Vol. 58 AUGUST, 1954 No. 8

THE JOURNAL OF PHYSICAL CHEMISTRY

DEBYE 70TH BIRTHDAY SYMPOSIUM, CORNELL UNIVERSITY, ITHACA, N. Y., MARCH, 1954

The Journal of Physical Chemistry is being published monthly in 1954
Notes and Communications to the Editor will be considered for
publication in THIS JOURNAL

THE JOURNAL OF PHYSICAL CHEMISTRY

(Registered in U. S. Patent Office)

Published monthly by the American Chemical Society at 20th and Northampton Sts., Easton, Pa.

Entered as second-class matter at the Post Office at Easton, Pennsylvania.

The *Journal of Physical Chemistry* is devoted to the publication of selected symposia in the broad field of physical chemistry and to other contributed papers.

Manuscripts originating in the British Isles, Europe and Africa should be sent to F. C. Tompkins, The Faraday Society, 6 Gray's Inn Square, London W. C. 1, England.

Manuscripts originating elsewhere should be sent to W. Albert Noyes, Jr., Department of Chemistry, University of Rochester, Rochester 3, N. Y.

Correspondence regarding accepted copy, proofs and reprints should be directed to Assistant Editor, Allen D. Bliss, Department of Chemistry, Simmons College, 300 The Fenway, Boston 15, Mass.

Business Office: American Chemical Society, 1155 Sixteenth St., N. W., Washington 6, D. C.

Advertising Office: Reinhold Publishing Corporation, 430 Park Avenue, New York 22, N. Y.

Articles must be submitted in duplicate, typed and double spaced. They should have at the beginning a brief Abstract, in no case exceeding 300 words. Original drawings should accompany the manuscript. Lettering at the sides of graphs (black on white or blue) may be pencilled in, and will be typeset. Figures and tables should be held to a minimum consistent with adequate presentation of information. Photographs will not be printed on glossy paper except by special arrangement. All footnotes and references to the literature should be numbered consecutively and placed in the manuscript at the proper places. Initials of authors referred to in citations should be given. Nomenclature should conform to that used in *Chemical Abstracts*, mathematical characters marked for italic, Greek letters carefully made or annotated, and subscripts and superscripts clearly shown. Articles should be written as briefly as possible consistent with clarity and should avoid historical background unnecessary for specialists.

Symposium papers should be sent in all cases to Secretaries of Divisions sponsoring the symposium, who will be responsible for their transmittal to the Editor. The Secretary of the Division by agreement with the Editor will specify a time after which symposium papers cannot be accepted. The Editor reserves the right to refuse to publish symposium articles, for valid scientific reasons. Each symposium paper may not exceed four printed pages (about sixteen double spaced typewritten pages) in length except by prior arrangement with the Editor.

Remittances and orders for subscriptions and for single copies, notices of changes of address and new professional connections, and claims for missing numbers should be sent to the American Chemical Society, 1155 Sixteenth St., N. W., Washington 6, D. C. Changes of address for the *Journal of Physical Chemistry* must be received on or before the 30th of the preceding month.

Claims for missing numbers will not be allowed (1) if received more than sixty days from date of issue (because of delivery hazards, no claims can be honored from subscribers in Central Europe, Asia, or Pacific Islands other than Hawaii), (2) if loss was due to failure of notice of change of address to be received before the date specified in the preceding paragraph, or (3) if the reason for the claim is "missing from files."

Subscription Rates: to members of the American Chemical Society, $8.00 for 1 year, $15.00 for 2 years, $22.00 for 3 years; to non-members, $10.00 for 1 year, $18.00 for 2 years, $26.00 for 3 years. Postage free to countries in the Pan American Union; Canada, $0.40; all other countries, $1.20. Single copies, $1.25; foreign postage, $0.15; Canadian postage $0.05. Back issue rates (starting with Vol. 56): nonmember, $1.50 per issue, foreign postage $0.15, Canadian postage $0.05; $12.50 per volume, foreign postage $1.20, Canadian postage $0.40; special rates for A.C.S. members supplied on request.

The American Chemical Society and the Editors of the *Journal of Physical Chemistry* assume no responsibility for the statements and opinions advanced by contributors to This Journal.

The American Chemical Society also publishes *Journal of the American Chemical Society*, *Chemical Abstracts*, *Industrial and Engineering Chemistry*, *Chemical and Engineering News*, *Analytical Chemistry*, and *Journal of Agricultural and Food Chemistry*. Rates on request.

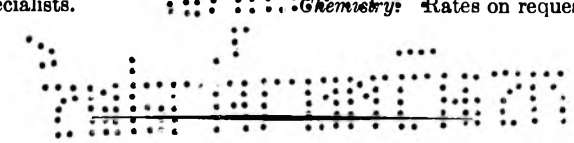

THE JOURNAL OF
PHYSICAL CHEMISTRY

(Registered in U. S. Patent Office) (Copyright, 1954, by the American Chemical Society)

VOLUME 58 AUGUST 18, 1954 NUMBER 8

THE EFFECTS OF HYDROSTATIC PRESSURE AND CENTRIFUGAL FIELDS UPON CRITICAL LIQUID–LIQUID INTERFACES

BY J. H. HILDEBRAND AND B. J. ALDER

Department of Chemistry and Chemical Engineering, University of California, Berkeley, California

J. W. BEAMS AND H. M. DIXON

Rouss Physical Laboratory, University of Virginia, Charlottesville, Virginia

Received March 27, 1954

Hydrostatic pressure applied to the system *n*-perfluoroheptane–2,2,4-trimethylpentane, raises the critical temperature for the appearance of the liquid–liquid interface at a uniform rate of 0.06656° per atmosphere between 1 and 64 atmospheres. In the system perfluoromethylcyclohexane–carbon tetrachloride, the rise through the same interval is 0.03875° per atmosphere. Centrifugal fields raise the apparent critical temperature linearly; at an acceleration of 10^8 cm. sec.$^{-2}$ a rise of 10° was found in the case of the former system and 7.7° for the latter. Subtraction of the hydrostatic pressure upon the interface from the centrifugal weight of liquid "above" it leaves, in the case of the former system, a rise of 1.9° at this acceleration to be attributed to a sedimentation effect arising from the large difference, 1,017, in the densities of the pure components at 25°. In the case of the latter system, where the density difference is only 0.180, the residual effect is not more than 0.2°, which lies within the limits of error of the experiment.

One of us[1a] not long ago described a hypothetical picture of the micro-effects of changing temperature in the critical region, and added: "If this is a reasonably accurate description of the process, there would seem to be room for slight disagreement as to the precise value of the critical temperature, particularly if we remember that we are observing," in the appearance of an interface, "the effects of small differences in density, which depend upon the gravitational field, and could be markedly changed in a centrifugal field." This paper describes an experimental study of the effects of a centrifugal field, which may be called a sedimentation effect, upon two different non-polar liquid pairs. One pair consisted of *n*-perfluoroheptane and 2,2,4-trimethylpentane ("isoöctane") whose densities, 1.707 and 0.690, respectively, at 25°, are very different; the other was perfluoromethylcyclohexane and carbon tetrachloride, whose densities, 1.795 and 1.615, are near together. The liquid–liquid curve for the former system was determined by Hildebrand, Fisher and Benesi,[2] the latter by Hildebrand and Cochran,[3] and with great precision by Zimm.[4]

The Effect of Hydrostatic Pressure.—Two non-polar liquids which differ sufficiently in their internal attractive forces to yield two liquid phases normally mix with considerable expansion and heat absorption,[1b] because the mixing process substitutes contacts between unlike molecules for contacts between like molecules, with a weakening of the internal forces, because the attraction between unlike molecules is normally closer to a geometric than to an arithmetic mean. In the case of the first pair, the expansion is as much as 4.9 cc. per mole of mixture, according to unpublished measurements kindly put at our disposal by Professor Robert Dunlap, of the University of Maine. The hydrostatic pressure of the liquid "above" the interface (in the sense of the centrifugal field) will add its component to the expected sedimentation effect, therefore one of us (Alder) measured, in the absence of a centrifugal field, the change in the critical temperature of the interface caused by hydrostatic pressure.

A mixture of the critical composition, 55.0 volume per cent. of isoöctane for the former system,

(1) (a) J. H. Hildebrand, *J. Colloid Sci.*, **7**, 551 (1952). See also (b) G. Jura, D. Fraga, G. Maki and J. H. Hildebrand, *Proc. Natl. Acad. Sci.*, **39**, 19 (1953).

(2) J. H. Hildebrand, B. B. Fisher and H. A. Benesi, *J. Am. Chem. Soc.*, **72**, 4348 (1950).

(3) J. H. Hildebrand and D. R. F. Cochran, *ibid.*, **71**, 22 (1949).

(4) B. H. Zimm, THIS JOURNAL, **54**, 1306 (1950).

56.0 volume per cent. of CCl_4 for the latter, was confined over mercury in the closed limb of a V-shaped tube. Air pressure, measured by a Bourdon gage,[5] was applied to the mercury in the other limb, and the temperature observed at which the interface just appeared. The liquid mixture could be stirred when necessary by a steel pellet moved by an external magnet. The results are given in Table I. The rise in the critical temperature is quite linear with pressure as shown by the correspondence between observed and calculated temperatures for the simple relations given.

TABLE I

EFFECT OF HYDROSTATIC PRESSURE UPON THE CRITICAL TEMPERATURE OF INTERFACES

	C_7F_{16}–i-C_8H_{18}			C_7F_{14}–CCl_4	
P, atm.	t_c Obs.	t_c Calcd.	P, atm.	t_c Obs.	t_c Calcd.
1.00	22.30	...	1.00	26.21	...
9.25	22.85	22.87	11.60	26.63	26.62
20.50	23.60	23.60	21.00	26.99	26.99
33.80	24.48	24.48	39.15	27.69	27.69
64.05	26.51	26.49	64.60	28.70	28.67
$\Delta t/\Delta P$	0.06656°/atm.			0.03875°/atm.	

In the case of C_7F_{14}–CCl_4, our value for t_c at 1 atmosphere is lower than those previously reported for this system. This may be the result of the care we took to purify our CCl_4 from traces of CS_2, which raises t_c, as might be expected. The behavior of these two-component systems under hydrostatic pressure is analogous to that of a one-component system, where Schneider and Habgood[6] found that the form of the liquid–vapor coexistence curve is very dependent upon the height of the column above the meniscus.

Volume Change upon Mixing.—The change in volume upon mixing can be related to the shift of the interface temperature with pressure by aid of the equations of regular solution theory which, although ignoring the clustering in the immediate vicinity of the critical point, have been used successfully to calculate critical compositions and temperatures.[7]

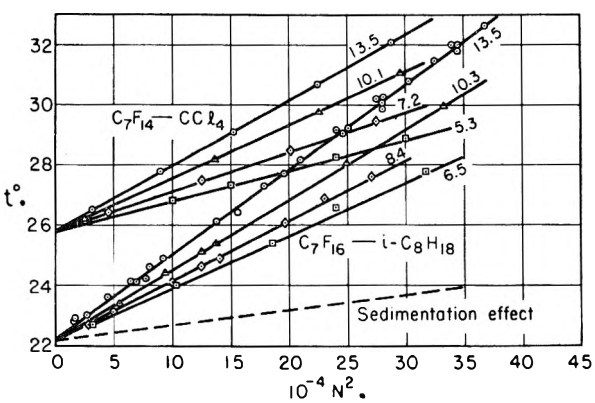

Fig. 1.—Effect of rotor speed upon t_c for different liquid depths, in mm.

(5) For details regarding the pressure system see E. W. Haycock, B. J. Alder and J. H. Hildebrand, *J. Chem. Phys.*, **21**, 1601 (1953).

(6) W. G. Schneider and M. W. Habgood, *ibid.*, **21**, 2080 (1953).

(7) J. H. Hildebrand and G. R. Negishi, *J. Am. Chem. Soc.*, **59**, 339 (1937); J. H. Hildebrand, *ibid.*, **59**, 2083 (1937); J. H. Hildebrand and R. L. Scott, "Solubility of Nonelectrolytes," Reinhold Publ. Corp., New York, N. Y., 1950, Chap. XVI.

Including the Flory–Huggins expression for entropy in the equation for activity, and setting its first and second derivatives with respect to composition equal to zero, yielded the following equations for critical composition and temperature

$$\frac{\varphi_1}{\varphi_2} = \left(\frac{V_2}{V_1}\right)^{1/2} \qquad (1)$$

$$RT_c = 2\phi_1^2 V_1(\delta_2 - \delta_1) \qquad (2)$$

Here the ϕ's denote volume fractions, the V's molar volumes, the δ's solubility parameters. This permits us to write

$$RT\left(\frac{\partial \ln a_2}{\partial P}\right)_{T,\phi} = \bar{V}_2 - V_2 = V_2\phi_1^2\left(\frac{\partial(\delta_2 - \delta_1)^2}{\partial P}\right)_{T,\phi}$$

$\bar{V}$ is partial molar volume. We have found by experiment that $RT_c = A + BP$, hence, by equation 2

$$B = 2\phi_1^2 V_1\left(\frac{\partial(\delta_2 - \delta_1)^2}{\partial P}\right)_{T,\phi}$$

and thus, $\bar{V}_2 - V_2 = (B/2)\,(V_2/V_1)$. Calculating the volume change upon mixing from $\Delta V^M = B/2(v_1(V_1/V_2) + \chi_2(V_2/V_1)$ we obtain for the system C_7F_{16}–i-C_8H_{18} at the maximum, 2.6 cc. per mole of mixture, rather less than the value calculated from Dunlap's densities. For C_7F_{14}–CCl_4 it is 1.5 cc.

The effect of centrifugal fields was investigated by Beams and Dixon at the University of Virginia in the vacuum contained centrifuge there developed.[8] It is hardly necessary to repeat here any details of its construction and operation, except as follows. Rotor speeds were determined to at least 0.5%. Temperatures, measured before and after each run, seldom differed by more than 0.1° because of the large heat capacity of the Duralumin rotor.

The separation into two phases starts at the "bottom" or peripheral end of the rotor cell, where the pressure is highest. It is observed as a sharp line of separation between the liquids both directly and by the schlieren optical method. The latter is more sensitive, but both give essentially the same results. When using the schlieren method, one notices as the rotor speed is slowly increased, with temperature constant, that within one or two r.p.s. turbulence begins in the cell and the liquids separate near the periphery of the cell. If, now, the rotor speed and temperature are held constant, the line of separation stays at a constant radial distance near the periphery. If, next, the rotor speed is increased, the line of separation moves toward the axis of rotation, and if the rotor speed is continually increased the interface moves upward.

The relation between rotational speed, N, in revolutions per second, and the observed temperatures of separation is shown in Fig. 1 for different depths of liquid in the cell, ΔR. It is to be seen that the centrifugal fields applied produce changes of many degrees in the temperature of separation.

Now there are two obvious ways to subtract the hydrostatic contribution in order to verify the existence of a pure sedimentation effect. The former is given by $2\pi^2\rho N^2(R_p^2 - R_s^2)$, where ρ is the density

(8) J. W. Beams, *J. Wash. Acad. Sci.*, **37**, 221 (1947).

of the liquid above the interface, R_s the radial distance to the surface, and R_p, the radial distance to the periphery, 6.20 cm., where the interface first appears. The value of ρ cannot be fixed with any certainty. According to the measurements of Dunlap, its value for a mixture of the composition we used should be close to 1.10 at 25°, but since the denser component has separated below the interface when this becomes visible, this may be regarded as a maximum value. If we calculate the hydrostatic pressure when $R_p = 7.2$ cm. and $R_s = 6.55$ cm. and $N^2 = 30 \times 10^4$ sec.$^{-2}$, assuming $\rho = 1.10$, we obtain 57.9×10^6 dynes cm.$^{-2}$ or 57.2 atmospheres. This alone, at the rate of 0.06656°/atm., would give a rise of 3.8°. The rise observed under these conditions was 5.3°, leaving 1.5° as the contribution of the sedimentation effect. The maximum in the solubility curve might be shifted by pressure to a different composition, but it is hardly to be expected that any such shift could be very far, and if it occurs it would have affected the static and centrifuge results nearly equally, except that the centrifugal field gives rise to a density gradient according to which the above difference could be regarded as a minimum.

Another, and we believe preferable, method of separating the sedimentation effect is to extrapolate to zero height above the interface. Figure 2 shows $R_p^2 - R_s^2$ plotted against Δt_c for five different values of N^2. The intersections of these lines with the zero ordinate may be taken as the value of the sedimentation effect at different centrifuge speeds. The dotted line in Fig. 2 represents this effect. Its value at $N^2 = 30 \times 10^4$ is 1.9°, agreeing satisfactorily with the above minimum of 1.5° for the same speed of rotation.

The same method of extrapolation applied to the system C_7F_{14}–CCl_4, whose components differ much less in density, gives intercepts amounting to not more than 0.2°, well within the experimental limits of uncertainty, and we have not thought it necessary to plot them. In this case, the rise found in the centrifuge corresponds closely with the rise calculated for the hydrostatic pressure alone. In the critical mixture, the density, calculated on an additive basis, is 1.67 at 25°. The actual value for the upper phase is doubtless smaller. When $N^2 = 30 \times 10^4$, $\Delta R = 1.35$ cm., the calculated hydrostatic pressure is 173 atm., and the calculated rise is 6.7° (also a maximum). The rise observed was 6.6°.

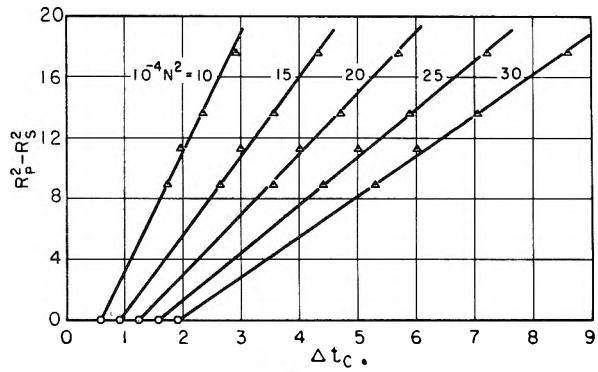

Fig. 2.—Extrapolation of Δt_c to zero liquid depth for constant rotor speeds: system C_7F_{16}–i-C_8H_{18}.

Discussion.—If these mixtures, in the region of light scattering, corresponded to ordinary emulsions, with globules of one density dispersed in a medium of different density, the sedimentation could be analyzed after the manner used by Perrin. These mixtures differ from true emulsions, however, in that they have a cell-like structure, made up of micro-regions which contain the components in different proportions, separated by density gradients instead of abrupt boundaries. The components of a critical mixture are present in nearly equal volume,[2,3] and the regions cannot properly be regarded as, respectively, outer and inner. As the temperature is lowered, the "cells" become larger and the composition gradients steeper, and eventually yield interfaces sharp enough to reflect light. Separation into upper and lower phases is brought about by the action of gravity or of a centrifugal field upon the regions of different density.

We have no desire to monopolize the theoretical analysis of these observations, and invite the attention of the investigators now interested in critical phenomena.

This work was supported, in part, by the Atomic Energy Commission.

DIELECTRIC RELAXATION, VISCOSITY AND MOLECULAR SHAPE[1]

BY CHARLES P. SMYTH

Department of Chemistry, Princeton University, Princeton, N. J.

Received April 19, 1954

Although the dielectric relaxation time of a liquid tends to increase with increase in the measured or macroscopic viscosity, it is much smaller than the value calculated from the viscosity and molecular radius, probably, because the molecular motion involved in dipole orientation requires much less translational motion of the molecules than that occurring in viscous flow. The relaxation times of nearly spherical molecules, which can rotate with little or no displacement of their neighbors, are found to show little dependence on the viscosity of the medium, in contrast to unsymmetrical molecules which displace their neighbors when they rotate. The van der Waals radii of six substituted methanes, which have nearly spherical molecules, have been calculated from atomic radii and bond lengths and used with the values of the critical wave length to calculate the internal or microscopic viscosity which hinders dipole orientation. The values calculated for the microscopic viscosity from the critical wave lengths are only 0.008 to 0.06 of the macroscopic. Lowering of the molecular relaxation time by the internal field may lower the microscopic viscosity by a factor of about 0.7 for all of these liquids but dibromodichloroethane. There appears to be little parallelism between the microscopic and the macroscopic viscosities and, indeed, a crystalline solid consisting of nearly spherical molecules may have a microscopic viscosity lower than that of the liquid state.

The directly observed dielectric relaxation time contained in the expressions for the real and imaginary parts of the dielectric constant is

$$\tau = \frac{1}{\omega_m} = \frac{\lambda_m}{6\pi \times 10^{10}} \qquad (1)$$

where ω_m is the critical angular frequency, for which the loss factor ϵ'' is a maximum, and λ_m is the corresponding critical wave length. In the original equations of Debye,[2] this macroscopic quantity was replaced by a molecular or microscopic relaxation time

$$\tau = \frac{\epsilon_\infty + 2}{\epsilon_0 + 2}\frac{1}{\omega_m} \qquad (2)$$

where ϵ_∞ is the optical or infinite frequency dielectric constant and ϵ_0 is the static dielectric constant. In early work, the relaxation time used was the microscopic given by eq. 2, which is based on the Lorentz internal field, but, in view of the inadequacy of this expression for the internal field in polar liquids, the macroscopic relaxation time given by eq. 1 has been generally used in recent years. Powles[3] has proposed a reasonable, though approximate, expression for the internal field in a dielectric subjected to an alternating electric field, which leads to

$$\tau = \frac{2\epsilon_0 + \epsilon_\infty}{3\epsilon_0}\frac{1}{\omega_m} \qquad (3)$$

This gives only a small difference between the microscopic and the macroscopic relaxation times, the microscopic never being less than $^2/_3$ of the macroscopic, while eq. 2 would require the microscopic relaxation time of water to be only about $^1/_{16}$th of the macroscopic.

Debye assumed the relaxing or orienting dipolar molecule to be a sphere of radius a moving in a continuous viscous fluid possessing a coefficient of internal friction η and obtained

$$\tau = 4\pi\eta a^3/kT \qquad (4)$$

It has been customary to use for η the experimentally measured macroscopic viscosity instead of the unknown microscopic internal friction coefficient. With reasonable values for a, Mizushima and Debye[2] were able to represent the dispersion and absorption of several alcohols satisfactorily, but it was pointed out that to do so for glycerol required the use of a radius value 0.35 Å., which is far too small.

Oncley[4] has used the macroscopic relaxation time given by eq. 1 for dilute solutions of proteins in water and alcohols and has found the values of the relaxation times to be of just the magnitudes to be expected from the values of molecular weight, asymmetry and hydration determined by other methods. In other words, the differences between the microscopic and macroscopic relaxation times are small in spite of the large static dielectric constant values, which would give a maximum difference between the macroscopic value from eq. 1 and the microscopic from eq. 2. This would seem to justify the neglect of any distinction between the macroscopic and the microscopic relaxation times, but the force of this evidence is weakened by the fact that Kirkwood and Shumaker[5] have shown that dipole fluctuation arising from the mobile distribution of protons in the molecules can give rise to a dielectric increment and a relaxation time of the order observed for typical proteins. The relaxation times of the large protein molecules show approximately the proportionality to viscosity required by eq. 4 even when the macroscopic viscosity is used, presumably, because the solvent molecules surrounding those of the solute are so small in comparison with the large solute molecules as to give an approximation to the homogeneous fluid postulated in the derivation of eq. 4. Such a proportionality would seem impossible in the case of molecules whose dielectric relaxation times arose from mobile distribution of protons in the molecule.

The lack of proportionality between the relaxation times for small molecules and the macroscopic viscosities is evident in the results of a number of early measurements. For example, twelve sets of measurements[6] by various investigators on nitrobenzene in various solvents gave relaxation times from which eq. 4 gave apparent radius values for the molecule varying from 0.25 to 2.4 Å. It is to

(1) This research has been supported in part by the ONR.

(2) P. Debye, "Polar Molecules," Chemical Catalog Co., New York, N. Y., 1929, Chap. V.

(3) J. G. Powles, *J. Chem. Phys.*, **21**, 633 (1953).

(4) J. L. Oncley, in "Proteins, Amino Acids and Peptides," by E. J. Cohn and J. T. Edsall, Reinhold Publ. Corp., New York, N. Y., 1943, Chap. 22.

(5) J. G. Kirkwood and J. B. Shumaker, *Proc. Natl. Acad. Sci.*, **38**, 855 (1952).

(6) F. H. Müller, *Ergeb. exakt. Naturw.*, **17**, 164 (1938).

be noted, moreover, that taking the cube root in calculating a does a great deal to reduce discrepancies. A convenient way of avoiding this ironing out of discrepancies is to calculate the hypothetical volume V_D of the N molecules in a mole from the relation[7]

$$V_D = \frac{4\pi a^3 N}{3} = \frac{\tau RT}{3\eta} \qquad (5)$$

Values of V_D obtained for a variety of liquids were commonly only 10 to 20% of the directly measured molar volume, $V = M/d$, where M is the molecular weight and d the density, while if the liquid were a system of close-packed molecular spheres, the ratio of the actual volume of the spheres to the total volume of the liquid would be 0.74. The values of V_D for the straight-chain alkyl bromides[8] rise continuously from a value of 8.19 cc. at 25° for ethyl bromide to 13.84 cc. for n-hexyl bromide and then decrease to 8.55 cc. for n-hexadecyl bromide, a value less than 3% of M/d. Although the relaxation times increase with increasing chain lengths for these straight-chain molecules, it appears that orientation of the extended molecule by turning around its long axis and increased opportunity for orientation by twisting around the C–C bond, probably, cause the increase in relaxation time to fall farther and farther behind the increase in viscosity. The influence of at least one of these two factors is evidenced by the fact that the relaxation time 8.6×10^{-11} sec. at 25° for α-bromonaphthalene, which has a somewhat flat, rigid molecule, is 2.5 times the value 3.4×10^{-11} for n-dodecyl bromide,[8] which has the same number of carbon atoms arranged in a long flexible chain, while the viscosity, 4.52 centipoises, of α-bromonaphthalene is only 1.25 times the value 3.60 of n-decyl bromide.[9]

The viscosities of a variety of fatty acid esters are slightly lower than those of alkyl bromides of approximately the same molecular length, but the critical wave lengths are only about half as large.[10] The rate of increase of the critical wave length with increase in viscosity is much less for the esters than for the alkyl bromides.

The results which have been discussed as typical indicate that the molecular or microscopic viscosity in eq. 4 is much smaller than the directly measured or macroscopic viscosity which is available for calculating the molecular radius. This is not surprising when it is considered that the process of viscous flow used in measuring the macroscopic viscosity involves both translational and rotational motion of the molecules, while dipole orientation which determines the dielectric relaxation time primarily involves only molecular rotation, which may, however, necessitate some displacement and, hence, translational motion of the neighboring molecules.

The molecules of methyl and halogen-tetrasubstituted methanes have the shape of a tetrahedron with rounded corners and indented edges. Their roughly spherical symmetry makes possible the orientation of their dipoles by molecular rotation in the crystal lattice. For such molecules in a liquid eq. 4 should be at its best. For several of them, Table I lists the observed critical wave length given by eq. 1, the value of the internal field factor in eq. 3, the apparent value of the radius a of the molecule given by eq. 4, the value a_v of the van der Waals radius calculated from bond lengths and the van der Waals radii of atoms and groups, the measured macroscopic viscosity η used in calculating a, and a microscopic viscosity η_m calculated by putting in eq. 4 the value of τ given by eq. 1 and the value of a_v for a.

TABLE I

CRITICAL WAVE LENGTHS (CM.), VISCOSITIES (CPS.) AND RADII (Å.) OF LIQUIDS WITH NEARLY SPHERICAL MOLECULES AT 20°

	λ_m	$\frac{2\epsilon_0 + \epsilon_\infty}{3\epsilon_0}$	a	a_v	η	η_m
$(CH_3)_3CCl$[11]	0.9	0.73	1.42	3.55	0.53	0.034
$(CH_3)_2CCl_2$[12]	0.9	.72	1.12	3.55	1.09	.034
$(CH_3)CCl_3$[12]	1.1	.76	1.19	3.55	1.12	.042
$(CH_3)_3CBr$[8]	1.2	.73	1.33	3.7	0.81	.040
CBr_2Cl_2[13]	0.7	.99	0.74	3.7	2.90	.024
$(CH_3)_2C(NO_2)_2$[12]	(2.5)(60°)	.69	1.24	3.5	2.23	.100

In spite of the reduction of the discrepancies as a result of the cube root relation, the apparent radii a calculated by means of eq. 4 are only 0.2–0.4 of the van der Waals radii a_v. For all of the molecules but dibromodichloromethane, the discrepancy would be slightly increased by calculating the relaxation time with eq. 3 and considerably increased by calculating it with eq. 2. The discrepancy is greatest for dibromodichloromethane, which has a much higher macroscopic viscosity and smaller dipole moment,[13] 0.26×10^{-18}, than the methyl halogen-substituted methanes, which have moments $1.8–2.2 \times 10^{-18}$. The calculated microscopic viscosities show discrepancies with the measured macroscopic viscosities analogous to those between the apparent volumes V_D calculated by means of eq. 5 and the measured volumes. However, while the apparent volumes V_D are significant mainly in showing the extent of the deviation from the calculated behavior, the values of the microscopic viscosity η_m should have a real, though approximate, physical significance. The obvious physical significance is that the resistance to rotation of the nearly spherical molecules is very much smaller than the resistance to translational motion, since the microscopic viscosities in Table I are only 0.008 to 0.06 of the macroscopic, which involve both kinds of motion. There appears to be little parallelism between the values of the microscopic and the macroscopic viscosities, which latter tend to increase with increasing molecular polarizability, but do not evidence an effect of molecular moment, except, perhaps, in the case of 2,2-dinitropropane. The microscopic viscosities calculated with eq. 1 and 4 show a small value for dibromodichloromethane, which has a very small dipole mo-

(7) W. P. Conner and C. P. Smyth, *J. Am. Chem. Soc.*, **65**, 382 (1943).

(8) E. J. Hennelly, W. M. Heston, Jr., and C. P. Smyth, *ibid.*, **70**, 4102 (1948).

(9) W. M. Heston, Jr., E. J. Hennelly and C. P. Smyth, *ibid.*, **72**, 2071 (1950).

(10) P. L. McGeer, A. J. Curtis, G. B. Rathmann and C. P. Smyth, *ibid.*, **74**, 3541 (1952).

(11) A. J. Curtis, P. L. McGeer, G. B. Rathmann and C. P. Smyth, *ibid.*, **74**, 644 (1952).

(12) Unpublished measurements by Mr. R. S. Holland.

(13) Unpublished measurements by Dr. R. C. Miller.

ment, somewhat larger values for the four methyl halogen-tetrasubstituted methanes, which have good-sized moments, and a considerably larger value for 2,2-dinitropropane, which has a large moment, about 4×10^{-18}, acting near the outer end of the molecular radius. If, however, the relaxation times are calculated by means of eq. 3 instead of eq. 1, the values of η_m are decreased by the factors $(2\epsilon_0 + \epsilon_\infty)/3\epsilon_0$, which reduces or eliminates the differences between the four methyl halogen-tetrasubstituted methanes and dibromodichloromethane, but still leaves the value for 2,2-dinitropropane much higher. The use of eq. 2 to calculate the relaxation time would leave the value of η_m for dibromodichloromethane practically unchanged, but would lower the values for the other five tetrasubstituted methanes to 0.012–0.016. As the measurements on 2,2-dinitropropane are at 60°, its viscosities, both microscopic and macroscopic, would, doubtless, still be highest of all, if extrapolated down to 20°.

Solutions of the three methylchloromethanes in heptane and in a viscous paraffin oil were investigated[11,12] in the belief that the critical wave lengths of the nearly spherical molecules would show little dependence upon the viscosity of the medium. This was borne out by the result that the critical wave lengths and, consequently, the microscopic viscosities, increased only 50% from heptane to nujol, although the macroscopic viscosity increased 257-fold. The long, flexible molecule of *n*-tetradecyl bromide gives much longer critical wave lengths than these spherical molecules, the values at 20° being 12.3 cm. in the pure liquid, 4.1 in heptane, and 19 in nujol.[10] The almost fivefold increase from heptane to nujol solution, still very small in comparison to the 257-fold increase in macroscopic viscosity, is attributable to the fact that dipole orientation involving either the entire molecule or a molecular segment should require some displacement of the surrounding molecules and, hence, greater dependence upon the macroscopic viscosity. The somewhat flattened, rigid molecule of α-chloronaphthalene gives a sixfold increase in critical wave length from heptane to nujol.[11] The departure of the molecules from spherical form evidently causes or increases translational motion of the surrounding molecules when dipole orientation occurs and, consequently, increases the microscopic viscosity and decreases somewhat the great difference between it and the macroscopic viscosity.

The tendency of the critical wave length of the pure polar liquid to be considerably longer than that of a dilute solution of the same substance of about the same viscosity has been attributed[11] to hindrance of molecular rotation by dipole–dipole interaction, which is present in the pure liquid and largely absent in the dilute solution. These differences in the relaxation times are reduced when they are calculated by eq. 3 and still more reduced when they are calculated by eq. 2, which, probably, effects too great a reduction in the values for the pure liquids. While the increase of the critical wave length and macroscopic relaxation time of the dielectric by the internal field would seem to be a general phenomenon, its exact interpretation is somewhat obscured by uncertainty as to the internal field. The results obtained with the reasonable approximation for the effect of the field given by eq. 4 indicate that the molecular or microscopic relaxation time is reduced by the occurrence of dipole–dipole interaction.

The *reductio ad absurdum* of the use of the macroscopic viscosity as determining dielectric relaxation time occurs in the case of solids in which molecular symmetry around one or more axes permits dipole orientation by molecular rotation. In several of the substituted methanes, which have been considered, the dielectric relaxation time is actually shortened by solidification of the liquid.[14] In fact, the almost negligible loss and the high dielectric constant at 3.22 cm. of solid *t*-butyl chloride for some distance below the melting point show that this short wave length is still far above the critical wave length. It is evident that a crystalline solid consisting of nearly spherical molecules may have a microscopic viscosity lower than that of the liquid state.

(14) J. G. Powles, D. E. Williams and C. P. Smyth, *J. Chem. Phys.*, **21**, 136 (1953).

THE ELECTROKINETIC PROPERTIES OF DILUTE MONODISPERSE SULFUR HYDROSOLS

BY ROBERT H. SMELLIE, JR., AND VICTOR K. LA MER

Department of Chemistry of Columbia University, New York, N. Y., and Trinity College, Hartford, Conn.

Received April 19, 1954

Monodisperse sulfur hydrosols prepared by the reaction of very dilute acid and thiosulfate consist of *positively* charged particles, in contrast to the negatively charged particles reported previously by all who have used more concentrated reagents or other methods. These positively charged particles have an isoelectric point (*p*H 4), which is higher than for mechanical dispersions of solid (rhombic) sulfur particles (*p*H 2.7). The positive charge observed for sols prepared from very dilute reagents persists only in the absence of significant (10^{-5} *M*) amounts of polythionate, thus allowing the less strongly adsorbed H^+ to be effective. The addition of pentathionate (1 to 5 $\times$ 10^{-5} mole/l.) reduces or even reverses the positive charge. At higher initial thiosulfate concentrations polythionate is formed as a by-product in the reaction and the positively charged particles are converted to negative during the development. Sulfite ion is responsible for the negative charge at high *p*H. Positively charged sols were also prepared by adding water to sulfur in dilute solutions in ethyl alcohol or acetone. Traces of acetic acid are necessary for the production of a positive charge in these sols. Mechanisms by which H^+ ion could be exchanged on the surface of the particles are discussed. The small distribution in mobility (charge) of the particles was comparable with the known small distribution (σ = 10%) in radii of particles prepared by these methods. The surface charge density appears to be uniform and the particles may be considered to be monodisperse both in respect to charge as well as radius at high positive and negative charge but not near the isoelectric point.

Introduction

The development of methods for preparing[1] monodisperse sulfur sols has resulted in the solution of a number of problems previously unattainable with polydisperse sols.[1-5] The electrokinetic behavior of a sol is an important factor when considering stability and coagulation,[6-8] but had not been studied in any of our previous investigations.

Under the proper conditions a reliable estimate of the magnitude of the charge,[7-9] the specific adsorption of certain ions and their effect on the charge may be determined by this method.

The results of previous investigations of the electrokinetic behavior of sulfur hydrosols cannot be utilized in considering the behavior of sulfur in our dilute monodisperse sols. The earlier studies were made on sols originally prepared from concentrated reagents, and were confined primarily to the effect of salts[10,11] on concentrated sols.

In these cases repeated purification by dialysis[12] (or electrodialysis) would reduce the ion concentrations only to a point which is still much greater than in the sols prepared by La Mer and collaborators. In fact, attempts to dialyze these sols lead to partial dissolution of the particles and coagulation. The reason is now apparent.[13] As dialysis proceeds, the *p*H of the sol is raised to such a value that HSO_3^- is converted to $SO_3^=$ and the reaction

$$S + SO_2^= = S_2O_3^=$$

proceeds at a rapid rate dissolving much of the suspended sulfur.

Measurements were made on growing sols by microelectrophoretic methods in order to correlate the electrokinetic behavior with chemical and physical evidence obtained under the same conditions. The excellent reproducibility of these sols with respect to particle size and number means reproducibility of surface area. Thus one of the major uncertainties usually associated with electrokinetic investigation was eliminated. The possibility of correlating electrophoretic behavior with particle radius or area was thus indicated.

However, since these dilute sols could not be safely dialyzed, the independent action of certain electrolytes and non-electrolytes could not be studied with sols prepared from thiosulfate and acid. Such information could be obtained by using alcohol–sulfur–water sols.[5]

In the study of proteins, acidimetric titration determines the amount of H^+ ion bound. The amount of bound ion often parallels the charge as determined by electrophoresis.[14] Acidimetric titrations could not be utilized for this purpose in the present investigation. However, other valuable information was obtained.

Experimental

I. Preparation and Reproducibility of Sols.—Dilute monodisperse sols were prepared by adding sodium thiosulfate and hydrochloric acid to distilled water according to the methods of La Mer and collaborators.[1] These sols were grown in a thermostat at 25 $\pm$ 0.03°. Organosulfur–water sols were prepared by adding distilled water to alcohol or acetone solutions of sulfur.[5]

The reproducibility of thiosulfate–acid sols was established by particle size and number measurements using a Beckman spectrophotometer.[1] The number of particles per cc. was also determined by direct counting under the microscope in the electrophoresis cell. The particles were counted in several different sections of the cell after they all had settled to the bottom using a calibrated net reticule visible under dark field illumination. Knowing the average number of particles in the field, the area of the field, and the

(1) (a) V. K. La Mer and M. Barnes, *J. Colloid Sci.*, **1**, 71 (1946); (b) M. Barnes, A. Kenyon, E. M. Zaiser and V. K. La Mer, *ibid.*, **2**, 349 (1947); (c) E. M. Zaiser and V. K. La Mer, *ibid.*, **3**, 571 (1948).

(2) I. Johnson and V. K. La Mer, *J. Am. Chem. Soc.*, **69**, 1184 (1947).

(3) H. Reiss and V. K. La Mer, *J. Chem. Phys.*, **18**, 1 (1950); H. Reiss, *ibid.*, **20**, 482 (1952).

(4) M. Kerker and V. K. La Mer, *J. Am. Chem. Soc.*, **72**, 3516 (1950).

(5) V. K. La Mer and R. H. Dinegar, *ibid.*, **72**, 4847 (1950).

(6) F. Powis, *J. Chem. Soc.*, **109**, 734 (1916).

(7) J. Th. G. Overbeek, "Advances in Colloid Science," Vol. III, Interscience Publ., Inc., New York, N. Y., 1950, pp. 97–134; "Colloid Science," (Kruyt), Vol. I, Elsevier Press, Houston, Texas, 1952, Chap. V.

(8) J. Th. G. Overbeek, *ibid.*, Chap. V, VII.

(9) H. A. Abramson and H. Muller, *Phys. Rev.*, **41**, 386 (1932).

(10) H. Freundlich and P. Scholz, *Kolloid-Beih.*, **16**, 234 (1932).

(11) S. Oden, "Der Kolloide Schwefel."

(12) W. Pauli, *J. Colloid Sci.*, **2**, 333 (1947).

(13) R. H. Dinegar and R. H. Smellie, *ibid.*, **7**, 370 (1952).

(14) R. K. Cannan, A. Kibrick and A. H. Palmer, *Ann. N. Y. Acad. Sci.*, **41**, 243 (1941); *J. Biol. Chem.*, **142**, 803 (1942).

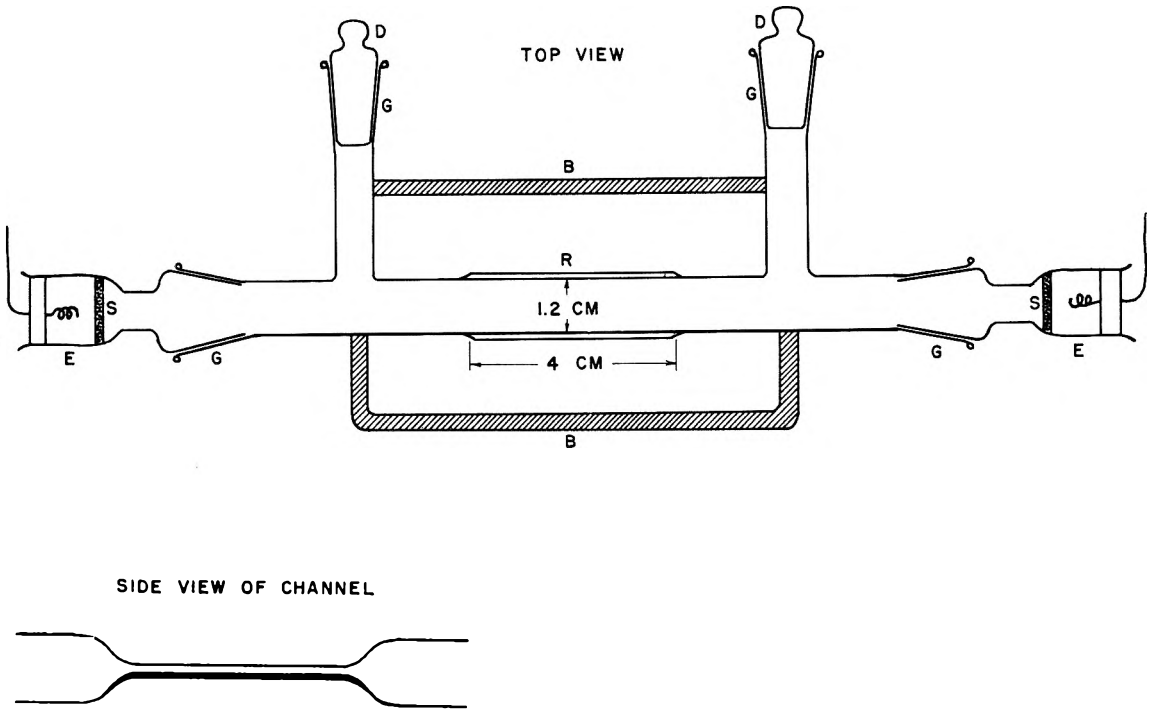

Fig. 1.—Electrophoresis cell: B, glass reinforcing bars; D, ground glass caps; E, electrode compartments; G, ground glass joints; S, sintered glass discs.

height of the cell, the number of particles per cc. of sol can be calculated.

The results of these counts showed excellent agreement (see Table I) with those previously obtained with the Beckman spectrophotometer and offer a further demonstration of the reliability of the method.

TABLE I

COMPARISON OF NUMBER OF PARTICLES (10^6/CM.^{3}) BY DIRECT MICROSCOPIC COUNT AND BY SPECTROPHOTOMETRY[10]

$Na_2S_2O_3$ = 0.0020 *M*

HCl, *M*	Hours after mixing	No. of particles (10^{-6}/cm.^{3}) Direct	Ref. 1c
0.002	4	2.7	2.7
.002	24	1.7–2.2	..
.003	4	5.5	5.44

II. Method and Apparatus.—The microelectrophoretic method was most suitable for the following reasons: (a) A macro method requires too long a period of time for a single observation. A detailed study of the variation of electrophoretic mobility with particle growth could not be made by such a method. (b) Dilute sols such as these should not be subjected to extended electrophoresis, since the great mobility of H^+ ion could produce disturbances in ionic distribution. No appreciable effect should be noted in the short times required for a single observation by the micro method (5–20 seconds). The reversal of polarity after each observation, assures the uniform distribution of ions. (c) Direct observation of the velocity distribution among the particles is possible. (d) The number of particles may be counted simultaneously with observations of the electrophoretic mobility.

The most reliable type of cell is one containing a rectangular cross-section in the region of observation.[15] In addition, the sample of sol should make contact with the electrode compartment only through conducting barriers to prevent mixing of electrolytes with the sample. The electrode–electrolyte combination was of the reversible type, *i.e.*, Cu; $CuSO_4$.

A cell meeting these requirements was manufactured by the Pyrocell Mfg. Co., New York (Fig. 1). The top glass in the rectangular section was about 0.2 mm. thick. With the rectangular channel of the cell about 0.6 mm. deep, it is possible to use a 44× objective on the microscope since the total distance that must be penetrated is about 0.8 mm. With a thicker top glass it would not be possible to focus on the bottom of the cell with this objective. The advantage to be gained by using an objective of such high power is discussed below.

The cell was cleaned with 95% alcohol to remove sulfur and flushed with water, allowed to stand in chromic acid–sulfuric acid solution for several hours, rinsed with distilled water, and dried in the oven.

In filling the cell, the detachable electrode compartments containing the copper electrodes and 0.5 *M* copper sulfate solution were put in place and the cell filled with sol through one of the tubes D (Fig. 1), while rocking to remove air bubbles. The ground glass caps were then carefully put into place. If the sol particles are large (radius *ca.* 0.4) they settle rapidly. A fresh sample of the sol can be quickly introduced through D, thus restoring the particle distribution. The whole cell assembly was set in a carriage on the microscope stage for horizontal support. *p*H measurements were made with a glass electrode.

After the cell had been assembled, filled and placed on the microscope stage, the copper electrodes were connected to a source of d.c. potential ranging between 90 and 250 volts. The sources were a series of 45 volt "B" batteries or a full wave rectifier power supply with variable output. The current was measured to *ca.* 0.5% by means of a sensitive milliammeter. The potential source (with the milliammeter in series) was connected to a double pole–double throw switch to allow reversing the polarity at the copper electrodes. With applied potentials between 90 and 250 volts the currents drawn were very small, ranging between 0.02 to 1.5 milliamperes.

The room temperature was adjusted to 25 ± 1° and the temperature of the sol in the electrophoresis cell did not vary from 25° by more than a few tenths of a degree.

III. Optical Requirements.—Dark field illumination must be used for reliable results. A substage condenser with a central opaque disc provided a satisfactory dark field for observing the sol particles. A white light or a Gates sodium lamp was used as a source of illumination. The latter is monochromatic and was the most satisfactory for observing sols containing very small particles.

For accurate focusing an objective with a small depth of focus must be used. Employing a 44× objective, focusing is accurate to ±2 microns, as determined by observation. Objectives of lower power are usually used with microelec-

(15) D. C. Henry, *J. Chem. Soc.*, 997 (1938).

trophoresis cells.[16] The accuracy of focusing is important since the mobility of the particles varies with position in the cell according to the relationship derived by Smoluchowski,[17] and modified by Komagata.[18] To provide homogeneous immersion, the bottom of the cell was brought into contact with the condenser by means of a film of immersion oil. By a combination of 44× objective, 10× ocular, and dark field illumination, the particles were easily observed.

IV. Mobility Measurements—Theory.—The mobility, v, of a particle under the influence of a potential gradient X is given by

$$v = XD\zeta/4\pi\eta \qquad (1)$$

where D is the dielectric constant, η the viscosity (both within the double layer) and ζ is the so-called zeta or electrokinetic potential.[19] The utilization of this equation has been the subject of much dispute.[8] Henry[8,20] has concluded that the thickness of the double layer and the radius of the particle will determine whether the value 4 may be used in the denominator. Another factor is the magnitude of the conductivity of the particles compared to that of the liquid.[8,20]

The most satisfactory method for obtaining the potential gradient is one in which the current passing through the cell and the specific resistance of the sol are measured.[21] Knowing the cross-sectional area of the rectangular part of the cell in addition to the other two quantities, the potential gradient may be calculated as

$$X = RI/q \qquad (2)$$

where

X = potential gradient in v./cm.
R = specific resistance of sol (in ohm-cm.)
I = current in amperes
q = cross-sectional area in cm.^{2}

In mobility measurements the time required for a particle to traverse a known distance is determined. A net reticule in the eyepiece of the microscope is calibrated by means of a stage micrometer, thus giving the value of each unit of the reticule in terms of absolute distance. The mobility in terms of cm.^{2} volt^{-1} sec.$^{-1}$ may be calculated from the measured mobility and the potential gradient.

Variation of Mobility with Position in the Cell and the Determination of the True Mobility.—Due to the electroosmotic flow of the liquid at the upper and lower walls of the cell and the return flow through the center of the cell, the observed mobility of the particles will vary with their position with respect to these walls,[17] as shown by Ellis.[22] To obtain the true mobility, observations must be made at different levels within the cell and the true value determined by integration.[22,23]

When the ratio of the cell width to depth is very large a more convenient method may be employed which requires making measurements only at the so-called stationary levels, approximately 0.2 and 0.8 of the depth of the cell. At these levels the true velocity of the particles may be obtained, by utilizing the equation of Smoluchowski for the flow of liquid between two parallel plates.[17]

Another relationship which may be derived from Smoluchowski's equation also gives the true mobility. In this case measurements are made at levels $^1/_6$ and $^1/_2$ of the thickness of the channel, *i.e.*

$$V = \frac{3}{4} V_{1/6} + \frac{1}{4} V_{1/2} \qquad (3)$$

This relationship was used when the mobilities at the 0.2 and 0.8 levels were too small for accurate measurement. Figure 2 shows that the mobility *vs.* level varies in accordance with theory with a maximum in the center of the cell. Comparison of the mobility obtained by direct measurement at the stationary levels with integration and by means of eq. 3 shows agreement within 5%. Between 5 and 8 observations were taken at each level.

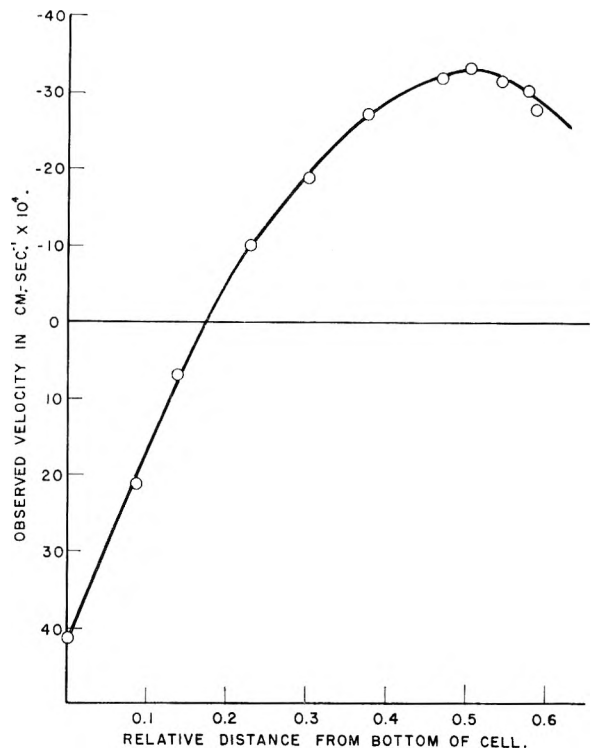

Fig. 2.—Variation of negative particle velocity with position in the electrophoresis cell.

The majority of the observations were made at the stationary or at the $^1/_6$ and $^1/_2$ levels. At least 10 and in most cases 20–25 observations were made. The spread in velocity distribution varied somewhat depending upon the order of magnitude of the mobility. In many cases the maximum deviation from the average value was less than 5% and in others as much as 30–40%. Where a large spread was observed, at least 25 observations were made. The average of all the values was close to the average of the extreme values. For sols in which the particles settle rapidly, the mobility measurements may be made as the particles reach the lower stationary level.

Direct measurement of the particle size distribution was not made on the sols employed, but indirect methods, based on the sharpness of the red-green ratio[2] and polarization ratio[4] of the higher order Tyndall spectra, which sols prepared in this manner exhibit, lead uniformly to the conclusion that the standard deviation from the mean radius is of the order of 10 to 20%.

This conclusion from the higher order Tyndall spectra has been confirmed by a method of direct photography of monodisperse aerosols by P. K. Lee (*J. Sci. Instr.*, in press).

Since deviations in surface area will be twice the deviations in radius it would appear that the surface charge density on the particles at higher charge but not near the isoelectric point is reasonably constant and that the distribution in mobility under these conditions arises primarily from distribution in radii. For the alcohol–water sols of radius 0.5 μ, the electrophoretic mobility at pH 6.9 was -1.3 ± 0.3 μ/sec./v./cm., corresponding to a calculated charge of 1500 electrons per particle or a surface density of 23 abs. e.s.u. cm.$^{-2}$.

Discussion of Experimental Results[24]

I. Acid–Thiosulfate Sols.—To determine the mobility of sol particles in the medium in which

(16) See H. A. Abramson, "Electrokinetic Phenomena and Their Application to Biology and Medicine," Chemical Catalog Company, New York, N. Y., 1934.

(17) M. Smoluchowski, "Graetz Handbuch," Vol. II, p. 366.

(18) S. Komagata, *Researches Electrotech. Lab., Tokyo*, No. 348 (1933).

(19) M. Smoluchowski, *Bull. Acad. Sci. Cracovie*, 182 (1903).

(20) D. C. Henry, *Proc. Roy. Soc. (London)*, **A133**, 106 (1931).

(21) H. A. Abramson, *J. Gen. Physiol.*, **12**, 469 (1929); H. A. Abramson and E. B. Grossman, *ibid.*, **14**, 563 (1931).

(22) R. Ellis, *Z. physik. Chem.*, **78**, 321 (1912).

(23) A. W. Thomas, "Colloid Chemistry," McGraw-Hill Book Co., Inc., New York, N. Y., 1934, pp. 212–217.

(24) These experiments were completed in 1950. Mr. Anthony J. Petro of the Trinity College Laboratories has since confirmed some of them and is studying the effect of particle size and sulfite ion concentration on mobility at high pH.

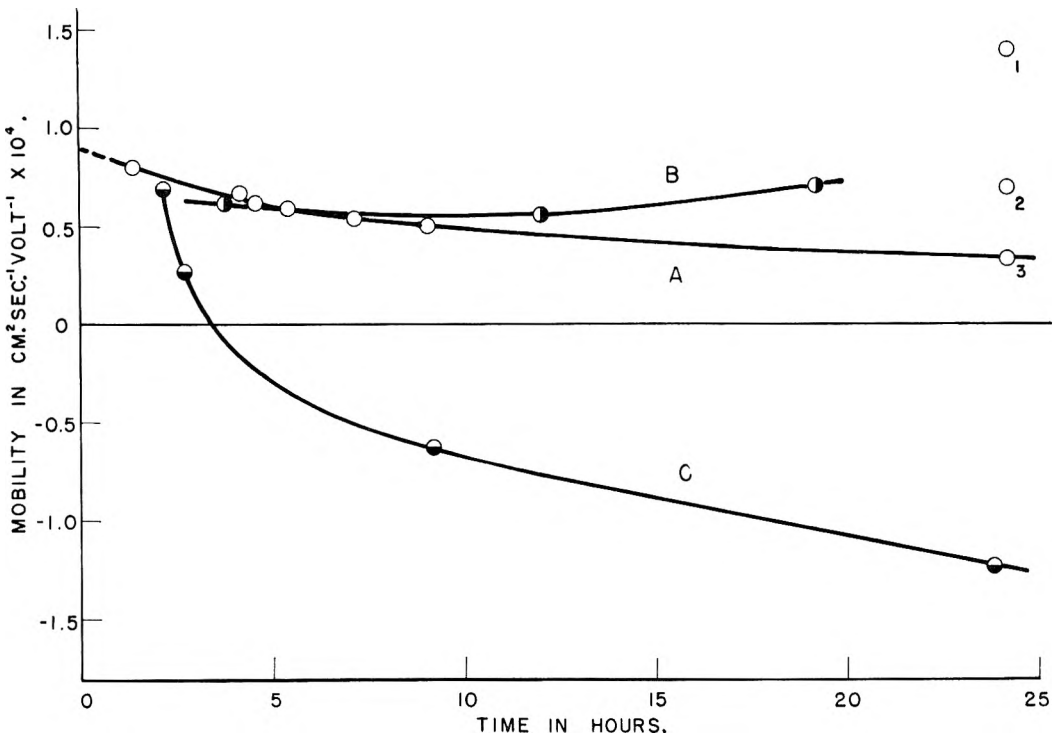

Fig. 3.—Variation of mobility with time in growing sols; initial, concentration given. Sol A (data from 7 sols). HCl 0.0020 M, $Na_2S_2O_3$ 0.0020 M. O_1, sample from top of volumetric flask; O_2, sample from middle of flask; O_3, contents of flask shaken before taking sample. B (data from 2 sols). HCl 0.0030 M, $Na_2S_2O_3$ 0.0020 M. C (data from 2 sols). HCl 0.0020 M, $Na_2S_2O_3$ 0.0030 M.

they are growing, the mobility was measured without adjustment of the ionic strength or pH. The results as a function of time are shown in Fig. 3.

For sols in which the initial thiosulfate concentration is 0.002 M or less, the charge on the particles is positive and remains so for at least 24 hours. However, in a sol in which the initial thiosulfate concentration is 0.003 M (0.002 M H^+), the particles are positively charged during the first few hours of growth, and pass over to a negative charge which increases with time.

Data on particle number and radii as a function of time for these concentrations are to be found in ref. 1c, pp. 587–589, where a similar behavior was noted as a result of polythionate formation at higher thiosulfate concentrations. (See ref. 25, Table II, for recalculation of polythionate concentrations based on data of ref. 1c, using a better value of the second dissociation constant of H_2SO_3.)

TABLE II

EFFECT OF ADDITION OF SODIUM PENTATHIONATE ON THE ELECTROPHORETIC MOBILITY OF MONODISPERSE S HYDROSOL

Initial concentrations; HCl = 0.002 M; $Na_2S_2O_3$ = 0.002 M.

Time after mixing, hr.	r, μ	Added $Na_2S_5O_6 \times 10^5$, mole/l.	Mobility, cm.² v.⁻¹ sec.⁻¹
4	0.35	0	+0.65
4	.35	1	+ .26
4	.35	2	− .02
7	.42	4	− .53[a]

[a] Shifts to −0.71 in one-half hour following addition. Measurements made immediately after polythionate addition.

That positively charged particles could be produced in sols prepared from thiosulfate and acid is contrary to expectations based upon studies by all previous workers, of sols prepared from concentrated solutions of the same reagents. The negative charge on the particles of these concentrated sols has been attributed to pentathionate ion attached to the surface of the sulfur particles.[26]

Using acidimetric and iodine titrations Dinegar, Smellie and La Mer[25] have demonstrated that in these dilute sols the concentration of polythionate calculated as pentathionate was always less than 10^{-5} M within 24 hours after mixing the reagents. Since the pentathionate ion concentration is extremely small, other species can determine the charge in these dilute sols, H^+ ion is the predominant species, thus accounting for the positive charge observed on the particles.

Sodium pentathionate was prepared by the method of Kurtenacker and Fluss.[27] To samples of a sol prepared from 0.002 M H^+ ion and 0.002 M $S_2O_3^-$, sodium pentathionate in varying amounts was added so that final concentrations between 1–5 $\times$ 10^{-5} M were obtained. The results are shown in Table II.

In all cases the original positive mobility was immediately lowered. When the concentration of pentathionate was 2 $\times$ 10^{-5}, the mobility of a 4-hour sample was reduced from +0.65 $\times$ 10^{-4} cm.² volt^{-1} sec.$^{-1}$, its original value, to a small negative value. Other concentrations have a corresponding effect on the charge. The addition of pentathionate to a 7-hour sample immediately produced a

(25) R. H. Dinegar, R. H. Smellie and V. K. La Mer, *J. Am. Chem. Soc.*, **73**, 2050 (1951).

(26) C. H. Freundlich and P. Schulz, ref. 10; also ref. 12.

(27) A. Kurtenacker and W. Fluss, *Z. anorg. Chem.*, **210**, 125 (1933)

negative charge which increased with time. These experiments demonstrate that the concentration of pentathionate in the original sol never exceeded 10^{-5} M for at least 24 hours after mixing reagents.

When the pH of a sol containing positively charged particles was increased by addition of NaOH, the particles showed a decrease in charge, passed through an isoelectric point at pH 4, and then attained a negative charge at higher pH. Figure 4 shows the variation of mobility with pH for three sols. In these experiments the pH was varied by dropwise addition of 0.1 N sodium hydroxide to 50- or 100-cc. samples of the sol. The volume change was less than 2%, and ionic strength remains essentially constant up to pH 7–9. Buffer solutions were not used because of the danger of specific adsorption of anions in the buffer. The variation of mobility with pH is similar to that found for proteins and other amphoteric substances.

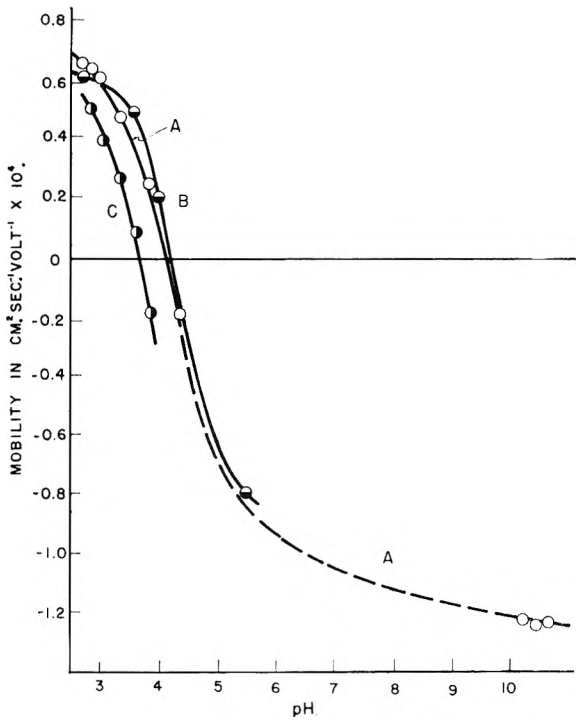

Fig. 4.—Variation of mobility with pH: A, 4-hour sol: HCl 0.0020 M, $Na_2S_2O_3$ 0.0020 M, particle radius 0.35 micron. B, 4-hour sol: HCl 0.0020 M, $Na_2S_2O_3$ 0.0010 M, particle radius 0.35 micron. C, 8-hour sol: HCl 0.0020 M, $Na_2S_2O_3$ 0.0020 M, particle radius 0.42 micron.

Other interpretations of this type of mobility–pH curve are possible. Competitive adsorption between a positive and a negative ion or an exchange process at the surface of the sulfur particles are possibilities. In any case hydrogen ion is fundamentally responsible for the production of a positive charge. Figure 5 shows the data of Fig. 4 (for pH values below 4) plotted as a_{H+}/u $vs.$ a_{H+}.

One of the sols definitely exhibits a linear dependence. The data for the other two sols are not sufficient to unequivocally demonstrate a linear dependence in these cases. An equation of the form $a_{H+}/u = \alpha + \beta a_{H+}$ could be interpreted by any one of the following assumptions: (1) The

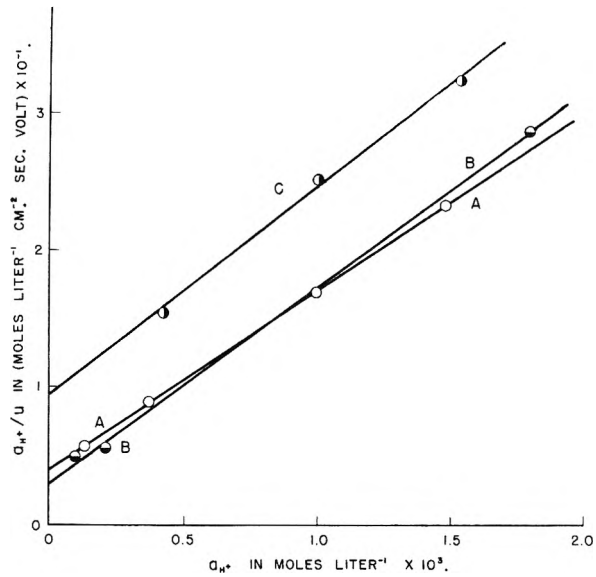

Fig. 5.—Data of Fig. 4 plotted as a_{H^+}/u $vs.$ a_{H^+}: a_{H^+} = activity of hydrogen ion in solution; u = mobility of particles.

charge is due to adsorption of H^+ ion. The amount of negative ions adsorbed is insignificant. (2) Hydrogen ion is transferred to the surface of the particle by a neutral carrier, such as weak acid. A neutral molecule could approach and interact with the surface of the particles with less difficulty than a hydrated proton. (3) An amphoteric substance resides at the surface of the particles.

To demonstrate that these interpretations lead to essentially equivalent expressions, it is necessary to find a relationship between electrophoretic velocity and surface charge by combining the fundamental equation of electrokinetics (eq. 1) with some form of the Debye–Hückel theory. The validity of this procedure is dependent upon a number of factors, which have been treated in detail by Overbeek.[7,8]

When the electrokinetic potential (ζ) is very small[7]

$$Q = D\zeta a(1 + \kappa a) \qquad (4)$$

where

Q = charge on particle
D = dielectric constant
ζ = zeta potential
a = radius of the particle

and κ is the characteristic thickness of the ionic atmosphere.

For the sols considered here $\kappa \sim 2.5 \times 10^6$ cm.$^{-1}$, the radius of the particles is about $0.4\ 10^{-4}$ cm. and the value of κa is 100. In this case $\kappa a >> 1$ and

$$Q = D\zeta\kappa a^2 \qquad (5)$$

For a spherical particle, surface area $= 4\pi a^2$ and the surface charge density σ, when $\kappa a >> 1$ is given by

$$\sigma = D\zeta\kappa/4\pi \qquad (6)$$

When κa is very large, the relation between ζ and mobility is correctly given by eq. 1.[7] Therefore

$$v = \sigma X/\kappa\eta \qquad (7)$$

and the velocity in terms of unit potential gradient, u, is given by

$$u = \sigma/\kappa\eta \qquad (8)$$

Considering the possibility of adsorption, the amount of H^+ adsorbed per unit area will be proportional to the charge density.

By employing the Langmuir adsorption isotherm

$$\sigma = \frac{Aa_{H^+}}{1 + Ba_{H^+}} \text{ and } u = \frac{1}{\kappa\eta}\left[\frac{Aa_{H^+}}{1 + Ba_{H^+}}\right] \qquad (9)$$

A and B are constants. This gives upon rearrangement

$$\frac{a_{H^+}}{u} = \alpha + \beta a_{H^+} \qquad (10)$$

where

$$\alpha = \kappa\eta/A \text{ and } \beta = \kappa\eta B/A$$

In case 2 a mechanism is considered whereby neutral molecules of a weak acid can transfer H^+ ion to the surface of the particles. This may be formulated as follows

$$S + HA \rightleftarrows SH^+ + A^-$$

$$\frac{[SH^+][A^-]}{[S][HA]} = K$$

Here

$[S]$ = surface concn. of sites on particle
$[SH^+]$ = surface concn. of positive charges
$[HA]$ = concn. of weak acid molecules in soln.
$[A^-]$ = concn. of A^- ions in soln.

Let $[S]_0$ = the concentration of sites on the bare surface, which will be a constant for the same surface material. Then

$$[S] = [S]_0 - [SH^+]$$

$$\frac{[SH^+][A^-]}{([S]_0 - [SH^+])[HA]} = K$$

and

$$[SH^+] = \frac{K[S]_0[HA]}{[A^-] + K[HA]}$$

Letting $[T]$ = total concentration of weak acid, and using the relations

$$[T] = [HA] + [A^-]$$

and

$$\frac{[H^+][A^-]}{[HA]} = K_1$$

it can be shown that

$$[HA] = \frac{[T][H^+]}{K_1 + [H^+]}$$

and

$$[A^-] = \frac{K_1[T]}{K_1 + [H^+]}$$

and

$$[SH^+] = \frac{K[S]_0[H^+]}{K_1 + K[H^+]}$$

Identifying $[SH^+]$ with σ and using eq. 8

$$u = \frac{1}{\kappa\eta}\left[\frac{K'[S]_0a_{H^+}}{K_1 + K'a_{H^+}}\right]$$

In the third case, it may be assumed that the amphoteric substance on the surface is a neutral (adsorbed) molecule which reacts as follows

$$A + H^+ \rightleftarrows AH^+$$

$$A \rightleftarrows B^- + H^+$$

where

A denotes neutral molecules at the surface
H^+, the hydrogen ion in solution
AH^+, the positively charged surface complex, and
B^-, the negative ions on surface produced by dissociation of A

If the concentration of B^- is negligible, then the charge is given by the concentration of AH^+. This is similar to case 1 and leads to eq. 10.

In Fig. 5, sol A exhibits a linear relationship. The data for sols B and C also seem to be linear, but the data for sols B and C are not yet sufficient to establish whether or not the behavior is in complete conformity with eq. 10. The mobility values for sol C are considerably lower than those of sols A and B for all pH values studied. The difference between the mobility values of sols A and C is essentially the same at all pH values between 2.7 and 3.9, and the isoelectric point for sol C is lower by about 0.4–0.5 pH unit than the isoelectric point of sol A. Since the ionic strengths of these two sols are the same within 2%, the lower mobilities and the lower isoelectric point for sol C cannot be reasonably accounted for by any factor, except possibly the specific adsorption of a significant amount of a negative ion, thus reducing the effective positive charge. In sol C the samples were taken after eight hours of growth, compared with four hours for sol A. In sol C the total sulfite concentration and the particle radius are greater than in sol A. If polythionates were also formed in the chemical reaction, the amount present after eight hours of sol growth, although very small, might be sufficient to cause a reduction in the positive mobility of the particles as compared to those of sol A. Some adsorption of bisulfite ion, due to the presence of a greater concentration of this ion in solution after eight hours, may also be a possibility. Further consideration is given to the influence of certain negatively charged species in the sections which follow.

Mobility Measurements at High pH.—A few minutes after the adjustment of the pH of sol A to pH 10.4 the mobility was found to have a value of -1.2×10^{-4} cm.^{2} volt^{-1} sec.$^{-1}$ (Fig. 4). However, the negative mobility decreased more rapidly with time (Fig. 6), than can be attributed to the decreases in pH (less than 0.1 unit in 45 minutes). Other measurements between pH 10.3 and 10.7 showed that the mobility was the same immediately after pH adjustment.

A reasonable explanation for this behavior is that $SO_3^=$ ion is the charging species at high pH. Dinegar and Smellie[13] have demonstrated that at pH $\cong$ 4 the growth of the particle ceases; instead they dissolve at a rate dependent upon the pH. They have shown that the dissolution of the particles is related to the diffusion of $SO_3^=$ ion to the surface. The primary reaction producing sulfur

$$S_2O_3^= + H^+ = S + HSO_3^-$$

is reversed above pH 4 by the reaction

$$S + SO_3^= = S_2O_3^=$$

Since the last reaction consumes $SO_3^=$ ion, the variation of mobility can be ascribed to a reduction of the concentration of this ion leading to a corre-

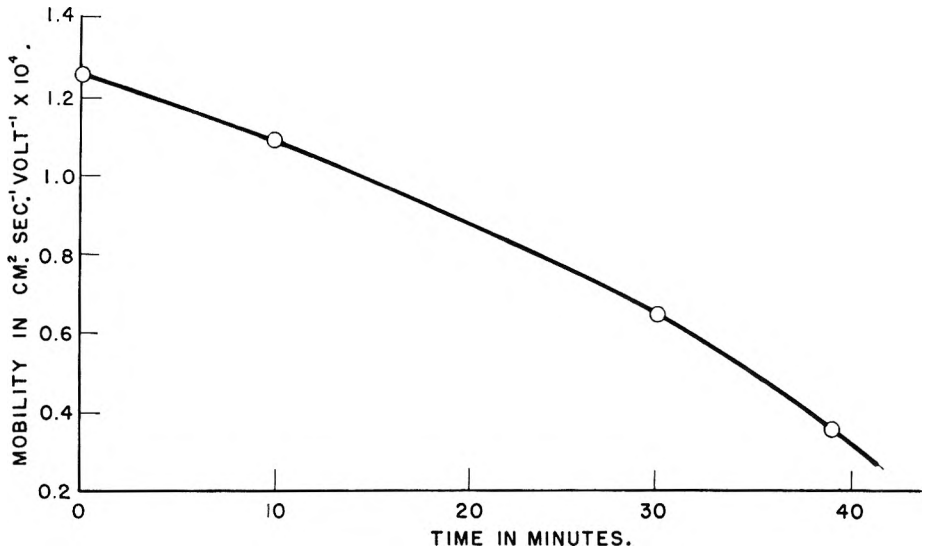

Fig. 6.—Variation of negative mobility with time after first observation following adjustment of *p*H to 10.47, for a 4-hour sol prepared as in A, Fig. 4.

sponding reduction of the concentration on the surface of the particles.

It can be shown that any reduction in mobility due to changes in size alone would be small, since the radius decreased from 0.35 to about 0.2 μ, corresponding to a change in mobility of less than 10%.[7,20]

Sols in which the Charge Becomes Negative during Growth.—In the case of a sol prepared from 0.002 *M* HCl and 0.003 *M* sodium thiosulfate, the initial positive charge on the particles changes to a negative charge within a few hours. This behavior might be associated with the production of some species, such as polythionate, in sufficient quantity to cause charge reversal. In sol A, Fig. 3, the charge decreases with time but the sign is not reversed. Experiments cited (Table II) have shown that added pentathionate ion can produce reversal of charge. However, this does not prove that the species responsible for reversal (or reduction) is pentathionate ion.

Preliminary experiments in which sodium sulfite was added to the sols (at *p*H 2.7–2.9) showed no appreciable effect on the original mobility of the particles indicating lower adsorption for HSO_3^- as contrasted with $SO_3^=$.

The rate of adsorption may be very important when ions are added to the sols. Equilibrium may not be established immediately and studies as a function of time should be made. This is especially true when the concentrations are in the order of 10^{-5} *M*. During the growth of particles the relative rates of production and/or adsorption of charging species may be changing so that equilibrium may not be established with respect to particle charge.

The Effect of Agar.—While experimenting with agar gel barriers in the electrophoresis cell, it was found that a negative charge was produced on particles of a sol in which the charge was originally positive. The direct addition of agar to the sols produces the same effect. The mobility was reduced in all cases to the same value -1.2×10^{-4} for several sols of different age and particle size. The agar evidently coats the particles producing a uniform negative charge. No change in the original mobility was observed with gelatin barriers.

II. Alcohol–Sulfur–Water and Acetone–Sulfur–Water Sols.—In sols prepared by adding water to alcohol or acetone solutions of sulfur which had been heated, the particles had isolectric points at *p*H values between 5.8 and 6.0. At higher *p*H values the particles exhibited large negative mobilities which increased with increasing *p*H. At *p*H values below about 6 the charge was positive. The mobilities at *p*H 2.7 were 1.78 for an alcohol–water sol and 1.74 for an acetone–water sol in 10^{-4} unit.

However, in sols prepared by dissolving sulfur in cold absolute alcohol and adding water the charge on the particles was negative even at *p*H 2.7. Potentiometric titration of these sols having positively charged particles indicated the presence of a weak acid. Acetic acid was suspected as responsible for the positive charge.

To test this assumption, sols were prepared by dissolving sulfur in absolute alcohol solution in the cold, diluting with water, HCl was then added to a final *p*H of 2.76. The measured mobility of -0.88×10^{-4} unit remained constant for more than an hour. Another sol was prepared in which 0.05 mole/l. of acetic acid was also added (*p*H = 2.75). The particles now had a positive charge with a mobility of 10^{-4} unit. (See Table III for summary of results.)

TABLE III

ALCOHOL–WATER HYDROSOLS. EFFECT OF METHOD OF PREPARATION

Preparation	*p*H	10^4 mobility, cm.² volt⁻¹ sec.⁻¹
Alcohol heated	6.0	Zero-isoelectric
	2.7	+1.78
	6.9	−1.3
Alcohol cold	2.7	Negative
	2.76	−0.88
	2.75	+1.0[a]
Mechanically dispersed sulfur	2.7	Zero[31]

[a] Acetic acid (0.05 *M*) added.

The mobility should be dependent upon the conductivity of the particles as compared to that of the liquid.[20] In several instances the mobility was lower when the sulfur particles were formed in a solution containing HCl (*p*H 2.7) than in the case where the HCl was added after the sol had been formed. The drop in mobility of about 40% may be due to incorporation of ions within the particles, thus increasing their conductivity. All sols compared exhibited the same bulk conductivity and *p*H.

According to Henry,[20] the electrophoretic mobility is related to the conductivity of the liquid K, and to the conductivity of the particles K' in the following manner for spherical particles

$$v = \frac{3K}{2K + K'} \times \frac{XD\zeta}{6\pi\eta}$$

The quantities D, X, ζ and η have the same meaning as in eq. 1.

This equation becomes identical with eq. 1 if $K >> K'$. If $K\zeta$ is comparable to K, the mobility will be reduced. The relatively low mobilities of sulfur particles in a dilute thiosulfate–acid sol may be due at least in part to the conductivity of the particles themselves. Pauli[12] claims that his particles consist of drops of supercooled liquid sulfur mixed with thiosulfuric acid[1,12] and possible water. If the surfaces of the particles are polarized, they should behave as insulators.[28] Emulsions of water (containing electrolytes) in organic solvents showed zero or extremely low mobilities.[29] In these cases the specific conductance of the water droplets is much greater than that of the organic liquid, *i.e.*, $K' >> K$, and therefore v is very small.

In the positively charged alcohol–sulfur–water and acetone–sulfur–water sols a plot of a_{H^+}/u *vs.* a_{H^+} (for *p*H values below 5) is linear. The data of Hazel and Ayers[30] for a hydrous ferric oxide sol are also linear when plotted in the same way for *p*H values below 8. The isoelectric point for this sol is approximately *p*H 8.6. Some of their data are plotted on Fig. 7. A plot of $-$(log intercept of eq. 10) *i.e.*, $-\log \alpha$ *vs.* (*p*H of the isoelectric point) is linear for thiosulfate–acid, alcohol–sulfur–water sols and the data of Hazel and Ayers[30] for a hydrous ferric oxide sol. A plot of (slope of eq. 10)$^{-1}$ *i.e.*, β^{-1} *vs.* (*p*H of the isoelectric point) is also essentially linear (Fig. 8).

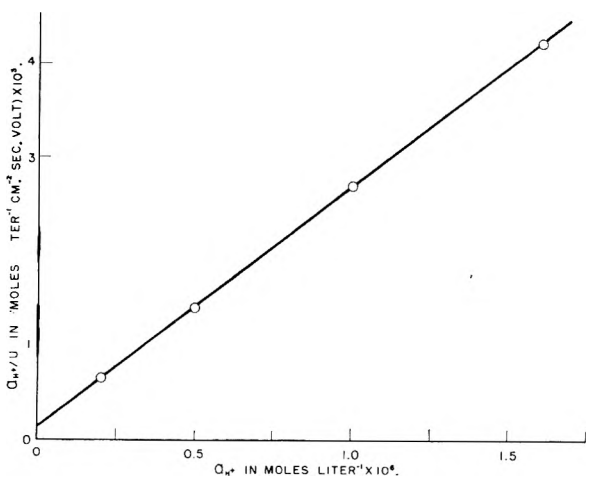

Fig. 7.—Plot of c_{H^+}/u *vs.* a_{H^+} for the data of Hazel and Ayers for a hydrous ferric oxide sol.

Miscellaneous Observations.—In sols prepared from thiosulfate and acid the mobility of the particles was dependent upon the position in the flask from which the sample was taken. After a period of about 20 hours, mobilities of particles in samples taken from the top of the flask differed considerably from the mobilities in samples taken from the bottom. Shaking the flask to redistribute the particles produced a uniform charge on their surface, since the particles now exhibited the same mobility.

Observations of mobility near the isoelectric point showed particles both positively and negatively charged. These particles could be made to collide and sometimes stick together by careful manipulation in the electrophoresis cell.

Sols in which the charge on the particles reverses during growth exhibited some coagulation ten or more hours after the charge reversal. In several cases as many as five or six elementary particles were joined together. These combinations exhibited no charge. Binary combinations of elementary particles were observed in large numbers. These combinations showed a lower mobility than the elementary particles.

V. Conclusion.—The isoelectric point of mechanically dispersed rhombic sulfur is at a *p*H of approximately 2.7.[31] Obviously, since the particles in the dilute thiosulfate–acid sols are positively charged at this *p*H and the isoelectric point is at a *p*H of approximately 4, the surfaces in each case cannot be the same. It seems likely, therefore, that the production of a positive charge on the surface of dilute monodisperse particles is not due to hydrogen ion adsorption alone but involves one of the other possible mechanisms discussed under "Acid–Thiosulfate Sols." The fact that acetic acid is necessary to produce a positive charge in sols prepared from alcohol–sulfur solutions and water lends support to an exchange mechanism by means of the weak acid molecule. If this mechanism were operative in the dilute thiosulfate–acid sols, the weak acid, H_2SO_3, could be responsible for depositing H^+ ion on the particles below *p*H 4.

Meyer[32] found that dilute selenium hydrosols prepared from sodium selenosulfate were positively charged at acid *p*H values and negatively charged in the alkaline *p*H region. The behavior of these sols is similar to that described here and indicates that in this case also no strongly adsorbable negative ions are present at acid *p*H values.

Since sulfites are produced in the reaction between the selenosulfate and H^+ ions, sulfurous acid will also be present. The exchange mechanism might also be possible in this case. Further information could be obtained by studying the effect of weak acids with different dissociation constants at constant ionic strength. The value of the dissociation constant should influence the magnitude of

(28) H. Bull and K. Sollner, *Kolloid-Z.*, **60**, 263 (1932).
(29) A. Gyamant, *Z. physik. Chem.*, **102**, 74 (1922).
(30) F. Hazel and G. H. Ayers, THIS JOURNAL, **35**, 2931 (1931).
(31) J. Perrin, *J. chim. phys.*, **2**, 601 (1904).
(32) J. Meyer, *Z. Elektrochem.*, **25**, 80 (1919).

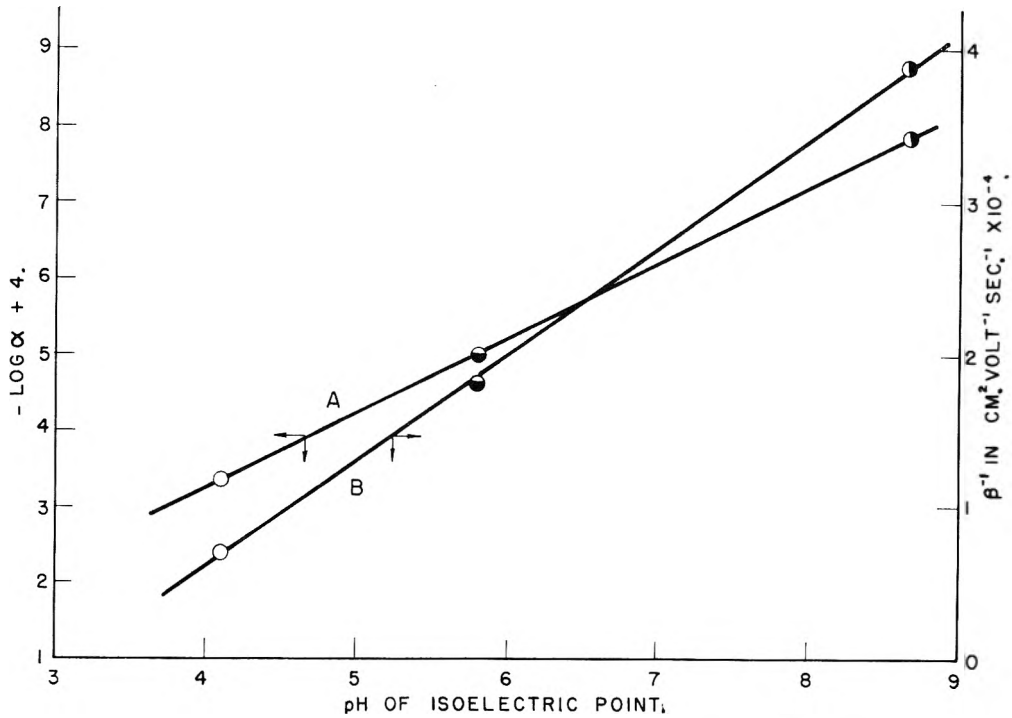

Fig. 8.—Shows a plot of $-\log \alpha$ *vs.* (*p*H of the isoelectric point) (line A) and a plot of β^{-1} *vs.* (*p*H of the isoelectric point) (line B). ○, data of sol A (Fig. 5); ◒, data of alcohol–sulfur–water sol containing acetic acid; ◑, data of Hazel and Ayers (Fig. 7).

the mobility in the acid *p*H region as shown by the theoretical developments under "Acid–thiosulfate." If weak acids with about the same values for the dissociation constant are chosen, the effect of the respective anions may be determined.

Pauli[12] has taken exception to the belief that pentathionate ion is responsible for the production of a negative charge in the more concentrated thiosulfate–acid sols. He considers that thiosulfate ion is responsible for this charge. The present investigation demonstrates that his view is not correct. The addition of very small amounts of pentathionate ion (2×10^{-5} *M*) to dilute sols reverses the charge. However, the thiosulfate concentration is 2×10^{-3} *M* yet a positive charge on the particles is observed. It is demonstrated in the present investigation that, when pentathionate is present, it will be more effective than thiosulfate in determining the charge on the particles.[33,34]

(33) M. Choucroun, private communication.

(34) H. V. Tartar and H. H. Garretson, *J. Am. Chem. Soc.*, **63**, 808 (1941).

THE STATISTICAL MECHANICAL BASIS OF THE DEBYE–HÜCKEL THEORY OF STRONG ELECTROLYTES

By John G. Kirkwood and Jacques C. Poirier

Contribution No. 1209 from the Sterling Chemistry Laboratory, Yale University, New Haven, Connecticut

Received April 19, 1954

The potentials of mean force of sets of *n* ions, averaged over the configuration space of all other ions in the system, are expanded as power series in a charging parameter ξ. Equations are derived relating coefficients of the various powers of ξ in these expansions, using the method of semi-invariants. The validity of the linearized Poisson–Boltzmann equation for the coefficient of the first power of ξ in the expansion of the potential of mean force of an ion pair, when ion size is neglected, is demonstrated. The validity of the Debye–Hückel limiting law is thus shown in an unambiguous way. A systematic procedure of obtaining the coefficients of higher powers of ξ is outlined. When ion size is considered, the linearized integral equation for the potential of average force of a pair of ions possesses oscillating solutions at high ionic strength, corresponding to stratifications of average space charge of alternating sign in the neighborhood of each ion.

Introduction

The Debye–Hückel[1] theory of solutions of strong electrolytes remains one of the outstanding achievements of modern theoretical chemistry. Not only does it provide a general understanding of the unique aspects of electrolyte solutions, arising from the long range Coulomb forces between the ions, but all experimental evidence appears to confirm its limiting laws, as the ionic strength approaches zero, as rigorously exact quantitative relationships. However, although the validity of limiting laws is

(1) P. Debye and E. Hückel, *Physik. Z.*, **24**, 185 (1923).

seldom seriously questioned any longer, their precise theoretical foundation leaves something to be desired. As R. H. Fowler[2] pointed out, the Poisson–Boltzmann equation on which the Debye–Hückel theory is based is not consistent with the exact principles of statistical mechanics, and this is reflected in the failure of the mean electrostatic potentials calculated by the theory to satisfy the conditions of integrability as functions of the ionic charges. Nevertheless, the solutions of the linearized Poisson–Boltzmann equation, upon which the limiting laws are based, do satisfy the conditions of integrability, which is presumptive evidence that only the non-linear terms are in error. Onsager[3] and Kirkwood[4] carried out detailed analyses of the problem along similar lines and reached a provisional conclusion that departures from the principle of superposition, upon which the Poisson–Boltzmann equation is based, lead to errors in the potential of mean force between an ion pair, which is of the same order in the ionic charges as the non-linear terms in the Poisson–Boltzmann equation. The principle of superposition states the average force acting upon a third ion in the neighborhood of an ion pair is the sum of the average forces which would act upon it if each ion of the pair were present alone. Their arguments, justifying the validity of the linearized Poisson–Boltzmann equation and the limiting laws, were, however, incomplete in the sense that it was necessary to employ the principle of superposition in order to estimate the error introduced into the Poisson–Boltzmann equation by departures from superposition. Therefore, it was only demonstrated that the use of the approximate principle of superposition was consistent with the rigorous validity of the linearized Poisson–Boltzmann equation, not that this equation was in fact valid. More recently, Mayer[5,6] has presented a theory of strong electrolytes, based upon a cluster development of the partition function of the type used in the theory of imperfect gases and solutions. After forcing converge of the cluster sums with factors $e^{-\alpha R}$ in the Coulomb potentials of the ions, he was able to obtain the Debye–Hückel limiting law by the summation of selected terms in the cluster development, corresponding to ring graphs alone. However, explicit proof that clusters corresponding to graphs of more complex topological types do not contribute terms of the same order as the limiting law is, to say the least, not transparent and obvious.

For these reasons, it seemed to us worthwhile to re-examine the statistical mechanical basis of the Debye–Hückel theory by means of a systematic development of the potentials of average force in sets of n ions, in power series in the ionic charging parameters, along the lines of the earlier work of Onsager and Kirkwood. In this manner, we shall be able to demonstrate the validity of the linearized Poisson–Boltzmann equation for the coefficient of the first power of the development of the potential of average force of an ion pair in a power series in the charging parameter of either ion, when ion size is neglected, and thus to demonstrate the validity of the Debye–Hückel limiting law in an unambiguous fashion. A systematic method for determining the coefficients of higher powers of the charging parameters is outlined. When ion size is taken into account in a symmetrical manner for both ions of a pair, the linearized integral equation for the potential of average force cannot be converted into a Poisson–Boltzmann equation, but is equivalent to a differential-difference equation which possesses oscillating solutions at high ionic strength, corresponding to stratifications of average space charge of alternating sign in the neighborhood of each ion, simulating the types of radial distribution to be expected in concentrated solutions and in molten salts.

I.

We shall find it profitable to begin with a brief review of some of the general relationships between the excess electrical chemical potentials $\mu_\alpha^{(e)}$ of the ions of the several types $\alpha = 1...\nu$, present in an electrolyte solution, the mean electrostatic potential $\bar{\psi}_\alpha$ in the neighborhood of an ion of type α, carrying a fraction ξ_1 of its full charge, and the radial distribution functions $g_{\alpha\beta}^{(2)}$ of ion pairs, one of which carries a fraction ξ_1 of its full charge. The mean electrostatic potential $\bar{\psi}_\alpha(R)$ at a distance R from an ion of type α, satisfies the exact Poisson equation

$$\nabla^2\bar{\psi}_\alpha = -\frac{4\pi}{D}\sum_{\beta=1}^{\nu}\frac{N_\beta}{v}e_\beta g_{\alpha\beta}^{(2)}$$
$$g_{\alpha\beta}^{(2)} = e^{-W_{\alpha\beta}^{(2)}/kT} \qquad (1)$$

where $W_{\alpha\beta}^{(2)}$ is the potential of mean force acting on an ion pair of type $\alpha\beta$. Equation 1 is valid by definition of the radial distribution functions $g_{\alpha\beta}^{(2)}$, which are so defined that $N_\beta g_{\alpha\beta}^{(2)}/v$ is the average particle density of ions of type β at a distance R from an ion of type α. The excess electrical chemical potential may be determined in several equivalent ways.

$$\mu_\alpha^{(e)} = e_\alpha\int_0^1\bar{\psi}_\alpha(\xi_1)\mathrm{d}\xi_1 \qquad (2)$$

$$\mu_\alpha^{(e)} = \sum_{\beta=1}^{\nu}\frac{N_\beta}{v}\int_0^1\int V_{\alpha\beta}^{(1)}[g_{\alpha\beta}^{(2)}(\xi_1, R) - 1]\mathrm{d}v\mathrm{d}\xi_1$$

where $V_{\alpha\beta}^{(1)}$ is the electrostatic energy of an ion pair of type $\alpha\beta$, and the volume integral extends over all relative configurations of the pair, while the integrals over the charging parameter ξ_1, of one ion of the pair extend from zero to unity, all other ions in the system remaining fully charged (Guntelberg path). As alternative methods, the Debye charging process, in which all ions are charged simultaneously, may be employed, or the general expressions for the chemical potentials of the components of a solution of Kirkwood and Buff[7] may be used. If the exact potentials $\bar{\psi}_\alpha$ or radial distribution functions $g_{\alpha\beta}^{(2)}$ are employed, all methods of determining the chemical potential are consistent and lead to the same result. The Poisson–Boltzmann equa-

(2) R. H. Fowler, "Statistical Mechanics," Cambridge University Press, New York, N. Y., 1929, Chap. XIII.
(3) L. Onsager, *Chem. Revs.*, **13**, 73 (1933).
(4) J. G. Kirkwood, *J. Chem. Phys.*, **2**, 767 (1934).
(5) J. E. Mayer, *ibid.*, **18**, 1426 (1950).
(6) J. Poirier, *ibid.*, **21**, 965 (1953).
(7) J. G. Kirkwood and F. P. Buff, *ibid.*, **19**, 774 (1951).

tion of the Debye–Hückel theory is obtained from eq. 1 with the use of the approximation

$$W_{\alpha\beta}^{(2)} = e_\beta \psi_\alpha (R) \tag{3}$$

An analysis of the limit of validity of this approximation will be the special subject of this investigation.

II.

We suppose that the potential, V_N, of the intermolecular force acting on a system of N ions occupying a volume v may be expressed in the form

$$V_N = \sum_{\substack{i<j \\ =1}}^{N} V_{ij}(R_{ij})$$

$$V_{ij} = V_{ij}^{(0)} + V_{ij}^{(1)} \tag{4}$$

where $V_{ij}^{(0)}$ is the potential of the short range intermolecular force, van der Waals and repulsive, acting between the ion pair ij and $V_{ij}^{(1)}$ is the potential of the long range Coulomb force. If the system of ions is immersed in a solvent, for example water, the potential V_N is to be interpreted as the potential of mean force, arising both from other ions and the solvent molecules, averaged over all configurations of the solvent molecules in a canonical ensemble. The Coulomb potential $V_{ij}^{(1)}$ may be defined as

$$V_{ij}^{(1)} = \frac{e_i e_j}{D R_{ij}} \tag{5}$$

where e_i and e_j are the charges of the respective ions, R_{ij} the distance between them, and D the macroscopic dielectric constant of the solvent, if we agree conventionally to absorb effects of departures of the local dielectric constant from D in the short-range part $V_{ij}^{(0)}$ of the potential. That such departures contribute only short-range terms, diminishing more rapidly than R_{ij}^{-3} requires separate proof which will not be given here. We shall also neglect departures from superposition, implicit in eq. 4, arising from the polarization of each ion by the total electric field of all others.

We now assign to each ion i a charging parameter, ξ_i, ranging from zero to unity and introduce the potential $V_N(\xi_1 \ldots \xi_N)$ for the system, in which each ion carries the charge $\xi_i e_i$, a fraction ξ_i of its full value

$$V_N(\xi_1 \ldots \xi_N) = V_N^{(0)} + \sum_{\substack{i<j \\ =1}}^{N} \xi_i \xi_j V_{ij}^{(1)}$$

$$V_N^{(0)} = \sum_{\substack{i<j \\ =1}}^{N} V_{ij}^{(0)} \tag{6}$$

$$V_{ij}^{(1)} = e_i e_j / D R_{ij}$$

where $V_N^{(0)}$ is the potential of the short-range intermolecular forces.

The potential of mean force $W_N^{(n)}(1 \ldots n)$ for a set of n ions, averaged over the configuration space of the other $N - n$ ions is given by the theory of the canonical ensemble in the following form

$$e^{-\beta W_N^{(n)}(1 \ldots n)} = v^n \int^v \cdots \int^v e^{-\beta[A_N - V_N(\xi)]} \prod_{j=n+1}^{N} dv_j \tag{7}$$

$$\beta = 1/\kappa T$$

where the integration extends over the configuration space of the residual set of $N - n$ ions, and it is understood that $W_N^{(n)}$, A_N and V_N depend upon the charging parameters ξ_j of eq. 6. For brevity, the coördinates of the n ions are denoted by 1, 2, . . n. Properly the potentials of average force should be labeled with the ion types of the set n. However, to avoid excessive complication in notation, this labeling will be introduced explicitly only in our final equations. We now select any one of the ions, say ion 1, of the set n and write

$$A_N - V_N = A_N(0) - V_N(0) + \mu_1^e - \xi_1 \sum_{j=2}^{n} \xi_j V_{ij}^{(1)} - \xi_1 V_{1,N-n}^{(1)}$$

$$V_{1,N-n}^{(1)} = \sum_{j=n+1}^{N} \xi_j V_{ij}^{(1)} \tag{8}$$

where $A_N(0)$ and $V_N(0)$ are the Helmholtz free energy and potential of intermolecular force when ξ_1 is equal to zero, ion 1 uncharged, μ_1^e the electrostatic contribution to the chemical potential of ion 1, equal to $A_N - A_N(0)$, and $V_{1,N-n}^{(1)}$ is the electrostatic energy arising from the interaction of fully charged ion 1 and the $N - n$ ions of the residual set. Introduction of eq. 8 into eq. 7 leads to the expression

$$e^{-\beta W_N^{(n)}(1 \cdots n)} = e^{\beta\left[\mu_1^e - W_N^{(n,0)}(1 \cdots n) - \xi_1 \sum_{j=2}^{n} \xi_j V_{ij}^{(1)}\right]} \langle e^{-\beta \xi_1 V_{1,N-n}^{(1)}} \rangle_{\xi_1 = 0}$$

$$e^{-\beta \mu_1^e} = \langle e^{-\beta \xi V_{1,N-1}^{(1)}} \rangle_{\xi_1 = 0}$$

$$\langle e^{-\beta \xi_1 V_{1,N-n}^{(1)}} \rangle_{\xi_1 = 0} = \frac{\int^v \cdots \int^v e^{-\beta \xi_1 V_{1,N-n}^{(1)}} e^{-\beta[A_N(0) - V_N(0)]} \prod_{j=n+1}^{N} dv_j}{\int^v \cdots \int^v e^{\beta[A_N(0) - V_N(0)]} \prod_{j=n+1}^{N} dv_j} \tag{9}$$

where $W_N^{(n,0)}(1 \ldots n)$ is the potential of average force acting on the set n, when ion 1 is discharged, $\xi_1 = 0$, and the averages are to be calculated in an ensemble in which ion 1 is discharged.

By the theory of semi-invariants,[8,9] we may write

$$\langle e^{-\beta \xi_1 V_{1,N-n}^{(1)}} \rangle_{\xi_1 = 0} = e^{\sum_{s=1}^{\infty} \frac{(-\beta \xi_1)^s}{s!} \Lambda_s^{(n)}}$$

$$\sum_{r=1}^{s} \binom{s-1}{r-1} \Lambda_s^{(n)} M_{r-s}^{(n)} = M_s^{(n)}; \quad s = 1, \cdots \infty$$

$$M_s^{(n)} = \frac{\int^v \cdots \int^v [V_{1,N-n}^{(1)}]^s e^{\beta[A_N(0) - V_N(0)]} \prod_{j=n+1}^{N} dv_j}{\int^v \cdots \int^v e^{\beta[A_N(0) - V_N(0)]} \prod_{j=n+1}^{N} dv_j} \tag{10}$$

$$\Lambda_1^{(n)} = M_1^{(n)}$$

$$\Lambda_2^{(n)} = M_2^{(n)} - M_1^{(n)2}$$

$$\Lambda_3^{(n)} = M_3^{(n)} - 3M_2^{(n)}M_1^{(n)} + 2M_1^{(n)3}$$

where the quantities $M_s^{(n)}$ are the moments of $V_{1,N-n}^{(1)}$, the electrostatic energy of interaction of ion 1 with the $N - n$ ions of the residual set.

(8) H. Cramer, "Mathematical Methods of Statistics," Princeton University Press, Princeton, N. J., 1946, p. 185.

(9) A similar expansion recently has been used by R. W. Zwanzig in the formulation of a general statistical mechanical perturbation theory, *J. Chem. Phys.* (in press).

Equations 9 and 10 lead to the following expressions for the potentials, $W_N^{(n)}$

$$W_N^{(n)}(1 \ldots n) = W_N^{(n,0)}(1 \ldots n) + \xi_1 \sum_{j=2}^{n} \xi_j V_{1j}^{(1)} + \sum_{s=1}^{\infty} \frac{(-\beta)^{s-1}}{s!} \xi_1^s [\Lambda_s^{(n)} - \Lambda_s^{(1)}] \quad (11)$$

as power series in the charging parameter ξ_1 of ion 1. Therefore, we may write

$$W_N^{(n)}(1 \ldots n) = W_N^{(n,0)}(1 \ldots n) + \sum_{s=1}^{\infty} \xi_1^s W_N^{(n,s)}(1 \ldots n)$$

$$W_N^{(n,s)}(1 \ldots n) = \frac{(-\beta)^{s-1}}{s!} [\Lambda_s^{(n)} - \Lambda_s^{(1)}] + \delta_{s1} \sum_{j=2}^{n} \xi_j V_{1j}^{(1)} \quad (12)$$

$$\delta_{s1} = \begin{cases} 1 s = 1 \\ 1 s = 0 \end{cases}$$

as the desired power series. Although the quantities $\Lambda_s^{(n)}$ do not converge individually for Coulomb forces, they may be made to converge by replacing $1/R_{ij}$ by $e^{-\alpha R_{ij}}/R_{ij}$ where α is a positive real number. The differences $\Lambda_s^{(n)} - \Lambda_s^{(1)}$ do converge in the limit $\alpha = 0$, and are properly defined as such limits.

We now proceed to consider the first of the set of eq. 12, determining $W_N^{(n,1)}(1 \ldots n)$, the coefficient of the linear term in ξ_1, which assumes the form

$$W_N^{(n,1)}(1 \ldots n) = \sum_{j=2}^{n} \xi_j [V_{1j}^{(1)} - \bar{V}_{1j}^{(1)}] + \sum_{j=n+1}^{n} \frac{\xi_j}{v} \int^v V_{1j}^{(1)} [e^{-\beta[W_N^{(n+1,0)}(1..nj) - W_N^{(n,0)}(1..n)] - e^{-\beta W_N^{(2,0)}(1j)}}] dv_j$$

$$\bar{V}_{1j}^{(1)} = \frac{1}{v} \int^v V_{1j}^{(1)} e^{-\beta W_N^{(2,0)}(1j)} dv_j \quad (13)$$

The effect of the short-range interactions of uncharged ion 1 with the other ions of the system may be taken into account by a Mayer cluster expansion, which with the neglect of terms of order $1/v$, yields

$$W_N^{(n+1,0)}(1 \ldots nj) = W_{N-1}^{(n)}(2 \ldots nj) + \sum_{l=j,2}^{n} V_{1l}^{(0)} \quad (14)$$

where $W_{N-1}^{(n)}(2 \ldots nj)$ is the potential of average force acting on the set of n ions, $2 \ldots nj$, in a system of $N - 1$ ions, from which ion 1 is absent. With the neglect of short-range cluster contributions, we may therefore write eq. 13 in the form

$$W_N^{(n,1)}(1 \ldots n) = \sum_{j=2}^{n} \xi_j [V_{1j}^{(1)} - \bar{V}_{1j}^{(1)}] + \sum_{j=n+1}^{n} \frac{\xi_j}{v} \int^v V_{1j}^{(1)} e^{-\beta V_{1j}^{(0)}} \times [e^{-\beta[W_{N-1}^{(n)}(2..nj) - W_{N-1}^{(n-1)}(2..n)]} - 1] dv_j \quad (15)$$

If we now expand $W_{N-1}^{(n)}(2 \ldots nj)$ in the power series

$$W_{N-1}^{(n)}(2 \ldots nj) = W_{N-1}^{(n,0)}(2 \ldots nj) + \xi_j W_{N-1}^{(n,1)}(2 \ldots nj) + 0(\xi_j^2)$$

$$W_{N-1}^{(n,0)}(2 \ldots nj) = W_{N-2}^{(n-1)}(2 \ldots n] + \sum_{l=2}^{n} V_{jl}^{(0)} \quad (16)$$

in the charging parameter ξ_j of ion j and ignore terms $W_N^{(n)} - W_{N-1}^{(n)}$ and $W_{N-1}^{(n-1)} - W_{N-2}^{(n-1)}$, which bear a ratio of order $1/N$ to terms retained, we obtain the following integral equations

$$W_N^{(n,1)}(1 \ldots n) = \sum_{j=2}^{n} \xi_j (V_{1j}^{(1)} - \bar{V}_{1j}^{(1)}) + \sum_{=n+1}^{n} \frac{\xi_j}{v} \int^v V_{1j}^{(1)} e^{-\beta V_{1j}^{(0)}} \left[e^{-\beta \xi_j W_N^{(n,1)}(2..nj) - \beta \sum_{l=2}^{n} V_{jl}^{(0)}} - 1 \right] dv_j \quad (17)$$

which are valid with the neglect of terms of the order $\xi_j^2 W_N^{(n,2)}$ in the exponential of the integrand on the right-hand side of eq. 12. If the short-range intermolecular forces are idealized as those acting between rigid spheres of equal diameter a, and the charging parameters ξ_j are subject to the restraint of electro-neutrality, $\sum_{j=1}^{N} \xi_j e_j = 0$, eq. 17 simplifies to the form

$$W_N^{(n,1)}(1 \ldots n) = \sum_{j=2}^{n} \xi_j V_{1j}^{(1)} + \sum_{j=n+1}^{N} \frac{\xi_j}{v} \int_{\omega_n}^{v} V_{1j}^{(1)} [e^{-\beta \xi_j W_N^{(n,1)}(2..nj)} - 1] dv_j \quad (18)$$

where the region ω_n, bounded by n spheres of radius a, concentric with each of the ions of the set n, is excluded from the domain of integration over the coördinates of each ion j of the residual set, $N - n$. Although there is no difficulty in principle in treating more complicated short-range forces, we shall henceforth restrict ourselves to the case of rigid spheres for the sake of simplicity. If the size of ion 1 is neglected in eq. 18, and only ω_{n-1}, the region of repulsion of ions $2, \ldots n$, is excluded from the domain of integration of ion j, eq. 18 may be transformed into the Poisson–Boltzmann equation by taking the Laplacian of both sides

$$\nabla_1^2 W_N^{(n,1)} = -4\pi \sum_{j=n+1}^{N} \frac{\xi_j e_j}{Dv} e^{-\beta \xi_j W_N^{(n,1)}(12..n)} \quad (19)$$

However, neither eq. 18 nor eq. 19 with the neglect of the size of ion 1, is a valid equation for $W_N^{(n,1)}$, since terms of order $\xi_j^2 W^{(n,2)}$ have been discarded in the exponential appearing in the integrand on the right-hand side of eq. 15. We are therefore only justified in keeping linear terms in ξ_j the expansion of the exponential

$$e^{-\beta[W_{N-1}^{(n)}(2..nj) - W_{N-1}^{(n-1)}(2..n)]} = e^{-\beta \sum_{l=2}^{n} V_{jl}^{(0)}} [1 - \beta \xi_j W_{N-1}^{(n,1)}(2 \ldots nj) + 0(\xi_j^2)] \quad (20)$$

With the linearization of the exponential of eq. 18 according to eq. 20, we obtain the following linear integral equations for the $W_N^{(n,1)}$, valid to terms of the order of ξ_j^3 in the charging parameters of the ions of the residual set, $N - n$

$$W_N^{(n,1)}(1 \ldots n) = \sum_{j=2}^{n} \xi_j V_{1j}^{(1)} - \beta \sum_{j=n+1}^{n} \frac{\xi_j^2}{v} \int_{\omega_n}^{v} V_{1j}^{(1)} W_N^{(n,1)}(2 \ldots nj) dv_j \quad (21)$$

The linear equations 21 constitute a self-consistent set of integral equations, closed for each ion set n, while the non-linear equations, eq. 18, are inconsistent with the exact statistical mechanical theory in retaining some terms of order ξ_j^3 and higher, but not all, since terms of the order $\xi_j^3 W_N^{(n,2)}$ are neglected. This does not mean that the non-linear equations 18 and 19 may not provide a useful approximation, but accounts for the fact that their solutions fail to satisfy the rigorous criterion of integrability.

In order to proceed to the next higher approximation, terms in $W_N^{(n,2)}$ and $W_N^{(n,1)^2}$ must be retained in the expansion of the exponential, eq. 20, and the second of eq. 12 must be employed to determine $W_N^{(n,2)}$

$$W_N^{(n,2)}(1 \ldots n) = -$$
$$\frac{\beta}{2}\sum_{j=n+1}^{N}\frac{\xi_j^2}{v}\int_{\omega n} V_{1j}^{(1)2}[e^{-\beta[W_N^{(n)}(2..nj)-W_N^{(n-1)}(2\cdots n)]}-1]\mathrm{d}v_j$$
$$-\frac{\beta}{2}\sum_{\substack{j\neq j'\\=n+1}}^{N}\frac{\xi_j\xi_{j'}}{v^2}\int_{\omega n}\int_{\omega n} V_{1j}^{(1)}V_{1j'}^{(1)}[e^{-\beta\,W_N^{(n+1)}(2..njj')}- W_N^{(n-1)}(2..n)] - e^{-\beta W_N^{(2)}(jj')}]\mathrm{d}v_j\mathrm{d}v_{j'} \quad (22)$$
$$+\frac{\beta}{2}[W_N^{(n,1)}(1\ldots n)-\sum_{j=2}^{n}\xi_j V_{1j}^{(1)}]^2$$

where terms of negligible order have been neglected and the short-range forces are assumed to be those between rigid spheres as in eq. 18 and 21. A rather tedious analysis leads to the following approximation to $W_N^{(n,2)}$, valid to terms in ξ_j^4

$$W_N^{(n,2)}(1\ldots n) = \frac{\beta^2}{2}\sum_{j=n+1}^{N}\frac{\xi_j^3}{v}\int_{\omega n} V_{1j}^{(1)2}W_N^{(n,1)}(2\ldots nj)\mathrm{d}v_j \quad (23)$$

If terms to the order ξ_j^4 are retained in the expansion of the exponential in the integrand of eq. 17, and short-range forces are idealized as those between rigid spheres, eq. 14 becomes

$$W_N^{(n,1)}(1\ldots n) = \sum_{j=2}^{n}\xi_j V_{1j}^{(1)} \quad (24)$$
$$-\beta\sum_{j=n+1}^{N}\frac{1}{v}\int_{\omega n}\{\xi_j^2 V_{1j}^{(1)}W_N^{(n,1)}(2\ldots nj) - \xi_j^3 V_{1j}^{(1)}\left[\frac{\beta}{2}W_N^{(n,1)^2}-W_N^{(n,2)}\right]\}\mathrm{d}v_j$$

Simultaneous solution of eq. 23 and 24 would yield a consistent approximation to $W_N^{(n)}$ $(1\ldots n)$ to terms of order ξ_j^3, and would provide correct expression for the terms proportional to c log c in the excess chemical potential of an unsymmetrical electrolyte present in solution at concentration C. The solution of eqs. 23 and 24 will be reported in a later article. Extension of the method outlined to the determination of higher approximations to the potentials of mean force could be made in a systematic way, but would be lengthy and tedious.

We now return to the linear integral equations, eq. 21. The integrals on the right-hand converge in the limit of zero ion size a, and the equations become

$$W_N^{(n,1)}(1\ldots n) = \sum_{j=2}^{n}\xi_j V_{1j}^{(1)} -$$
$$\beta\sum_{j=n+1}^{N}\frac{\xi_j^2}{v}\int_{v} V_{1j}^{(1)}W_N^{(n,1)}(2\ldots nj)\mathrm{d}v_j \quad (25)$$

Equations 25 may be exactly solved by superposition in the following form

$$W_N^{(n,1)}(1\ldots n) = \sum_{j=2}^{n} w_N^{(n,1)}(1j)$$
$$w_N^{(n,1)}(1j) = \xi_j V_{1j}^{(1)} -$$
$$\beta\sum_{l=n+1}^{N}\frac{\xi_l^2}{v}\int_{v} V_{1l}^{(1)}w_N^{(n,1)}(jl)\,\mathrm{d}v_l \quad (26)$$
$$w_N^{(n,1)}(1j) = W_{N-n+2}^{(2,1)}(1j)$$
$$W_N^{(2,1)}(12) = \xi_2\frac{e_1e_2}{DR_{12}} - \sum_{l=3}^{N}\frac{\xi_l^2e_1e_l}{vDkT}\int_{v}\frac{1}{R_{1l}}W_N^{(2,1)}(2l)\mathrm{d}v_l$$

Thus we observe that the entire set of linear integral equations 25 are rigorously solved by the superposition principle, which was implicit in the original Poisson–Boltzmann equation of the Debye–Hückel theory, if ion size is neglected.

It is of interest to investigate the solutions of eq. 21 for ion pairs, $n = 2$, without the neglect of ion size. For this purpose we introduce the more explicit notation $W_{\alpha\beta}^{(2,1)}(R_{12})$ for two ions of types α and β, where it is to be understood that there are $N_1, N_2 \ldots N_\nu$ ions of the several types $1 \ldots \nu$ present in the volume v, with $N = \sum_{\alpha=1}^{\nu} N_\alpha$, and R_{12} is the distance between the pair of ions. Equations 5 and 21 then lead to the following system of integral equations for the functions $W_{\alpha\beta}^{(2,1)}$ when all ξ_j are set equal to unity, corresponding to full charge for all the ions except ion 1

$$W_{\alpha\beta}^{(2,1)}(R_{12}) =$$
$$\frac{e_\alpha e_\beta}{DR_{12}} - \sum_{\gamma=1}^{\nu}\frac{N_\gamma e_\gamma e_\alpha}{DvkT}\int_{\omega_{13},\omega_{23}}\frac{W_{\beta\gamma}^{(2,1)}(R_{23})}{R_{13}}\mathrm{d}v_3 \quad (27)$$
$$\alpha,\beta = 1, \ldots \nu$$

where ω_{13} and ω_{23}, spherical regions of radius a, concentric with ions 1 and 2 are to be excluded from the domain of integration in the space of ion 3. The system of eq. 27 may be solved in the form

$$W_{\alpha\beta}^{(2,1)}(R_{12}) = \frac{e_\alpha e_\beta}{DR_{12}}\varphi(R_{12})$$
$$\varphi(R) = 1 - \kappa^2\int_a^\infty K(R,r)\varphi(r)\mathrm{d}r$$
$$K(R,r) = R;\ a \le R \le r - a$$
$$= \frac{1}{2}(R + r - a);\ r - a < R \le r + a \quad (28)$$
$$= r;\ r + a < R < \infty$$
$$\kappa^2 = \frac{4\pi}{DkT}\sum_{\gamma=1}^{\nu}\frac{N_\gamma e_\gamma^2}{v}$$

after the introduction of dipolar coördinates, R_{13} and R_{23} in the integration over the configuration space of ion 3, where κ is the familiar Debye–Hückel parameter, proportional to the square root of the ionic strength. The integral equation for $\varphi(R)$ may be solved by the method of Laplace transforms

$$G(z) = \int_a^\infty e^{-zR}\varphi(R)\mathrm{d}R$$
$$G(z) = \frac{B(z)}{z^2 - \kappa^2\cosh za}$$
$$B(z) = z - \kappa^2 G(0) - z^2\sigma(z)$$

$$\sigma(z) = \int_0^a e^{-zR}\,\varphi(R)\,dR$$

$$\int_0^c k(R - r)\varphi(r)dr = f(R);\ 0 \leq R \leq a$$

$$f(R) = \frac{1}{2\pi i}\int_{c-i\infty}^{c+i\infty} \frac{z - \kappa^2 G(0)}{z^2 - \kappa^2 \cosh za}\, e^{zR}dz \qquad (29)$$

$$k(t) = \frac{1}{2\pi i}\int_{c-i\infty}^{c+i\infty} \frac{e^{zt}}{z^2 - \kappa^2 \cosh za}\, dt$$

where the path of integration is to be taken along a line parallel to the imaginary axes with the constant C lying between zero and the least positive real part of the zeros of the function $z^2 - \kappa^2 \cosh za$. The function $\varphi(R)$ is then given by the expression

$$\varphi(R) = \frac{1}{2\pi i}\int_{c-i\infty}^{c+i\infty} \frac{B(z)e^{zR}}{z^2 - \kappa^2 \cosh za}\, dz$$

$$\varphi(R) = \sum_{n=1}^{\infty} A_n e^{-z_n R};\ R > a \qquad (30)$$

$$A_n = \frac{-B(-z_n)}{2z_n - \kappa^2 a \sinh z_n a}$$

$$z_n^2 - \kappa^2 \cosh z_n a = 0$$

where the sum extends over all zeros of $z^2 - \kappa^2 \cosh za$ with positive real part. The explicit determination of the coefficients A_n may be carried out after numerical solution of the fifth of eq. 29, an integral equation for $\varphi(R)$ on the finite interval $0 \leq R \leq A$. Since we desire only to discuss the general properties of the function $\varphi(R)$, this calculation will not be presented here.

If we examine the roots z_n of the equation

$$z^2 - \kappa^2 \cosh za = 0$$

$$z_n = \alpha_n \pm i\beta_n \qquad (31)$$

we find that if a is set equal to zero, there is only one root $Z_1 = \kappa$ with positive real part, and the solution, eq. 27 for $\varphi(R)$ reduces to the Debye–Hückel first approximation $e^{-\kappa R}$. For finite a and small κa there are two positive real roots, the smaller one approximating κ at low ionic strengths, which makes the dominant contribution to $\varphi(R)$, so that $\varphi(R)$ resembles the Debye–Hückel form. As the ionic strength increases, the two real roots approach equality, become equal at $\kappa a = 1.03$ and then move into the complex plane as complex conjugates. For values of κa greater than 1.03, $\varphi(R)$ exhibits the oscillations characteristic of the potentials of mean force in the liquid state, and around each ion there develops a statistical stratification of the average space charge due to the other ions with alternating zones of excess positive and excess negative charge. It is attractive to consider the application of these ideas to an elucidation of the structure of concentrated electrolyte solutions and fused salts, although it would no doubt be necessary to go beyond the linear approximations, eq. 24 to the potentials of mean interionic forces in order to obtain more than a qualitative description.

ISOTONIC SOLUTIONS. II. THE CHEMICAL POTENTIAL OF WATER IN AQUEOUS SOLUTIONS OF POTASSIUM AND SODIUM PHOSPHATES AND ARSENATES AT 25°[1]

BY GEORGE SCATCHARD AND R. C. BRECKENRIDGE

Department of Chemistry, Massachusetts Institute of Technology, Cambridge, Mass.

Received April 19, 1954

The chemical potential of water in aqueous solutions of potassium and sodium primary and secondary phosphates and arsenates and in equimolal mixtures of the secondary and tertiary salts at 25° was determined by isotonic comparison with sodium chloride solutions from 0.1 to 1.1 *M* NaCl. The osmotic coefficients are expressed as the Debye–Hückel term and LaMer–Gronwall–Greiff second term for a size of 5.35 Å. plus a term $Bc/(1 + Dc)$, in which B and D are specific parameters. This permits analytic expressions for the activity coefficients. The coefficients of the ternary salts are computed by the specific ion interaction assumption that νB and D are linear functions of the equivalent fraction. The activity and osmotic coefficients of the primary sodium salts are less negative than those of the potassium salts, the coefficients of the sodium secondary and tertiary salts are more negative. The coefficients of the arsenates are less negative than those of the corresponding phosphates. The basis of Brönsted's theory of specific ion interaction is reexamined, and the theory is used to determine the coefficients in mixtures and specific effects on chemical equilibria.

Our interest in aqueous solutions of sodium and potassium phosphates was aroused by the fact that sodium phosphate buffers are much more acid than potassium buffers of the same ratio of acid to base.[2] The effect may be as great as one *p*H unit in one molal solution. Measurements of the osmotic coefficients also permit a continuation of the comparison of the individual salts started by Scatchard and Prentiss.[3]

(1) Adapted from the Ph.D. Thesis of Robert G. Breckenridge, M.I.T., 1942.

(2) E. J. Cohn, private communication (about 1938).

(3) G. Scatchard and S. S. Prentiss, *J. Am. Chem. Soc.*, **56**, 807 (1934).

Experimental

The apparatus used was that of Scatchard, Hamer and Wood,[4] and the only change in procedure was that two of the cups contained the reference sodium chloride solutions, and each of the other four contained a solution of a salt being studied. The four primary and secondary phosphates were studied together in one series, the corresponding four arsenates in another, and the four secondary–tertiary mixtures in a third series.

The salts used for this study were prepared in this Laboratory and at the Harvard Medical School. The sodium chloride was prepared by precipitation by hydrogen chloride gas from a saturated solution of Mallinckrodt C.P. analytical reagent sodium chloride in conductivity water. The product was

(4) G. Scatchard, W. J. Hamer and S. E. Wood, *ibid.*, **60**, 3061 (1938)

dried at 300° for 24 hours, recrystallized once from conductivity water and again dried at 300° for 48 hours. It was pulverized in an agate mortar, air dried at room temperature and then stored over calcium chloride.

The primary and secondary phosphates were prepared by Dr. T. L. McMeekin in the Laboratory of Physical Chemistry at the Harvard Medical School. Pure primary phosphates were made as described by Sørensen[5] and these were converted to the secondary salts by adding the proper amounts of pure hydroxides. For these measurements, the potassium dihydrogen phosphate was dried at 120° for 24 hours, then pulverized, air dried and stored over calcium chloride.

Primary sodium phosphate crystallizes as a hydrate, so this salt was made up as a stock solution in conductivity water and its concentration determined by precipitating the phosphorus as magnesium ammonium phosphate and weighing as magnesium pyrophosphate.[6] The secondary salts were received as solutions and were used without further treatment, the concentrations being determined by analysis as for the primary sodium phosphate.

The primary and secondary arsenates were made by adding the calculated amount of Mallinckrodt C.P. hydroxide to a sample of Mallinckrodt analytical reagent arsenic oxide and recrystallizing the salt thus obtained. The sodium salts were recrystallized three times. Since these are obtained as hydrates, stock solutions were made up and the concentrations determined by precipitation of the arsenic as magnesium ammonium arsenate and weighing as magnesium pyroarsenate. The primary potassium arsenate was recrystallized five times from conductivity water and dried at 120° for 48 hours. The salt was then powdered, air dried and stored as before. The secondary potassium arsenate was prepared by adding pure hydroxide to the pure primary salt and recrystallizing twice. The salt was used from a stock solution similar to the sodium salts.

The mixtures of secondary and tertiary salts were prepared by adding the calculated amount of pure alkali hydroxide to a solution of the corresponding secondary salt. Highly concentrated solutions of Mallinckrodt C.P. hydroxide were prepared in conductivity water. After several hours digestion on a steam-bath they were filtered through hardened paper from the insoluble carbonate.[7] The filtrates were diluted with carbon dioxide free conductivity water to about 2.4 normal and stored in paraffined bottles equipped with dispensing burets and soda lime guard tubes. These solutions were standardized against primary-standard grade potassium acid phthalate that had been dried for 12 hours at 120°. Three or four stock solutions of each mixture were made by weighing the proper amount of each solution, and the ratio of total cation concentration to total anion concentration was determined for each stock solution.

Results

The results of the isotonic measurements are given in Table I as the equilibrium concentrations, and the values of $M\phi$, in which M is the total number of moles of ions per kilogram of water, and ϕ the osmotic coefficient, $\phi = (\ln a_0)/0.01816M$, a_0 is the activity of the water. The values of the osmotic coefficient of sodium chloride were calculated from the equation which corresponds to that for the activity coefficient given by Scatchard, Batchelder and Brown[8]

$$\phi = 1 - (A/\alpha)\, Z(x)/2 + 0.0126m + 0.0141m^2 \quad (1)$$

in which

$$A = \epsilon^2/kTD_0 \quad (2)$$

$$\alpha = a(8\pi N\epsilon^2\rho_0/1000\ kTD_0)^{1/2} \quad (3)$$

$$x = \alpha(\Sigma_i m_i z_i^2/2)^{1/2} \quad (4)$$

$$Z = [1 + x - 1/(1 + x) - 2\ln(1 + x)]/x^2 \quad (5)$$

and ϵ is the protonic charge, k is Boltzmann's constant, T is the absolute temperature, N is Avogadro's number, D_0 and ρ_0 are the dielectric constant and density of the solvent, z_i is the valence of the species i, and a is the nearest distance of approach of two ions. For water at 25°, A is 2.342×10^8 and

TABLE I

ISOTONIC RATIOS

	Phosphates, m				
NaCl	KH_2PO_4	NaH_2PO_4	K_2HPO_4	Na_2HPO_4	$M\phi$
0.95289	1.25414	1.16786	0.87287	0.99143	1.7794
.92773	1.21154	1.13048	.84496	.96044	1.7310
.89267	1.15619	1.08708	.81181	.....	1.6636
.88989	1.15350	1.07920	.80950	.91084	1.6582
.79265	1.00109	0.94255	.71311	.78756	1.4728
.78377	0.98764	.93161	.69869	.77661	1.4559
.77198	.96882	.92395	.69160	.....	1.4335
.72093	.89257	.84678	.63960	.69920	1.3368
.69512	.85528	.81201	.61294	.66951	1.2881
.61902	.74374	.71390	.53961	.57979	1.1444
.60786	.73077	.....	.52691	.56745	1.1235
.60115	.72163	.68806	.52661	.56186	1.1113
.55410	.65576	.63224	.47941	.51034	1.0234
.54381	.64174	.61672	.....	.49806	1.0029
.48114	.55594	.53736	.40794	.42892	0.8876
.46114	.53097	.51426	.....	.40728	.8505
.44452	.50715	.49313	.37579	.39045	.8205
.42844	.48849	.47391	.....	.....	.7900
.40561	.45757	.....	.34194	.35275	.7478
.38264	.42976	.41913	.31915	.32961	.7054
.37021	.41453	.....	.30597	.31453	.6825
.32862	.36330	.35475	.26985	.27747	.6060
.24445	.26331	.25964	.19786	.20016	.4515
.20494	.21872	.21513	.16452	.16467	.3792
.19085	.20218	.19933	.15183	.15253	.3534
.18440	.19548	.19285	.14636	.14731	.3414
.12992	.13535	.13383	.10129	.10115	.2418
.11553	.12018	.....	.08947	.09002	.2154

	Arsenates, m				
NaCl	KH_2AsO_4	NaH_2AsO_4	K_2HAsO_4	Na_2HAsO_4	$M\phi$
1.10091	1.38515	1.28602	0.88646	1.02910	2.0655
1.05953	1.33171	1.23628	.85201	0.98517	1.9841
0.94722	1.16684	1.08849	.75837	.86336	1.7685
.90452	1.10423	1.03391	.72368	.81780	1.6865
.87140	1.06030	0.99270	.69447	.78341	1.6230
.83938	1.01075	.95284	.66878	.75385	1.5471
.76296	0.90912	.85606	.60558	.67167	1.4048
.71489	.84383	.79636	.56473	.62295	1.3160
.66215	.77330	.72935	.52417	.56957	1.2154
.61583	.71072	.67560	.48434	.52613	1.1277
.60048	.68949	.65594	.47161	.51041	1.1048
.58344	.67013	.63707	.45604	.49363	1.0789
.52662	.59678	.57119	.41130	.44103	0.9729
.52469	.59387	.56771	.40982	.43950	.9686
.51910	.58436	.55621	.40362	.42755	.9584
.46120	.51520	.49268	.35522	.37976	.8506
.42670	.47451	.45236	.33076	.34878	.7868
.42578	.47147	.45179	.32942	.34666	.7851
.31380	.33904	.32708	.32740	.24892	.5787
.29636	.32006	.30785	.22601	.23449	.5467
.28545	.30649	.29819	.21645	.22463	.5267
.24142	.25765	.24940	.18247	.18803	.4460
.23250	.24666	.23956	.17347	.18030	.4297
21205	.22398	.21845	.15898	.16358	.3922
.15172	.15898	.11193	.11283	.11481	.2817

(5) S. P. L. Sørensen, *Compt. rend. trav. Lab. Carlsberg*, **8**, 1 (1909); *Biochem. Z.*, **21**, 131 (1909); **22**, 352 (1909).

(6) F. P. Treadwell and W. T. Hall, *Analytical Chemistry*, John Wiley and Sons, Inc., New York, N. Y., 1935.

(7) J. B. Niederl, "Micro-Quantitative Organic Analyses by the Method of Pregl," John Wiley and Sons, Inc., New York, N. Y., 1938.

(8) G. Scatchard, A. C. Batchelder and A. Brown, *J. Am. Chem. Soc.*, **68**, 2320 (1946).

TABLE I (*Continued*)

Secondary–tertiary mixtures,

A = 2.4915	D = 2.5311	G = 2.5063	K = 2.4558
B = 2.4917	E = 2.5198	H = 2.5710	L = 2.5355
C = 2.4976	F = 2.5043	I = 2.5026	M = 2.4990
		J = 2.4820	

m

NaCl	K_2HPO_4 + K_3PO_4		Na_2HPO_4 + Na_3PO_4		K_2HAsO_4 + K_3AsO_4		Na_2HAsO_4 + Na_3AsO_4		$M\phi$
1.11186					0.77710	I			2.0870
1.03158					.72088	I			1.9313
0.94722					.65683	G			1.7885
.90449					.63352	I			1.6902
.88199	0.68282	A	0.85427	D			0.76524	K	1.6433
.83248	.65152	A	.79448	D			.71218	K	1.5486
.77602	.60347	A	.72586	D			.65819	K	1.4412
.76745					.53357	I			1.4249
.76296					.53371	G			1.4178
.73128	.56599	A	.67221	D			.61054	K	1.3564
.70575	.54340	A	.63981	D			.58785	K	1.3081
.66215					.45787	H			1.2270
.63814	.48890	A	.56679	D			.52108	K	1.1807
.63755	.48697	C	.57167	F	.44975	J	.51547	M	1.1796
.57209	.43590	A	.49551	D			.45770	K	1.0570
.55756	.42412	C	.48517	F	.39194	J	.44355	M	1.0299
.51910					.35098	H			0.9584
.42884	.32087	C	.35368	F	.29912	J	.32966	M	.7953
.42670					.28980	H			.7868
.42578					.28729	H			.7850
.37610	27952	B	.30027	E			.28286	L	.6934
.33784	24878	C	.26710	F	.23050	J	.25187	M	.6230
.32829	24097	C	.25825	F			.24421	M	.6053
.29881	21807	C	.23411	F	.20569	J	.22056	M	.5512
.24142					.15609	H			.4459
.24114	.17328	C	.18125	F	.15883	J	.17352	M	.4455
.21892	.15608	B	.16032	E			.15563	L	.4048
.15172					.093837	H			.2817
.14437	.09997	B	.10138	E			.09860	L	.2685
.14143	09732	C	.09976	F	.08968	J	.09722	M	.2629
.11444	07762	C	.07894	F	.07117	J	.07664	M	.2134
.10975	.07752	C	.07894	F	.06475	H			.2047

$\alpha/a = 0.3281 \times 10^8$. For sodium chloride we used $a = 4.72$, $\alpha = 1.55$.

To obtain an analytical expression for the phosphates and arsenates we used the method of Scatchard and Epstein[9] to determine a size $a = 5.33$, $\alpha = 1.75$ for all the salts. Then we used the more general expression

$$\phi = 1 - (A/\alpha)Z(x)(\Sigma_i m_i z_i^2)/2(\Sigma_i m_i) - (A/\alpha)^2[X_2(x)/2 - 2Y_2(x)](\Sigma_i m_i z_i^3)^2/(\Sigma_i m_i)(\Sigma_i m_i z_i)^2 + Bc/(1 + Dc) \quad (6)$$

with c the equivalent concentration, to determine the specific parameters B and D. The second term in this expression is that of LaMer, Gronwall and Greiff,[10] who tabulate values of $[X_2(x)/2 - 2Y_2(x)]$ up to $x = 0.4$. We used values up to $x = 3.2$.

$$X_2(x) = -\frac{1}{2}\frac{x^2}{(1+x)^2}e^{3x}\int_{3x}^{\infty}\frac{e^{-u}}{u}du \quad (7)$$

$$Y_2(x) = \frac{1}{x^4}\int_0^x u^3 X_2(u)du \quad (8)$$

X_2 was calculated from elementary functions and tables of the exponential integral. Y_2 was determined by graphical integration. Table II contains, for steps in x of 0.2 from 0.4 to 3.2, the values of

$$-10^2[X_2(x)/2 - Y_2(x)] \text{ and } -10^2[X_2(x)/2 - 2Y_2(x)]$$

which are the combinations most used in $\ln \gamma$ and in ϕ. For a single salt, with cation 3 and anion 4

$$(\Sigma_i m_i z_i^2)/(\Sigma_i m_i) = -z_3 z_4,$$
$$\text{and } q_2 = (\Sigma_i m_i z_i^3)/(\Sigma_i m_i z_i^2) = z_3 + z_4$$

which is zero for symmetrical salts.

TABLE II

ELECTROSTATIC INTERACTION TERMS

x	$-10^2[X_2/2 - Y_2]$	$-10^2[X_2/2 - 2Y_2]$	x	$-10^2[X_2/2 - Y_2]$	$-10^2[X_2/2 - 2Y_2]$
0.4	0.4324	0.0982	2.0	0.2159	−0.1062
.6	.4575	.0548	2.2	.1913	− .1103
.8	.4370	.0140	2.4	.1702	− .1120
1.0	.3975	− .0240	2.6	.1520	− .1122
1.2	.3547	− .0528	2.8	.1360	− .1116
1.4	.3138	− .0741	3.0	.1223	− .1100
1.6	.2769	− .0891	3.2	.1103	− .1079
1.8	.2442	− .0996			

The parameters B and D are listed in Table III, which includes values for the ternary phosphates and arsenates extrapolated on the assumptions that

(9) G. Scatchard and L. F. Epstein, *Chem. Revs.*, **30**, 211 (1942).

(10) V. K. La Mer, T. H. Gronwall and L. J. Grieff, THIS JOURNAL, **35**, 2245 (1931).

νB and D are linear functions of the equivalent fraction. These assumptions will be discussed later.

TABLE III

SPECIFIC COEFFICIENTS

Salt	$-B$	D	Salt	$-B$	D
KH_2PO_4	0.303	0.639	K_2HAsO_4	0.084	0.436
NaH_2PO_4	.256	.767	Na_2HAsO_4	.154	.352
K_2HPO_4	.260	.966	KH_2AsO_4	.262	.762
Na_2HPO_4	.256	.503	NaH_2AsO_4	.139	.335
K_3PO_4	.162	.889	K_3AsO_4	.042	.776
Na_3PO_4	.263	.465	Na_3AsO_4	.234	.632

Equation 6 represents the results within the scatter of the measurements for the primary and secondary salts, and for the mixtures of secondary and tertiary salts above 0.1–0.15 m. In dilute solutions of these mixtures the measured osmotic coefficients are consistently high and appear to extrapolate to a limit greater than unity. For both of the sodium salts and for the potassium phosphates the maximum discrepancy is 2%. For potassium arsenate, however, it reached 8% and the measurements in more concentrated solutions scatter abnormally. There seems to have been an impurity which contributed about 0.003 to M (0.012 for potassium arsenate) for any value of M. This type of behavior would result from the hydrolysis or from the absorption of carbon dioxide from the atmosphere, but the amount seems very large. We have ignored the measurements in very dilute solutions. The results for the mixtures are therefore uncertain to about $0.003/M$ ($0.012/M$ for potassium arsenate). The extrapolated values for the tertiary salt have about twice this uncertainty in addition to any uncertainty in the assumptions.

Table IV contains the osmotic coefficients, and Table V the activity coefficients, as $1 + \log \gamma$, calculated from these parameters. The equation for the activity coefficients which corresponds to equation 6 is

$$\ln \gamma_{\pm} = z_+z_-(A/\alpha)x/2(1 + x) + z_+z_-(z_+ + z_-)^2(A/\alpha)^2 [X_2(x)/2 - Y_2(x)] + (B/D) \ln (1 + Dc) + Bc/(1 + Dc) \quad (9)$$

Since the experimental work of this paper was completed, Stokes[11] has published the results of isotonic (isopiestic) measurements on sodium and potassium primary phosphates. Her results for the

TABLE IV

OSMOTIC COEFFICIENTS

Primary Salts

m	Debye	KH_2PO_4	NaH_2PO_4	KH_2AsO_4	NaH_2AsO_4
0.1	0.937	0.909	0.913	0.913	0.924
.2	.928	.875	.884	.883	.902
.3	.925	.848	.862	.861	.887
.4	.923	.826	.844	.842	.874
.5	.922	.807	.829	.827	.862
.6	.921	.790	.816	.813	.852
.7	.921	.774	.804	.801	.842
.8	.920	.760	.794	.790	.833
.9	.921	.748	.784	.781	.825
1.0	.921	.736	.776	.772	.817
1.1	.921	.725	.768	.674	.809
1.2	.921	.715	.761	.757	.802
1.3	.922	.706	.755	.750	.796

Secondary Salts

m	Debye	K_2HPO_4	Na_2HPO_4	K_2HAsO_4	Na_2HAsO_4
0.1	0.849	0.805	0.802	0.833	0.820
.2	.839	.764	.754	.811	.785
.3	.839	.739	.720	.799	.761
.4	.839	.722	.693	.790	.742
.5	.840	.708	.670	.784	.726
.6	.843	.698	.651	.779	.712
.7	.845	.690	.634	.775	.700
.8	.847	.684	.620	.771	.689
.9	.849	.679	.608	.769	.679
1.0	.851	.674	.596	.766	.670
1.1	.853	.671	.586	.764	.663

Tertiary Salts

m	Debye	K_3PO_4	Na_3PO_4	K_3AsO_4	Na_3AsO_4
0.1	0.748	0.709	0.678	0.738	0.689
.2	.742	.678	.618	.724	.640
.3	.746	.665	.579	.724	.612
.4	.752	.658	.550	.726	.593
.5	.759	.655	.527	.730	.579
.6	.766	.654	.508	.734	.569
.7	.772	.653	.492	.738	.561

TABLE V

ACTIVITY COEFFICIENTS AS $1 + \log \gamma$

Primary Salts

m	Debye	KH_2PO_4	NaH_2PO_4	KH_2AsO_4	NaH_2AsO_4
0.1	0.897	0.871	0.876	0.875	0.885
.2	.873	.824	.833	.832	.850
.3	.858	.789	.801	.799	.824
.4	.848	.759	.775	.773	.804
.5	.839	.732	.752	.750	.786
.6	.833	.709	.732	.730	.770
.7	.828	.688	.715	.712	.755
.8	.823	.668	.698	.695	.742
.9	.819	.650	.684	.680	.730
1.0	.815	.633	.670	.666	.718
1.1	.812	.618	.657	.653	.707
1.2	.809	.603	.645	.641	.697
1.3	.807	.589	.634	.630	.687

Secondary Salts

m	Debye	K_2HPO_4	Na_2HPO_4	K_2HAsO_4	Na_2HAsO_4
0.1	0.722	.0683	.0681	.0709	0.697
.2	.671	.600	.593	.644	.622
.3	.642	.546	.532	.606	.572
.4	.622	.504	.484	.576	.533
.5	.607	.471	.443	.553	.500
.6	.596	.444	.408	.533	.472
.7	.586	.420	.377	.517	.447
.8	.578	.398	.349	502	424
.9	.571	.380	.234	.489	.404
1.0	.565	.363	.301	.477	.385
1.1	.560	.348	.279	.467	.367

Ternary Salts

m	Debye	K_3PO_4	Na_3PO_4	K_3AsO_4	Na_3AsO_4
0.1	0.529	0.494	0.467	0.520	0.475
.2	.449	.388	.335	.432	.353
.3	.406	.324	.247	.383	.275
.4	.377	.279	.180	.350	.217
.5	.356	.244	.126	.326	.171
.6	.340	.216	.079	.306	.133
.7	.328	.193	.039	.290	.100

(11) J. M. Stokes, *Trans. Faraday Soc.*, **41**, 685 (1945).

sodium salt average 0.4% higher than ours, for the potassium salt hers are 0.1% lower. Only in the dilute solutions is the difference from this average greater than 0.2%.

Discussion

The comparison of the osmotic coefficients may be made without involving any theory except that necessary for interpolation, and it makes but little difference which concentration is chosen for the comparison. The osmotic coefficients are all smaller than those calculated from electrostatic theory. The primary phosphates have the smallest coefficients of any salt of the same cation and a univalent anion listed by Robinson and Stokes.[12] Primary sodium arsenate also lies below any other sodium salt, but potassium primary arsenate has a larger coefficient than the nitrate or bromate. The coefficient of every arsenate is larger than that of the corresponding phosphate, and the difference is such that the smaller arsenate coefficient is nearly the same as the larger phosphate coefficient. For the primary salts the coefficient of the potassium salt is smaller than that of the sodium salt, for the secondary salts the coefficient of the potassium salt is larger. The difference between the primary arsenates is somewhat less than that for the nitrate, chlorate and perchlorate ions, and that for the phosphates is very much less.

Scatchard and Prentiss[3] divided the alkali salts of univalent anions into three classes: the first includes the halides except the fluorides and their osmotic coefficients decrease with increasing size of the cation; the second includes the hydroxides, fluorides and salts of carboxylic acids and their osmotic coefficients increase with increasing size of the cation; the third consists of salts of oxygenated anions such as the nitrates, chlorates and perchlorates, and the order is the same as in the first, but the salts of larger cations have very much smaller osmotic coefficients. The difference between the third and first class is less marked at 25° than at 0°, but is still significant.

The primary phosphates and arsenates appear to combine the characteristics of the second and third classes. The potassium salts behave like the nitrates and perchlorates, the sodium salts have an additional factor reducing their osmotic coefficients, which is greater for the phosphate than for the arsenate. The primary phosphate ion is the weaker base, so the basic strength cannot explain quantitatively the behavior of class two. Perhaps the smaller size of the phosphate ion is more important in its interaction with sodium ion than in that with a proton. This fact is brought out even more clearly, however, by a comparison of the hydroxide and fluoride ions.

Our knowledge of the alkali salts of bivalent and trivalent anions is much more limited than that of the salts of univalent anions, but the same factors are obviously operative. For the potassium salts ϕ''' decreases continuously as the valence of the anion changes, and for the sodium salts it increases, though to a smaller extent. The phosphates always have larger values than the arsenates.

(12) R. A. Robinson and R. H. Stokes, *Trans. Faraday Soc.*, **45**, 642 (1949).

Salt Mixtures

To relate our results to the *p*H measurements, or to any study of chemical equilibria, it is necessary to consider the activity coefficients of salts in salt mixtures. We use essentially the "specific ion interaction" theory of Brönsted.[13] If we expand the term $Bc/(1 + Dc)$ in equation 6 for the osmotic coefficient, it becomes

$$Bc - BDc^2 + - - - -$$

This corresponds to a virial expansion, so for mixtures the first term must be at most a quadratic function of the composition and the second a cubic. Then our parameters must have the forms

$$B = \Sigma_i c_i b_i/c + \Sigma_{ij} c_i c_j b_{ij}/2c^2 \quad (10)$$

$$D = \Sigma_i c_i d_i/c \quad (11)$$

in which c_i is the equivalent concentration of species i, $c = \Sigma_i {}^+c_i = \Sigma_j {}^-c_j$ is the total equivalent concentration and $\nu c = \Sigma_i c_i \nu_i = \Sigma_i m_i = \Sigma_i N_i/V_0 N_0$, if $\Sigma_i{}^+$ is the sum over all cations and $\Sigma_i{}^-$ the sum over all anions. The parameter b_i corresponds to the interaction of the ion i with the solvent, and may be interpreted as a chemical solvation or as a change in the association of the solvent. The parameter b_{ij} corresponds to the interaction of an i ion with a j ion. Brönsted called $b_i c_i$ the salting out term, and $b_{ij} c_i c_j/c$ the interaction term. The specific ion interaction theory is merely the statement that b_{ij} is zero if the product of the valences $z_i z_j$ is positive. It is powerful enough, however, to determine the osmotic coefficient and the mean activity coefficient of any salt in any mixture of salts of the same valence type from the osmotic coefficients or the mean activity coefficients of the single salts. For mixtures of different valence types a further assumption is necessary. Since ternary collisions between ions, and therefore the third virial coefficient, must involve at least two ions of the same sign, Brönsted's theory is obviously limited to the second virial coefficient. However, since D for a mixture can also be derived from those of the component salts solutions, there is no loss of power in the extended equation, although there is considerable loss in convenience.

To save space we will derive immediately the expression for the general case, without Brönsted's theory, and derive the simpler cases from the general expression.

We will use the superscript $'$ to denote the Debye–Hückel approximation, $''$ to denote the Gronwall–La Mer second term, and $'''$ to denote the short range term in solutions so dilute that $Dc << 1$.

For a single salt with cation 3 and anion 4

$$(\phi'''/c)_{34} = B_{34} = b_3 + b_4 + b_{34}/\nu_{34} + (b_{33} + b_{44})/2\nu_{34} \quad (12)$$

$$\ln \gamma_{34}''' = 2B_{34} \quad (13)$$

In any salt mixture

$$\nu\phi'''/c \equiv \nu B = \Sigma^{+-}{}_{ij} x_i y_j \nu_{ij} B_{ij} + \Sigma^{++}{}_{ij} x_i x_j [(b_i - b_j)(\nu_j - \nu_i)/2 + (2b_{ij} - b_{ii} - b_{jj})/4] + \Sigma^{--}{}_{ij} y_i y_j [(b_i - b_j)(\nu_j - \nu_i)/2 + (2b_{ij} - b_{ii} - b_{jj})/4] \quad (14)$$

$$\nu_{34}(\ln \nu_{34}''')/c = \Sigma^{+}{}_i x_i \nu_{i4} B_{i4} + \Sigma^{-}{}_j y_j \nu_{3j} B_{3j} + \Sigma^{+}{}_i x_i [(b_3 - b_i)(\nu_i - \nu_3) + (2b_{3i} - b_{33} - b_{ii})/2 + \Sigma^{-}{}_j y_j [(b_4 - b_j)(\nu_j - \nu_4) + (2b_{4j} - b_{44} - b_{jj})/2] \quad (15)$$

(13) J. N. Brönsted, *J. Am. Chem. Soc.*, **44**, 877, 938 (1922); **45**, 2898 (1923).

The parts of equation 6 which correspond to ϕ' and ϕ'' and the part of equation 10 which corresponds to ln γ_{34}' apply equally to mixtures, but, if there is more than one valence type, ln γ_{34}'' is changed. In general

$$\ln \gamma_{34}' = z_3 z_4 (A/\alpha) x/2(1 + x) \quad (16)$$

$$\ln \gamma_{34}'' = z_3 z_4 q_2^2 (A/\alpha)^2 \quad [X_2(x)/2 - Y_2(x)] + z_3 z_4 q_2 (z_3 + z_4 - q_2)(A/\alpha)^2 Y_2(x) \quad (17)$$

Specific Ion Interaction

Brönsted's theory makes each term b_{ij}, b_{ii}, b_{jj} in equation 14 equal to zero. The same result may be obtained by the less drastic, though perhaps not more probable, assumption that each b_{ij} is the average of the corresponding b_{ii} and b_{jj}. With either assumption, the terms involving $(2b_{ij} - b_{ii} - b_{jj})$ in equations 14 and 15 are zero. If all salts are of the same valence type each $(\nu_j - \nu_i)$ is zero for either cations or anions, and only the terms in B_{ij} remain. They can be determined from measurements on the single salts. In this case the assumption of equal collision diameters a leads to electrostatic terms independent of the composition. In a binary mixture with a common ion, say 34 and 54, the osmotic coefficient is a linear function of the composition, with slope $(B_{54} - B_{34})c$ and the logarithm of the mean activity coefficient of any salt with anion 4 and cation of the same valence as 3 and 5, has this same slope. The mean activity coefficient of 34 in 54 is the same as that of 54 in 34.

$$(\ln \gamma_{34}''')_{54} = (\ln \gamma_{54}''')_{34} = (B_{34} + B_{54})c \quad (18)$$

Brönsted[13] derived this relation and illustrated it with a figure (*J. Am. Chem. Soc.*, **45**, 2902 (1923)). In a mixture without a common ion, ϕ is no longer linear, though each ln $\gamma_{\pm}'''$ is linear, and is determined from the reciprocal salt pair $(\ln \gamma_{34}''')_{56} = (B_{36} + B_{54})c$. For salts too insoluble for the direct determination, B may be determined from the solubility in a solution of a salt with a common ion as $(\ln \gamma_{AgCl}''')_{AgNO_3} = (B_{AgCl} + B_{AgNO_3})c$.

The fundamental assumption of Brönsted cannot be universal. It must fail badly for interactions such as that of CN^- with $Fe(CN)_3^-$, $Fe(CN)_4^=$ and $Fe(CN)_6^{\equiv}$, and may fail less drastically in other cases. It is, however, extremely useful.

Brönsted made an error in neglecting the effect of b_i on the activity coefficient of species i in any solution. However, this error affects only his results for mixtures of different valence types and for single ion activities because he applied it to mixtures of the same valence type by a thermodynamic method which corrected the error. Guggenheim,[14] who repeats the figure and properly credits it to Brönsted, avoids the thermodynamic error by the usually improbable assumption that every b_i is zero. Güntelberg[15] credits Brönsted only with the results Güntelberg got by applying Brönsted's assumptions in a way which did not correct the error, and credits Guggenheim with equation 18. Harned and Owen[16] repeat this error and also give a slope of ϕ different from that of ln $\gamma_{\pm}$ for both Brönsted and Guggenheim.

(14) E. A. Guggenheim, *Phil. Mag.*, [7] **19**, 588 (1935).

(15) E. Güntelberg, "Studier over Elektrolyte—Activiteter I Vandige Opløsninger," G. E. C. Gads, Copenhagen, 1938.

(16) H. S. Harned and B. B. Owen, "The Physical Chemistry of Electrolytic Solutions," Reinhold Publ. Corp., New York, N. Y., 1943.

Solvation and Salting Out

Mixtures of salts of different valence types require more careful consideration. Scatchard[17] correlated the osmotic coefficients of the alkali halides with the assumption that every b_i is zero. The usual treatment of hydration attributes all but the Debye–Hückel interaction to this term. The correct compromise must be that the solvation of an ion affects other ions of the same sign, but not as much as it affects ions of the opposite sign, or that there are b_i terms, but they do not account for all of the salting out.

For the complex anions such as the phosphates and arsenates, hydration should be small because the first shell of the central ion is already full. This corresponds to the fact that the non-electrostatic effects are negative for these salts. We should expect, moreover, that the hydration per mole is greater the higher the valence, so that the difference in the hydration per equivalent may be very small. We may assume then without too much error that $(b_i - b_j)$ is zero for the anions in these systems. This is the assumption which we made in extrapolating to the parameters for the tertiary salts.[18]

Chemical Equilibria

We will illustrate the treatment of chemical equilibria by the dissociation of the primary phosphate ions. The concentration of hydrogen ion is given in terms of the buffer ratio by

$$\ln (H^+) - \ln (U^-/D^=) - \ln K = \ln \gamma_U/\gamma_D\gamma_H = 2 \ln \gamma_{3U} - 3 \ln \gamma_{H3D} \quad (19)$$

If U^- represents $H_2PO_4^-$, $D^=$ represents $HPO_4^=$ and 3 is a univalent cation other than H^-. For a solution in which $(K^+) = xc$, $(Na^+) = (1 - x)c$, $(D^=) = yc$, and $(U^-) = (1 - y)c$, Brönsted's theory states that

$$(2 \ln \gamma_{3U}''' - 3 \ln \gamma_{H3D}''')/c = -2(1 - y)B_{HU} - \frac{3}{2}yB_{HD} + 2[(1 - x)B_{NaU} + xB_{KU}] - 3[(1 - x)B_{NaD} + xB_{KD}]$$

$$= -2B_{HU} + 2B_{NaU} - 3B_{NaD} + \left[\frac{3}{2}B_{HD} - 2B_{HU}\right]y + [2(B_{KU} - B_{NaU}) - (3(B_{KD} - B_{NaD})]x \quad (20)$$

Our measurements do not include the equilibrium constant, K, or B_{HU} or B_{HD}, so they cannot tell the hydrogen ion concentration at any buffer ratio, its change with total concentration at constant buffer ratio, or the effect of changing the buffer ratio. But they do give the effect of replacing sodium by potassium at any buffer ratio. For this substitution the ionic strength is unchanged, and therefore the electrostatic term is unchanged. Since, $(b_D - b_U)$ $(\nu_D - \nu_U)$ is independent of the cation any error due to hydration also cancels in this difference.

Our values of the constants yield

$$[d \ln (H^+)/dx] = -0.082c \text{ for phosphates}$$
$$= -0.456c \text{ for arsenates}$$

(17) G. Scatchard, *Chem. Revs.*, **19**, 309 (1936).

(18) For mixtures in which the solvation-salting out term predominates it is more accurate to take

$$\phi'''/c = B = \Sigma^{+-}{}_{ij} x_i x_j B'_{ij} + \Sigma^{+-}{}_{ij} x_i y_j [b_{ij}(1/\nu - 1/\nu_{ij}) - (b_{ii} + b_{jj})/2\nu_{ij}] + \Sigma^{++}{}_{ij} x_i x_j b_{ij} + \Sigma^{=}{}_{ij} y_i y_j b_{ij})/2\nu$$

and to assume that all but the first term vanishes. The corresponding treatment of activity coefficients eliminates the b_i's of the solvent salts, but not b_3 and b_4.

The difference between the two salts may be exaggerated by the fact that each depends upon four measurements. The change is in the direction of the change in "activity" of the hydrogen ion as measured with a saturated potassium chloride bridge.

Single Ion Activities

We will define single ion activities as those measured with a use of a saturated potassium chloride bridge. "Such a definition does not contradict any measurements or theories which do not involve single ion activities."[19] We will assume that equations similar to 15, 16 and 17 apply to these single ion activities, with the clear understanding that this assumption is of a very different sort from those we have made hitherto. It leads to the results

$$-\ln \gamma_k' = -z_k^2(A/\alpha)x/(1+x) \quad (21)$$

$$-\ln \gamma_k'' = -z_k^2 q_2^2 (A/\alpha)^2[X_2(x)/2 - Y_2(x)] - z_k^2 q_2 (z_k - q_2)(A/\alpha)^2 Y_2(x) \quad (22)$$

$$\ln \gamma_k''' = \Sigma_i c_i (b_i + b_k \nu_i/\nu_k + b_{ik}/\nu_k) \quad (23)$$

in which Brönsted's specific ion interaction theory says that b_{ik} is zero if $z_i z_k$ is positive. In the salt ij

$$(\ln \gamma_k''')/c = (b_i + b_j) + b_k(\nu_i + \nu_j)/\nu_k + (b_{ik} + b_{kj})/\nu_k \quad (24)$$

and either b_{ik} or b_{kj} is zero. The coefficient of b_k depends only upon the valence type of the salt.

If we consider the change in the activity coefficient of hydrogen ion in going from a sodium phosphate buffer to a potassium phosphate buffer of the same buffer ratio and concentration, the change in $\ln \gamma_H'''/c$ is $b_K - b_{Na}$. If there is univalent anion X such that $b_{KX} = b_{NaX}$, $(b_K - b_{Na}) = (\phi_{KX} - \phi_{NaX})/c$. It is not too improbable that the chloride ion fulfills this condition. If so $(b_K - b_{Na}) = -0.04$, which corresponds to about two more moles of water combining with sodium ion than with potassium ion. It increases the effect of changing cation on *p*H measurements.

From equation 23 we see that for the single salt 34 the ratio of the individual ion activities to the mean activity is

$$(\ln \gamma_3/\gamma_{34})'''/c = (b_3\nu_4/\nu_3 - b_4) + b_{34}(\nu_4 - \nu_3)/\nu_3(\nu_3 + \nu_4)$$
$$(\ln \gamma_4/\gamma_{34})'''/c = (b_4\nu_3/\nu_4 - b_3) + b_{34}(\nu_3 - \nu_4)/\nu_4(\nu_3 + \nu_4)$$

For a symmetrical salt, $\nu_3 = \nu_4$, the differences reduce to $(b_3 - b_4)$ and $(b_4 - b_3)$. Brönsted[13] and Guggenheim[14] define individual ion activities as equal to mean activities. This follows from Guggenheim's assumption that all the b_i's are zero. If we assume that $b_i = b_j$ for potassium chloride, and that b_{ij} is the same for the alkali chlorides and for hydrogen chloride

$$b_{Na} - b_{Cl} = b_{Na} - b_K = (\phi_{NaCl}''' - \phi_{KCl}''')/c = \frac{1}{2}(\ln \gamma_{NaCl}''' - \ln \gamma_{KCl}''')/c$$

Thus, the logarithm of the activity of chloride ion in sodium chloride is the mean of the logarithms of the mean activities of sodium chloride and of potassium chloride, and similarly for hydrogen chloride. This latter result of our assumptions may be compared with the measurements of Scatchard[20] with hydrochloric acid and a saturated potassium chloride bridge. The agreement is better than it is with the other assumptions which have been made, but not much better.

More Concentrated Solutions

Equation 6 may be used for salt mixtures with

$$B = \Sigma^{+-}{}_{ij} x_i y_j \nu_{ij} B_{ij}/\nu$$

and

$$D = \Sigma^{+}{}_i x_i d_i + \Sigma^{-}{}_j y_j d_j = \Sigma^{+-}{}_{ij} x_i x_j D_{ij}$$

but the term in $\ln \gamma'''$, like the long range terms, requires modification.

The value of the free energy which corresponds to this osmotic coefficient may be written

$$G'''/RT = \frac{\Sigma^{+-}{}_{ij} N_i N_j \nu_{ij} B_{ij}/\nu_i\nu_j}{\Sigma^{+}{}_i N_i d_i/\nu_i + \Sigma^{-}{}_j N_j d_j/\nu_j} \ln [1 + (\Sigma^{+}{}_i N_i d_i/\nu_i + \Sigma^{-}{}_j N_j d_j/\nu_j)/N_0 V_0] \quad (25)$$

The corresponding activity coefficients are given by

$$\nu_3 \ln \gamma_3''' = (\Sigma^{-}{}_j y_j \nu_{3j} B_{3j}/D) \ln (1 + Dc) + (\nu B d_3/D^2)[Dc/(1 + Dc) - \ln (1 + Dc)] \quad (26)$$

$$\nu_4 \ln \gamma_4''' = (\Sigma^{+}{}_i x_i \nu_{i4} B_{i4}/D) \ln (1 + Dc) + (\nu B d_4/D^2)[Dc/(1 + Dc) - \ln (1 + Dc)] \quad (27)$$

$$(\nu_3 \ln \gamma_3''' + \nu_4 \ln \gamma_4''')/\nu_{34} = [(\Sigma^{+}{}_i x_i \nu_{i4} B_{i4} + \Sigma_j \nu_{3j} B_{3j})/\nu_{34} D] \ln (1 + Dc) + (\nu B D_{34}/\nu_{34} D^2)[Dc/(1 + Dc) - \ln (1 + Dc)] \quad (28)$$

Equation 28 is too intricate for much simple generalization. For the same valence type, if the D's are all equal but Dc is not negligible relative to unity, the same simple relations hold as when Dc is negligible except that the slope of $\ln \gamma$ with composition is no longer proportional to c. If the D's are very different, but $Bc/(1 + Dc)$ is nearly the same, the slope of the two mean activity coefficient curves may have opposite signs. Even in this case, however, each slope is nearly independent of the composition, that is the Harned rule holds to a good approximation in cases for which the other simple relations fail badly. This one additional term is sufficient to imitate many of the experimental results, but this fact does not show that it is sufficient to explain them.

To explain the discussion of Brönsted's theories at the celebration of Debye's birthday one must go back to 1921–1923, and picture the effects on students of electrolyte solutions of the impacts in rapid succession of Lewis' use of exact thermodynamics culminating in Lewis and Randall, Brönsted's theory of reaction rates, Brönsted's theory of specific ion interaction, and the Debye–Hückel theory. All but the specific ion interaction have received ample recognition. Yet this theory, paired with that of Debye and Hückel, can be so useful that they should be included in the undergraduate curriculum. For this purpose the La Mer–Gronwall–Greiff second term and the third virial coefficient may well be omitted, and the specific ion interaction theory may be presented as an approximation which may become worse as the solution becomes more concentrated,[17] but may hold up to high concentrations.

(19) G. Scatchard, *Science*, **95**, 27 (1942).

(20) G. Scatchard, *J. Am. Chem. Soc.*, **47**, 696 (1925).

SOLUBLE CRYSTALLINE POLYPHOSPHATES—THEIR PURIFICATION, ANALYSIS AND PROPERTIES

BY OSCAR T. QUIMBY

Miami Valley Laboratories, The Procter & Gamble Company, Cincinnati 31, Ohio

Received April 19, 1954

Application of tracer techniques has shown that sodium pyrophosphate is readily obtained in 99.9% purity, but that sodium triphosphate is not easily obtained in higher than 99% purity, the chief impurity being pyrophosphate formed during the triphosphate recrystallizations. While some orthophosphate is probably also formed during triphosphate purification, it is either more readily removed than pyrophosphate or formed in lesser quantities; at any rate the orthophosphate content of a quadruply recrystallized triphosphate seldom exceeds 0.1% as Na_2HPO_4. The purity attainable for the newly-discovered, crystalline hexaguanidinium tetraphosphate has not been so extensively investigated, but is probably at least 95%, and may be as high as 99%. The hexaguanidine salt, derived from the easily available tetrametaphosphate, provides the tetraphosphate in stable and convenient form, ready for instant use in any situation where a tetraphosphate ion is desired. Methods of analysis have been developed recently which are specific for individual polyphosphate species. The most versatile of these is based on paper chromatography studies in Canada and in France. Chromatography is capable of determining ortho-, pyro-, tri-, tetra-, trimeta- and tetrametaphosphates in the presence of one another and is also capable of extension to other condensed phosphates. In our own laboratories certain specific analytical methods have been developed. For commercial sodium tripolyphosphate (or triphosphated detergents) isotope dilution methods specific for pyro- and for triphosphate have been developed. They are based on the isolation of the "pure" sodium salts as already indicated. Attempts to obtain a pure pyrophosphate by precipitation with zinc ions in the presence of triphosphate, or to obtain a pure triphosphate by precipitation with tris-(ethylenediamine)-cobalt(III) ion in the presence of pyrophosphate, failed because either polyphosphate tends to cocrystallize with the other. In spite of such difficulties it was possible to develop a colorimetric method for triphosphate in commercial triphosphate or triphosphated detergents, using the tris-(ethylenediamine)-cobalt(III) ion. When samples are available in crystalline form, *e.g.*, commercial tripolyphosphate, analysis by X-ray diffraction gives the polymorphic distribution in addition to an estimate of triphosphate content. The stability of polyphosphates toward hydrolysis in solution decreases in the order pyro-, tri-, tetraphosphate. In the hydrolysis or reversion of triphosphate there is an important difference between solution hydrolysis and that which accompanies the dehydration of the hexahydrate $Na_5P_3O_{10}\cdot 6H_2O$. In the former, all evidence is consistent with cleavage of triphosphate to give equimolar amounts of pyro- and orthophosphate. In the latter, considerably more than a mole of pyrophosphate is often found for each mole of orthophosphate. This fact necessitates a revision of the hexahydrate hydrolysis reaction offered by Raistrick and supported by Thilo and Seeman, namely, $Na_5P_3O_{10}\cdot 6H_2O \rightarrow Na_4P_2O_7 + NaH_2PO_4 + 5H_2O$. Some additional reaction must be invoked which produces more pyrophosphate, *e.g.*, $2Na_5P_3O_{10}\cdot 6H_2O \rightarrow Na_4P_2O_7 + 2Na_3HP_2O_7 + 11H_2O$. A combination of the two can explain the observations below the temperature of recondensation (120°). Above 120° both simple dehydration directly to $Na_5P_3C_{10}$ (II) and formation of $Na_5P_3O_{10}$ (II) by recondensation (reversal of above reactions) occur, the one which dominates depending on the speed of escape of the water. The interaction of calcium and triphosphate ions in solution is briefly discussed.

Introduction

Condensed sodium phosphates have received considerable attention in recent years, with the result that most of the crystallizable species have now been fairly well characterized. The present survey deals with recent progress in characterizing the soluble crystalline polyphosphates: pyro-, tri- and tetraphosphate.

Prior to the classic work of Partridge, Hicks and Smith,[1] little phase information was available on the occurrence of sodium triphosphate $Na_5P_3O_{10}$ and still less on that of sodium tetraphosphate $Na_6P_4O_{13}$. This study and that of Ingerson and Morey[2,3] demonstrated for the Na_2O–P_2O_5 system that $Na_5P_3O_{10}$ is stable below a temperature of about 620° and that $Na_6P_4O_{13}$ does not occur, a mixture of $Na_5P_3O_{10}$ plus $Na_3P_3O_9$ always being found in well-crystallized samples of the tetraphosphate composition. This was confirmed by other less extensive studies.[4–7]

In the Na_2O–P_2O_5–H_2O system not only is the tetraphosphate unstable, but so also are the triphosphate and pyrophosphate, as shown by numerous studies of the hydrolysis of the latter two phosphates[8–13] in aqueous solutions. Ingerson and Morey,[2] however, state that the normal pyrophosphate $Na_4P_2O_7$ is thermodynamically stable in certain parts of the Na_2O–P_2O_5–H_2O system.

In spite of its lack of thermodynamic stability the tetraphosphate can be prepared in aqueous solutions by mild alkaline hydrolysis of cyclic sodium tetrametaphosphate, another metastable substance. This has been accomplished by three groups of investigators,[7,14–16] but none of them succeeded in isolating a crystalline tetraphosphate. Thilo and Rätz[14] obtained insoluble calcium, silver and zinc tetraphosphate precipitates, all of which were amorphous to X-rays. Westman, *et al.*,[7,15] and Ebel[16] obtained tetrametaphosphate hydrolysates, the bulk of whose phosphate ions differed chromatographically from the common phosphate species, namely, ortho, pyro, tri, trimeta and tetrameta, in just the way one would expect for tetraphosphate ions.

While the data summarized below emphasize (1) purification and analysis of sodium triphosphate, and (2) isolation and purification of crystalline tet-

(1) E. P. Partridge, V. Hicks and G. W. Smith, *J. Am. Chem. Soc.*, **63**, 454 (1941).

(2) E. Ingerson and G. W. Morey, *Am. Mineral.*, **28**, 448 (1943).

(3) G. W. Morey and E. Ingerson, *Am. J. Sci.*, **242**, 1 (1944).

(4) K. R. Andress and K. Wüst, *Z. anorg. allgem. Chem.*, **237**, 113 (1938).

(5) O. T. Quimby, unpublished studies (1938–1940).

(6) P. Bonneman-Bémia, *Ann. chim.*, **16**, 395 (1941).

(7) A. E. R. Westman, A. E. Scott and J. T. Pedley, *Chemistry in Canada*, 35 (1952).

(8) S. J. Kiehl and W. C. Hansen, *J. Am. Chem. Soc.*, **48**, 2802 (1926).

(9) J. Muus, *Z. physik. Chem.*, **159A**, 268 (1932).

(10) S. J. Kiehl and E. Claussen, Jr., *J. Am. Chem. Soc.*, **57**, 2284 (1935).

(11) R. Watzel, *Die Chemie*, **55**, 356 (1942).

(12) R. N. Bell, *Ind. Eng. Chem.*, **39**, 136 (1947).

(13) J. R. Van Wazer, E. J. Griffith and J. F. McCullough, *J. Am. Chem. Soc.*, **74**, 4977 (1952).

(14) E. Thilo and R. Rätz, *Z. anorg. Chem.*, **260**, 255 (1949).

(15) A. E. R. Westman and A. E. Scott, *Nature*, **168**, 740 (1951).

(16) J. P. Ebel, *Bull. soc. chim.*, 991, 1085 (1953).

raphosphates of organic bases, properties of both polyphosphates and analyses for pyrophosphate ions also receive attention.

Triphosphate (and Pyrophosphate) Purification

The compound $Na_5P_3O_{10}$ was made as early as 1895, as demonstrated by the optical properties reported by Schwarz.[17] However, lack of adequate methods of analysis has until recently prevented a critical examination of methods of purification. By using tracer methods to follow the purification of triphosphate,[18] it has been found that commercial triphosphate of 85–94% purity expressed as $Na_5P_3O_{10}$ can be brought to a purity of 99% (anhydrous basis) by three to five crystallizations from water–ethanol mixtures at room temperature, followed by air drying. Occasional samples of 99.5% purity have been obtained.

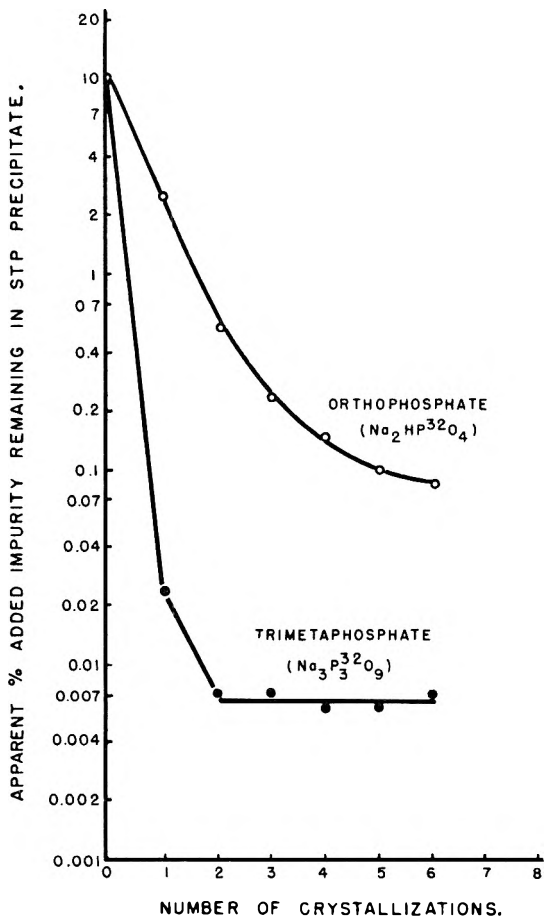

Fig. 1.—Removal of added impurity ($Na_2HP^{32}O_4$ or $Na_3P^{32}{}_3O_9$) from sodium triphosphate (STP) by fractional crystallization; phosphate/water ratio 1 g./8 ml., ethanol/water volume ratio 1/4, room temperature 25–35°.

Method.—The method of purification is simple. One makes an aqueous solution containing 12–15% of commercial triphosphate (usually 85–94% $Na_5P_3O_{10}$), filters to remove any insoluble matter, and precipitates most of the triphosphate as hexahydrate $Na_5P_3O_{10}\cdot 6H_2O$ by adding ethanol slowly with stirring until the ratio of ethanol to water is about 1/4 by volume. After a total of 30 minutes of stirring the hexahydrate crystals are filtered off and washed twice with 1:1 mixtures of ethanol and water, using an aspirator to remove most of the adhering liquid. The damp crystals are then redissolved in the minimum amount of water and the process repeated. If the original purity was below 90% the sample is given four or five crystallizations; if the original purity was above 90% one less crystallization is needed. Finally the crystals of hexahydrate are air-dried at room temperature, preferably at relative humidities of 40–60%. Heat should not be used in any part of the process; drying of the crystals is to be avoided in intermediate stages, as is vacuum-drying on the final stage. The yield of purified $Na_5P_3O_{10}$ is usually 40–45% of the weight of commercial triphosphate taken.

Removal of Ortho- or Trimetaphosphate.—When 10% ortho- or trimetaphosphate, tagged with P^{32}, is added to pure inactive triphosphate and the mixture purified by recrystallizations similar to the method described above, the added impurity is readily reduced to a level of 0.1% or less, as illustrated by Fig. 1. For the orthophosphate this has been confirmed by other methods[17] on inactive triphosphate preparations. Since these impurities are usually present in much smaller quantities than 10%, it is apparent that impurity levels below 0.1% can be achieved easily by the recrystallization method.

Removal of Pyrophosphate.—While tagged pyrophosphate is less readily removed (Fig. 2), nevertheless one sees that four crystallizations bring the *added* pyrophosphate to a level of 0.5% or less provided the original sample contained no more than 20 g. of $Na_4P_2O_7$ to 80 g. of $Na_5P_3O_{10}$. That the *total* pyrophosphate is not necessarily reduced to this level is shown by a reverse experiment in which 10–30% tagged triphosphate, purified by a process

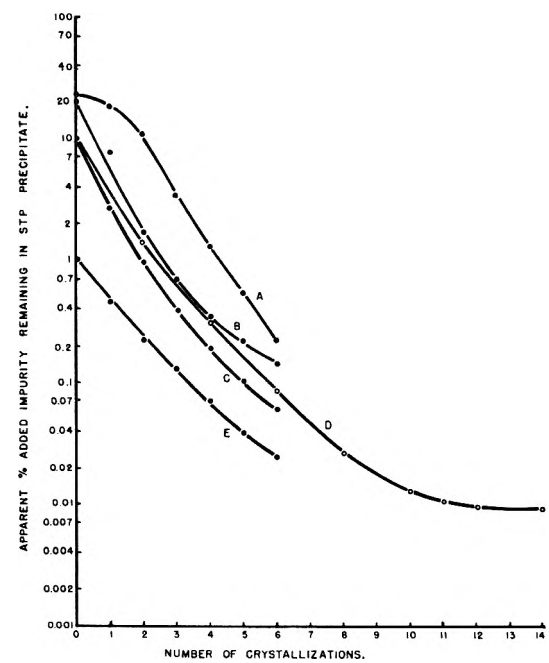

Fig. 2.—Removal of added pyrophosphate impurity ($Na_4P^{32}{}_2O_7$) from STP by fractional crystallization; phosphate/water ratio 1 g./8 ml., ethanol/water volume ratio 1/4, except for curve B where it was 1/5, room temperature 25–35°.

(17) F. Schwarz, *Z. anorg. Chem.*, **9**, 249 (1895).

(18) O. T. Quimby, A. J. Mabis and H. W. Lampe, *Anal. Chem.*, **26**, 661 (1954).

similar to the above, is added to inactive pyrophosphate, and the pyrophosphate purified by the same process except that more water is required to dissolve the phosphate.[18] As expected the activity falls rapidly during the first few crystallizations (Fig. 3) because tagged triphosphate is being lost.

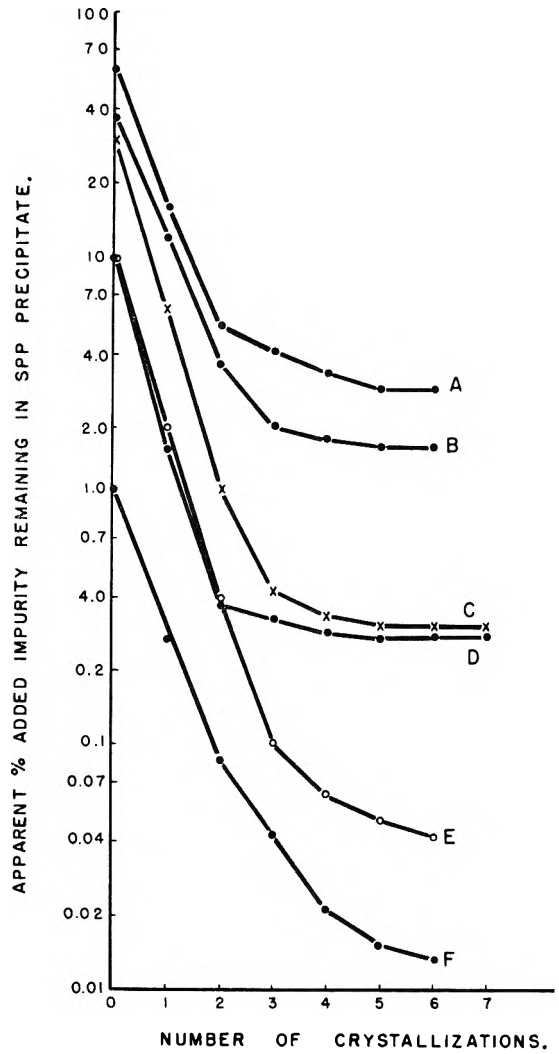

Fig. 3.—Removal of added triphosphate impurity ($Na_5P^{32}{}_3O_{10}$) from sodium pyrophosphate (SPP) by fractional crystallization; phosphate/water ratio 1 g./14 ml., ethanol/water volume ratio 1/4, room temperature 25–35°.

However, all of these curves eventually level out because the tagged triphosphate contains tagged pyrophosphate (usually about 1%) which is, of course, retained by the pyrophosphate. For example, a mixture supposedly containing 70% $Na_4P_2O_7$ + 30% $Na_5P^{32}{}_3O_{10}$ acts as if it contained 70% $Na_4P_2O_7$ + 0.3% $Na_4P^{32}{}_2O_7$ + 29.7% $Na_5P^{32}{}_3O_{10}$. Thus, additional pyrophosphate is formed during the purification of triphosphate. Calculations based on the solution hydrolysis rate given for room temperature in the "Hydrolysis" section show that hydrolysis would not account for so much new pyrophosphate. Possibly the explanation is that the pyrophosphate impurity formed during triphosphate purification arises from surface decomposition of hexahydrate crystals during drying. At least this would not be surprising in view of the labile nature of the hexahydrate.[6,19–21]

Critical Ratio of $Na_5P_3O_{10}$ to $Na_4P_2O_7$.—For isolation of pure sodium triphosphate from a mixture containing both pyro- and triphosphate, the initial weight ratio $Na_5P_3O_{10}/Na_4P_2O_7$ must exceed 7/3, preferably be 4/1 or greater.[18] This is readily apparent from the fractional crystallization data of Fig. 4. In like manner this ratio must be less than 7/3, preferably less than 3/2, in order to yield pure pyrophosphate.

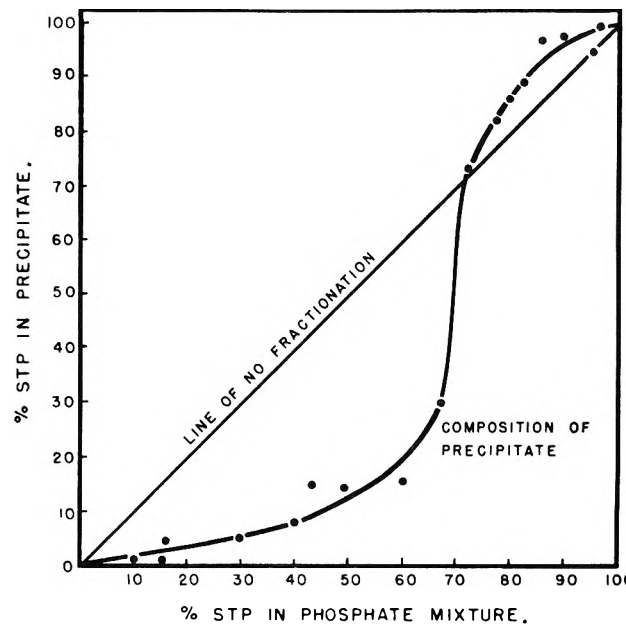

Fig. 4.—Purification diagram for sodium triphosphate—sodium pyrophosphate mixtures by fractional crystallization; phosphate/water ratio 1 g./14 ml. for less than 70% STP in mixture, 1 g./8 ml. otherwise, ethanol/water volume ratio 1/4, room temperature 25–35°.

Analysis

Until recently the available solution methods for determining triphosphate[22,23] were indirect and hence subject to interference from other polyphosphate ions. Accordingly several attempts have been made to develop methods *specific* for the triphosphate ion.

X-Ray Diffraction.—Methods based on measuring intensities of diffraction peaks have been in use for some time.[19,24] They are especially useful when information is desired on the polymorphic nature of a solid sample, for they provide a convenient way of estimating relative amounts of triphosphate present as Phase I, Phase II and hexahydrate. Some examples are given on commercial sodium triphosphate in Table I where the components listed have been adjusted to a total of 100%. Such samples may also contain small amounts of

(19) B. Raistrick, *Roy. Coll. Sci. J.*, **19**, 9 (1949).

(20) E. Thilo and H. Seeman, *Z. anorg. allgem. Chem.*, **267**, 65 (1951).

(21) O. T. Quimby, *Chem. Revs.*, **40**, 141 (1947). (See also the section below on decomposition accompanying dehydration of $Na_5P_3O_{10}\cdot 6H_2O$.)

(22) R. N. Bell, *Ind. Eng. Chem., Anal. Ed.*, **19**, 97 (1947).

(23) B. Raistrick, F. J. Harris and E. J. Lowe, *Analyst*, **76**, 230 (1951).

(24) A. J. Mabis and O. T. Quimby, *Anal. Chem.*, **25**, 1814 (1953).

orthophosphate and/or trimetaphosphate, but their sum seldom exceeds 2%. Since commercial triphosphate contains no hexahydrate as made, X-rays may be used to determine the progress of hydration from exposure to humid atmosphere. Such a method shows not only the amount of hexahydrate produced at any stage, but indicates that Phase I hydrates faster than Phase II.

TABLE I

X-RAY ANALYSES OF SOME COMMERCIAL TRIPHOSPHATES

Sample	% Triphosphate present as $Na_5P_3O_{10}$ (I)	$Na_5P_3O_{10}$ (II)	$Na_5P_3O_{10}\cdot 6H_2O$	$Na_4P_2O_7$, %
A	65.5	29	None	5.5
B	9.5	83	None	7.5
C	27.5	58.5	None	12

While the X-ray method is specific for triphosphate, it is not a general-purpose tool for quantitative analysis, because it requires that the sample be solid and fully crystallized. The importance of this is shown in the analyses of partially dehydrated hexahydrate discussed in the later section on stability of $Na_5P_3O_{10}\cdot 6H_2O$.

On wholly crystallized samples, the X-ray diffractometer method involving an internal standard[24] gives a total triphosphate determination with an average deviation of ±3% absolute if the triphosphate is present in one form and of ±5% if all three forms are present.

This method is of course not limited to determining the triphosphate species, for pyrophosphate as crystalline $Na_4P_2O_7$ can also be determined with slightly greater precision.[24] It will be seen from Table I that pyrophosphate is the chief impurity in commercial sodium triphosphate. Other crystalline species, such as trimetaphosphate, might also be determined by the X-ray method if present in sufficient concentration.

Precipitation by Zinc.—The Bell method of analysis has never been claimed to give high precision in determining either tri- or pyrophosphate; for even the author used the word "estimation" rather than "determination" in the title of his paper.[22] Nevertheless, it is true that this method often gave a fair estimate of triphosphate content—no mean achievement in the light of the mutual interferences revealed by P^{32} tracer studies[25] to be discussed below.

The Bell method was developed by modifying the older method of Britzke and Dragunov[26] for determining pyrophosphate by titrating the hydrogen ions liberated by adding excess zinc ion at *p*H 3.8. But since both pyro- and triphosphate liberate hydrogen ions, it was necessary to obtain an independent measure for one of them and this was done by weighing the pyrophosphate as the zinc salt after two precipitations.

While the precipitation of pyrophosphate by zinc at *p*H 3.8 is quantitative in absence of triphosphate, tracer studies showed that, in the presence of triphosphate, (1) the precipitation is incomplete in both the first and the second precipitation; (2) both precipitates are contaminated with triphosphate; (3) repeating the precipitation as many as four times continues to reduce, but does not eliminate, such contamination. (4) Precipitation of zinc pyrophosphate fails to occur in the presence of massive amounts of triphosphate. For the case of the two precipitations called for by the method, the weight yield of zinc precipitate is usually equal to or slightly higher than that expected for quantitative precipitation of the pyrophosphate alone, provided the weight ratio of $Na_5P_3O_{10}/Na_4P_2O_7 = 3$ or less. Thus, the net effect of the two precipitations is that the pyrophosphate remaining in solutions is fully or a little more than compensated weight-wise by the triphosphate contamination of the zinc pyrophosphate precipitate. Table II gives examples of the recovery of P^{32} put in as pyrophosphate. Note that at weight ratios of 9 or higher pyrophosphate often does not precipitate at all, an observation also recorded by others.[27,28]

TABLE II

PYROPHOSPHATE RECOVERY IN BELL METHOD

Phosphate composition	% of total pyro found: Wt. Zn precipitate	Counting P^{32}
10% $Na_5P_3O_{10}$ + 90% $Na_4P_2{}^{32}O_7$	101	95
25% $Na_5P_3O_{10}$ + 75% $Na_4P_2{}^{32}O_7$	95	90
50% $Na_5P_3O_{10}$ + 50% $Na_4P_2{}^{32}O_7$	108	97
75% $Na_5P_3O_{10}$ + 25% $Na_4P_2{}^{32}O_7$	99	84
90% $Na_5P_3O_{10}$ + 10% $Na_4P_2{}^{32}O_7$	No pptn.	

In view of the uncertainties in the pyrophosphate precipitation and the fact that pyrophosphate contributes two moles of H^+ to approximately one H^+ for the triphosphate, it is remarkable that the method has given such reasonable estimates of triphosphate content, based on the acidity not accounted for by the pyrophosphate as calculated from the weight of zinc precipitate. However, when pyrophosphate fails to precipitate the titration is all calculated to triphosphate and gives impossibly high values.

It is possible that a method for determining pyrophosphate might still be evolved by modifying the Bell procedure. For instance, by using a limited excess of zinc at *p*H 3.8 one could estimate pyrophosphate by centrifuging off the precipitate and determining the excess of zinc in the supernatant. By suitable control of $Na_5P_3O_{10}/Na_4P_2O_7$ ratio and by making calibration curves in such a way as to correct for triphosphate interference, a reliable determination of pyro- in the presence of triphosphate, may yet result, after the manner of the cobalt method developed for triphosphate by Weiser[29] as indicated in the next section.

Precipitation by Tris-(ethylenediamine)-cobalt-(III) Ion.—From solutions containing only triphosphate ions at *p*H 3–4 the cobalt reagent precipitates triphosphate (practically quantitatively)[30] as $Co(en)_3H_2P_3O_{10}\cdot 2H_2O$. This is shown in Fig. 5, which also shows that pyrophosphate by itself does not precipitate under these conditions. Nevertheless, such contamination. (4) Precipitation of zinc pyrophosphate fails to occur in the presence of massive amounts of triphosphate. For the case of the two precipitations called for by the method, the weight yield of zinc precipitate is usually equal to or slightly higher than that expected for quantitative precipitation of the pyrophosphate alone, provided the weight ratio of $Na_5P_3O_{10}/Na_4P_2O_7 = 3$ or less. Thus, the net effect of the two precipitations is that the pyrophosphate remaining in solutions is fully or a little more than compensated weight-wise by the triphosphate contamination of the zinc pyrophosphate precipitate. Table II gives examples of the recovery of P^{32} put in as pyrophosphate. Note that at weight ratios of 9 or higher pyrophosphate often does not precipitate at all, an observation also recorded by others.[27,28]

(25) O. T. Quimby and H. W. McCune, unpublished results.

(26) E. V. Britzke and S. S. Dragunov, *J. Chem. Ind.* (*Moscow*), **4**, 29 (1927).

(27) A. B. Gerber and F. T. Miles, *Ind. Eng. Chem., Anal. Ed.*, **13**, 406 (1941).

(28) H. Schmid and W. Dewald, *Fette u. Seifen*, **55**, 19 (1953).

(29) H. J. Weiser, unpublished results, Methods Development Group, Chemical Division, The Procter & Gamble Company.

(30) H. W. McCune and G. J. Arquit, presented before the Division of Physical and Inorganic Chemistry of the Am. Chem. Soc. at Chicago, September, 1953.

less, tracer studies[30] (*cf.* also Table III) have shown that a similar precipitate from a mixture of pyro- and triphosphate (1) does not contain all of the triphosphate; (2) is contaminated by pyrophosphate; (3) contains less pyrophosphate with each succeeding precipitation, but requires many precipitations (6–10) for production of a triphosphate of 99% purity, and (4) is not precipitated at all if the ratio of pyro- to triphosphate is too high.

TABLE III

PRECIPITATION OF $Co(en)_3H_2P_3O_{10}$ IN PRESENCE OF PYROPHOSPHATE

*p*H	Molar ratio tri/pyro	Ppt. yield, % of theory	Contamination as % $Co(en)_3HP^{32}{}_2O_7$
3.5	6.5/1	100	2.7
3.5	1.08/1	101	10.6
3.5	1/3.23	73	15.5
2.5	4/1	104	6.9
3.0	4/1	107	..
4.0	4/1	106	8.1
4.5	1/2	34	24

Thus, the behavior with the cobalt reagent is a replica of that with zinc ions, except that pyro- and triphosphate have exchanged roles. These two condensed phosphates are so similar in structure that each is prone to enter a crystal lattice of the other. It is therefore difficult to obtain a pure pyrophosphate or a pure triphosphate precipitate, if the other species is present even in small quantities.

In spite of the pyrophosphate interference with the triphosphate precipitation by $Co(en)_3^{+3}$, Weiser[29] was able to develop a colorimetric method for determining triphosphate in materials such as commercial triphosphate and triphosphated detergents, both of which contain pyrophosphate. He accomplished this by preparing a calibration curve using mixtures of purified pyro- and triphosphate. To either such a known mixture or the sample an excess of the cobalt reagent is added, the precipitate is removed by filtration and the excess of reagent in the filtrate is measured with a colorimeter. Translation of the colorimeter reading into triphosphate content by means of the special calibration curve proved to be an effective way of correcting for the pyrophosphate contamination of the precipitate. Replicate analyses showed an average deviation, expressed as parts per hundred parts of triphosphate, of 0.5 in commercial triphosphate and of 0.6 in triphosphated detergents. The uncertainty in the true value is somewhat larger since the triphosphate used for calibration probably had a purity near 99% rather than the assumed 100%.

The presence of 10% tetraphosphate or of as little as 2% sodium polyphosphate glass prevents completely the precipitation of tris-(ethylenediamine)-cobalt dihydrogen triphosphate in the colorimetric method.[29] Smaller amounts interfere, causing the triphosphate analysis to come out low. This may sometimes be overcome by adding some pure triphosphate to reduce the contaminant to triphosphate ratio.

Isotope Dilution.—The fastest approach to a pure tri- or pyrophosphate phase known at present occurs upon recrystallization of the sodium salts from aqueous media. As indicated in the section on purification of triphosphate, this was accomplished at room temperature by adding ethanol to an aqueous tri- or pyrophosphate solution to induce crystallization as $Na_5P_3O_{10}\cdot 6H_2O$ or $Na_4P_2O_7\cdot 10H_2O$. If the initial weight ratio of $Na_5P_3O_{10}$ to $Na_4P_2O_7$ is less than 3/2 four crystallizations under the conditions recommended[18] reduces the triphosphate impurity to less than 0.5% as $Na_5P_3O_{10}$. Similarly, when this ratio is 4/1 or greater, four crystallizations reduce the pyrophosphate originally present as such to an insignificant level. Unfortunately, however, some pyrophosphate is made in the recrystallization process,[18] so that it is difficult to reduce the pyrophosphate content of the anhydrous salt below 1% as $Na_4P_2O_7$.

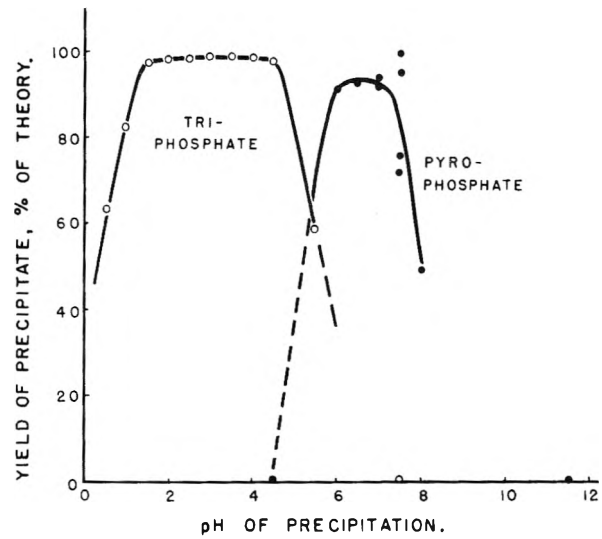

Fig. 5.—Effect of *p*H on precipitation of $Co(en)_3^{+3}$ by pure tri- or pyrophosphates; concentration of phosphate 0.02–0.05 *M*, Co reagent used in 6–20% excess.

Since a reproducible state of purity is attainable for both species, it is therefore possible to utilize the recrystallization process as the basis for determination of both pyro- and triphosphate by isotope dilution.[18] The results have a precision of 1–1.5% absolute on such samples as commercial tripolyphosphate and synthetic detergents containing triphosphate. The method has the advantage of being specific for the species being determined. However, when either the pyro- or triphosphate content of the phosphate is less than 20% the relative error becomes rather large because of the necessity of adding pure inactive pyro- or triphosphate for ratio adjustment.

Chromatography.—Two laboratories[7,16] have recently developed paper chomatography to the point where quantitative analyses can be made for each of the following phosphate species: ortho, pyro, tri, tetra, trimeta and tetrameta. It involves an unambiguous separation of the species, followed by determining the total phosphorus in each separated phosphate. The accuracy is of the order of 3–5%. An advantage of the chromatographic method, as applied to determination of pyro- and triphosphates for example, is that tetra- and higher polyphosphates do not interfere provided the conditions of experiment (*p*H, temperature, etc.) are chosen so as to make negligible the

production of the lower members by hydrolysis of the higher polyphosphates.

Solubility

Table IV contains phase data on the metastable binary system $Na_5P_3O_{10}$–H_2O. These were obtained at the Armour Research Foundation,[31] using

TABLE IV

HETEROGENEOUS EQUILIBRIA IN THE SYSTEM $Na_5P_3O_{10}$–H_2O AT 0 TO 50°

(Data of Jones, Cook and McCrone[31])

Temp., °C.	$Na_5P_3O_{10}$, wt. %	Time allowed, hr.	Crystal phase
−0.45	3.03	F.p. detn.	Ice
−0.74	5.54	F.p. detn.	Ice
−0.93	7.36	F.p. detn.	Ice
−1.08	8.91	F.p. detn.	Ice
−1.11	9.44	F.p. detn.	Ice
−1.22	10.45	F.p. detn.	Ice
−1.33	12.13	F.p. detn.	Ice
−1.41	13.92	F.p. detn.	Ice very near euctectic
0.00	13.98	50	$Na_5P_3O_{10}\cdot 6H_2O$
9.04	13.19	5.5	$Na_5P_3O_{10}\cdot 6H_2O$
14.70	13.00	116	$Na_5P_3O_{10}\cdot 6H_2O$
17.82	13.02	53.5	$Na_5P_3O_{10}\cdot 6H_2O$
20.10	12.92	143.2	$Na_5P_3O_{10}\cdot 6H_2O$
24.78	12.97	F.p. detn.	$Na_5P_3O_{10}\cdot 6H_2O$
24.87	12.96	51	$Na_5P_3O_{10}\cdot 6H_2O$
25.00	12.96	219	$Na_5P_3O_{10}\cdot 6H_2O$
29.84	13.02	72	$Na_5P_3O_{10}\cdot 6H_2O$
30.00	13.06	74.8	$Na_5P_3O_{10}\cdot 6H_2O$
30.01	13.23	75	$Na_5P_3O_{10}\cdot 6H_2O$
30.51	13.26	67	$Na_5P_3O_{10}\cdot 6H_2O$
30.81	13.26	3	$Na_5P_3O_{10}\cdot 6H_2O$
30.87	13.30	3	$Na_5P_3O_{10}\cdot 6H_2O$
30.93	13.26	3.5	$Na_5P_3O_{10}\cdot 6H_2O$
31.11	13.44	21.1	$Na_5P_3O_{10}\cdot 6H_2O$
31.31	13.28	67	$Na_5P_3O_{10}\cdot 6H_2O$
31.81	13.48	26	$Na_5P_3O_{10}\cdot 6H_2O$
32.39	13.32	3.5	$Na_5P_3O_{10}\cdot 6H_2O$
33.95	13.30	77.2	$Na_5P_3O_{10}\cdot 6H_2O$
34.83	13.38	66.5	$Na_5P_3O_{10}\cdot 6H_2O$
35.03	13.50	3.5	$Na_5P_3O_{10}\cdot 6H_2O$
39.83	13.57	65.8	$Na_5P_3O_{10}\cdot 6H_2O$
40.06	13.68	3.0	$Na_5P_3O_{10}\cdot 6H_2O$
44.97	14.02	3.0	$Na_5P_3O_{10}\cdot 6H_2O$
44.98	13.85	67	$Na_5P_3O_{10}\cdot 6H_2O$
50.07	14.34	1.0	$Na_5P_3O_{10}\cdot 6H_2O$

sodium triphosphate from commercial tripolyphosphate which had been purified by four crystallizations similar to those described under "Purification," except that a larger ethanol:water volume ratio (1:3) was used. While the purified triphosphate was not analyzed by the more reliable methods, the purity expected from the method of purification would be 98–99%. The solubility increases slowly with time and reaches the saturation value in a day or two at 0°, and in a few hours at 45–50°. Since hydrolysis, detected by analysis for orthophosphate, also causes an increase in solubility with time, the equilibrium solubility was recognized as a steady state between two periods of increasing solubility. Because of this limitation the data given at 55° and higher are not trustworthy; significant hydrolysis occurred before solubility equilibrium was attained. Approximate values at 55 and 70° were 14.8 and 16.5%, respectively.

At temperatures below 40° the data of Table IV agree reasonably well with the "approximate solubility" data reported graphically by Van Wazer,[32] but differ from them in showing a shallow minimum at about 20°.

Stability

Since triphosphate is metastable in contact with water, it is of interest to examine its rate of hydrolysis under various conditions.

Hydrolysis in Aqueous Solutions.—It has been shown that triphosphate hydrolyzes first to a mixture of ortho- and pyrophosphate, and ultimately to orthophosphate. At room temperature, however, the hydrolysis is rather slow as shown by the data for three concentrations and three methods of analysis in Table V. The concentration decreases linearly with time, *i.e.*, appears to follow a zero-order law. In 150 days the extent of decomposition was so slight that the *p*H remained practically unchanged at a value near that for pure $Na_5P_3O_{10}$, namely, 10.0. Thus, at *p*H values of 9–10 and at concentrations of 0.1 to 10.0 g./ml. the initial specific reaction rate k corresponds to the disappearance of 0.01 to 0.02% of the total triphosphate per day. The specific reaction rate appears to increase somewhat with increasing concentration, a trend contrary to that previously reported by Green[33] on very dilute solutions (6.5 to 65 p.p.m.) at *p*H 9 and 190°F. (88°C.), based on rate

TABLE V

HYDROLYSIS OF SODIUM TRIPHOSPHATE (STP) IN AQUEOUS SOLUTIONS AT 25–28°

Initial concn. 0.1 g./100 ml. Anal. for pyro by iso. diln.[a]			Initial concn. 0.7 g./100 ml. Anal. for tri by Co method[b]		Initial concn. 10 g./100 ml. Anal. for tri by G–M titrn.[c]	
Time, days	$Na_4P_2O_7$, %	Calcd. % of total STP remaining	Time, days	Total STP remaining, %	Time, days	Total STP remaining, %
0	0.37	99.5	0	98.9, 98.6	0	99 (assumed)
9	.49	99.3	7	99.1	14	98
20	.40	99.4	14	98.6	41	100
43	.77	98.9	35	98.0	70	100
76	.92	98.7	70	97.0	78	98
103	1.2	98.5	106	97.55	121	92
146	3.3	95.5	146	97.25	148	94.5
k = 0.010% $Na_5P_3O_{10}$/day			k = 0.013% $Na_5P_3O_{10}$/day		k = 0.02% $Na_5P_3O_{10}$/day	

[a] Analysis made for pyrophosphate by inverse isotope dilution[18] and calculating the triphosphate assuming one mole of triphosphate disappeared for each mole of pyrophosphate formed. Initial orthophosphate content = 0.15% as Na_2HPO_4. Thus, 100 − 0.37 − 0.15 = 99.48% $Na_5P_3O_{10}$ present initially. [b] Analysis made by the Weiser[29] colorimetric cobalt method. [c] Analysis made by a modified Gerber–Miles titration.[27]

(31) S. P. Jones, J. W. Cook and W. C. McCrone, research project at Armour Research Foundation, Chicago, Illinois, sponsored by the Procter & Gamble Co.

(32) J. R. Van Wazer, "Encyclopedia of Chem. Technology," Vol. X, edited by Kirk and Othmer, Interscience Publishers, Inc., 1953, p. 413.

(33) J. Green, *Ind. Eng. Chem.*, **42**, 1542 (1950).

of appearance of orthophosphate. Probably this simply means that dependence of rate on concentration cannot be determined from the data of Table V, primarily because of the use of analytical methods of widely differing accuracy. The least accurate rate, *i.e.*, that dependent on the titration method, may be in error by a factor of two. Suffice it to say that the widely different methods have given *about* the same hydrolysis rate.

It is well known that rate of hydrolysis of any condensed phosphate increases rapidly with increasing temperature. Following the disappearance of triphosphate at 180°F. (82°C.) by means of the cobalt method[29] in a solution initially containing 10 g. of $Na_5P_3O_{10}$ per 100 ml. gave the data of Table VI. Again the initial decrease of triphosphate concentration with time is approximately linear and the specific reaction rate derived from this part of the curve corresponds to disappearance of about 40% of the triphosphate during the first day (1.7%/hr.). This calculation ignores any effect of the change in *p*H which had fallen to about 7.5 by the end of the first day. The 2,000- to 4,000-fold increase in rate resulting from raising the temperature from 27 to 82° corresponds to a 4- to 4.5-fold increase for each 10° rise in temperature. For comparison, it may be noted that the above value appears consistent with the higher rate (5.8%/hr.) reported by Green[33] for triphosphate at a concentration of 65 p.p.m., controlled *p*H of 7, and temperature of 190°F. (88°C.). Both the lower average *p*H and the higher temperature used by Green would increase the rate. Van Wazer and co-workers[13] reported an even faster rate (14%/hr.) at a still higher temperature (90°) for a 1.29% $Na_5P_3O_{10}$ solution held at *p*H 7. Allowing for the small effect of the temperature difference, the rates determined by Green and by Van Wazer still differ markedly for some unknown reason.

TABLE VI

HYDROLYSIS OF SODIUM TRIPHOSPHATE (STP) IN AQUEOUS SOLUTION AT 180°F. (82°C.)

Initial concn. 10 g./100 ml.

Time, hr.	Total STP remaining, %
0	98.6, 98.9
4	91.4
7.5	84.9
16	72.0, 69.2
24	51.1, 52.9
40	29.7
48	21.1
64	6.3
72	4.0

Initial $k = 1.7\%$/hr.

Hydrolysis during Dehydration of Hexahydrate Crystals.—It has become increasingly evident[6,19–21] that hexahydrate does not lose water at any temperature below some point in the interval 130–140° without undergoing more or less hydrolysis. At 120° the amount of hydrolysis is relatively small if a shallow layer of hexahydrate crystals is quickly brought to temperature and the water vapor pumped off or swept away; however, in an ordinary oven the escape of water vapor is so delayed that almost complete decomposition into ortho- and pyrophosphates occurs. At 95–105° there is much hydrolysis regardless of how fast the water is removed. In one room temperature experiment nearly half of the water was removed from hexahydrate in a vacuum over P_2O_5; the *p*H of the product (1% solution in CO_2-free water) fell from 10.0 to 8.4 and about 40% of the triphosphate was converted to a mixture of ortho- and pyrophosphates. Because of this tendency to hydrolyze it is impossible to obtain satisfactory equilibrium measurements of the partial pressure of water vapor over hexahydrate crystals,[31] even at relatively low temperatures of 40–50°. Surface hydrolysis always modifies the system so that one always has more than the three phases demanded by the equation

$$Na_5P_3O_{10}\cdot 6H_2O \rightleftharpoons Na_5P_3O_{10}(II) + 6H_2O \quad (a)$$

Such surface hydrolysis becomes appreciable at 70–80° and quite rapid at 90° as demonstrated by the weight-loss data of Bonneman-Bémia.[6]

From studies of the dehydration of hexahydrate in open containers at temperatures near 100°, Raistrick[19] and Thilo and Seeman[20] conclude that what happens is

$$Na_5P_3O_{10}\cdot 6H_2O \longrightarrow Na_4P_2O_7 + NaH_2PO_4 + 5H_2O \quad (b)$$

According to Thilo and Seeman, heating the resultant equimolar mixture of pyro- and orthophosphate for a long time at the same temperature, or better for a shorter time at a slightly higher temperature, *e.g.*, 105–120°, simply results in recondensation thus

$$Na_4P_2O_7 + NaH_2PO_4 \longrightarrow Na_5P_3O_{10} + H_2O \quad (c)$$

Looking first at the recondensation reaction (c), experiments were made with equimolar mixtures of pure $Na_4P_2O_7$ and pure NaH_2PO_4 to see whether any triphosphate forms at 105–120°. In one case the mixture was put into solution and spray-dried to ensure an intimate mixture in the solid state; the only phase revealed by X-ray diffraction was $Na_4P_2O_7$, but diffuse halos indicated the presence of amorphous material. Upon analysis for triphosphate it was found to contain essentially no triphosphate (Table VII). Furthermore, heating this spray-dried mixture for 6 hours at 120° caused the appearance of Na_2HPO_4 in the X-ray pattern,

TABLE VII

ATTEMPTED CONDENSATION OF AN APPROXIMATELY EQUIMOLAR MIXTURE OF $Na_4P_2O_7$ AND NaH_2PO_4

	Triphos. as $Na_5P_3O_{10}$, %[a]	Loss in oven htg., % wt.	Tot. H_2O (ign. loss), %	*p*H of prod. (1% soln.)
A. Prod. htg. hexahydrate, 12 hr., 95°	34, 35, 30	(12.8)	11.50	8.11
B. Prod. htg. hexahydrate, 72.5 hr., 95°	5	18.1	...	
C. Mech. mixt. 0.98 mole $Na_2H_2PO_4$: 1.00 $Na_4P_2O_7$	...	..	...	7.66
D. Prod. C spray-dried from solution	2, 0	..	8.87	7.42
E. Prod. D heated 6 hr. at 120°	2, 2, 1	(2.8)	6.22	7.23

[a] By colorimetric $Co(en)_3^{+3}$ method of Weiser.[29] Results of 2% or less are probably not significantly different from zero.

TABLE VIII

ROUGH ANALYSES OF PRODUCTS OF HEATING 1/8 TO 1/2 INCH LAYERS OF HEXAHYDRATE IN OPEN DISHES

Sample	Oven temp., °C.	Heating, hr.	H_2O loss, %	Product *p*H in 1% soln.	P_2O_5, wt. % Molybd. total	Color ortho	Bell pyro	Bell tri	Moles pyro / Moles ortho
20-77	R.T.	None	None	10.0	45.6	...	N.F.	44.2	
28-3A	95	6	10.5	8.5	...	4	17	25	2
28-3E	95	20	19.0	7.75	...	14	34	3	1.2
28-3J	95	69	19.9	7.79	...	17	34	10	1.0
28-3N	95	162	19.6	7.82	...	16	39	3	1.2
20-80A	105	0.5	1.8	9.73	44.1	1	6	39	...
20-80B	105	1	2.9	9.51	46.3	3	11	32	2
20-80C	105	2	3.6	9.22	46.4	3	11	32	2
45-24A	105	2.5	13.0	...	51.9[a]	8	24[b]	17	1.5
45-24B	105	24	19.4	...	57.6[a]	16	38[c]	0	1.2
20-80F	105	70	20.1	8.23	56.3	13	42	6	1.6
20-80G	120	0.5	9.3	8.78	...	7	13	28	0.9
20-80H	120	1	17.2	8.23	54.4	12	36	6	1.3
20-80I	120	2	19.6	8.00	54.4	12	36	6	1.3
20-80L	120	70	20.5	8.20	57.0	10	41	7	2
28-5	120	6	18.5	7.9	...	11	39[d]	7	1.8
45-11	120	6	19.9	7.95	55.6	8	40[e]	3	2.5

[a] Two end-point determination of total P_2O_5, *cf.* Andrews.[36] [b] Quantitative X-ray analysis[18] (BeO internal standard) revealed 23% $Na_4P_2O_7$, 19% $Na_5P_3O_{10}\cdot 6H_2O$, no $Na_5P_3O_{10}$ or orthophosphate. [c] X-Ray analysis (BeO): 41% $Na_4P_2O_7$, nothing else crystalline. [d] After 2.5 years aging in bottle, X-ray analysis (BeO) revealed 28% $Na_4P_2O_7$ + a larger amount of $Na_3HP_2O_7\cdot H_2O$, but no $Na_5P_3O_{10}$ or orthophosphate. [e] X-Ray analysis (BeO): 43% $Na_4P_2O_7$, nothing else crystalline.

TABLE IX

ROUGH ANALYSES OF PRODUCTS OF HEATING VARIOUS DEPTHS OF HEXAHYDRATE AT 95° IN OPEN DISHES

Sample	Depth of cryst. layer, in.	Heating, hr.	H_2O loss, %	Product *p*H in 1% soln.	P_2O_5, wt. % Molybd. total	Color in ortho	Bell pyro	Bell tri.	Moles pyro / Moles ortho
28-3A	1/8	6	10.5	8.50	...	4	17	25	2
28-3B	5/8	6	3.4	9.00	47.0	0	2	41	...
28-3C	2	6	0.5	9.47	...	0	0	44	...
28-3D	8	6	1.3	8.91	45.7	0.5	3	41	...
28-3E	1/8	20	19.0	7.75	...	14	34	3	1.2
28-3F	5/8	20	17.5	7.75	...	27[a]	32	3	0.6
28-3G	2	20	17.5	8.01	54.6	4	41	9	5
28-3H	8	20	11.0	7.98	50.7	14[a]	41	5	1.5
28-3I	1/8	69	19.9	7.79	..	17	34	10	1.0
28-3J	5/8	69	19.1	2.65	..	21	36	1	0.9
28-3K	2	69	17.8	8.03	..	6	43	3	4
28-3L	8	69	16.7	7.91	..	10	44	1	2
28-3M	1/8	162	19.6	7.82	..	16	39	3	1.2
28-3N	5/8	162	19.5	7.71	..	18	38	2	1.1
28-3P	2	162	17.5	8.06	..	5	46	2	5
28-3R	8	162	16.7	7.90	..	10	43	3	2

[a] Ortho content probably too high because sum of ortho + pyro + tri-P_2O_5 exceeds the total P_2O_5.

but no formation of triphosphate. Thus, recondensation to triphosphate is unimportant at 120° or below. In fact, there was probably some hydrolysis of the pyrophosphate, because both the spray-drying and the further heating at 120° caused the 0.98:1.00 molar mixture of NaH_2PO_4 and $Na_4P_2O_7$ to drop in *p*H (Table VII).

Turning back to the initial decomposition, which is said to occur according to reaction (b), one can say that it is qualitatively adequate, but is really an oversimplification. It calls for a product with a *p*H of 7.6–7.7, as compared with hexahydrate decomposition products having a *p*H of 7.7–8.2 (Tables VIII and IX). Equation (b) calls for a water loss of 18.9%, as compared with observed losses up to 20.5%, depending on depth of hexahydrate crystals, temperature and time of heating. It also calls for a product containing an equimolar mixture of pyro- and orthophosphate, whereas hexahydrate decomposition products made at 95–120° usually contain relatively more pyrophosphate even in the early stages as shown by the approximate analyses in Tables VIII and IX.

One remarkable fact about such products of dehydrating hexahydrate at 90–120° to a steady state is that the X-ray diffraction pattern shows sharp lines for but one species, namely, $Na_4P_2O_7$. This observation has been reported by others.[15,20] Attempts to make the orthophosphate evident by slurrying such products with a little water, allowing them to dry slowly at room temperature, and re-X-raying the air-dried product fails to reveal orthophosphate in the vast majority of cases. Product 28-5 of Table VIII, like so many others with an oven water loss of 17–21% and a *p*H of 7.7–8.2, initially gave sharp diffraction lines for $Na_4P_2O_7$ only, plus

the usual broad halo showing the presence of considerable material amorphous to X-rays. After aging 2.5 years in a screw-capped bottle, quantitative analysis by X-ray diffraction[24] showed 28% $Na_4P_2O_7$ plus what appeared to be an appreciably larger amount of $Na_3HP_2O_7 \cdot H_2O$; no orthophosphate was detected; in fact, all lines were accounted for by $Na_4P_2O_7$ and $Na_3HP_2O_7 \cdot H_2O$. Upon slurrying the aged 28-5 with water and air-drying, the sample now showed only diffraction lines for $Na_4P_2O_7 \cdot 10H_2O$; again no orthophosphate was evident. On the other hand, synthetic mixtures made from pure $Na_4P_2O_7$ and NaH_2PO_4 or from pure $Na_3HP_2O_7$ and Na_2HPO_4 in 1:1 molar ratio, slurried with water and air-dried at room temperature or oven-dried always showed $Na_3HP_2O_7 \cdot H_2O$ + Na_2HPO_4 and/or $Na_2HPO_4 \cdot 2H_2O$. Thus, qualitative X-ray evidence says that orthophosphate is usually present in concentrations below that called for by equation (b).

The rough analyses for pyro- and orthophosphate in Tables VIII and IX tell a similar story. The pyrophosphate analyses are the more nearly correct the closer the triphosphate composition approaches zero, but are probably high by no more than 5% relative error in any case. The orthophosphate data, obtained by a colorimetric molybdate determination without separation from the condensed phosphates, are probably a little high due to hydrolysis of condensed phosphates during the development of the blue color; in the case of products 28-3F and 28-3H in Table IX, the ortho P_2O_5 appears to be significantly high because too much P_2O_5 is accounted for. It is probable that the pyro/ortho ratios given in Table VIII are approximately correct in most cases. This ratio usually exceeds 1:1.

TABLE X

TRACER ANALYSES OF A PRODUCT MADE BY HEATING A 1/8-INCH LAYER OF HEXAHYDRATE CRYSTALS FOR TWO HOURS AT 105°

Phosphate species	Reported as	Wt. %	Method of anal.
Tri	$Na_5P_3O_{10}$	24	Isotope diln.[18]
Pyro	$Na_4P_2O_7$	58	Inverse iso. diln.[18]
Ortho	Na_2HPO_4	19	Extractive colorim.[34]
Moles pyro/moles ortho		1.6	

much more decomposed than sample 20-80C in Table VIII or sample 10-105B in Table XI is not known, but all three samples clearly show a molar pyro/ortho ratio much greater than 1/1.

Another series of partially dehydrated samples was prepared at 95–140° by choosing a time of heating that would yield a product about 1/3 to 2/3 decomposed. The products were analyzed for pyro- and triphosphate by a modified Gerber and Miles titration method,[27] for orthophosphate by the Martin and Doty extractive procedure,[34] and for total P_2O_5 by the two-end-point method.[36] The results (Table XI) show that at all temperatures above 95° the molar ratio of pyro- to orthophosphate is greater than 1.00. This is true even at 150° where appreciable recondensation eventually takes place as indicated by rise in *p*H and by increase in intensity of $Na_5P_3O_{10}$(II) diffraction lines if the heating is prolonged.

It is therefore evident by a variety of methods that products of dehydrating hexahydrate at 90–120° are extensively decomposed into pyro- and orthophosphates, but, unlike the solution hydrolysis of triphosphate, they often contain more moles of pyrophosphate than orthophosphate. It therefore seems highly probable that at least two mechanisms are involved in this solid state hydrolysis of triphosphate. One probably is the simple hydrolytic cleavage of the triphosphate ion equivalent to equation (b) and the initial step can be represented thus

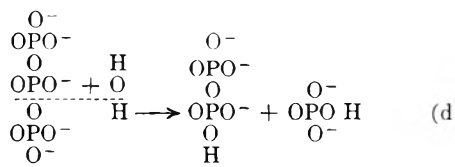

(d)

This may be followed by a second reaction such as

$$Na_3HP_2O_7 + Na_2HPO_4 \longrightarrow Na_4P_2O_7 + NaH_2PO_4 \quad (e)$$

But some other reaction capable of giving more pyrophosphate must be involved. Conceivably it could be some such reaction as

$$2Na_5P_3O_{10} + H_2O \longrightarrow Na_4P_2O_7 + 2Na_3HP_2O_7 \quad (f)$$

Ignoring the question of mechanism of such a reaction, one finds that it is reasonably consistent with the observed facts as follows

(1) The $Na_4P_2O_7$ phase is always detected by X-rays and orthophosphate is not. Recall that oven drying a 1/1 molar mixture of $Na_4P_2O_7$ and NaH_2PO_4 or of $Na_3HP_2O_7$ and Na_2HPO_4 fails to give

TABLE XI

TITRATION ANALYSES OF PRODUCTS OF HEATING 1/2-INCH LAYERS OF HEXAHYDRATE IN OPEN DISHES

Sample	Oven temp., °C.	Time of htg.	Prod. H_2O content	Prod. *p*H 1% soln.	P_2O_5, wt. % Total 2 EP	Colorim. ortho	Titrn. pyro	Titrn. tri	Moles pyro / Moles ortho
10-29A	95	7 hr.	19.0	8.6	47.4	4.2	6.9	36.3	0.82
10-105A	95	12 hr.	11.5	8.1	51.3	10.8	20.8	19.7	0.95
10-105B	105	2 hr.	14.0	8.4	49.4	6.1	17.8	25.5	1.47
10-24B	105	2.5 hr.	13.5	8.1	49.4	9.2	23.8	16.4	1.29
10-24C	120	50 min.	12.8	8.3	51.3	7.1	17.8	26.4	1.25
10-105C	150	20 min.	5.3	8.3	54.7	7.2	20.5	26.8	1.42
10-24D	150	25 min.	4.7	8.0	55.4	11.3	29.2	14.9	1.29

As a further check a sample made by heating hexahydrate for two hours at 105° was analyzed by recently developed methods known to be both reliable and specific for the species being determined.[18,34,35] Why this sample (Table X) is so

(34) J. B. Martin and D. M. Doty, *Anal. Chem.*, **21**, 965 (1949).

(35) H. W. Lampe, unpublished work, Research Department, Chemical Division, The Procter & Gamble Co.

(36) J. T. R. Andrews, *J. Am. Oil Chem. Soc.*, **31**, 192 (1954).

$Na_4P_2O_7$ + amorphous but shows $Na_3HP_2O_7 \cdot H_2O$ and Na_2HPO_4 by X-ray diffraction.

(2) The material amorphous to X-rays may well be largely $Na_3HP_2O_7$ which is known not to crystallize readily. Also recall that an aged decomposition product (28-5 in Table IX) contained much $Na_3HP_2O_7 \cdot H_2O$. Some amorphous Na_2HPO_4 and/or NaH_2PO_4 is probably present also.

(3) Equation (f) together with (b) or (d) accounts for water losses between 5 and 5.5 moles quite as well as the recondensation hypothesis (equation (c)).

(4) The range of *p*H values 7.7–8.3 is better accounted for by a combination of equations (f) with (d) or (b) than by (b) alone (Table XII). Recall that heating a 1/1 molar mixture of $Na_4P_2O_7$ and NaH_2PO_4 actually pushed the *p*H downward from 7.6 (Table VII).

TABLE XII

SOME PERTINENT *p*H VALUES

Salts mixed	Molar ratio	*p*H of 1% soln.
$Na_4P_2O_7 + NaH_2PO_4$	1:1	7.63
$Na_3HP_2O_7 + Na_2HPO_4$	1:1	7.63
$Na_4P_2O_7 + Na_3HP_2O_7$	1:2	8.11

(5) Most of the molecular weight data of Thilo and Seeman[20] are accounted for. Thus, hexahydrate samples which have been heated at 95–98° so as to lose 5 moles of water give molecular weights close to the 193 demanded by equation (b) or (d). Those which have been heated at 100–120° so as to lose 5 to 5.5 moles (18.9–20.8%) of water have molecular weights between 193 and 251, the latter value corresponding to complete conversion *via* equation (f). Only when hexahydrate is heated so that more than 5.5 moles of water is lost does one have to invoke the recondensation to triphosphate *via* equation (c) or (g).

$$Na_4P_2O_7 + 2Na_3HP_2O_7 \longrightarrow 2Na_5P_3O_{10} + H_2O \qquad (g)$$

Recondensation has been detected at temperatures above 120° by X-rays. Thus, products made by heating hexahydrate for 1/2 hour at 150° show little or no $Na_5P_3O_{10}$(II), besides the $Na_4P_2O_7$ plus amorphous material. But similar products heated for a much longer time, *e.g.*, 70 hours, at 150° reveal an increase in $Na_5P_3O_{10}$(II) content by X-rays. Such samples have lost at least 5.5 moles of water and their *p*H has risen from a minimum near 8.0 (1/2 hour) to 8.4–8.6 (20 hr. or more). Thus, in dehydrating triphosphate hexahydrate the temperature 120° causes only hydrolysis, but higher temperatures may cause appreciable recondensation after the initial extensive hydrolysis.

Lest it be supposed that reaction (a) is never a factor another set of experiments must be mentioned. At 135–230° $Na_5P_3O_{10}$(II) is formed if the water is quickly flashed out. As an example of this, hexahydrate in 1/2-inch depth in a 10-mm. test-tube was heated suddenly to temperature (oil-bath), held there for 10 minutes to allow the water vapor to escape into the laboratory atmosphere, and the samples chilled by means of an ice-bath. By X-raying at room temperature it was shown that such products heated at 70–120° were largely hexahydrate, and one heated at 135° still contained at least some hexahydrate in addition to considerable $Na_5P_3O_{10}$(II), but at 150–230° $Na_5P_3O_{10}$(II) was the only crystalline species evident. None of these products had a *p*H below 9.4. A somewhat similar product,[35] made by heating hexahydrate for two hours in an oven at 200°, gave the following analysis

94% $Na_5P_3O_{10}$ (isotope dilution[18])
5.2% $Na_4P_2O_7$ (inverse isotope dilution[18])
1.8% Na_2HPO_4 (Martin and Doty[34])

An alternative mechanism of triphosphate decomposition might be a disproportionation in which both more and less condensed phosphates are formed. The only slight indication of such a reaction is the failure of hexahydrate decomposition products to give a precipitate with tris-(ethylenediamine)-cobalt(III) ion under the conditions specified by Weiser.[29] The inhibitory effect is large enough to prevent precipitation when 1–2 g. of pure triphosphate is added to each gram of decomposition product and a suitable aliquot of the resulting solution taken for the test. While this does not prove the presence of higher polyphosphates, it is true that they can prevent precipitation of $Co(en)_3H_2P_3O_{10}$, and therefore such compounds may be present. However, the amount of more condensed phosphate need not be large. Hence, decomposition of hexahydrate at 90–120° should be regarded as due mainly to reactions such as (b) and (f).

Reaction with Calcium Ions in Dilute Solutions

For dilute systems containing $CaCl_2$ and $Na_5P_3O_{10}$ the boundary between homogeneous and heterogeneous regions at 60° is shown in Fig. 6; it was determined turbidimetrically[37] after attainment of steady state, which often required only 10–30 minutes, but sometimes required 1–3 hours. The heterogeneous region is rather wide and comes close to the calcium axis, so that the area of clear solutions is very narrow on this side (Fig. 6A). Of more interest is the behavior on the other side DE where, in general, more than a mole of triphosphate per mole calcium is required to prevent precipitation (Fig. 6B). The right branch DE of this curve shifts to the right as sodium salts are added to the solutions (Table XIII), that is, more sodium triphosphate is required to clarify the sodium rich solutions. This rightward shift increases with increasing concentra-

TABLE XIII

EFFECT OF SODIUM SALTS ON SOLUBILITY OF CERTAIN CALCIUM TRIPHOSPHATE PRECIPITATES

Kind of Na salt	Concn. of Na salt, g./l.	Ca^{+2} concn., mmoles/l.	$P_3O_{10}^{-5}$ concn. mmoles/l. required to suppress pptn.
None	..	1.2	1.2
Na_2SO_4	5	1.2	1.5
Na_2SO_4	10	1.2	2.0
None	..	3.6	4.0
Na_2SO_4	2.5	3.6	5.5
Na_2SO_4	5.0	3.6	8.0
NaCl	10	3.6	14.0

(37) J. A. Gray and K. E. Lemmerman, unpublished results, Research Department, Chemical Division, The Procter & Gamble Company.

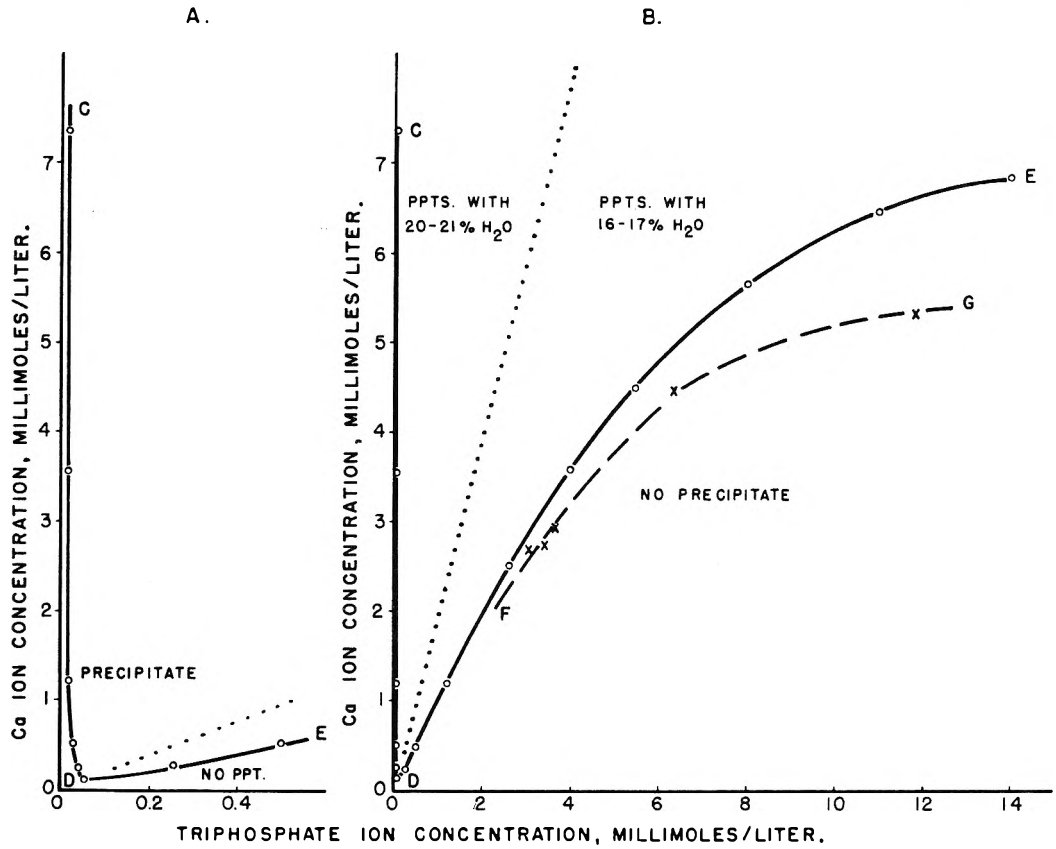

Fig. 6.—Region of calcium triphosphate precipitation at 60° in the system $CaCl_2$-$Na_5P_3O_{10}$-H_2O. Solid curve CDE obtained turbidimetrically; dashed curve FG, saturated solutions obtained from compositions between dotted line and curve DE.

tion of sodium salt and also becomes more marked the higher the calcium level. These observations suggest that the precipitates along the right boundary of the heterogeneous region contain sodium, an inference verified by semi-quantitative spectroscopic analyses of a few of the precipitates.

In the very dilute region near the minimum D in the above curve conductometric evidence was found which is consistent with the existence of a soluble 1:1 calcium:triphosphate complex $CaP_3O_{10}^{-3}$. The conductometric measurements[37] were made by the Job[38] method of continuously varying the Ca^{+2}:$P_3O_{10}^{-5}$ ratio, the concentration being deliberately chosen so low that no precipitate could form at any ratio.

Search in the long ultraviolet region (available range 210–400 mμ) showed no characteristic absorption for Ca^{+2} or $P_3O_{10}^{-5}$ ions,[39] hence no effort was made to investigate calcium triphosphate soluble complexes spectroscopically.

While further study may well reveal more than one soluble calcium triphosphate complex, as has been observed for certain metals with pyrophosphate,[40] nevertheless, it has been tentatively assumed that $CaP_3O_{10}^{-3}$ is the only one involved in the region of the clarification points along the right branch of the curve in Fig. 6. Its dissociation constant K_D has been estimated from measurements[37] of the clarification of calcium oxalate suspensions by sodium triphosphate, giving 2.1×10^{-7} at 60° and 3.1×10^{-7} at 30°. The latter value is near that reported by Topley[41] for 25°. Apparently temperature has negligible effect on stability of the complex within the range tested.

The boundary between heterogeneous and homogeneous compositions along the high triphosphate branch has also been determined by analysis (FG, Fig. 6), using radioactive tracers Ca^{45} acetate and $Na_5P^{32}{}_3O_{10}$. Total compositions between the right branch DE of the curve and the dotted line in Fig. 6 were made. After equilibration at 60° the precipitates were filtered off and the saturated solutions analyzed for Ca and for triphosphate by counting. The total activity was determined first, then the $P^{32}{}_3O_{10}$ was determined by interposing between solution and counter an aluminum foil thick enough to absorb the less powerful beta radiation from Ca^{45} and calcium was determined by difference between the total activity and that due to P^{32}. It will be seen that these solution compositions fall to the right of the turbidimetric curve, the more so the higher the calcium level. The substitution of acetate for chloride probably had little effect. More important is the fact that each composition from which precipitation took place contained more Na^+ than the saturated solution and hence more Na^+ than the corresponding point on the turbidi-

(38) P. Job, *Ann. chim.*, [10] **9**, 113 (1928).

(39) H. V. Meek, unpublished results, Research Department, Chemical Division, The Procter & Gamble Company.

(40) L. B. Rogers and C. A. Reynolds, *J. Am. Chem. Soc.*, **71**, 2081 (1949).

(41) B. Topley, *Quart. Revs.*, **3**, 345 (1949).

metric curve DE (*cf.* Fig. 6 and Table XIII). This alone probably accounts for the observed difference.

The precipitates within the heterogeneous region of Fig. 6 have been characterized[37] by X-ray pattern and approximate analyses, but not sufficiently to allow a complete definition of the equilibrium solid phases. Most precipitates made from compositions to the left of the dotted line of Fig. 6 are amorphous to X-rays and in air-dried form contain 20–21% H_2O, while those from compositions to the right of this line are crystalline and in air-dried form contain 16–17% H_2O. Abbreviated attempts to determine their composition by the tracer method of analysis already described indicate great variation in composition in both regions, higher Ca/P_3O_{10} ratios usually being found in the former than in the latter. However, occasional reversals were encountered with respect to all three properties. The crystalline patterns were in general similar, but scarcely any two were identical suggesting that mixtures of crystalline species were involved. Whether this variability of composition is due solely to properties of the mixed Na^+–Ca^{+2}–$P_3O_{10}^{-5}$–acetate–H_2O system or to some thermal decomposition (hydrolysis) of the triphosphate during the one-half to three hours equilibration at 60° was not determined.

Because the *p*H is observed to drop during precipitations in calcium-rich compositions, the possibility of a basic precipitate such as $Ca_3(P_3O_{10})(OH)\cdot 5H_2O$ must be considered. In the region to the right of the dotted line of Fig. 6, the precipitates often contain significant amounts of sodium, but frequently not enough to correspond to the salt $NaCa_2P_3O_{10}\cdot 4H_2O$ reported by Bonneman-Bémia[6] as the product of room-temperature precipitation between $CaCl_2$ and $Na_5P_3O_{10}$ at or near the 1:1 molar ratio.

While the main outlines of the interaction of Ca^{+2} and $P_3O_{10}^{-5}$ ions are now evident, much remains to be done before a complete description can be given.

Tetraphosphate

While sodium tetraphosphate is clearly metastable in the Na_2O–P_2O_5–H_2O system, nevertheless it can be prepared in aqueous solutions at low temperatures by alkaline hydrolysis thus

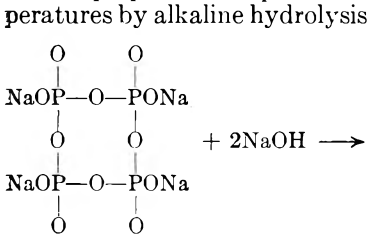

Tetrametaphosphate

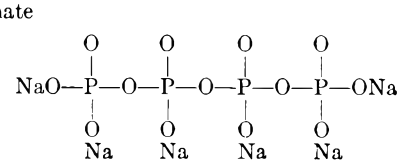

Tetraphosphate

Thilo and Rätz[14] carried out the hydrolysis at 40°, using exactly two moles of NaOH per mole of tetraphosphate. While they claimed complete conversion to tetraphosphate in 100 hours, their evidence was largely qualitative. Thus, impurities were removed by repeated acetone precipitation of the tetraphosphate as a viscous liquid. The viscous solution gave a Na:P ratio of 6:4 and an amorphous precipitate with calcium, silver or zinc. Tri- or pyrophosphate gives crystalline precipitates with zinc and frequently also with calcium. Westman, *et al.*,[7,15] used a higher hydrolysis temperature (70°) and after 2 hours found 60% of the phosphorus in tetraphosphate form, based on colorimetric P determination after chromatographic separation of phosphate species. The remainder was largely present as tetrametaphosphate, but some was present as lower phosphates, tending to show that higher temperatures are unfavorable to obtaining high yields of pure tetraphosphate. This has been confirmed by our own experience, in some preliminary experiments in which concentrated NaOH was used to open the tetrametaphosphate ring. This was tried because, when a moderately concentrated solution of trimetaphosphate $Na_3P_3O_9$ is treated with concentrated sodium hydroxide (30–40%), the phosphate can be precipitated almost quantitatively as the hexahydrate of triphosphate, $Na_5P_3O_{10}\cdot 6H_2O$. The conversion of trimeta- to triphosphate is fast at temperatures of 50–75°, being complete in about an hour. But when the analogous reaction is tried with tetrametaphosphate at temperatures of 50–100°, any crystalline products precipitated always proved to be some one of the known sodium phosphates (X-ray pattern), usually $Na_4P_2O_7$ and/or $Na_5P_3O_{10}$. In one case the product was largely anhydrous sodium triphosphate $Na_5P_3O_{10}$(II).

Bell, Audrieth and Hill[42] were unable to detect tetraphosphate in the products of solution hydrolysis of tetrametaphosphate. This may have been due partially to their use of high temperature (100°), which may not allow the tetraphosphate concentration to become large, but probably more to their method of analysis (*cf.* Bell[11]), which, as they point out, counts tetraphosphate as triphosphate, and hence gives no way to detect tetraphosphate.

Purification

Starting Material.—Our own efforts to obtain a pure tetraphosphate followed similar lines. The starting material was a technical grade sodium tetrametaphosphate $Na_4P_4O_{12}\cdot 4H_2O$ obtained from the Victor Chemical Works, Chicago, Illinois. It was purified by two crystallizations from water at room temperature by adding ethanol as nonsolvent (300 g. of crude $Na_4P_4O_{12}\cdot 4H_2O$, 2 kg. of H_2O, 1 l. of ethanol in the first crystallization, *ca.* 245 g. of $Na_4P_4O_{12}\cdot 4H_2O$, 1 kg. of H_2O and 500 ml. of ethanol in the second crystallization). Both the first and the second crop of crystals were washed first with 20% ethanol, then with 50% ethanol. The yield of crystals, air-dried to constant weight, was 232 g. of $Na_4P_4O_{12}\cdot 4H_2O$. By acid–base titration it was found that the spread between the *p*H 4–5 and the *p*H 9–10 end-points decreased to the expected zero value in the two crystallizations

	Ml. 0.1 *N* NaOH per g air-dried product
Orig. material	4.67
After 1st crystn.	0.58
After 2nd crystn.	0.00

(42) R. N. Bell, L. F. Audrieth and O. F. Hill, *Ind. Eng. Chem.*, **44**, 568 (1952).

The product was further characterized as follows

	Found	Theory for $Na_4P_4O_{12}\cdot 4H_2O$
*p*H of 1% solution, CO_2-free, 25°	6.4, 6.5	...
% P_2O_5 by titration method[36]	59.5, 59.2	59.17
% Volatile, 2 hr., 400°	15.6, 15.4	15.00

Its X-ray pattern was identical to that of Bell, Audrieth and Hill[42] for $Na_4P_4O_{12}\cdot 4H_2O$ (low-temperature form).

Conversion to Sodium Tetraphosphate.—Since preliminary experiments had demonstrated that the tetraphosphate decomposes rapidly at elevated temperatures in aqueous systems, solutions of the sodium salt (11.5%) were prepared at room temperature 25–28°, usually with a 100% excess of NaOH for retarding the subsequent hydrolysis of the tetraphosphate. In one such solution titrations of excess base at intervals showed that the theoretical 2.00 moles of NaOH had been used up in three weeks and that only 0.15 mole more NaOH consumption had occurred in six months. Thus, the further hydrolysis (degradation of the tetraphosphate) is quite slow at room temperature. Once the tetraphosphate solution is made, it can be kept for six months with little decomposition, especially if stored in the refrigerator.

From the above 11.5% solution a concentrated viscous solution (*ca.* 44% $Na_6P_4O_{10}$) can be made by adding 1 volume of ethanol for each volume of water. Thilo and Rätz[14] got a similar concentrate, using acetone instead of ethanol. Impurities including the excess of NaOH are largely eliminated by two such precipitations. Two such concentrated solutions gave average chain lengths of 4.02 and 3.95, respectively, as determined by the method of Samuelson[43] or Van Wazer.[44]

All attempts to crystallize and purify the tetraphosphate started from the 11.5% solution (the NaOH was always neutralized just before use) or from the 44% concentrate. A wide variety of tests, paralleling the attempts by Thilo and Rätz,[14] failed to induce crystallization of sodium tetraphosphate itself. After the discovery that hexaguanidinium tetraphosphate could be crystallized from formamide-rich mixtures of formamide with water alone (or with water and ethanol), similar attempts were made on the sodium salt without success, except that a trace of cloud formed in one solution containing formamide, ethanol and water; after standing for a month at 0°, a very few crystals were obtained with an X-ray pattern differing from patterns of known sodium phosphates. This approach is far less attractive than that involving the guanidinium salt. Even if the sodium salt is eventually crystallized, it will be hygroscopic and hence not generally useful as a source of tetraphosphate reagent.

Metal Ion Tetraphosphates.—Attempts to find a metal ion whose tetraphosphate is crystalline and has solubility characteristics favoring purification were unsuccessful. Metal ions such as Ag, Ba, Ca and Zn not only give rather insoluble amorphous precipitates as reported by Thilo and Rätz,[14] but also precipitate the lower phosphate impurities and hence are not useful for purification.

Lithium was tried because certain lithium phosphates have a rather low solubility (*e.g.*, Li_3PO_4). In this case, the free tetraphosphoric acid, prepared by ion exchange, was neutralized with LiOH and unsuccessful attempts were made to precipitate the Li salt. Because of its high water solubility the Li tetraphosphate could be recovered only as a concentrated and extremely viscous solution which dried at room temperature to an amorphous solid.

Tris-(ethylenediamine)-cobalt(III) ion did not give a precipitate with tetraphosphate at any *p*H tried (2.5 to 10).

Tetraacridinium Tetraphosphate.—In biochemical studies a crystalline acridine salt of adenosine triphosphoric acid has served as (a) a derivative of definite melting point for identification[45] purposes, (b) a means of purifying the adenosine triphosphate,[46] and (c) a reagent stable on storage.[46] It therefore seemed desirable to see whether a crystalline acridinium tetraphosphate could be prepared.

Since double decomposition between sodium tetraphosphate and acridinium chloride (AdH)Cl either gave no precipitate or precipitated (AdH)Cl, the acridinium tetraphosphate was prepared by neutralizing tetraphosphoric acid. The acid was prepared by passing 1% Na tetraphosphate through an ion-exchange column (IR 100 or 120), the acid dropping directly into an alcoholic solution of acridine. Initially six moles of acridine was used for each mole of tetraphosphate, but it was soon found that acridine is too weak a base to neutralize the weak hydrogens. Accordingly, about four moles (preferably 4.2 moles) was used in most cases and gave the same product (X-ray pattern) as six moles. The yellow product approximates the composition of the tetraacridinium salt $(AdH)_4H_2P_4O_{13}\cdot xH_2O$, the wet solid being crystalline (Table XIV), but the air-dried sample, which is within 5% of the $(AdH)_4H_2P_4O_{13}$ composition (Table XV) is largely amorphous to X-rays. Each product precipitated from the dilute solution as described, was recrystallized 1–3 times, either from water or from water–ethanol mixtures, by dissolving at 35–45° and cooling to 0°. Except for the solvent containing 50 volume % ethanol, these solvents gave products deficient in acridine as shown by the analyses in Table XV. The acridine was determined by adding the theoretical amount of NaOH, extracting the acridine with ethyl ether, evaporating the ether, and weighing the acridine. The P_2O_5 determinations were by the two-end-point method described by Andrews.[36] The preparation *via* 50% ethanol is preferred since it gives the correct Ad:P ratio and allows purification so that the phosphate has the desired chain length of four. After purification the tetraacridinium salt can be converted to an aqueous solution of the tetra-, penta- or hexasodium salt by the process described above for determining acridine. The main defect of the tetraacridinium salt as a reagent is its lack of stability in storage (compare preparations C with D and E with F in Table XV). The tetraphosphate also darkened during storage, other acridinium phosphates did not. Thus, it seemed better to change to a strong base so that the two weak hydrogens could also be neutralized. This led to the preparation of the guanidinium salt.

Hexaguanidinium Tetraphosphate.—This salt crystallizes readily and has been made both by

(43) O. Samuelson, *Svensk. Kem. Tid.*, **56**, 343 (1944).

(44) J. R. Van Wazer, *J. Am. Chem. Soc.*, **72**, 647 (1950).

(45) T. Wagner-Jauregg, *Z. physiol. Chem.*, **239**, 188 (1936).

(46) J. Baddiley, A. M. Michelson and A. R. Todd, *J. Chem. Soc.* 582 (1949).

TABLE XIV

X-RAY PATTERNS OF ACRIDINIUM (AdH) AND GUANIDINIUM (GuH) PHOSPHATES

Cu Kα, λ = 1.5418 Å., specimen-to-film = 7.16 cm., Ni filter. Moisture content of AdH salts unknown; all were X-rayed in air-dried form except for the tetraphosphate, which was X-rayed in wet crystal form. V = very, S = strong, M = moderate, W = weak, b = broad

$(AdH)H_2PO_4$		$(AdH)_2H_2P_2O_7$		$(AdH)_3H_2P_3O_{10}$		$(AdH)_4H_2P_4O_{13}$		$(AdH)_6P_6O_{18}$		$(AdH)_4P_4O_{12}$		$(GuH)_4P_2O_7 \cdot H_2O$				$(GuH)_4P_2O_7$				$(GuH)_6P_6O_{18}$				$(GuH)_6P_4O_{13} \cdot H_2O$	
d, Å.	*I*	*d*, Å.	*I*	*d*, Å.	*I*	*d*, Å.	*I*	*d*, Å.	*I*	*d*, Å.	*I*	*d*, Å.	*I*	*d*, Å.	*I*	*d*, Å.	*I*	*d*, Å.	*I*	*d*, Å.	*I*	*d*, Å.	*I*	*d*, Å.	*I*
7.14	VVS	12.4	M	12.3	VW	13.8	S	17.0	M	14.6	VW	11.3	VW	1.76	Mb	9.14	VVW	1.73	VVW	12.3	VW	1.89	VW	9.13	S
5.13	VVS	10.3	S	9.78	VW	12.0	VW	9.70	S	10.4	S	8.01	VS	1.74	VW	8.37	VVS	1.69	Mb	7.96	VW	1.85	W	8.51	S
4.37	VVS	8.25	S	8.51	VVS	10.8	VS	8.38	VVS	8.31	S	6.58	VS	1.69	VVW	7.42	VVW	1.66	VVW	7.57	M	1.82	VW	6.63	VVS
4.24	M	7.47	VVS	7.47	W	9.45	VVS	6.59	M	6.92	W	5.86	VVSb	1.68	W	6.63	VVS	1.63	W	6.83	VS	1.77	W	6.15	W
3.95	M	6.22	S	6.63	W	8.78	VVW	5.77	M	6.18	W	5.13	VW	1.64	M	6.18	M			6.47	M	1.75	VVW	5.92	W
3.69	M	5.28	S	6.05	W	7.68	VW	5.33	S	5.65	W	4.86	M	1.62	M	5.80	M			6.15	M	1.73	VW	5.33	S
3.52	VVS	4.66	M	5.46	VVS	7.09	M	5.11	VS	5.23	VVS	4.55	S			5.48	W			5.54	S	1.71	W	4.56	M
3.36	S	4.43	M	4.70	M	6.55	M	4.59	Sb	4.68	M	4.30	S			4.64	VVSb			5.33	S			4.29	S
3.20	VW	3.98	M	4.25	M	5.99	M	4.16	VW	4.22	M	4.03	S			4.30	M			4.68	M			4.08	VW
3.09	VVS	3.73	W	3.79	M	5.51	S	3.95	W	4.05	M	3.92	S			4.13	W			4.51	VW			3.88	VS
3.00	M	3.48	VVS	3.47	VS	5.06	VS	3.76	VW	3.72	W	3.69	Sb			3.99	VVS			4.29	M			3.73	VS
2.80	M	3.32	VVW	3.29	S	4.76	W	3.57	VS	3.60	M	3.52	M			3.78	W			4.09	VS			3.63	W
2.73	M	3.21	S	3.07	M	4.57	W	3.43	VS	3.35	VVS	3.36	VS			3.66	S			3.97	M			3.48	VW
2.57	W	3.08	S	2.80	W	4.13	VW	3.26	VVS	3.19	VW	3.30	M			3.59	VS			3.79	VW			3.40	S
2.44	VW	3.06	Wb	2.49	VVW	3.88	M	3.06	M	3.08	M	3.18	M			3.49	VS			3.61	VS			3.36	S
2.34	VVW	2.66	W	2.29	VVW	3.76	S	2.93	M	2.94	VW	3.00	S			3.39	VS			3.48	M			3.12	S
2.27	VW	2.49	VVW	2.10	VWb	3.53	VVS	2.73	W	2.80	W	2.89	W			3.31	M			3.41	VS			3.07	W
2.20	VW	2.38	VW	1.92	W	3.31	VVS	2.65	M	2.62	W	2.81	S			3.17	W			3.20	VW			2.94	M
2.15	W	2.24	VW	1.76	W	3.23	S	2.55	VVW	2.40	VWb	2.66	S			3.02	S			3.16	S			2.87	VW
1.98	Wb	2.14	W			3.13	M	2.44	Sb	2.21	VWb	2.59	Wb			2.90	Mb			3.06	S			2.78	W
1.93	Wb	2.04	VW			2.97	Sb	2.30	VW	2.09	VWb	2.51	Wb			2.75	S			3.01	W			2.72	W
1.87	VVW	1.98	VVW			2.85	M	2.19	VVW	2.04	VWb	2.42	W			2.71	W			2.95	W			2.67	W
1.82	W	1.90	W			2.74	M	2.11	W	1.93	VVW	2.34	W			2.68	VW			2.92	W			2.57	M
1.74	M	1.81	VVW			2.64	W	2.05	W	1.81	VVW	2.30	W			2.62	S			2.78	Mb			2.43	M
1.67	Wb	1.76	VW			2.43	W	1.99	W	1.76	W	2.27	S			2.45	M			2.68	M			2.33	VW
1.62	VVW	1.71	VW			2.18	M	1.93	W	1.70	W	2.18	VW			2.41	M			2.54	W			2.27	VW
1.58	VW	1.65	VWb			2.14	VW	1.88	W	1.67	VVW	2.12	M			2.37	W			2.51	W			2.20	VW
						1.98	W	1.80	M	1.60	VVW	2.07	VW			2.28	W			2.45	W			2.17	VW
						1.91	W	1.74	W	1.54	VVW	2.04	VW			2.22	W			2.39	W			2.13	VVW
						1.76	W	1.70	M	1.49	VVW	2.01	VW			2.16	VW			2.33	VW			2.05	W
						1.73	VVW	1.68	VW			1.97	M			2.10	VW			2.28	W			1.96	VW
						1.70	M	1.63	VWb			1.94	M			2.08	VVW			2.23	W			1.92	VVW
						1.65	W	1.61	VWb			1.90	VW			2.04	VVW			2.18	VVW			1.89	VW
						1.62	VW					1.87	VW			2.02	VWb			2.12	VWb			1.83	VW
												1.84	VVW			1.97	M			2.07	VW			1.76	VVW
												1.83	VW			1.88	M			2.02	VWb			1.74	W
												1.81	VW			1.82	M			1.99	VW			1.70	VW
												1.79	VW			1.76	VVW			1.94	VVW			1.66	W

TABLE XV

ANALYSES AND APPROXIMATE SOLUBILITIES OF TETRAACRIDINIUM TETRAPHOSPHATE

Preparation	A	B	C	D[a]	E	F[a]	G	Theory for $(AdH)_4H_2P_4O_{13}$
Mol. ratio used, Ad:P	1.05:1	1.05:1	7:8	7:8	1.05:1	1.05:1	1.05:1	1:1
Crystd. from	H_2O	H_2O	H_2O	H_2O	50% EtOH	50% EtOH	60% EtOH	..
No. crystn.	2	4	3	3	2	2	2	..
Approx. soly. (t, °C.), %	1.5(45)	1.5(45)	3(40)	3(40)	3(35)	3(35)	3(35)	..
Approx. soly. at 0°, %	0.3	0.3	0.5	0.5	0.4	0.4	0.4	..
% Acridine, Et_2O extn.	63.7	63.4	61.5	60.4	64.3	64.0	58.3	68.0
% P_2O_5, two-end-point	27.1	26.3	27.7	27.8	25.6	26.0	23.9	26.9
Av. chain length of phosphate	4.00	3.84[b]	3.93	3.72	4.00	3.48	4.08	4.00
Mol. ratio found, Ad/P	0.93	0.95	0.88	0.86	1.00	0.98	0.97	1.00

[a] Preparation D is preparation C, reanalyzed after storage for one month. Preparation F is preparation E reanalyzed after storage for 18 mo. [b] Sample too small for reliable titrations.

TABLE XVI

ANALYSES OF CRYSTALLINE GUANIDINIUM POLYPHOSPHATES

	Tetraphosphate data				Triphosphate data		Pyrophosphate data	
	Found	Found	Found	Theory for $(GuH)_6P_4O_{13}\cdot H_2O$	Found	Theory for $(GuH)_5P_3O_{10}$	Found	Theory for $(GuH)_4P_2O_7\cdot H_2O$
Sample no.	04-42	04-92	04-99		04-85A		04-75B	
No. crystn.	1	2	3		2		3	
pH of 1% soln.		9.62	9.68		10.08		10.28	
pH of 0.5% soln.	9.32		9.70		....		...	
% Volatile[a]	1.9	2.23	2.30	...	0.1	0.0	4.36	4.17
% H_2O of constitution[b]	...	0.55	0.57	...				
% Total H_2O	...	2.78	2.87	2.54				
% N, orig. sample	36.7	34.6	...	35.5	37.2	38.0	39.0	38.9
% N, after dehydn.	...	34.7	...					
% P_2O_5, M. & D., ref. 33	40.2	39.9	...	40.0	38.3	38.5	32.3	32.8
% Purity by titration from pH 4+ to 9.5 end-point	101	97	98	97.5	100	100	97	96
Water soly., 27°, % anhyd. salt	...	63	...		74		17.4	

[a] Volatile 20 hr., 120° for the tetraphosphate, 2 hr., 110° for others. [b] Obtained by titration to upper end-point near pH 10.

neutralizing tetraphosphoric acid with guanidine $HN{=}C(NH_2)_2$ (abbreviation Gu) and by double decomposition between Na tetraphosphate and guanidinium chloride (GuH)Cl. The X-ray pattern of the two products was identical. Only the more convenient double decomposition will be described. While the salt can be obtained by low temperature evaporation of a concentrated water solution, it is more convenient to use formamide containing some water as the solvent.

While the optimum conditions have not been precisely established, a successful preparation (77% yield) of the hexaguanidinium salt was obtained by the following procedure: To 10 g. of the sirupy liquid (4.4 g. of crude $Na_6P_4O_{13}$) add the solution obtained by dissolving 12 g. of guanidinium chloride in 24 ml. of water. Then dilute the mixture with 120 ml. of formamide. If the solution is not clear dilute until clear with water:formamide in the ratio of 1:4 by volume. Induce crystallization by scratching the walls of the beaker or more conveniently by seeding (a small portion of the solution diluted with formamide and ethanol often starts crystallizing) and stir the solution for one hour. After filtering wash the crystals three times each with formamide and ethanol, then air-dry. The product so obtained was already fairly close to the composition of pure hexaguanidinium salt, for its P_2O_5-content was 39.5 (theory = 40.0 P_2O_5 for monohydrate) and it contained no chloride. Tests have not been made to determine how much the excess of guanidinium chloride or the concentration of formamide can be reduced without altering the completeness or the course of the reaction. In precipitating the triphosphate, by the corresponding double decomposition, the phase precipitated was the desired pentaguanidinium triphosphate when the precipitating solvent was 90% formamide, but was the sodium salt $Na_5P_3O_{10}\cdot 6H_2O$ when the precipitating solvent was 50% formamide. The triphosphate experience led to the use of high formamide concentrations in tetraphosphate preparations.

For further purification the above tetraphosphate sample was treated thus: To 10 g. of air-dried hexaguanidinium tetraphosphate in 15 ml. of water add 2 g. of (GuH)Cl in 5 ml. of water and dilute with 16–17 ml. of formamide. Induce crystallization and proceed as above. The yield here is about 90% and may be decreased by using more solvent if greater purification is desired. Analytical information on the product is summarized in Table XVI and accords reasonably with the composition $(GuH)_6P_4O_{13}\cdot H_2O$. Note that oven drying causes some hydrolysis, *i.e.*, formation of acid salts equivalent to 0.5–0.6% water of constitution, but does not drive off guanidine.

For comparison two other guanidine phosphates were prepared, namely, pentaguanidinium triphosphate and tetraguanidium pyrophosphate. The former precipitated as the anhydrous salt, the latter as the monohydrate. The triphosphate was obtained by double decomposition with (GuH)Cl in mixed solvent (formamide/water volume ratio 9/1). The pyrophosphate was similarly obtained, but did not require so much formamide, being obtained from a solvent of approximately equal volumes of formamide and water. Analyses are given in Table XVI and X-ray patterns in Table XIV.

Analyses

So far paper chromatography studies by Westman, *et al.*,[7] and by Ebel[47] provide the only method which is capable of determining tetraphosphate in the presence of other known species of condensed phosphates. As a consequence their work provides the most convincing proof available that tetraphosphate ion exists, and specifically that it can be made by mild hydrolysis of the tetrametaphosphate. The

(47) J. P. Ebel, *Bull. soc. chim.*, 1089 (1953).

method gives results with an accuracy of 3 to 5% for tetraphosphate as for other ions.

Other data also serve to establish the identity of tetraphosphate and are particularly useful to one who wants to prepare a sample of pure tetraphosphate for use in his own laboratory. Thus, the X-ray patterns (Table XIV) on the acridinium salts show that the tetraphosphate is distinct from ortho-, pyro-, tri-, trimeta- or tetrametaphosphate. Similarly for the guanidinium salts, the tetraphosphate gives a pattern distinct from that of pyro- or triphosphate; ortho- and metaphosphates were not made. With $Co(en)_3^{+3}$ tetraphosphate gives no precipitate at any *p*H tried (2.5 to 10). The usefulness of this test is lessened by the fact that a triphosphate contaminated with 10% tetraphosphate also fails to precipitate as noted by Weiser.[29] The rate of hydrolysis in the extractive molybdate procedure described in the next section can also be used for qualitative differentiation between tetra- and other crystallizable condensed phosphates. Also recall that tetraphosphate gives amorphous precipitates with zinc, while pyro- and triphosphate give crystalline products.

While precipitates are formed when tetraphosphate reacts with ions such as acridinium, barium, silver or zinc, they are not useful for analysis because pyro- and triphosphates give similar precipitates.

Properties

Only qualitative or semi-quantitative information is available in most cases. For instance, the solubility of sodium, lithium or guanidinium salts in water is very high, probably over 50% in all three cases. From the isolation of the 44% concentrate in solution form, it is evident that the solubility of $Na_6P_4O_{10}$ is more than 44%. While only qualitative information is available on the lithium salt, the drying of its aqueous solutions to a glass indicates a very high solubility. The hexaguanidinium tetraphosphate is highly soluble (Table XVI), much more so than the tetraguanidinium pyrophosphate; even so it is somewhat less soluble than the pentaguanidinium triphosphate.

From the difficulties in obtaining a pure tetraphosphate upon alkaline cleavage of the tetrametaphosphate ring, it is clear that the tetraphosphate is less stable than the triphosphate in alkaline media. Four pieces of evidence suggest that alkaline media tend to split the tetraphosphate ion into two pyrophosphate fragments.

(a) Thilo and Rätz[14] observed crystals of $Na_3HP_2O_7 \cdot H_2O$ growing at room temperature in a concentrated $Na_6P_4O_{13}$ solution that had dried to a glassy consistency and stood for a few weeks longer.

(b) Tetrametaphosphate was almost completely converted to pyrophosphate in the following experiment: 40 g. of NaOH in pellet form was added slowly to 10.0 g. of $Na_4P_4O_{12} \cdot 4H_2O$ in 45 ml. of water with stirring and cooling to hold the temperature at 50 to 60°. The product which finally precipitated was filtered and washed free of NaOH with ethanol. It was largely $Na_4P_2O_7 \cdot 10H_2O$, by X-ray pattern, but contamination by Na_3PO_4 and Na_2CO_3 was detected. Its moisture content was 42.5% (theory for $Na_4P_2O_7 \cdot 10H_2O$, 40.4%). The yield of anhydrous material calculated as $Na_4P_2O_7$ was 102% of the theoretical.

(c) In an attempt to salt out crystals of $Na_6P_4O_{13}$ by adding sodium acetate to the viscous liquid, the small amount of precipitate obtained proved to be $Na_4P_2O_7$ by X-ray.

(d) Upon drying the hexaguanidinium tetraphosphate monohydrate, analysis showed that it had suffered hydrolysis because titratable hydrogens were present (samples 04-92 and 04-99 in Table XVI). However, a test for orthophosphate in the dried product was negative. Presumably, then, the acidity produced by the drying is present in the dried product as acid pyrophosphate.

That the pyrophosphate reaction is likely to predominate in the alkaline hydrolysis of tetraphosphate (or its precursor tetrametaphosphate) is fairly well indicated by the above observations, but one experiment which is contrary should also be mentioned. A solution of 10 g. of $Na_4P_4O_{12} \cdot 4H_2O$ in 47 ml. of water was warmed to 60° and pellets of NaOH were added up to a total of 25 g. The only difference between this and experiment (b) above is that the temperature went to 92° in the early stages and the solution was hotter than 60° for perhaps 5 minutes. The product which precipitated in the late stages of this preparation was largely $Na_5P_3O_{10}$ (II) by X-ray diffraction! No other analyses were made. Since triphosphate was produced, then orthophosphate would also be expected as one of the products. Thus, except for the experiment in which the temperature went to 92°, alkaline media appear to favor cleavage of middle P–O–P links over that of similar end links.

In acid solutions there is also evidence that tetraphosphate is less stable than triphosphate. This is made evident by a test similar to the extractive procedure of Martin and Doty[34] for determining orthophosphate in the presence of other easily hydrolyzed phosphates. For example, if 1 mg. of sodium tetraphosphate in 5 ml. of water is treated with 1 ml. of the acid ammonium molybdate reagent and shaken with 2 ml. of a benzene–isobutanol mixture (1:1 by volume), a distinct yellow color develops in the organic layer within half an hour. Pyro-, tri-, trimeta- or tetrametaphosphate will do so only after three hours or more. While it is not possible to state from the available data whether such lowering of the *p*H has affected the cleavage of end P–O–P links more than middle P–O–P links, the data do indicate that the introduction of a middle P–O–P into triphosphate to make tetraphosphate does favor the acid hydrolysis of the end P–O–P link. Thus, tetraphosphate yields orthophosphate faster than triphosphate.

Acknowledgment.—It is a pleasure to acknowledge the assistance of my Procter & Gamble colleagues. Besides those already mentioned, Messrs. F. L. Jackson, F. P. Krause and H. Nordsieck have been especially helpful.

CHELATION OF ALKALINE EARTH IONS BY HYDROLYZED MALEIC ANHYDRIDE COPOLYMERS

BY H. MORAWETZ, A. M. KOTLIAR AND H. MARK

Polytechnic Institute of Brooklyn, Brooklyn 1, New York

Received April 19, 1954

The chelation of Mg, Ca, Sr and Ba with hydrolyzed maleic anhydride–styrene and maleic anhydride–vinyl ethyl ether copolymers was studied by the effect of low concentrations of alkaline earths salts on the titration curve of the polymer in strong potassium nitrate solution. Bjerrum's method of calculating chelate formation constants was modified to take account of the variation of the effective ionization constant with the charge of the polyelectrolyte. Apparent chelate formation constants increased, in general, with the charge of the polyanion in the case of the styrene copolymer, while the reverse was found with the vinyl ether copolymer. The results were interpreted as due to a superposition of an electrostatic and a saturation effect.

The interactions of polyelectrolytes with their counter-ions have been studied intensively in recent years. In view of the high charge of the polymeric ion, the counter-ions are subjected to strong electrostatic forces, which manifest themselves in the characteristic titration behavior of polymeric acids,[1] low activity coefficients of the ions in such solutions[2,3] and the electrophoretic transport of part of the counter-ions with the polyion.[4]

Most of the work to date was restricted to systems with monovalent counter-ions, although the effect of divalent counter-ions on the titration[5] and solution viscosity[6] of polyelectrolytes was briefly mentioned, and the gelation of polycarboxylic acids with divalent cations was studied in some detail.[7,8] The interpretation of the behavior of such systems is complicated by the fact that complex formation of divalent cations with carboxyl groups may be superimposed on the electrostatic effect. Gregor and Luttinger[9] have observed a pronounced shift in the titration curve on addition of small concentrations of cupric salt to polyacrylic acid in strong salt solution and interpreted this finding as evidence of chelation. Before such data can be translated into chelate formation constants, a modification of Bjerrum's procedure[10] consistent with polyelectrolyte theory is required. The study of the chelation of alkaline earth cations with hydrolyzed maleic anhydride copolymers offers two advantages for a preliminary study of this problem: there is no uncertainty about the number of ligands bound by the chelating ion, and formation constants of analogous succinic acid chelates, similar to the complex formed by the polyacid but without the complications peculiar to polyelectrolyte equilibria, have been reported.[11]

Results and Discussion

Two hydrolyzed copolymers of maleic anhydride with vinyl ethyl ether (VEE/MA) and styrene (ST/MA), respectively, were titrated with sodium hydroxide in 1 *N* potassium nitrate solution. Since it is known that maleic anhydride adds to styrene and vinyl ether radicals very much more rapidly than to its own radical, the hydrolyzed copolymers contain pairs of carboxyl groups isolated by the comonomer from similar pairs. Titration curves of such "polydicarboxylic acids" should have a break at half-neutralization, since the double ionization of a carboxyl pair is improbable while there remain any un-ionized carboxyl pairs. Ferry and his collaborators[12] reported such a break in the titration curve of hydrolyzed styrene–maleic anhydride copolymers, but found little evidence of it in titrating a hydrolyzed copolymer of maleic anhydride and vinyl ethyl ether, which is much more expanded in aqueous solution. When small amounts of alkaline earth nitrates were added, the second half of the titration curve was displaced to lower *p*H values. The total salt concentration being very much larger than that of the alkaline earth salt added, the effect could not be due to a change in the electrical free energy of ionization and had to be ascribed to complex formation.

Let us denote by A the stoichiometric concentration of carboxyl pairs, (HA^-) and ($A^=$) being the concentrations of the singly and doubly ionized species and (X) the concentration of carboxyl pairs complexed with an alkaline earth ion. Since complexing is observed only in the second half of the titration curve, we may assume that the concentration of un-ionized carboxyl pairs is negligible so that for a degree of neutralization of the second carboxyl α_2

$$(HA^-) = A(1 - \alpha_2) + (OH^-) \qquad (1)$$

$$A\alpha_2 = (A^=) + (X) + (OH^-) \qquad (2)$$

We shall assume that the electrical free energy of dissociation ΔF_{el}[1] depends only on the average charge Z per carboxyl pair, *i.e.*, that as long as Z is held constant, ΔF_{el} is independent of the number of ions chelated. Thus

$$\frac{(H^+)(A^=)}{(HA^-)} = K_a = K_0 \exp(-\Delta F_{el}/RT) = f(Z) \qquad (3)$$

where

$$Z = 1 + \alpha_2 - 2(X)/A - (OH^-)/A \qquad (4)$$

(1) A. Katchalsky and J. Gillis, *Rec. trav. chim.*, **68**, 879 (1949).
(2) W. Kern, *Makromol. Chem.*, **2**, 269 (1948).
(3) A. Katchalsky and S. Lifson, *J. Polymer Sci.*, **11**, 409 (1953).
(4) J. R. Huizenga, P. F. Grieger and F. T. Wall, *J. Am. Chem. Soc.*, **72**, 2636, 4228 (1950).
(5) A. Katchalsky and P. Spitnik, *J. Polymer Sci.*, **2**, 432 (1947).
(6) T. Alfrey, R. M. Fuoss, H. Morawetz and H. Pinner, *J. Am. Chem. Soc.*, **74**, 438 (1952).
(7) F. T. Wall and J. W. Drenan, *J. Polymer Sci.*, **7**, 83 (1951).
(8) H. Deuel and H. Solms, *Kolloid-Z.*, **124**, 65 (1951).
(9) H. P. Gregor and L. Luttinger, private communication.
(10) J. Bjerrum, "Metal Ammine Formation in Aqueous Solution," P. Haase and Son, Copenhagen, 1941.
(11) A. E. Martell and M. Calvin, "Chemistry of the Metal Chelate Compounds," Prentice-Hall, Inc., New York, N. Y., 1952, p. 517.
(12) J. D. Ferry, D. C. Udy, F. C. Wu, G. E. Heckler and D. F. Fordyce, *J. Colloid Sci.*, **6**, 429 (1951).

By proper substitution from (1), (2) and (4) into equation (3) we obtain

$$\frac{(H^+)}{1 - \alpha_2 + (OH^-)/A} = \frac{2f(Z) + (H^+)}{Z} \qquad (5)$$

The function $f(Z)$ is known from titration data obtained in the absence of chelating ions, and Z can be evaluated from (5), leading to (X) and ($A^=$) by the relations (4) and (2). The chelate formation constant

$$K_f = \frac{(X)}{(M^{++})(A^=)} \qquad (6)$$

can now be calculated, since the free metal concentration (M^{++}) is the difference between the stoichiometric metal concentration and the chelate concentration (X).

Tables I and II give the titration data obtained with copolymers VEE/MA and ST/MA in the presence and absence of alkaline earth cations. Figure 1 gives plots of K_a as a function of Z for the two copolymers. It can be seen that the apparent dissociation constant of the styrene copolymer falls off continuously with increasing charge on the polyion as would be expected. The apparent initial increase in the K_a values of the vinyl ether copolymer with increasing degree of neutralization is undoubtedly due to the error introduced in neglecting the presence of un-ionized carboxyl pairs at low values of α_2, and the K_a values obtained in this region were not used in subsequent calculations. It has been pointed out previously[12] that the differences in the titration behavior of these two polyelectrolytes are due to the tighter coiling of the styrene copolymer.

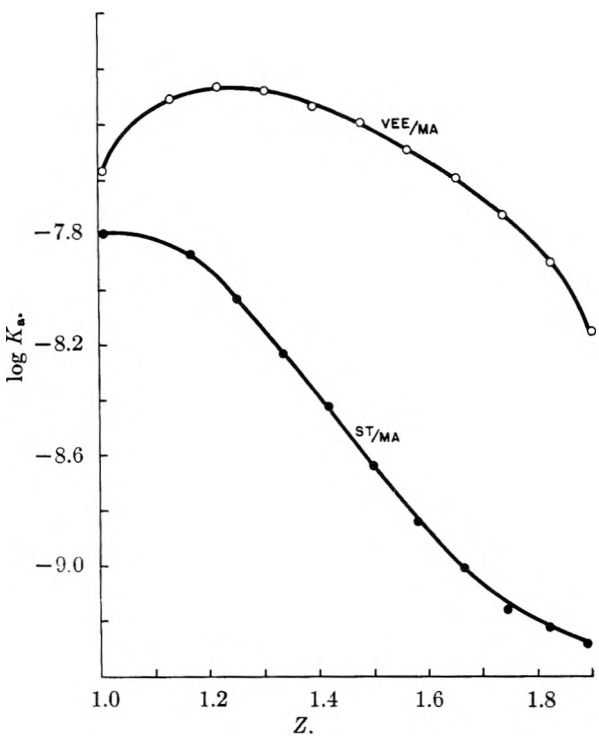

Fig. 1.—Apparent dissociation constants of VEE/MA and ST/MA as a function of copolymer charge density.

The results of the calculations of chelate formation constants are represented on Figs. 2 and 3.

TABLE I

EFFECT OF ALKALINE EARTH IONS ON THE TITRATION OF COPOLYMER VEE/MA IN 1 *N* POTASSIUM NITRATE AT 25°

		$-\Delta pH$					
	Blank titration	Ca^{++}		Mg^{++}		Ba^{++}	Sr^{++}
α_2	pH	0.0036 *M*	0.0018 *M*	0.0036 *M*	0.0018 *M*	0.0036 *M*	0.0036 *M*
0.042	6.21	0.19	0.08	0.17	0.06		
.128	6.48	.25	.11	.21	.10		
.215	6.70	.29	.15	.25	.11	0.10	0.09
.302	6.93	.39	.19	.29	.16	.15	.14
.389	7.14	.45	.23	.34	.19	.19	.18
.476	7.36	.51	.28	.39	.23	.25	.23
.562	7.60	.58	.31	.45	.27	.30	.29
.649	7.87	.65	.35	.52	.32	.37	.36
.736	8.18	.74	.40	.59	.35	.45	.44
.823	8.57	.72	.40	.66	.36	.51	.50

TABLE II

EFFECT OF 0.0036 *M* ALKALINE EARTH IONS ON THE TITRATION OF COPOLYMER ST/MA IN 1 *N* POTASSIUM NITRATE AT 25°

		$-\Delta pH$			
	Blank titration				
α_2	pH	Ca^{++}	Mg^{++}	Ba^{++}	Sr^{++}
0.083	6.76	0.18	0 09		0.06
.167	7.17	.22	.12	0.07	.08
.250	7.55	31	.18	.09	.13
.333	7.93	.44	.29	.16	
.417	8.27	.53	.37	.19	.24
.500	8.64	.70	.51	.29	.34
.583	8.98	.86	.61	.34	.42
.667	9.30	.94	.70	.41	.50
750	9.62	.98	.76	.48	.59
833	9.88	.96	.68	.44	.56

They may be interpreted as due to two opposing factors: the electrostatic free energy of chelate dissociation would tend to produce K_f values increasing with the charge of the polyion. A superimposed saturation effect hinders the production of chelates with high densities of alkaline earth ions bound to the chain. With the less expanded styrene copolymer the electrostatic factor predominates, while the reverse is true of the vinyl ether copolymer. The slight increase in the K_f of magnesium and VEE/MA at any given Z, when the metal concentration was reduced by one-half, is in qualitative agreement with this interpretation. It should also be pointed out that solvation effects, which are difficult to evaluate, were not taken into account in assuming that the chelate formation constant depends only on the charge density of the polymer.

Table III gives a comparison between the values of K_f of alkaline earth complexes with the polyelectrolytes used in the present study (at an arbitrarily chosen value of $Z = 1.3$) and the analogous complexes with succinic acid.[11] At this charge the chelate formation constant of VEE/MA is between

TABLE III

COMPARISON OF CHELATE FORMATION CONSTANTS OF ALKALINE EARTHS WITH VEE/MA, ST/MA AND SUCCINIC ACID

	log K_f			
	Ca^{++}	Mg^{++}	Ba^{++}	Sr^{++}
VEE/MA ($Z = 1.3$)	2.45	2.30	2.00	1.96
ST/MA ($Z = 1.3$)	2.11	1.74	1.36	1.46
Succinic acid	1.16	1.02	0.97	0.75

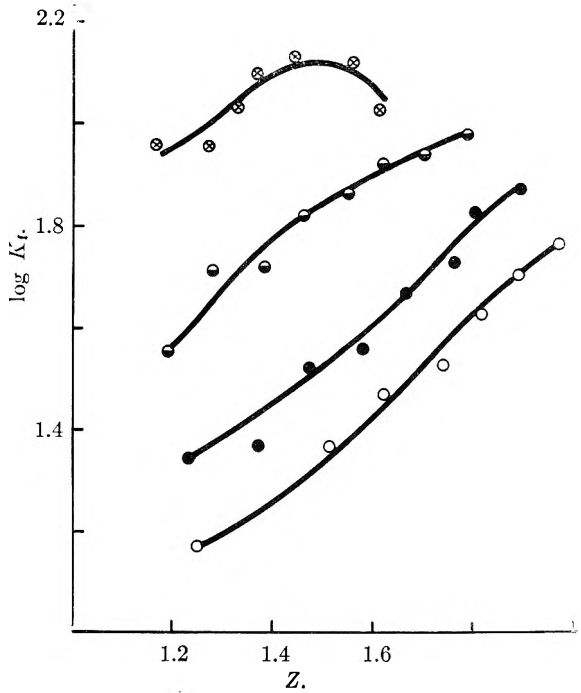

Fig. 2.—Chelate formation constant of copolymer ST/MA with 0.0036 *M* alkaline earths: ⊗, $CaNO_3$; ●, $SrNO_3$; ◒, $MgNO_3$; ○, $BaNO_3$.

ten and twenty times as high as the corresponding value for succinic acid, while somewhat lower values of K_f were obtained for copolymer ST/MA.

Experimental

Preparation of Polymers.—Forty grams of maleic anhydride and 20 g. of the comonomer were dissolved in 400 ml. of butanone and 100 mg. of azo-bis-isobutyronitrile initiator was added. The polymerization was carried out at 70°, the copolymer was precipitated in hexane, dissolved in hot water, dialyzed and freeze dried. The vinyl ethyl ether copolymer (VEE/MA) contained 62 mole % of vinyl ethyl ether, the styrene copolymer (ST/MA) 54 mole % of styrene as calculated from titration data. The maleic anhydride copolymers were fully hydrolyzed, since boiling with alkali before dialysis did not alter their titration behavior.

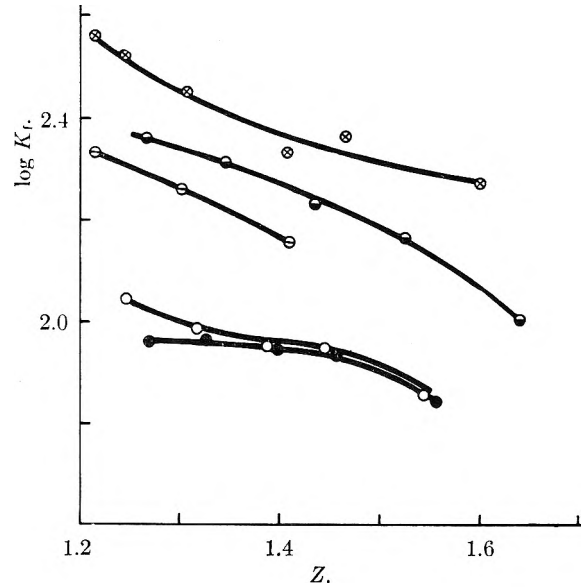

Fig. 3.—Chelate formation constants of copolymer VEE/MA: ⊗, 0.0018 *M* $CaNO_3$; ○, 0.0036 *M* $BaNO_3$; ◒, 0.0018 *M* $MgNO_3$; ●, 0.0036 *M* $SrNO_3$; ⊖, 0.0036 *M* $MgNO_3$.

Titration.—The *p*H determinations were carried out with a Cambridge Instrument Co. research model *p*H meter with external shielded electrodes. During titration, solutions were held at 25° to within 0.1°, stirred and protected by a stream of nitrogen from atmospheric CO_2. Four minutes were allowed for equilibrium after each addition of base; longer time intervals produced no further *p*H change. All titrations were carried out in the presence of 1 *N* potassium nitrate.

Acknowledgment.—This study was supported by a research grant from the Monsanto Chemical Company.

TITRATION OF POLYELECTROLYTES AT HIGHER IONIC STRENGTHS

BY R. A. MARCUS

Polytechnic Institute of Brooklyn, Brooklyn 1, New York

Received April 19, 1954

The titration behavior of polyelectrolytes at higher ionic strengths is treated on the basis of the nearest neighbor interaction between the fixed ions. This point of view suggests a quantitative comparison of the behavior of polymeric and dibasic acids. The application of these considerations to existing work on the correlation of viscosity and titration curves of polymeric acids is briefly discussed.

Introduction.—The correlation of various properties of polyelectrolytes, such as viscosity and titration behavior, has been the subject of a number of recent theoretical treatments.[1] These approaches have had varying degrees of success and while differing in a number of important respects, have in common the assumption that both the fixed and mobile ions in the polyelectrolyte system may be treated as a continuous charge distribution.

The purpose of the present note is to examine a different approach to the titration behavior of these systems, one which does not involve the latter assumption but instead assumes that the important interactions between the fixed ions on the polyelectrolyte are nearest neighbor interactions. It is expected that the repulsions between the immobile ions will vanish rapidly with distance, R, at the higher ionic strengths, in the first approximation as $e^{-\kappa R}/R$ where κ is the reciprocal Debye length. On this basis nearest neighbor interaction will begin to predominate when $\kappa R \sim 1$ where R is the distance between nearest neighbors. When $R \sim 5$ Å. this will occur when the salt concentration exceeds 0.4 *M*.

(1) A. Katchalsky, O. Kunzle and W. Kuhn. *J. Polymer Sci.*, **5**, 283 (1950); J. Hermans and J. T. G. Overbeek, *Rec. trav. chim.*, **67**, 761 (1948); G. E. Kimball, M. Cutler and H. Samelson, THIS JOURNAL, **56**, 57 (1948).

If these considerations are valid a correlation between the titration behavior of a polymeric acid and of a suitable dibasic acid is to be anticipated. An examination of available data on polyacrylic and glutaric acids supports this. A treatment of the dependence of pK on the degree of neutralization is given in the following section using, at first, the Bragg–Williams approximation and later, the more exact Ising method.

Theory of Nearest Neighbor Interaction.—The polymer chain is considered to have N_a neutralized and N_b unneutralized acidic groups. We suppose that the free energy f_a of an immobile ion, A, and its counter ion atmosphere are modified by an amount $f_{aa}/2$ for each A nearest neighbor and by $f_{ab}/2$ for each B neighbor, there being only two neighbors in all. Additivity of these effects will be assumed. Corresponding quantities for the uncharged acidic group B will be denoted by f_b, $f_{ab}/2$ and $f_{bb}/2$, respectively. The total free energy of such an assembly depends on the number of pairs, N_{ab}, of nearest AB neighbors and may be written as

$$F_{ab} = f_aN_a + f_bN_b + f_{aa}N_{aa} + f_{bb}N_{bb} + f_{ab}N_{ab} - kT \ln g(N_a, N_b, N_{ab}) \quad (1)$$

where $g(N_a, N_b, N_{ab})$ is the number of ways of distributing, for a given N_a, N_b and N_{ab}, the A and B groups along the chain and where the number of AA pairs, N_{aa}, and of BB pairs, N_{bb}, is given by $2N_{aa} + N_{ab} = 2N_a$, $2N_{bb} + N_{ab} = 2N_b$. The free energy of this system, F, equals $-kT \ln$ (P.F.) $= -kT \ln \Sigma(\text{P.F.})_{ab} = -kT \ln \Sigma_{exp}(-F_{ab}/kT)$ where (P.F.) is the partition function for all configurations while $(\text{P.F.})_{ab}$ is the partition function for only those configurations corresponding to a given N_{ab}. The summation is over all N_{ab} consistent with the values of N_a and N_b. From equation 1 it then follows that

$$F = N_a(f_a + f_{aa}) - N_b(f_b + f_{bb}) - kT \ln \Sigma g(N_a, N_b, N_{ab}) \exp(-N_{ab}w/kT) \quad (2)$$

where

$$w = f_{ab} - f_{aa}/2 - f_{bb}/2$$

In the Bragg–Williams approximation N_{ab} in the exponential in the last term is replaced by $\bar{N}_{ab}$, the average value of N_{ab} when A and B are randomly distributed along the chain. The last term in equation 2 thus becomes $\exp(-w\bar{N}_{ab}/kT)\Sigma g$. The total number of ways of arranging the N_a A's and N_b B's along the chain, Σg, is $(N_a + N_b)!/N_a!N_b!$ $\bar{N}_{ab}$ is readily evaluated by observing that in this random case the probability of an adjacent pair of sites having an A on the first site and a B in the second is $N_a/(N_a + N_b) \times N_b/(N_a + N_b)$, so that the chance that this link is an AB link is twice this. Since there are $(N_a + N_b)$ such pairs of adjacent sites, $\bar{N}_{ab} = 2N_aN_b/(N_a + N_b)$. It then follows that $(\partial F/\partial N_a)$ is given by

$$\left(\frac{\partial F}{\partial N_a}\right)_{N_a + N_b} = f_a + f_{aa} - f_b - f_{bb} + 2w(1 - 2\alpha) \quad (3)$$

where

$$\alpha = N_a/(N_a + N_b)$$

Equating this to the partial molecular free energy, μ, of the hydrogen ions in a solution in which their activity is a_{H^+}, $\mu = f_H + kT \ln a_{H^+}$, it follows that

$$pK = p\text{H} - \log\frac{\alpha}{1 - \alpha} = \frac{\Delta f}{2.3kT} + \frac{2w}{2.3kT}(1 - 2\alpha) \quad (4)$$

where

$$f = f_a + f_{aa} + f_H - f_b - f_{bb}$$

Thus the pK is a linear function of α in this approximation and the change in pK, from $\alpha = 0$ to $\alpha = 1$ is $\Delta pK = -4w/2.3kT$. The major contribution to w is f_{aa}, the repulsion of the immobile ions, and it follows that f_{aa} is positive and w negative, as observed. Both Δf and w will depend on the counter ion atmosphere and hence upon the salt concentration.

If the repulsion of nearest neighbor ions is very pronounced, then the A and B groups are not distributed randomly along the chain. Using the approach employed by Ising in an analogous problem in ferromagnetism, an equation may be derived which takes into account in an exact manner such deviations from randomness. From such a treatment we find[2]

$$\left(\frac{\partial F}{\partial N_a}\right)_{N_a + N_b} = f_a + f_{aa} - f_b - f_{bb} + kT \ln \frac{\sqrt{4\alpha(1 - \alpha)(e^{2w/RT} - 1) + 1} + 2\alpha - 1}{\sqrt{(4\alpha(1 - \alpha)(e^{2w/RT} - 1) + 1)} + 1 - 2\alpha} \quad (5)$$

and from this, that

$$pK = \frac{\Delta f}{2.3kT} + \log \frac{(\sqrt{4\alpha(1 - \alpha)(e^{2w/RT} - 1) + 1} + 2\alpha - 1)(1 - \alpha)}{(\sqrt{4\alpha(1 - \alpha)(e^{2w/RT} - 1) + 1]} + 1 - 2\alpha)\alpha} \quad (6)$$

where w and Δf retain their previous significance. As before, the change in pK from $\alpha = 0$ to $\alpha = 1$, ΔpK, is $-4w/2.3kT$. This is as expected since in both cases a dissociating acid group is in an environment of other undissociated groups when $\alpha = 0$ and in an environment of neutralized groups when $\alpha = 1$. When $-2w << kT$, equation 6 reduces to 4, as it should. A comparison between these equations is given in Fig. 1 for $\Delta pK = 1.0$. In this case $-2w/kT = 2.3/2$, which is not negligible compared with unity. When $\Delta pK = 0.5$ equations 4 and 6 are essentially equivalent.

Comparison with Experimental Data.—A survey of the titration behavior of polyelectrolytes[3,4] indicates three common types of pK–α curves: linear (as in Fig. 1), S-shaped (as in Fig. 1) with a maximum slope at $\alpha = 1/2$, inverted S-shaped with a minimum slope at $\alpha = 1/2$. Frequently the curvature in the latter cases is not particularly pronounced and its observance may well depend on the

(2) An evaluation of the last term in equation 2 is given, for example, in Rushbrooke's "Statistical Mechanics," Oxford University Press, New York, N. Y., 1949, p. 304, equation 42. Denoting this term by ΔF, subsequent equations are also given there for $(\partial\Delta F/\partial N_a)_{N_b}$ and $(\partial\Delta F/\partial N_b)_{N_a}$. It is observed that

$$\left(\frac{\partial F}{\partial N_a}\right)_{N_a + N_b} = f_a + f_{aa} - f_b - f_{bb} + \left(\frac{\partial\Delta F}{\partial N_a}\right)_{N_b} - \left(\frac{\partial\Delta F}{\partial N_b}\right)_{N_a}$$

(3) *Cf.* P. Doty and G. Ehrlich, *Ann. Rev. Phys. Chem.*, **3**, 81 (1952)

(4) H. P. Gregor and L. Luttinger, private communication.

number of experimental points recorded. In the various data examined the first two curves, and therefore equations 4 and 6, satisfy reasonably well the modified, empirical, Henderson–Hasselbach equation, $pH = pK_m + n \log \alpha/(1 - \alpha)$, proposed by Katchalsky and Spitnik,[5] if α is, say, between 0.1 and 0.9; while the third type generally obeys the equation over a somewhat larger region. However, when $\alpha > 0.9$ the experimental error is larger, while when $\alpha < 0.1$ the interpretation of the data may be more vague since here, the calculation of α depends on a knowledge of the self-ionization of the acid.

Of particular interest is the comparison of the titration behavior of glutaric and polyacrylic (PAA) acids. A comparison with α,γ-dimethylglutaric acid would, it is true, be more suitable, but data on that acid do not appear to be available. The ratio of the first and second dissociation constants K_1/K_2, of glutaric acid is about 12, of which a factor of 4 is statistical and the remaining factor of 3 may be attributed to the repulsions of the neighboring ionic groups and more specifically to the term, $-2w/kT$, discussed earlier. An examination of some approximate titration curves of glutaric acid[4] indicates that $pK_2 - pK_1$ is lowered by about 0.08 and 0.19 unit in the presence of 0.2 and 2 M $NaNO_3$, respectively. If nearest neighbor interaction predominates in PAA, then one might anticipate that ΔpK for PAA would be about 2 log 3, 2(log 3 − 0.08), 2(log 3 − 0.19); that is, 0.96, 0.80, 0.58 in the presence of no salt, 0.2 M $NaNO_3$ and 2M $NaNO_3$, since there are two nearest neighbors in the polymeric acid and only one in glutaric acid.

The pK–α curves for PAA,[4] in solutions dilute with respect to PAA, appear to be linear or slightly S-shaped, as in Fig. 1. ΔpK is approximately 2.5, 1.2, 0.8 in the presence of 0, 0.2 and 2 M $NaNO_3$, respectively. The agreement between the observed ΔpK's and those calculated from the behavior of glutaric acid improves with increasing salt concentration, as expected, and the agreement in the latter cases is reasonable, considering the extrapolation errors and assumptions employed.[6]

(5) A. Katchalsky and P. Spitnik, *J. Polymer Sci.*, **2**, 432 (1947).

(6) Two procedures are available for this calculation of ΔpK for PAA. The values cited in the text are based on a linear extrapolation of data given in the region $\alpha = 0.2$ and $\alpha = 0.8$. Another procedure, and one which is more self-consistent, calculates ΔpK from the slope of the pK–α curve in this region using equation 6 and the relation $\Delta pK = (-2w/2.3kT)$. The values of ΔpK calculated by the latter procedure are but slightly less, as expected, and are found to be 1.0 and 0.7 in the presence of 0.2 and 2 M $NaNO_3$, respectively.

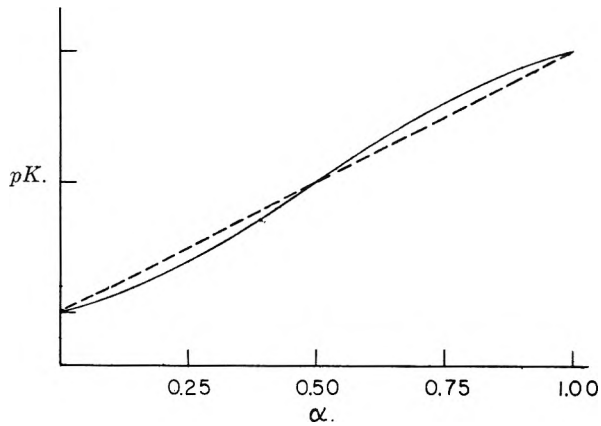

Fig. 1.—A plot of pK *versus* α when $\Delta pK = 1.0$ The dotted line is based on equation 4, and the full line on equation 6.

The titration behavior of dilute solutions of carboxylmethylcellulose[7] (CMC) is rather interesting. Extrapolating the linear curves of Hermans and Pals, one arrives at a rather rough value for ΔpK of about 1.8 in the absence of salt, a value somewhat less than that observed for PAA. This ΔpK decreases rapidly with increasing salt (NaCl) concentration so that at a salt concentration of 0.3 M, $\Delta pK \sim 0.2$, a value considerably smaller than that found for PAA. This CMC polymer differs from PAA in that the acid groups are, on the average, more widely spaced. In the presence of salt the nearest neighbor interaction will vary strongly with distance, R, approximately as $e^{-\kappa R}/R$, while at low salt concentration the interaction between all the immobile ions varies less strongly, as $1/R$. It is therefore expected that the former will be much more sensitive to change in nearest neighbor distance than the latter. This is consistent with the observed behavior of CMC and PAA.

In conclusion, it is observed that nearest neighbor interaction is expected to have a rather slight effect on viscosity. If such interaction is a large part of the total interaction, which in PAA it appears to be, then it must be taken into account in theories correlating viscosity and titration behavior. The neglect of this contribution to the interaction would tend to make ΔpK's calculated from viscosity behavior less than those observed experimentally.

Acknowledgment.—The author should like to express his appreciation to Dr. H. Morawetz, who suggested the problem and offered a number of helpful comments.

(7) D. T. F. Pals and J. J. Hermans, *Rec. trav. chim.*, **71**, 513 (1952).

THE MOLECULAR CONFIGURATION AND HYDRODYNAMIC BEHAVIOR OF CELLULOSE TRINITRATE

BY ALFRED M. HOLTZER,[1] HENRI BENOIT[2] AND PAUL DOTY

Gibbs Laboratory, Department of Chemistry, Harvard University, Cambridge, Mass.

Received April 19, 1954

Measurements of light scattering as a function of angle, and viscosity as a function of gradient have been made on acetone solutions of eleven samples of cellulose trinitrate in order to determine the dependence of the mean molecular size and the intrinsic viscosity on the degree of polymerization, N. It is found that the ratio of the mean square end-to-end length, $\overline{r^2}$, to the degree of polymerization increases with N until N is about 500 and thereafter remains essentially constant. This behavior is that predicted for randomly coiled chains with a negligible volume effect and with a stiffness characterized by a value of 35 Å. for b_0, the square root of the above ratio in the region of high N. Within probable error the intrinsic viscosity–molecular weight relation is given by $[\eta] = 5.0 \times 10^{-3} N_w$ throughout the range investigated (N_w = 250 to 9000). This shows that the hydrodynamic character of the chain molecules is not molecular weight dependent in this region, as has been claimed. Moreover, the molecular weight exponent of unity in the viscosity relation cannot be explained in terms of the volume effect on chain statistics because of the nature of the observed dependence of size on N. Viscosity measurements in various solvents support this view. With the value of b fixed the Kirkwood-Riseman expressions fit the intrinsic viscosity up to N = 1000 and much of the published sedimentation and diffusion data when the other parameter ζ is equal to 2.7×10^{-10}. For $N > 1000$, however, the viscosity behavior indicates a coil that is much more free draining than the theory would predict with the same values of b and ζ.

Although the common cellulose derivatives are among the most investigated of all high polymers, we have been prompted to undertake another study for several reasons. First, cellulose derivatives appear to be almost the only unbranched polymers readily available in a broad range of molecular weights that have sufficiently stiff chains to allow the radius of gyration to be measured in both the Gaussian and non-Gaussian molecular weight regions. Since we had earlier proposed[3] how the radius of gyration should depend on the molecular weight upon passing from the non-Gaussian to the Gaussian regions, we were anxious to test this experimentally. Moreover, such a study should, with present techniques of light scattering, lead to an unambiguous characterization of the size of cellulose molecules and thereby complete an investigation which was one of the first stimulated[4] by Debye's derivation of the particle scattering factor for a randomly coiled polymer molecule.[5]

Secondly, we wished to inquire into the intrinsic viscosity–molecular weight relationship since it had been reported[6,7] that in the case of cellulose nitrate a transition from one type of hydrodynamic behavior to another occurred with increasing molecular weight, and this would have, if true, considerable interest in conjunction with current theories of intrinsic viscosities.[8-11] In this problem we would want to use some of the highest molecular weight samples available and this would present the opportunity of tying down upper limits of the molecular weight of cellulose derivatives about which there is considerable disagreement.

Consequently, we obtained samples of the most highly nitrated cellulose nitrate, in order to ensure uniformity of substitution, prepared some fractions, and carried out viscosity, light scattering, and some osmotic pressure measurements in acetone solution. The viscosity measurements required particular attention in order to eliminate gradient dependence and the interpretation of the light scattering data required the use of some recent theoretical developments.[12]

Experimental Procedures

A. Samples.—The cellulose nitrate used came from three sources. Relevant information obtained from the supplier is summarized in the table.

Designation	Source	$[\eta]$ in EtAc at 20°	N, %	Source of supply
A	Lint cotton	49.5	14.1	Rayonier, Inc.
B	Chemical cotton	16.0	13.8	Hercules Powder Co.
C	Tire cord from cotton linters	5.27	13.7	Rayonier, Inc.

The Hercules sample was prepared by using 8 liters of an acid mixture containing 4875 g. of 85% H_3PO_4, 2725 g. of P_2O_5 and 7200 g. of 99% HNO_3. One hundred grams of air dry chemical cotton was nitrated for four hours at 0°, and washed with cold acetic acid. The nitrate was stabilized by boiling in alcohol to remove impurities. The Rayonier sample was nitrated by Mitchell according to a well-known procedure.[13]

All samples were purified in a preliminary way by dissolving in acetone, precipitating a very small fraction, and then precipitating the bulk of the polymer.

B. Fractionation.—Part of sample A was fractionated following the recommendations of Kinell and Ranby, based on ultracentrifuge studies of polydispersity and fractionation.[14] Pure hexane was added dropwise and with stirring to a 0.2% solution of the polymer in acetone. After the appearance of permanent cloudiness, the 20-liter cylindrical jar containing the mixture was then warmed in a large thermostat bath to about 35° until the solution became clear. The temperature of the bath was slowly decreased to 25.00 ±0.02°, and the stirring discontinued. When the precipitate settled out, a process varying in duration between one hour and overnight, the supernatant liquid was siphoned off. The polymer phase was, fortunately, always in the form of a transparent gel, indicating the absence of any sub-

(1) Union Carbide and Carbon Fellow, 1952–1953.

(2) Institute of Macromolecular Physics, The University, Strasbourg, France.

(3) H. Benoit and P. Doty, THIS JOURNAL **57**, 958 (1953).

(4) R. S. Stein and P. Doty, *J. Am. Chem. Soc.*, **68**, 159 (1946).

(5) P. Debye, personal communication (1945); THIS JOURNAL, **51**, 18 (1947).

(6) A. Munster, *Z. physik. Chem.*, **197**, 17 (1951); *J. Polymer Sci.*, **8**, 633 (1952).

(7) R. M. Badger and R. H. Blaker, THIS JOURNAL, **53**, 1056 (1949).

(8) P. Debye and A. M. Bueche, *J. Chem. Phys.*, **16**, 573 (1948).

(9) J. G. Kirkwood and J. Riseman, *ibid.*, **16**, 565 (1948).

(10) H. C. Brinkman, *Proc. Amsterdam Acad.*, **50**, No. 6 (1947).

(11) T. G. Fox and P. J. Flory, *J. Am. Chem. Soc.*, **73**, 1904, 1909, 1915 (1951).

(12) H. Benoit, *J. Polymer Sci.*, **11**, 507 (1953).

(13) R. L. Mitchell, *Ind. Eng. Chem.*, **38**, 843 (1946).

(14) Kinell and Ranby, "Advances in Colloid Science," Vol. III, H. Mark and E. J. W. Verwey, ed., Interscience Publishers, Inc., New York, N. Y., 1950.

stantial amount of crystallization, which would severely limit fractionation. The precipitate was redissolved in a small amount of acetone and the fraction reprecipitated with distilled water, washed with ethyl alcohol and stored alcohol-wet in the dark at 4°. The supernatant phase was titrated to cloudiness with hexane and the process repeated. In this way ten fractions were obtained, each weighing about a gram, and were designated A1–A10, 1 being the highest degree of polymerization.

The remainder of sample A was used to obtain two high molecular weight fractions by a somewhat more elaborate procedure. This fractionation involved a precipitation followed by three successive extractions designed to remove low degrees of polymerization species. The details of the procedure are shown in Fig. 1a. Circles represent jars. The line through each is a phase boundary, and the arrows indicate the history of the given phase. Equilibration at each point was assured by warming until homogeneous, and cooling to 25.00 ± 0.02°. To maintain proper relative quantities in precipitate and supernate, it was necessary to add some hexane or acetone in some of the steps. The concentration of polymer in each step was about 0.2%. In the top line the sample is titrated and the precipitate extracted three successive times. In the bottom line, the supernate of the first top-line precipitation is titrated, and the subsequent precipitate extracted with the supernatant from the top line jar just ahead of it. The entire sample was not fractionated in this way; only two high fractions were removed. Each fraction constituted about $^1/_{10}$ of the total quantity of polymer.

An analogous scheme, geared to remove low degree of polymerization fractions, was used to obtain two fractions from sample B, and two from C, as shown in Fig. 1b.

As in the high degree of polymerization case each of the two fractions made up about $^1/_{10}$ of the total polymer. The starting concentration here was about 1%, which on addition of hexane reduced to 0.5% at the first precipitation point, and to 0.02% in the final step.

Since all unfractionated samples were essentially completely nitrated, it was assumed that fractions were also trinitrates. This was checked in the case of fraction A8 by nitrogen analysis, and found to be correct.

C. Concentration Determinations.—The concentration of the solutions in all the experiments was determined by dry weight. In cases where the solution could be used immediately, the polymer, which was stored wet with alcohol, was heated to 50° overnight in a vacuum oven, and weighed into a volumetric flask, which was diluted to the mark when the nitrate was completely dissolved. When intermediate standing, or handling was likely to result in the evaporation of some solvent, a dry weight was determined by pipetting a known volume of solution into a weighing bottle, and evaporating to dryness, finally heating in a vacuum oven at 50° to constant weight. The two methods when checked against each other agreed within the precision of the analytical balance, indicating that there was neither evolution of gas from decomposition of the nitrate nor retention of acetone.

D. Viscosity Measurements.—All viscosity measurements except on the two very low degree of polymerization samples (C1 and C2) were made with a modified Ubbelohde-type capillary viscometer.[15]

The fact that solutions of high degree of polymerization cellulose and its derivatives show non-Newtonian behavior has long been recognized, and must be taken into account. The instrument was therefore constructed with three bulbs at different heights to allow measurements at three different gradients; and with a long, coiled capillary to give results in the range of low rates of shear. It was calibrated with chemically pure acetone, ethyl acetate and distilled water, and found to have negligible kinetic energy correction, in spite of the fact that flow times for acetone were only 83.0, 56.8 and 88.1 seconds for the three bulbs in order of decreasing height.

The average rate of shear on a given solution was calculated from the formula

$$\gamma = rhg/3l(\eta/d) \qquad (1)$$

where γ = rate of shear; r, radius of capillary; l, length of capillary; h, pressure head; g, acceleration of gravity; η, viscosity of liquid; d, density of liquid. The various parameters of equation 1 were determined in the following way: the radius, by measuring the weight of mercury contained in a given length; the length with a ruler; the height with a cathetometer.

(15) The viscometer was designed by Dr. Nathan Schneider of this Laboratory and constructed by Mr. H. Wayringer.

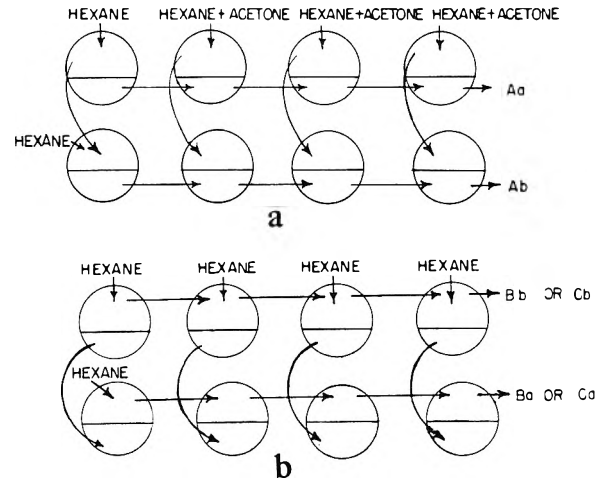

Fig. 1.—Schematic representation of the fractionation procedure: a, high molecular weights; b, low molecular weights.

It is convenient to express (1) in terms of the relative viscosity of the solution to that of solvent, η_{rel}. The assumption is made that the density of solution and solvent are the same. This yields

$$\gamma = \frac{rhg}{3l\nu_0\eta_{rel}} = \frac{k}{\eta_{rel}} \qquad (2)$$

where ν_0 is the kinematic viscosity of the solvent. The factor k is a constant for a given bulb, and a given kinematic viscosity of solvent. In this case, the calibration and the known kinematic viscosity of acetone give values of 531.0, 336.0 and 155.8 sec.$^{-1}$ for k in the top, middle and lowest bulbs, respectively.

The viscometer was immersed in a thermostat bath at 25.00 ± 0.02° and the flow times for a given solution were recorded to the nearest tenth of a second for the three bulbs. Dilutions were made by volume in the viscometer. For each concentration, the relative viscosity of the solution in each of the three bulbs was plotted as a function of the rate of shear Fig. 5, determined from relation 2. These three points invariably fell on a straight line which was extrapolated to zero gradient. One thus obtains the relative viscosity of the solution at zero rate of shear. These data were then treated in the customary way; plotted as log η_{sp}/c, against c, where c is concentration in grams/dl. and extrapolated to zero concentration. The values obtained for the intrinsic viscosity were found to be reproducible to within ±5% at high $[\eta]$.

E. Refractive Index Increment.—The difference in refractive index between solution and pure acetone was measured in a Rayleigh–Haber–Lowe interferometer manufactured by Zeiss.[16] A solution approximately 0.2% in concentration was made up by weight, and the reading converted to refractive index difference by the fundamental equation

$$n_1 - n_2 = \frac{\lambda}{d}(\Delta N)$$

where λ is the wave length of light; n_1, a refractive index of solution; n_2, of solvent; d, thickness of liquid through which the light passes; and ΔN, number of fringes. In practice, the readings were taken with white light and converted to the corresponding number of fringes in the blue by using a table of dial reading *versus* fringe number, which had been obtained with monochromatic light (4360 Å.) in a calibration experiment. The instrument gave values of dn/dc in close agreement with the literature for standard KCl solutions, bovine serum albumin and polystyrene in butanone. The values obtained for the cellulose trinitrate samples varied from fraction to fraction over a ±1.5% span, with an aver-

(16) N. Bauer and K. Fajans, "Physical Methods of Organic Chemistry," A. Weissberger, ed., Interscience Publishers, Inc., New York, N. Y., 1949.

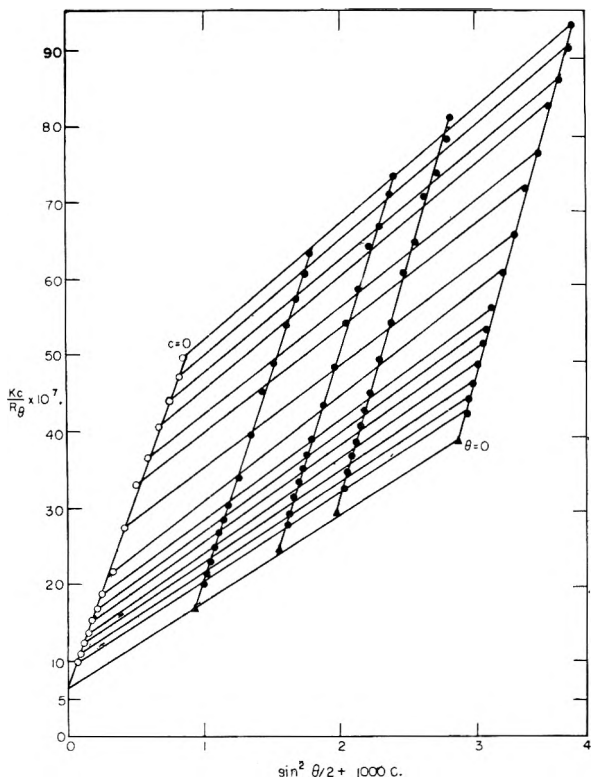

Fig. 2.—Light scattering data for cellulose nitrate sample A in acetone at 25°.

age figure of 0.105 cc./g. This is in good agreement with the data of Jullander,[17] but falls below the results of Badger and Blaker.[7]

F. Light Scattering.—"And all our yesterdays have lighted fools the way to dusty death."—Macbeth.

1. Procedure and Practical Matters.—The first prerequisite for a light scattering run is, obviously, dust-free solvent. Simple distillation, with a few Raschig rings in a column produces solvent which is quite dust-free. The entire apparatus must be flushed out well with acetone vapor, the condenser turned on, the receiving vessel filled and emptied two or three times, and the result is achieved. The solvent shows very few motes in a strong beam of light viewed with a 7 power lens at low scattering angles.

The cellulose nitrate solutions were cleaned free of dust and colloidal contaminants by centrifugation in the large rotor of a Spinco preparative ultracentrifuge. Modified polyethylene bottles served as centrifuge tubes. (A mold was made in plaster of Paris shaped to the bottom of the rotor holes. A commercially available 2-oz. polyethylene bottle was heated by immersing the flat bottom in a glycerine-bath at about 160°, until the bottom became clear in appearance. It was then rammed into the mold and blown into, hard, from the top. The bottle took the shape of the mold and could then be placed, flush, into the rotor.) The bottles were covered with Teflon gaskets and bakelite screw caps. The gap between the cap and rotor was filled by a collar of bakelite impregnated nylon, machined to fit. The collar was tapped, and the hole threaded. In this way, after centrifuging, a small screw could be inserted, the collar taken out, the cap unscrewed with the fingers, and the solution removed.

In general, the solutions were spun for one hour at 44,000 *g*. On one occasion, a high molecular weight sample gave indications of the presence of aggregation. This manifested itself by a faintly stippled appearance of the solution when viewed at low angles in a strong beam, and by an unusually high dissymmetry of scattering. This solution, when recentrifuged for three hours showed normal behavior.

Pipets were made with two glass projections: one, at a distance from the tip so that it rested on the lip of the centrifuge bottle when the end was two-thirds of the way into the solution; another, indicating the liquid level in the pipet when it contained 35 cc. of fluid, the amount required to make a measurement in the cell used. In this way the solution was transferred from the rotor into the light scattering cell. The solution was examined at low angles in a strong, parallel beam. If dust-free, the measurement was made using the unpolarized blue light (4360 Å.) of a mercury arc lamp, in a Brice–Phoenix light scattering photometer,[18] kept in a room thermostated at 25 ± 1°. The intensity of scattering for each solution was measured as a function of angle between 30 and 135°.

All scattering measurements were made in an Erlenmeyer-type cell. The uniformity of the cell was checked with clean fluorescein by measuring the angular envelope, which was constant to ±1%. The cell constant, used to convert Erlenmeyer measurements to absolute turbidities, was determined by measuring the 90° scattering of a given solution of Ludox in the Erlenmeyer, and in the square cell. This factor varied from 1.25 to 1.60 ± 1%, changing somewhat each time the mercury lamp was replaced. The angle made by the sides of the cell was sufficient, so that no correction for back reflection had to be applied to the data.[19] The back reflected beam was completely deflected to the cell floor and was not viewed by the phototube. This was checked empirically by measuring the same solution in the Erlenmeyer, and in a cylindrical cell. When the results were adjusted for the difference in cell constants, and the back-reflection correction applied to the cylindrical cell data, the results agreed over the whole angular range to within 2%.

The effect of concentration was studied by diluting with clean solvent by weight, stirring magnetically until homogeneous, and measuring as before.

2. Treatment of Light Scattering Data.—It has become customary, in handling light scattering data, to interpret the results according to the familiar equation[20]

$$Kc/R_\theta = 1/[M_w P(\theta)] + 2Bc \qquad (3)$$

by means of which the weight average molecular weight, M_w, and the *z*-average of $(\overline{r^2})$, the mean square end-to-end chain length, are determined, on the assumption that the chains are Gaussian. Now although this procedure is always valid provided we can make measurements at sufficiently low angles, under ordinary experimental conditions it can be strictly applied only to chain molecules having values of $(\overline{r^2})^{1/2}$ less than about 800 Å.

On the other hand, an expansion of $P(\theta)$ for large, rather than small, chains shows that a plot of Kc/R_θ against $\sin^2 \theta/2$ reaches an asymptote whose intercept yields the number average molecular weight, M_n, and whose slope is determined by the number average of $(\overline{r^2})$. In actual practice this asymptote should be accurately locatable when the *z*-average of $(\overline{r^2})^{1/2}$ exceeds 2000 Å. This leaves us with an intermediate range in which a knowledge of or an assumption about the polydispersity of the sample is a prerequisite to a precise determination of molecular weight and size, provided measurements are made only in the ordinary range of 30 to 135°. The dependence of the location of these three regions on polydispersity and other relevant details are discussed in the following paper.

It will be useful to anticipate the effects of this situation on the principal experimental results we expect to obtain. With regard to determining the value of the effective bond length *b* it is seen that in the low molecular weight range this will be obtained from $(\overline{r^2})_z$ and M_w so that the result will be somewhat in error numerically and depends to some extent on the polydispersity. In the region of the asymptotic behavior, however, number averages of both quantities will be obtained and the result will be correct and independent of polydispersity. In determining the intrinsic viscosity–molecular weight relation, we shall want the weight average molecular weight but this is directly obtainable only in the low molecular weight range. Elsewhere an estimate of the polydispersity will be required. The dependence of the result on the polydispersity will not be great enough to obscure the main effects we seek to establish but the inability to estimate it accurately can set a definite limit to the precision of the results obtained.

(17) I. Jullander, *Arkiv Kemi Mineral. Geol.*, **A21**, No. 8 (1945).

(18) B. Brice, M. Halwer and R. Speiser, *J. Opt. Soc.*, **40**, 768 (1950).

(19) A. Oth, J. Oth and V. Desreux, *J. Polymer Sci.*, **10**, 551 (1953).

(20) B. H. Zimm, *J. Chem. Phys.*, **16**, 1093 (1948); **16**, 1099 (1948).

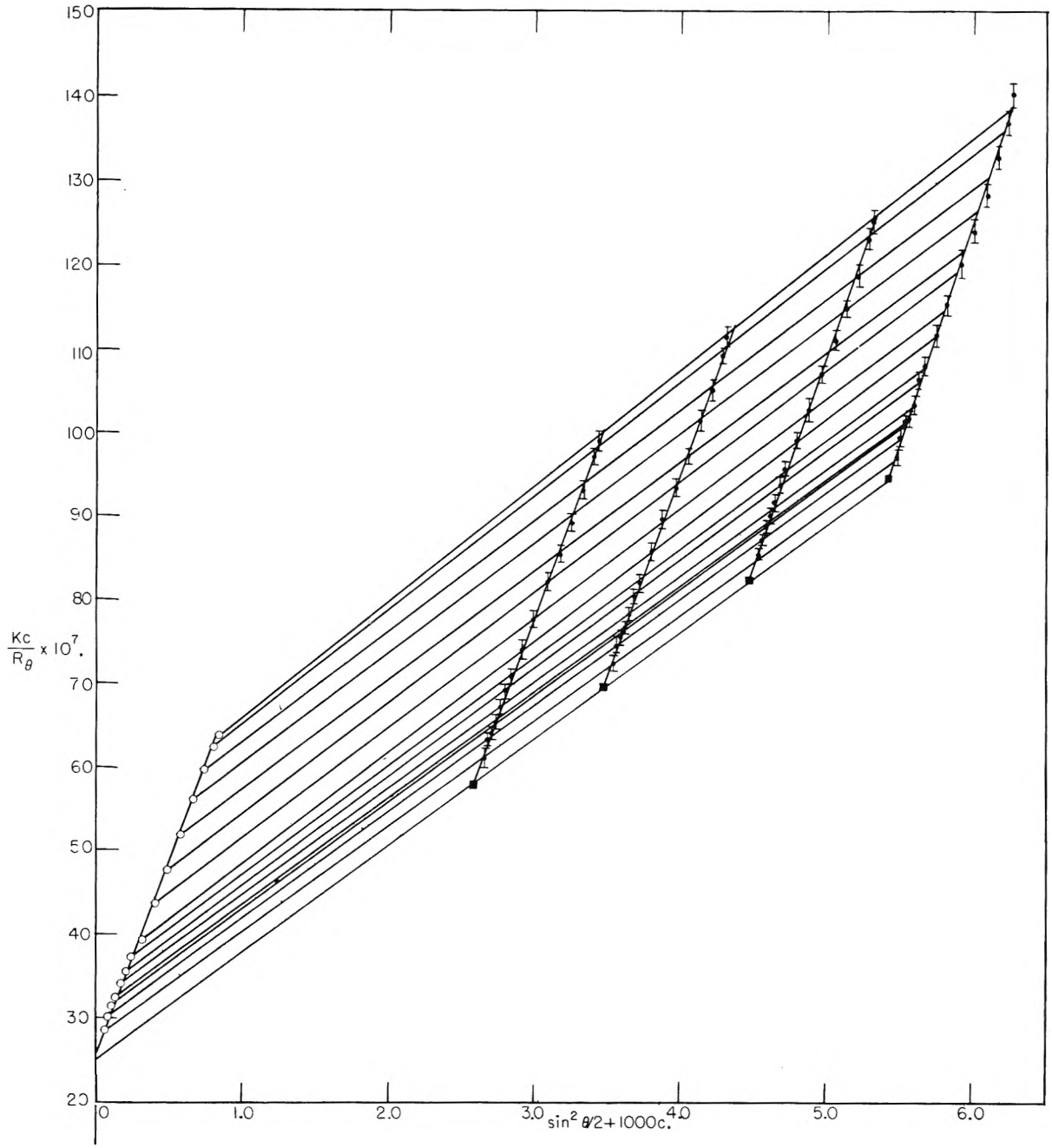

Fig. 3.—Light scattering data for cellulose nitrate sample Ba in acetone at 25°.

G. **Osmotic Pressure.**—Osmotic pressure measurements were made on three samples as a guide in polydispersity estimates and to check independently on the light scattering results.

A Fuoss–Mead type osmometer was used with a gel cellophane membrane. The membrane was washed free of preservative with running water and conditioned for use with acetone by soaking over successive nights in water–acetone mixtures of proportions 90:10, 75:24, 50:50, 25:75, 10:90, and finally in pure acetone.

It was found that acetone evaporated from the edges of the membrane, so the gap between metal plates was covered with adhesive tape which was then coated with glyptal over its whole surface and around the edges. The entire osmometer was packed tightly in a box with excelsior, and placed in a room thermostated at 25 ± 1°. The difference in levels in the capillaries was adjusted to approximate the equilibrium value, and then read until constant for at least an hour. Equilibrium was reached in all cases within three hours. The heights of the menisci were determined with a cathetometer having a precision of ±0.02 cm. The pressure was calculated directly from the head of acetone. The density of the acetone used, as determined pycnometrically, was 0.778.

Experimental Results

A. **Tabulation of Experimental Data.**—Representative light scattering plots are shown in Figs. 2 (sample A) and 3 (fraction Ba). These together with all others except those mentioned below showed linear reciprocal envelopes and likewise did not display any curvature in the zero angle line showing that the second virial coefficient was sufficient to characterize the data in the concentration range studied. For higher molecular weight samples, the highest concentration measured was about 0.2 g./dl. and for the lower molecular weight

samples about 0.5 g./dl. In all, measurements were made on eight fractions, two unfractionated polymers and one mixture. In all cases K is taken equal to 1.84×10^{-7}.

Osmotic pressure measurements were made of two fractions and one unfractionated polymer. Some results are shown in Fig. 4. Here the concentration range extended up to 1% but no curvature in the reduced osmotic pressure plot was evident.

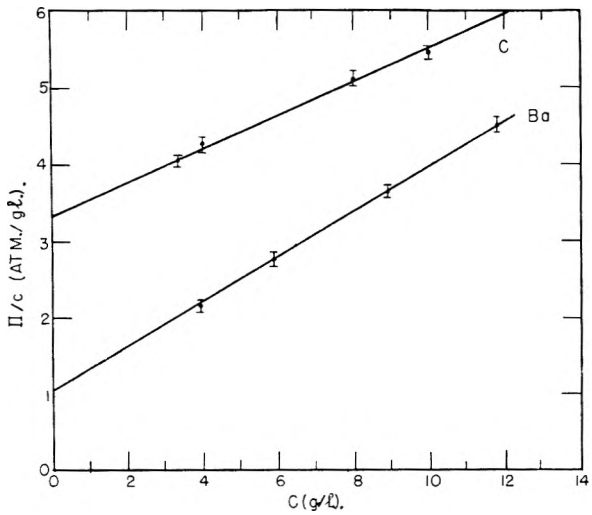

Fig. 4.—Osmotic pressure data for cellulose nitrate samples Ba and C in acetone at 25°.

As indicated in the previous section, viscosity measurements were made as a function of gradient and extrapolated to zero gradient. Only in the case of the two lowest molecular weight samples (Cb and Ca) was the gradient dependence negligible. A typical plot of η_{rel} against gradient is shown in Fig. 5 and the plot of the logarithm of the reduced specific viscosity against concentration for all of the samples is shown in Fig. 6. All measurements mentioned thus far have been in acetone. Some viscosity measurements have been made in other solvents: these are reported where needed in the discussion.

In Table I we have collected relevant quantities

TABLE I

DIRECT EXPERIMENTAL RESULT ON CELLULOSE NITRATE

Sample	Mol. wt. (L.S.)	$\sqrt{\overline{r^2_{exp}}}$ Å.	B (L.S.), mole cc./g.^{2} × 10^4	[η], dl./g.	Mol. wt. (O.P.)	B (O.P.),[c] mole-cc./g.^{2} × 10^4
Cb	77,000	380	5.5	1.23		
Ca	89,000	540	5.5	1.45		
C[b]	273,000	2250	5.0	3.54	74,000	8.95
Bb	360,000	1360	6.6	5.50	213,000	11.2
Ba	400,000	1500	6.6	6.50	234,000	11.9
M1[a]	640,000	2280	6.75	10.6		
A8	846,000	2165	6.9	14.9		
Ab[b]	1,270,000	3180	5.7	24.5		
A	1,550,000	3080	5.8	30.3		
A2[b]	2,510,000	4070	(0.9)	31.0		
Aa[b]	2,640,000	5450	11.8	36.3		

[a] M1 is a mixture of 0.742 part by weight of Ba and 0.258 part of Ab. [b] These samples exhibited some irregular features which are discussed in the text. [c] The striking difference in B determined by the two methods is being studied further and will not be discussed in this paper.

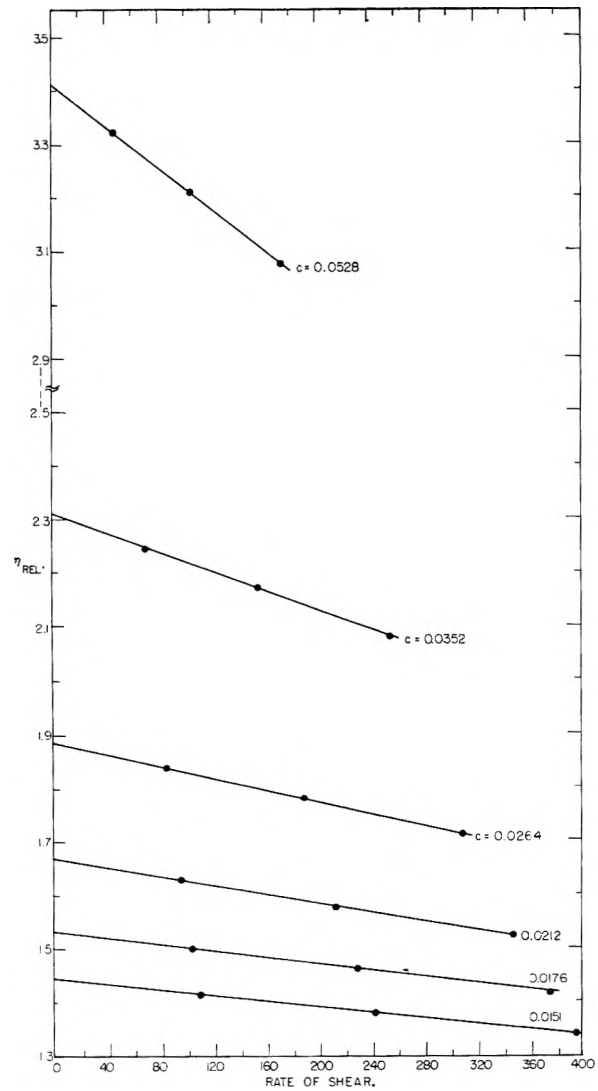

Fig. 5.—Relative viscosity as a function of gradient for cellulose nitrate sample Ab in acetone at 25°.

obtained from these data directly, that is, by customary extrapolation procedures, and the equations

$$(Kc/R\theta)_{c=0} = 1/M \qquad (4a)$$

$$\overline{r^2} = \frac{9\lambda'^2(\text{limiting slope})}{8\pi^2(Kc/R\theta)_{c=0}} \qquad (4b)$$

The reciprocal scattering envelopes for two samples, C and M1, were curved and are reproduced in the following article.[21] The results entered in Table I are obtained from extrapolation of the lowest angle data. The curvature in sample C is so pronounced however that there is considerable uncertainty in the molecular weight and size determinations. The three other samples marked in the Table also exhibited anomalies or presented unusual difficulties.

In the case of sample Ab we find that despite extensive fractionation that should have produced a fraction lying close in molecular weight to Aa and considerably above the unfractionated sample its molecular weight is indeed substantially lower. We

(21) H. Benoit, A. M. Holtzer and P. Doty, THIS JOURNAL, **58**, 635 (1954).

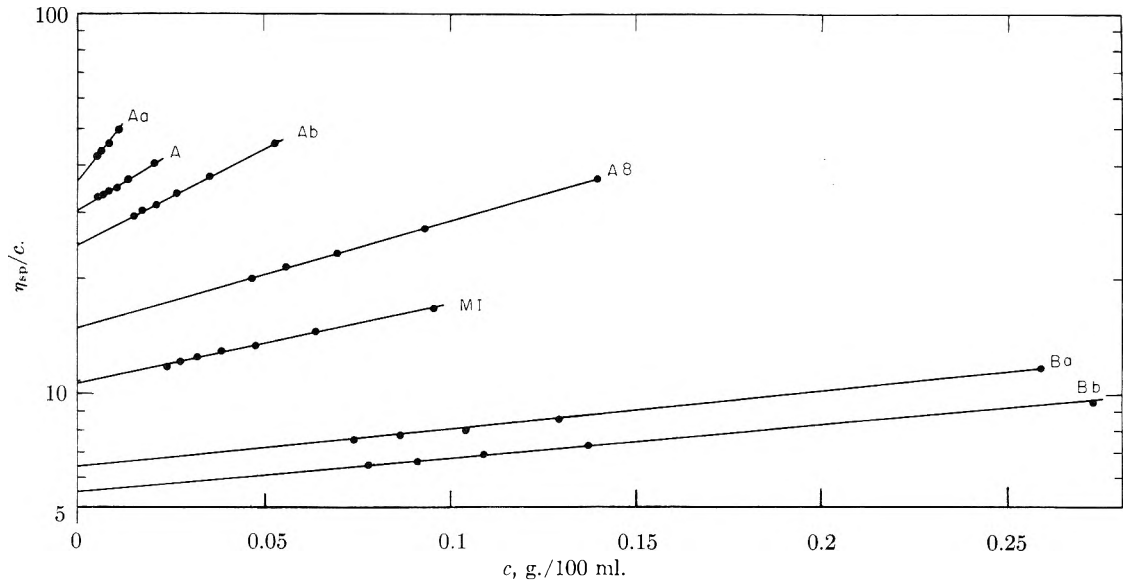

Fig. 6.—Log η_{sp}/c *vs.* c at zero gradient for cellulose nitrate samples in acetone at 25°.

suspect that degradation occurred during the fractionation or before measurements were made on it. Consequently, it may be that its molecular weight distribution is much broader than expected from its fractionation.

The second virial coefficients, B, for samples A2 and Aa differ widely from the others. The first measurements on Aa showed such marked downward curvature that extrapolation to zero angle was impossible. The concentration dependence at finite angles corresponded to $B = 0.8 \times 10^{-4}$. When further attempts at cleaning did not alter this situation, we suspected that trace amounts of metal ions might be causing association through occasional carboxyl groups on the cellulose nitrate.[22,23] Consequently, after adding some water to the acetone solution, this sample was passed through an ion-exchange resin (Dowex 50) followed by precipitation with hexane and washing with alcohol. When measurements were now made the results recorded in Table I were found. This strongly suggests that metal ion contamination plus the presence of groups with which they could associate were responsible for the original behavior. However, the sample purified in this way may not be completely representative because of possible chemical alteration. This was suggested by the fact that upon repeated passage through the ion-exchange resin the polymer became slightly yellow colored and, moreover, the resin gave off a strong phenolic odor. Returning now to sample A2 we find upon re-examination of the light scattering plot that a very mild curvature could be detected in the envelope although it lies within probable experimental error. Because of this and the very low value of B, the results for this sample as well must be considered with some reservations.

B. Results Derived from Experimental Data.—Recalling that our principal aim is to determine the variation of size as measured by the radius of gyration and the hydrodynamic behavior as measured by the viscosity as a function of molecular weight, we now set about putting the data summarized in the foregoing section into the most suitable form for this purpose.

First it is clear from Table I that the molecular sizes investigated extend from the range where the ordinary procedures are valid well into the range of the asymptotic behavior discussed earlier. Thus in the lower molecular weight range the values listed in Table I are M_w and $\sqrt{r_z^2}$, whereas in the higher range these are the values of $2M_n$ and $(3\overline{r_n^2})^{1/2}$. In both cases the subscript over $\sqrt{r^2}$ refers to the root mean square dimension of that particular average of molecular weight. Thus it is necessary to decide upon the relation of M_n to M_w to M_z before all the data can be converted into that of a single average. In addition we have the high angle data from samples C and M1 to evaluate and a decision must be made as to how to treat those samples (fortunately only two, Bb and Ba) which lie in the intermediate region where neither of the above procedures is likely to be exactly correct.

As a guide in these problems, osmotic pressure determinations of M_n were made in the three cases listed in Table I. In the case of the two intermediate fractions, this shows that the interpretation of the reciprocal of the intercept as M_w leads to the conclusion that $M_w = 1.7M_n$, whereas its interpretation as $2M_n$ leads to a 17% discrepancy. The other osmotic pressure measurement shows M_w to equal $3.7M_n$ assuming that the low angle data can be extrapolated reliably. The extrapolation of the high angle data leads to a value of M_n of 94,000. This is a maximum value and hence is not necessarily in conflict with the lower osmotic pressure result. Accepting this higher value, we still have $M_w = 2.9M_n$.

One might expect cellulose derivatives to have molecular weight distributions corresponding to that of polycondensation polymers where all bonds are equivalent, *i.e.*, with the ratio $M_n:M_w:M_z$ proportional to 1:2:3, and the fractions thereof to have very narrow distributions with the three average

(22) M. Wales and D. L. Swanson, THIS JOURNAL, **55**, 203 (1951).
(23) E. F. Evans and H. M. Spurlin, *J. Am. Chem. Soc.*, **72**, 4750 (1950).

TABLE II

TABULATION OF DERIVED RESULTS[a]

Sample	M_n	M_w	N_n	$\sqrt{\overline{r_n^2}}$ (Å.)	$\sqrt{\overline{r_n^2}}/L_n$	b (Å.)	b^2/b_0^2[b]	$\Phi \times 10^{21}$[c]
Cb	(45,000)	77,000	(152)	(271)	(0.346)	(22.0)	(0.395)	(2.24)
Ca	(52,500)	89,000	(178)	(344)	(.376)	(25.8)	(0.543)	(1.52)
C	74,000	273,000	250	(600)	(.466)	(38.0)	(1.18)	(1.41)
Bb	213,000	360,000	720	(868)	(.234)	(32.4)	(0.855)	(1.44)
Ba	234,000	400,000	790	(955)	(.235)	(34.0)	(0.940)	(1.41)
M1	211,000	640,000	711	906	.247	34.0	0.940	(1.87)
A8	424,000	(850,000)	1429	1250	.170	33.1	0.890	(2.42)
Ab	635,000	(1,270,000)	2150	1835	.166	39.6	1.27	(1.89)
A	775,000	(2,300,000)	2620	1760	.131	34.4	0.961	
A2	1,255,000	(2,510,000)	4230	2360	.108	36.3	1.07	(2.23)
Aa	1,320,000	(2,640,000)	4470	3150	.137	47.1	1.80	(1.15)

[a] Values in parentheses have been calculated using polydispersity assumptions described in the text. [b] The effective bond length in the Gaussian range, b_0, has been taken as the average value of b for samples Bb through A2. [c] Values of Flory's Φ have been calculated taking polydispersity into account as discussed in the text. For sample C a smoothed value of b = 30 Å. was used, because of uncertainty in the experimental result for this sample. Averaging all of these except the doubtful Aa, we find $\Phi = 1.91 \times 10^{21}$.

molecular weights nearly equal. However, it appears that the distributions in cellulose nitrate are much wider both for the unfractionated samples and for the fractions. In view of the limited observations on polydispersity and the likelihood that the higher molecular weight fractions have received less sharpening during the fractionation, it seems best to assume that the four higher fractions have a distribution corresponding to $M_w/M_n = 2$. For the four lowest fractions we can take $M_z/M_n = 2.5$ and $M_w/M_n = 1.7$ in keeping with the osmotic pressure measurements and the assumption that low angle behavior is being exhibited by the Ba and Bb fractions. We accept the osmotic pressure results for M_n of sample C and assume that $M_w/M_n = 3$ for sample A on the basis of our knowledge of the polydispersity of C, the other unfractionated sample.

With these estimates and assumptions about polydispersity, the desired results can be derived from the data assembled in Table I. These are listed in Table II. All values reported in parentheses are those which depend on an assumption of polydispersity. N_n and $\sqrt{\overline{r_n^2}}$ represent the number average degree of polymerization and the root-mean-square dimension thereof. The effective bond length b is $(\overline{r_n^2}/N_n)^{1/2}$ and Φ, the constant in the Flory–Fox viscosity equation is calculated from $[\eta]M_n/(\sqrt{\overline{r^2}^3})_n$.

Discussion

A. Size and Configuration of Cellulose Nitrate. —It will be recalled that for a freely jointed chain without volume effect the mean square of the radius of gyration, $\overline{\rho^2}$, or the mean square of the end-to-end length, $\overline{r^2}$, is proportional to the degree of polymerization N, provided N is sufficiently large. It has been shown[3] that when N is not large enough to meet this requirement of Gaussian behavior, $\overline{\rho^2}$ and $\overline{r^2}$ assume lower values than otherwise expected and these decrease continuously with decreasing values of N. For a given valence angle one can calculate the dependence $\overline{\rho^2}$ on N over the entire molecular weight range as a function of the mean value of the cosine of the angle between one bond and the plane of the two prior bonds. This quantity, denoted as $\overline{\cos\phi}$, also occurs in the expression for $\overline{r^2}$ (or $\overline{\rho^2}$) in the Gaussian region. That is

$$\overline{r^2} = Nl^2\left(\frac{1+\cos\theta}{1-\cos\theta}\right)\left(\frac{1+\overline{\cos\phi}}{1-\overline{\cos\phi}}\right) \qquad (5)$$

where l = 5.15 Å. and θ, the supplement of the valence angle is taken as 70°. Hence the value of $\overline{\cos\phi}$ should characterize the size of a chain molecule of given N in both the Gaussian and non-Gaussian ranges, and be independently measurable in both regions.

Having seen that cellulose nitrate is sufficiently stiff to permit measurements of the radius of gyration in the non-Gaussian as well as the Gaussian regions, we are interested in seeing if our measurements are consistent with the above prediction. From Table II it is seen that the effective bond length, b, which is equal to $\sqrt{\overline{r^2}/N}$, exhibits a nearly constant value of about 35 Å. for N greater than 500, if the two samples (C and Aa) about which we have greatest doubt, are excluded. Below N = 500 the value of b is substantially less. We can check this behavior quantitatively by comparing b^2/b_0^2 (where b_0 equals the average value at high N) as a function of N with the calculated relation based on the following choice of the value of $\overline{\cos\phi}$. The average of the seven samples (Bb to A2) gives b_0 = 34.8 A., and substitution of this in the above equation gives a value of 0.915 for $\overline{\cos\phi}$. Using this, the theoretical curve in Fig. 7 has been drawn. The fit of the points lies within the probable experimental error (±15% for b^2) in all but two cases.

We conclude that the variation of the size of cellulose nitrate with molecular weight in both the Gaussian and non-Gaussian regions can be accounted for in terms of a single parameter which in the case of acetone solutions at 25° equals 0.915 ± 0.01: this corresponds to b = 34.8 ± 2.2 Å.

Thus far it has been assumed that the volume effect plays no role in the chain statistics. The volume effect, if present, can be approximated by multiplying the right side of equation 5 by $(1 + kN^{1/2})$ where k is a constant. The uncertainty in our data is such that a value of k up to 6×10^{-3} could not be excluded. Indeed, a value of 2×10^{-3}

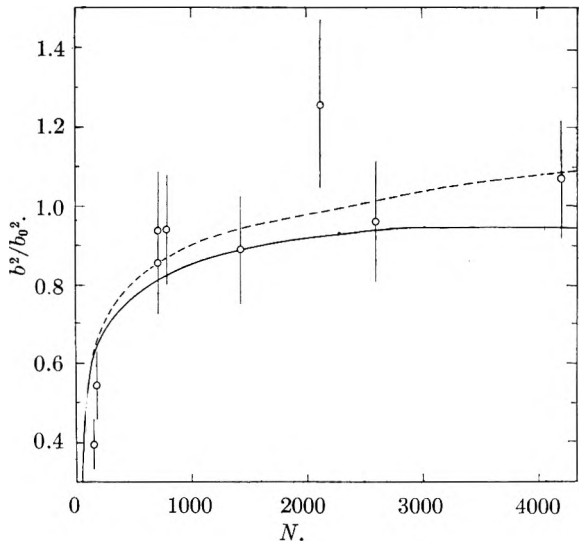

Fig. 7.—Dependence of b^2/b_0^2 on N for cellulose nitrate in acetone at 25°: solid curve, theoretical curve for b = 34.7 Å., $\overline{\cos \phi}$ = 0.915; dashed curve, theoretical curve with volume effect, $k = 2 \times 10^{-3}$.

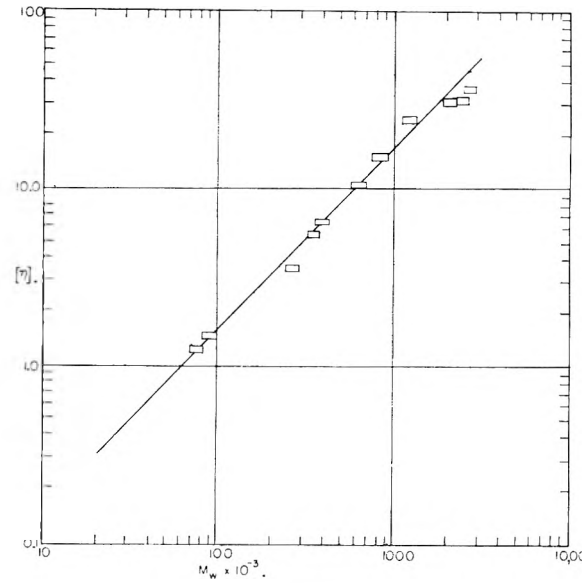

Fig. 8.—Log $[\eta]$ *vs.* log M_w for cellulose nitrate in acetone at 25°.

with $\overline{\cos \phi}$ unchanged fits the data quite well as is shown by the dashed line in Fig. 7.[24a] It is of interest to note that this value for k is very close to that calculated from the observed value of B and b_0 by means of the recently derived relation of Zimm, Stockmayer and Fixman[24b]

$$k = \frac{8}{3}\frac{3}{2\pi b_0^2}^{3/2}\frac{BM_0^2}{N_0} \qquad (6)$$

where M_0 is the weight of a glucose residue and N_0 is Avogadro's number. Substitution yields $k = 1.8 \times 10^{-3}$ indicating that the volume effect should be in the range compatible with our observations. This point is discussed further in the next section.

It is important to recognize that despite the detailed concern with polydispersity estimates these have not affected the character of the results but only the absolute values. Hence in comparing this with other work there are two points of interest: the dependence of b on N and the value of b_0. Only three light scattering studies appear to have been made: cellulose acetate in acetone,[4] cellulose nitrate in acetone[7] and cellulose nitrate in butanone and ethyl acetate.[25] In all of these b is found to decrease with N, the opposite of that found here and the opposite of that to be expected. These earlier results were obtained by assuming that the polydispersity was negligible. However, had we done the same, *i.e.*, employed the data in Table I directly, we would still have found b to increase with N and then become essentially constant. Therefore the difference appears to be in the experimental observations. It is evident that in the Stein and Doty and Badger and Blaker work dust and colloidal impurities had not been satisfactorily removed and these assumed greater importance with decreasing N.

The values of b_0 in these earlier measurements need not be identical because of differences in the cellulose derivatives or solvent. Nevertheless, the range observed, 70, 50 and 41 for the three studies, respectively, is too broad to accept. We believe that the value of 70 for cellulose acetate should be discarded. The value of 50 for cellulose nitrate is based on molecular weight measurements that seem to be too low as discussed in the next section. The two measurements in ethyl acetate that are in the Gaussian range in the Newman and Flory work give 36.5 Å. and this appears to be quite acceptable. However, if this is corrected to allow for these samples being in the asymptotic region, this value is reduced to 29.6 A. Such a value is too low since the value in ethyl acetate should be somewhat higher than in acetone.

The value of b_0 found in this study is about four times that found for typical vinyl polymers such as polystyrene. This increase is half due to the larger monomeric unit and half to a larger value of $\overline{\cos \phi}$, *i.e.*, to steric hindrance and potentials restricting rotation.

B. Molecular Weight Dependence of the Intrinsic Viscosity.—Since the intrinsic viscosity is very closely related to the weight average molecular weight, this average must be employed. One recalls that it is this average which is obtained directly from light scattering in the low molecular weight range but at higher values it is the M_n which is determined. Consequently, the higher molecular weight range will display some dependence upon our assumption about polydispersity. The results are shown in a log–log plot in Fig. 8. The points are shown as rectangles allowing a ±5% error in $[\eta]$ and a ±10% error in M_w. These estimates are probably somewhat high for the lower molecular weight fractions but may be substantially low for

(24) (a) The two lowest molecular weight points fall substantially below the calculated line. They can only be brought closer to a theoretical line by lowering the value of b_0. However, the higher molecular weight data, allowing for the maximum volume effect, would not permit less than a value of 33 Å. and this does not make a net over-all improvement.

(24b) B. H. Zimm, W. H. Stockmayer and M. Fixman, *J. Chem. Phys.*, **21**, 1716 (1953). We wish to thank Prof. Stockmayer for pointing this out and telling us of current work with M. Fixman which insures that higher terms than $1 + kN^{1/2}$ are not important in this case.

(25) S. Newman and P. J. Flory, *J. Polymer Sci.*, **10**, 121 (1953).

the higher molecular weight fractions and the unfractionated samples. It is seen that the data, which cover a 30-fold range in molecular weight, appear to be linear and can be well fitted by a line with a slope of unity. The value of the constant K_m, the Staudinger constant ($[\eta]/N_w$), is 5.0×10^{-3}.

Let us compare this value of K with other measurements assuming Staudinger's law is valid before taking up the possibility of curvature in the log–log plot. In a recent survey[26] it was concluded that all earlier reliable data give a value of $K = 10.5 \pm 1.0 \times 10^{-3}$ for cellulose nitrate of 13.8% N. All molecular weight measurements in the earlier investigations were made with osmotic pressure and yielded therefore number average molecular weights; fractions and unfractionated samples were used rather indiscriminately. If we assume that M_w/M_n equals approximately 2 as this present study suggests, it is seen that our work and the earlier work are in excellent agreement. In another survey of earlier work plus new measurements, Immergut and Mark[27] report an average value of the Staudinger constant of 10.3×10^{-3}. With this value so clearly established and with the equally clear proposition that the intrinsic viscosity depends on M_w and not on M_n, one is forced to conclude that M_w is related to M_n in a consistent way in the many studies that have now been made. Our results require that this relation is, on the average, $M_w = 2M_n$. This means that the log–log plot based upon osmotic pressure measurements should be a band, the width of which could be estimated from the range of M_w/M_n ratios. From our very limited observations, this range in fractions and unfractionated samples varies from 1.7 to 2.9, that is, over a factor of 1.7. Hence the band width should be about 0.23. In the compilation of Immergut and Mark[27] this width is about 0.17. Since experimental errors would tend to broaden the band, it appears that our estimate of the range of polydispersity is too great or that results differing more than 0.085 in log M from the mean have been rejected.

Turning now to the problem of curvature in the log $[\eta]$–log M_w plot, it is seen from an examination of Fig. 8 that there is no apparent curvature within the margin of error. Is this margin of error sufficiently small to check the claims of curvature? To answer this, one notes that the data of Munster,[6] which show the most pronounced curvature, are such that the slope in the region between $N = 500$ and 3000 should be about 0.80. Our data conform with the slope of unity certainly within ± 0.05 and, if accepted, invalidate the claim that substantial curvature exists. From examining Munster's work, it would appear that he did not measure viscosities as a function of gradient and extrapolate to zero gradient. If this is the case, the values of $[\eta]$ above $N = 500$ are increasingly in error. Correction for this would raise his points progressively and would probably restore a linear behavior. Moreover, the osmotic pressures measured for his highest fractions were in the range of 0.15 to 0.6 cm. and this must lead to considerable uncertainty in the molecular weight determination in this region.

Badger and Blaker[7] state that their data together with those of three other investigators suggest that K_m passes through a broad maximum near $N = 120$ and exhibit decreasing values as N increases up to 1000. Our data do not extend down this low in N but are in conflict with the downward trend in the values of K_m in the region of higher N. Examination of Badger and Blaker's work alone actually shows that it agrees quite well with Staudinger's law behavior and $K = 10.5 \times 10^{-3}$. However, the value of this constant is twice that which we find; it appears that these much lower molecular weights arise from the combined effects of a higher refractive index increment and a higher calibration constant.

Of the other data quoted by Badger and Blaker only those referring to cellulose acetate cover a sufficient range of N but this does show the downward trend in K_m clearly. Here again it appears that the criticism of neglect of gradient dependence can be made and in addition there is the possibility that the acetate content is varying systematically in the samples studied.

If now we accept the relation $[\eta] = 5.0 \times 10^{-3} N_w$, it is possible to estimate the magnitude of the highest molecular weight samples of cellulose. The information required is the intrinsic viscosity extrapolated to zero shear in acetone. Among the meager reports of this type of viscosity measurement in the literature, the only sample we find that is significantly higher than that reported here is a cellulose nitrate made from Delfos cotton having at 500 sec.$^{-1}$ an intrinsic viscosity in ethyl acetate of 63.[28] Using extrapolations of our own data, we estimate that this corresponds to a zero gradient viscosity in acetone of at least 46 and probably somewhat more. This would then place the weight degree of polymerization of the highest natural cellulose near 10,000.

C. The Relation of Hydrodynamic Behavior to Molecular Configuration.—Having concluded that the mean molecular configuration as a function molecular weight can be characterized by a single parameter, $\overline{\cos \phi}$, and that a transition from non-Gaussian to Gaussian statistics does occur within the normal molecular weight range, we find some difficulty in accommodating three other observations: (1) the hydrodynamic character as reflected in the intrinsic viscosity is oblivious to the non-Gaussian to Gaussian transition, (2) the exponent of unity in the viscosity–molecular weight relation suggests that the volume effect is so large that it should have dominated the molecular weight dependence of the effective bond length, b, and (3) the observed dependence of $[\eta]$, sedimentation constant, s_0, and diffusion constant, D_0, on molecular weight cannot be accounted for by a single choice of the Kirkwood–Riseman parameters b and ζ.

(1) Several theoretical developments[8-10] lead to the expectation that with increasing molecular weight several regions may be distinguished in the $[\eta]$–M relation: each region may be characterized

(26) P. Doty and H. M. Spurlin, "Cellulose," edited by Ott and Spurlin, Interscience Publishers, Inc., New York, N. Y., 1954.

(27) E. Immergut and H. Mark, *Ind. Eng. Chem.*, **45**, 2483 (1953).

(28) S. Newman, L. Loeb and C. M. Conrad, *J. Polymer Sci.*, **10**, 463 (1953).

by the value of the exponent a appearing in the relation $[\eta] = K'M^a$. At very low M rod-like behavior dominates and in this region a should increase toward a limiting value of 2. Before this value is reached the rod-like configurations are replaced by non-Gaussian coils and the value of a should diminish toward a value of 1. It should reach this value of unity when the chains become Gaussian. With a further increase in M there follows a transition from free draining to solvent immobilizing character with a consequent transition from 1.0 to 0.5 in the value of a. In practically all studies only a short range of the final region is observed and in this a single value of a serves as a satisfactory approximation. The present work shows for the first time that a transition from Gaussian to non-Gaussian configurations occurs in an accessible range of the molecular weight spectrum. It is consequently surprising to find no reflection of this transition in the $[\eta]$–M relation shown in Fig. 8. Two possible explanations may be offered. First, the effect may be too small to be distinguished with the present experimental error. Second, it may be that the first three regions described above are so telescoped that one passes directly from rod-like behavior with axial ratios so low that a equals about 1 to free-draining Gaussian coils where a also equals 1. A choice between these does not seem possible at present. The first suggestion corresponds to the views of Kuhn, Moning and Kuhn[29] and, as they show, the earlier data of Mosimann[30] on low molecular weight cellulose nitrate in acetone is in good accord with this. On the other hand, current investigations of the low molecular weight range by Schulz[31] and his co-workers support the second alternative.

(2) In examining the second observation, let us use the Flory method of dealing with the volume effect

$$[\eta] = K'M^a = KM^{1/2}\alpha^3 \qquad (7)$$

Taking $a = 1$ we have in the region of lowest M the approximation

$$K = [\eta]/M^{1/2} = 0.058[\eta]/N^{1/2} \qquad (8)$$

Using the result for the lowest fraction, we find $K = 0.0058$. Solving for α^2 one gets $\alpha^2 = 0.215N^{1/3}$. Reducing the above approximation by using this value of α^3 rather than unity for the lowest fraction, one obtains $\alpha^2 = 0.247N^{1/3}$. Now the quantity $(1 + kN^{1/2})$ which we used to approximate the volume effect in the previous section dealing with the dependence of b^2/b_0^2 on N is seen to be equal to α^2. Therefore by equating these, one finds that the value of k which corresponds to the volume effect necessary to account for $a = 1$ is 46×10^{-3}. It was found earlier that our data would only permit values of k as high as 6×10^{-3}.[32] For example, if the former value of k were valid, the dashed curve in Fig. 7 would be raised so that it would at $N =$ 2620 (M = 775,000) pass through $b^2/b_0^2 = 3.37$ instead of 1.07 as it does. Clearly then the dependence of $\overline{r^2}/N$ on N shows that the volume effect cannot be large enough, by a wide margin, to account for the viscosity–molecular weight dependence.

In order to obtain other evidence for or against the dominating role of the volume effect, the intrinsic viscosities listed in Table III were measured.

TABLE III

INTRINSIC VISCOSITIES OF TWO CELLULOSE NITRATE FRACTIONS IN SEVERAL SOLVENT MEDIA

Solvent	Ab	Ca
Acetone	24.5	1.45
Ethyl acetate	34.0	2.00
Ethyl acetate–ethanol (1:1)	27.0	1.70
Acetone–ethanol (1:1)	25.0	..

The addition of alcohol in equal volume brought both systems very close to precipitation but no effort was made to adjust each system separately. Two points are of particular interest in these measurements. First, it is seen that upon bringing cellulose nitrate in two different solvents to the verge of precipitation there is not a substantial drop in viscosity but rather only a small reduction in one case and none in the other. Although it would have been preferable to have used a pure "theta" solvent[11] rather than the solvent–non-solvent mixture, it is clear that there has been no tendency to remove the volume effect that would be present if the explanation of the exponent of unity did indeed arise from the volume effect. Second, it is seen that the ratio of the intrinsic viscosities in ethyl acetate to that in ethyl acetate–ethanol is the same for both the high and low molecular weight fractions. This indicates that the difference between the values of the viscosities in the two solvent systems is due to a difference in b_0 rather than to a difference in α. In other words, the value of the exponent a appears to be unchanged. These observations therefore support the proposal that the volume effect is not playing a dominant role.

Finally, it is of interest to compute the value of $\Phi(= [\eta]M/(\overline{r^2})^{3/2})$ which has assumed such an important role in viscosity theory. Because this depends on the number average of M and the number average of $(\overline{r^2})^{3/2}$ the calculation must allow for the polydispersity. This can be done in the following way.

The values of $[\eta]$ and M_n are taken directly from Table II. The value for the number average of $(\overline{r^2})^{3/2}$ is obtained by evaluating the number average of $M^{3/2}$ and using the experimental value of b found for the given sample. The number average of $M^{3/2}$ is given by

$$(M^{3/2})_n = M_n \int_0^\infty M^{1/2} f(M)\, dM \qquad (9)$$

where $f(M)$ is the normalized weight distribution function. Zimm has given a suitable distribution formula whose breadth is determined by a variable parameter z.[20] We find from our above estimates of polydispersity, that samples Cb, Ca, Ba and Bb correspond to a value $z = 1.43$; samples A and M1

(29) H. Kuhn, F. Moning and W. Kuhn, *Helv. Chim. Acta*, **36**, 731 (1953). See also E. H. Immergut and F. R. Eirich, *Ind. Eng. Chem.*, **45**, 2500 (1953).

(30) H. Mosimann, *Helv. Chim. Acta*, **26**, 369 (1943).

(31) Professor G. V. Schulz (Mainz), private communication.

(32) This value is in the range observed for vinyl polymers in thermodynamically good solvents.

to $z = 0.5$; and A8, Ab, A2 and Aa to $z = 1$. Distributions corresponding to these values have been used in the above equation to determine the number average of $M^{3/2}$, and thus, through b, the number average of $(r^2)^{3/2}$. In the case of sample C the value of b determined experimentally was not considered to be sufficiently precise since Φ depends on the reciprocal of b^3. Consequently, the smoothed value $b = 30$ Å. was used. The polydispersity correction here was made by extrapolation of the factors found in the other cases.

When the calculations are performed in this manner, one obtains the results listed in Table II. We find, contrary to earlier expectations,[25,33] that Φ shows very little dependence on molecular weight. The values in the first half are a little lower than in the latter half but the difference cannot be considered significant because of the magnitude of the polydispersity effect and of the rather large cumulative experimental error in Φ. We conclude therefore that Φ continues to serve as a very useful constant and exhibits here an average value (1.9×10^{21}) very close to that assigned it from studies on other polymers, and that its constancy within present precision does not depend necessarily upon the mean polymer configuration being in the Gaussian range.

(3) Having seen that absence of a substantial volume effect prevents an explanation of the near unity value of a by the Flory theory, it is of interest to examine the extent of agreement with the Kirkwood–Riseman treatment since it assumes the absence of the volume effect at the outset. The principal test here is to see whether $[\eta]$, s_0 and D_0 can be represented for any sample within the molecular weight range studied by a single assignment of values to the effective bond length, b, and the effective friction constant per monomer element, ζ. The value of b is not subject to assignment for the best fit of data but rather must be taken from the light scattering evaluation. Thus only the choice of ζ remains. However, this quantity appears in the viscosity equation in two places: one, as the first power where its value strongly influences $[\eta]$ and, two, as a factor in the argument of a slowly changing function, $F(\lambda_0 N^{1/2})$, which controls the nature of the molecular weight dependence. Unfortunately, a self-consistent value of ζ cannot be found for the two roles that it plays. If the values of $[\eta]$ for the lower half of the range of log M are matched, a value of about 2.7×10^{-10} is required but this in turn requires that a vary from 0.90 at $N = 200$ to 0.73 at $N = 9000$. On the other hand, if ζ is chosen so that the range of a is the lowest that remains consistent with the data ($0.96 \geq a \geq 0.85$ for the same range of N), one obtains a value of 0.9×10^{-10}. This choice, however, leads to values of $[\eta]$ that are about one-third too small. Thus it is clear that our data cannot be accommodated by a single assignment of values to b and ζ.

Upon turning to examine the corresponding situation in sedimentation and diffusion, one finds a much greater scatter of experimental data in the literature. However, the higher value of ζ (2.7×10^{-10}) is found to provide a reasonable fit of the s_0 values given by Kinell and Ranby.[34] For example, at $N = 256$, s_0 is calculated as 13.3 against 8.3 observed and at $N = 9000$, s_0 is calculated as 42.5 against 45 observed. Values of D_0 are subject to much greater uncertainty and do not extend to as high molecular weights. Using the measurements of Jullander,[35] one finds at $N = 256$, $D_0 = 10.7$ compared with observed values of about 7.0 and at $N = 1480$, D_0 is calculated as 3.0 compared with the experimental value of 2.3. Consequently, when the effects of polydispersity and error in extrapolation to zero concentration are taken into account, it appears that a choice of $\zeta = 2.7 \times 10^{-10}$ and $b = 35$ Å. permit a reasonable semiquantitative representation of sedimentation and diffusion data of cellulose nitrate at the present state of experimental precision. With the somewhat greater precision of viscosity–molecular weight studies, however, an internal inconsistency is found which lies beyond probable experimental error and suggests that the theory does not provide a quantitative representation of the hydrodynamic behavior in this system.

In conclusion it appears that the hydrodynamic characteristics of cellulose nitrate cannot be adequately accommodated by either of the modern points of view represented by the Flory–Fox and the Kirkwood–Riseman theories. The origin of the difficulty appears to lie in the very open and free-draining configurations characteristic of cellulose in derivatives in contrast to vinyl polymers. Consequently for an explanation of the behavior observed here, we must return to the older theories of Huggins,[36] Hermans,[37] Kuhn and Kuhn,[38] and Debye.[39] This means abandoning the Flory–Fox theory because it is based on a model requiring some degree of solvent immobilization and giving up the $F(\lambda_0 N^{1/2})$ factor in the Kirkwood–Riseman equation for $[\eta]$. When this is done, a value of 2.2×10^{10} for ζ offers a very good fit of the viscosity data and maintains the reasonable agreement already found for the more uncertain sedimentation and diffusion constants. This procedure is far from completely satisfying, however, since in principle the Kirkwood–Riseman theory should be internally capable of taking care of even a very porous coil, so long as it is Gaussian. Replacing the factor $F(\lambda_0 N^{1/2})$ by unity in the $[\eta]$ equation is completely *ad hoc* from the strict theoretical point of view.

Acknowledgments.—We are very indebted to the Office of Naval Research (Contract No. N5ori-07654) for the support of this work and to the Union Carbide and Carbon Corporation for a Fellowship held by one of us. We greatly appreciate receiving samples from the Hercules Powder Co. and from Dr. R. C. Mitchell of Rayonier, Inc. Numerous conversations with Dr. Harold Spurlin have been both useful and stimulating throughout the course of this work.

(33) P. Doty, N. S. Schneider and A. Holtzer, *J. Am. Chem. Soc.*, **75**, 754 (1953).

(34) P. Kinell and B. Ranby, "Advances in Colloid Science," Vol III, Interscience Publishers, New York, N. Y., 1949.

(35) I. Jullander, *Arkiv Kemi Mineral. Geol.*, **A21**, No. 8 (1945).

(36) M. L. Huggins, *J. Phys. Chem.*, **42**, 911 (1938); **43**, 439 (1939).

(37) J. J. Hermans, *Physica*, **10**, 777 (1943).

(38) W. Kuhn and H. Kuhn, *Helv. Chim. Acta*, **26**, 1324 (1943).

(39) P. Debye, *J. Chem. Phys.*, **14**, 636 (1946).

AN EXPERIMENTAL STUDY OF POLYDISPERSITY BY LIGHT SCATTERING[1]

BY HENRI BENOIT, ALFRED M. HOLTZER AND PAUL DOTY

Gibbs Laboratory, Department of Chemistry, Harvard University, Cambridge, Mass.

Received April 19, 1954

In the usual treatment of light scattering from solutions of randomly kinked chain molecules, the initial slope of the reciprocal angular envelope at zero concentration is used to obtain the dimension of the z-average molecular weight species, and the intercept at $\theta = 0$ is used to get the weight average molecular weight. The present paper describes in detail a method of utilizing data which fall on the asymptote of this angular envelope, rather than on the initial part. It is shown that such data provide the number average molecular weight, and the number average dimension. Hence, when asymptotic results are available, it is possible to study chain statistics without recourse to fractionation. The results of two separate tests of these conclusions are reported. The first involves a correlation of information from osmotic pressure and viscosity with that obtained from our interpretation of light scattering measurements on a very polydisperse sample of cellulose trinitrate in acetone. The second test employs light scattering data on two fractions of the same substance, and on a mixture of the two of known proportions. The experimental results are shown to be in good accord with the values expected from theory.

In a quite recent paper[2] it has been shown that the determination of the angular distribution of the light scattered by a solution of randomly kinked chain molecules can provide information about the polydispersity of the sample. In this paper we want to show more precisely the possibilities of the method; first by recalling its theoretical basis and then by examining the results obtained in two experimental cases.

Theoretical Basis of the Method

In order to determine the molecular weight, the size and the shape of polymer molecules in solution, one usually plots c/R_θ, the ratio of the concentration to the reduced intensity, multiplied by a numerical factor, K, as a function of $\sin^2(\theta/2)$ (where θ is the angle between the incident and the scattered beams). On extrapolating to zero concentration by the Zimm method,[3] one obtains an experimentally determined curve, which in the case of a monodisperse system is given by the equation

$$\left(\frac{Kc}{R_\theta}\right)_{c=0} = \frac{1}{MP(\theta)} \qquad (1)$$

where M is the molecular weight of the substance and $P(\theta)$ the particle scattering factor. Extrapolating this curve to $\theta = 0$, where $P(\theta) = 1$ by definition, one obtains the molecular weight of the sample.

In the case of a Gaussian chain, $P(\theta)$ has been shown by Debye[4] to be given by

$$P(\theta) = \frac{2}{N^2u^2}\left[Nu - 1 + \exp(-Nu)\right] \qquad (2)$$

with

$$u = \left[\frac{4\pi}{\lambda'}\sin\frac{\theta}{2}\right]^2\frac{b^2}{6} \qquad (2')$$

where N is the degree of polymerization; λ' the wave length of the light in solution; and b the effective bond length.

In the case of a polydisperse system of Gaussian chains, it is possible to insert (2) in (1) and then expand in terms of u and the different moments of the polymer distribution function.

(1) This work was supported by the Office of Naval Researeh under Contract No. N5ori-07654.

(2) H. Benoit, *J. Polymer Sci.*, **11**, 507 (1953).

(3) B. H. Zimm, *J. Chem. Phys.*, **16**, 1093, 1099 (1948).

(4) P. Debye, THIS JOURNAL, **51**, 18 (1947).

For small u one has the well-known result[3]

$$\left(\frac{Kc}{R_\theta}\right)_{c=0} = \frac{1}{M_w}\left[1 + N_z\frac{u}{3} + \ldots\right] \qquad (3)$$

and for large values[2]

$$\left(\frac{Kc}{R_\theta}\right)_{c=0} = \frac{1}{M_n}\left[\frac{1}{2} + N_n\frac{u}{2} + \ldots\right] \qquad (4)$$

In these expressions, M_w and M_n are, respectively, the weight average and the number average molecular weight, N_w and N_n are the corresponding averages for the degree of polymerization, and N_z is the so-called "z-average" degree of polymerization.[5]

Equation 3 shows, as is well known, that the intercept of the curve with the axis gives the weight average molecular weight, and that the initial slope gives the z-average end-to-end distance of the coils; *i.e.*, the end-to-end distance of a coil having molecular weight, M_z. That is, if we plot $(Kc/R_\theta)_{c=0}$ *vs.* $\sin^2\theta/2$, we have, from (3)

$$M_w = \frac{1}{(Kc/R_0)_{c=0}} \qquad (5a)$$

and

$$\overline{r_z^2} = \frac{9\lambda'^2\,(\text{initial slope})}{8\pi^2\,(Kc/R_0)_{c=0}} \qquad (5b)$$

Equation 4 is the equation of the asymptote to the experimental curve. The intersection of this line with the axis is $1/2M_n$, and its slope gives the number average dimension of the coil, according to the equations, easily obtained from (4)

$$M_n = \frac{1}{2\,(\text{intercept of asymptote})} \qquad (6a)$$

$$\overline{r_n^2} = \frac{3\lambda'^2\,(\text{slope of asymptote})}{8\pi^2\,(\text{intercept of asymptote})} \qquad (6b)$$

(5) If $f(N)$ is the normalized weight distribution function of the degree of polymerization in the sample, N_w, N_n and N_z are defined by the expressions

$$N_w = \int_0^\infty nf(N)\,dN$$

$$N_z = \frac{1}{N_w}\int_0^\infty N^2 f(N)\,dN$$

$$N_n = 1\Big/\int_0^\infty \frac{f(N)}{N}\,dN$$

and we also have the relation

$$M_x = N_x M_0$$

where M_0 is the molecular weight of the monomeric unit.

Therefore, if the molecular size is large enough, the precise determination of the angular distribution of the scattered light can give M_n, M_z, M_w and the dimensions of the molecules in the case of a polydisperse system of Gaussian coils.

It is also evident that, when possible, the determination of the asymptote is as important as the determination of the initial part of the curve, since it gives the same average for the molecular weight and the dimension. For instance, this shows that, for the study of the variation of $\overline{r^2}$ as a function of N, unfractionated materials suffice in the range of high molecular weight where the asymptote can be determined with some precision, since it gives the effective bond length, $b = \sqrt{\overline{r_n^2}/N_n}$, without ambiguity.

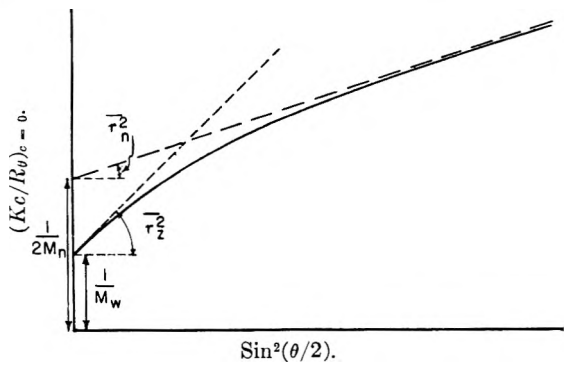

Fig. 1.—Schematic summary of quantities obtainable from the angular distribution of the light scattered by a solution of randomly kinked macromolecules.

Another remark can be made before we discuss the experimental data. Very often it is found in the study of the angular distribution of light scattered by polymer solutions of high molecular weight that the experimental curve, $(Kc/R_\theta)_{c=0}$, is, within probable error, a straight line. We see that this now has two possible interpretations, one of which is a special case of the other. The special case is that the molecular weight distribution[6] is one which approximates the ratio $M_z:M_w:M_n::3:2:1$, since under this condition $(Kc/R_\theta)_{c=0}$ is a straight line.[3] The other is that the measurements have been on the asymptote and that possible curvature at lower angles has been missed. Thus, although the data would be indistinguishable in the two cases, the results derived from their linear extrapolation would differ. In the latter case, equations 6 instead of 5 must be used. The molecular weight obtained is not M_w but $2M_n$ and the dimension is not a z-average but a number average. In the former case, these two interpretations coincide. In order to define the regions in which equations 5 and 6 apply, we have examined the theoretical curves of $1/P(\theta)$ over the whole practical range of polydispersity from the monodisperse case (extreme upward curvature) to the very polydisperse case (extreme downward curvature). We find that, for λ' of 3250 Å., angles of 30 to 135°, and distributions usually expected, equations 5 are valid for molecular sizes up to $\sqrt{\overline{r_z^2}} = 800$ Å. Where the molecular size exceeds $\sqrt{\overline{r_z^2}} = 3000$ Å., the curves have become essentially asymptotic and equations 6 apply. The curvature is therefore restricted to the molecular size range between these two limits. The extrapolation of experimental data falling in this region is consequently hazardous. For cases of moderate polydispersity, the curvature is diminished, the intermediate region contracts and extrapolation is less uncertain. Corrections which may be applied in these cases and a more detailed delination of the region of curvature are given in the Appendix.

In order to summarize this discussion, we have drawn in Fig. 1 a typical light scattering envelope with the values which can be obtained from the study of the initial part of the curve and of the asymptote.

Experimental

In order to use the results of these equations, we have performed two different experiments. We have first studied an unusually polydisperse, unfractionated sample of cellulose nitrate, sample C from the previous study.[7] For this sample we have evaluated the different average molecular weights and the corresponding dimensions directly from light scattering results, and these are compared with those obtained by other methods. The second experiment involved mixing two fractions of cellulose nitrate of known molecular weight and verifying that the values obtained for the various averages are those one can expect from the properties of the fractions. This choice of cellulose nitrate in acetone was made for the following reasons.

(a) For molecular weights greater than 150,000 it has been shown that cellulose trinitrate is a Gaussian chain.[7] This chain has a relatively large effective bond length which allows us to get the asymptotic behavior from light scattering experiments even for moderate molecular weights.

(b) Branching has never been found in cellulose derivatives. This is very important, since branching changes the shape of the particle scattering factor[2] and our preceding conclusions are only valid without this complication.

1. **Study of an Unfractionated Sample. Light Scattering.**—The measurements were made in the manner described in the previous paper.[7] The results shown in Fig. 2 show pronounced curvature. The intercept obtained by extrapolating the low angle data is not very precise but yields the approximate value of 273,000 for M_w. The initial slope is still more uncertain and we have preferred to use the initial slope of the curve corresponding to the lowest concentration. In this way the approximate radius of gyration $\sqrt{\overline{\rho_z^2}} = 920$ Å. is obtained. Since it has been shown that this sample lies in the range of Gaussian behavior, this value can be translated into the root-mean-square end-to-end length: $\sqrt{\overline{r_z^2}} = 2250$ Å.

In order to use the asymptote of the curve we must also be sure that all the curvature is due to the polydispersity and not to the stiffness of the coil. For this purpose we have used Peterlin's calculations[8] of the particle scattering factors for stiff coils. He employed as a model the worm-like chain of Porod and Kratky[9] which can be considered as the limiting case of a chain having a large number of elements and a cosine of the supplement of the valence angle, μ, near unity. The stiffness of such a coil is characterized by the parameter $x = L/q$ where L is the total length of the chain, and q a function which is infinite for a rod and is equal to the bond length for a completely flexible coil. For large x the chain is Gaussian, for $x = 0$, it is a rod, and Peterlin gives numerical evaluations of the particle scattering factor for different values of x. Keeping in mind that x is the limiting value of the quantity $N(1 - \mu)$, we can try to evaluate x for the cellulose chain. In this case the chain is characterized by the relation

$$\overline{r^2} = Nl^2 \frac{1+\mu}{1-\mu} = Nb_0^2$$

(6) P. J. Flory, *Chem. Revs.*, **39**, 137 (1946).

(7) A. Holtzer, H. Benoit and P. Doty, THIS JOURNAL, **58**, 624 (1954).

(8) A. Peterlin, *Makromol. Chem.*, **9**, 244 (1953).

(9) G. Porod and Kratky, *Monatsh.*, **80**, 251 (1949).

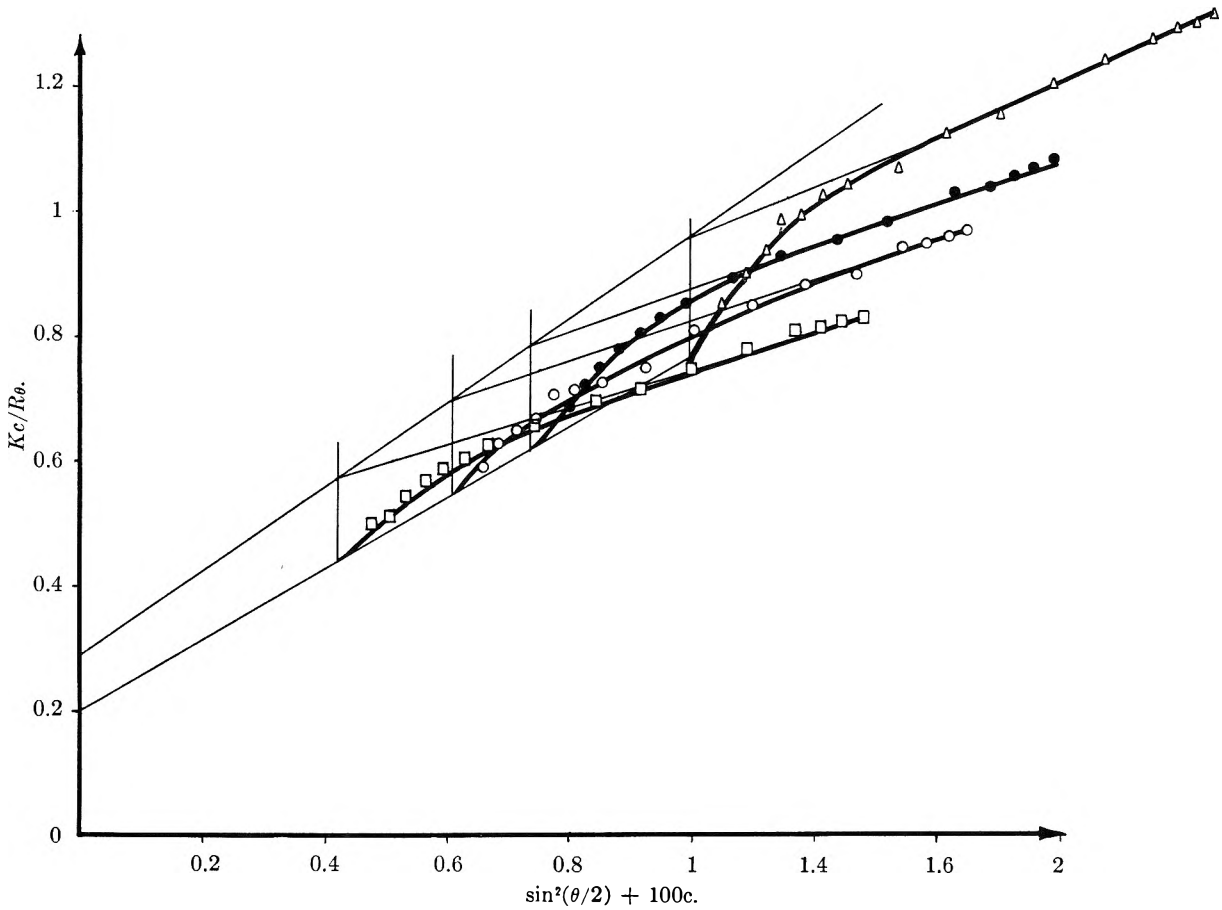

Fig. 2.—Light scattering data for cellulose nitrate sample C in acetone at 25°.

Using the value 5.15 Å. for the length, l_0 of the glucose unit, and for b_0 an experimental value of 35 Å., one obtains $\mu = 0.96$ and we find that $x = 50$, assuming that x equals $N \cdot (1 - \mu)$. In Fig. 3 we have plotted the values of $P^{-1}(\theta)$ as a function of $\sin^2 \theta/2$ (or more exactly $[4\pi/\lambda \sin \theta/2]^2\rho^2$, in order to have the same initial slope) for $x = \infty$, $x = 100$ and $x = 25$ in the range of practical interest for this case, *i.e.*, the value of $P^{-1}(\theta)$ between 1 and 3.[10] These results show that there is only a small difference between the curve $x = \infty$ (Gaussian coil) and the case where x is of the order of 50, and that this difference is of the order of magnitude of the experimental error. Therefore we shall make the assumption that, as a first approximation, the coil is Gaussian and that all the curvature of our curves is due to polydispersity. One also notes that experiments on fractionated samples of similar molecular weight yield envelopes which are linear, corroborating the above conclusion.

Under these circumstances the application of equation 6 to the asymptotic data gives

$$M_n = 94{,}000 \sqrt{\overline{r_n^2}} = 675 \text{ Å.} \quad b = \sqrt{\frac{\overline{r_n^2}}{N_n}} = 38 \text{ Å.}$$

Osmotic Pressure and Viscosity.—The osmotic pressure measurements have been described in the previous paper.[7] The molecular weight obtained by extrapolation to zero concentration in the usual way is equal to 74,000.

The viscosity was measured by the usual method of determining the flow time of a certain amount of solution through a capillary tube. The extrapolated intrinsic viscosity is not shear dependent for such a low molecular weight sample and has the value $[\eta] = 3.54$.

2. **Mixing Experiment.**—Light scattering and viscosity measurements in acetone were made on fractions designated Ba and Ab, and on a mixture containing 25.8% Ab and 74.2% Ba by weight. The viscosity results were extrapolated to zero gradient. As can be seen from Figs. 4 and 5 and Fig. 3 of the previous paper, the fractions gave linear envelopes, while that of the mixture showed downward curvature at high angles.

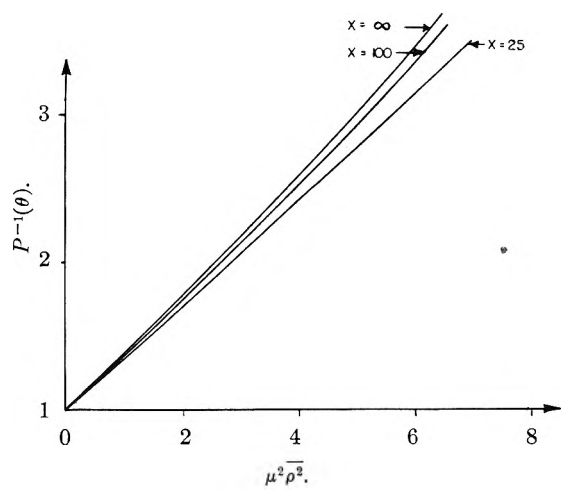

Fig. 3.—The effect of stiffness (after Peterlin) on the shape of the angular light scattering envelope. $x = \infty$ represents the Gaussian coil. A rod would have $x = 0$. Cellulose nitrate corresponds to $x = 50$.

The results obtained by treating the data as described in the first part are summarized in Table I, which also includes values for the mixture as calculated from the results on the individual fractions.

(10) We wish to thank Prof. A. Peterlin who was kind enough to supply the numerical values.

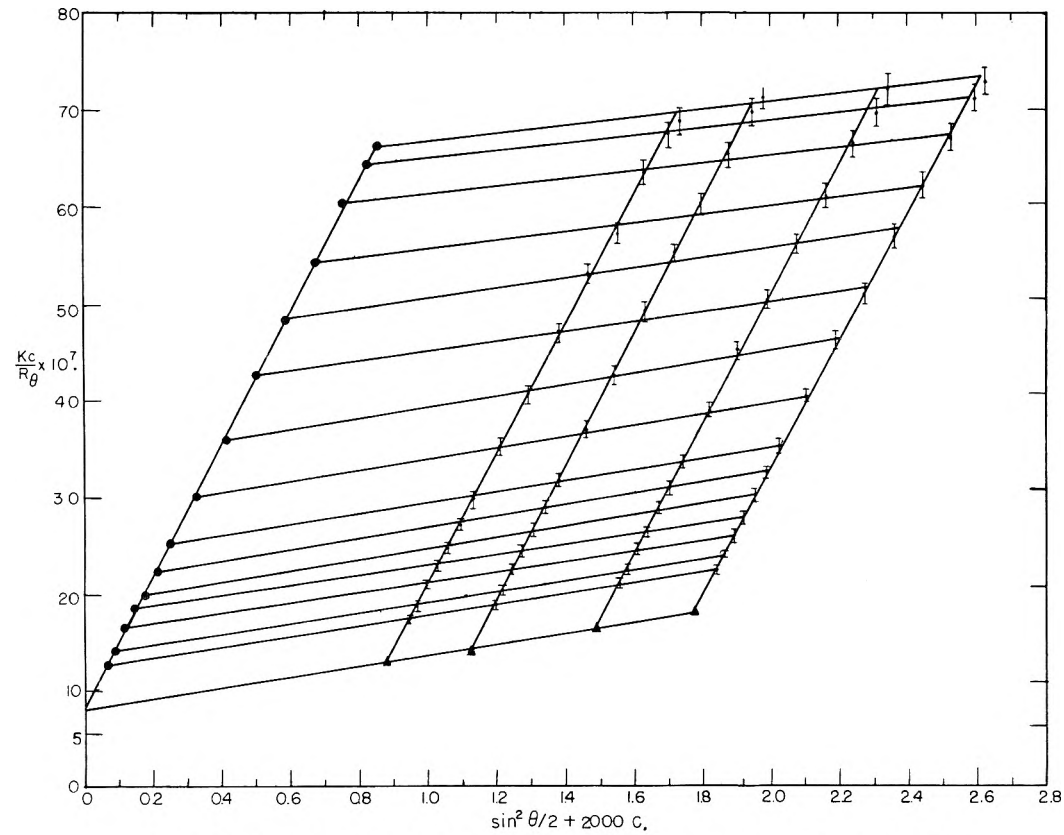

Fig. 4.—Light scattering data for cellulose nitrate fraction Ab in acetone at 25°.

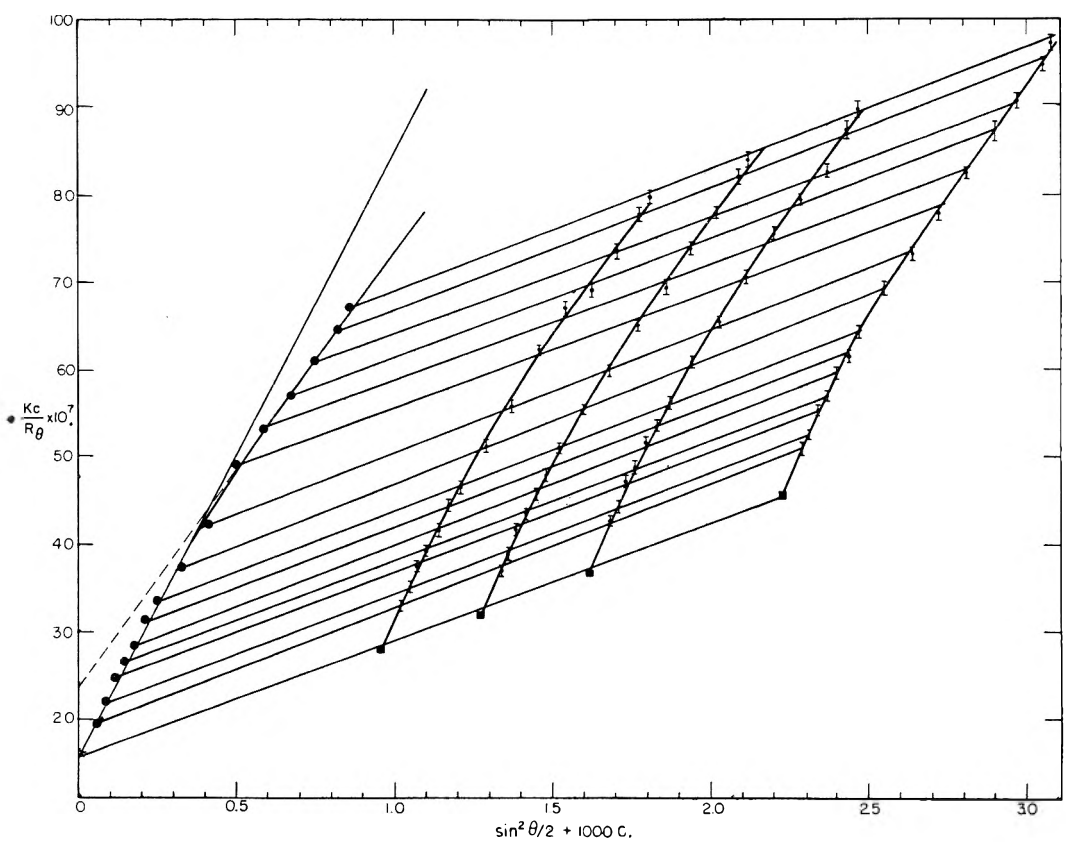

Fig 5.—Light scattering data for cellulose nitrate sample M1 (a mixture of 74.2% Ba and 25.8% Ab) in acetone at 25°

TABLE I

RESULTS CALCULATED FROM LIGHT SCATTERING ON TWO FRACTIONS AND A MIXTURE

		M_n	M_w	$\sqrt{\overline{r_n^2}}$ (A.)	b (Å.)	$[\eta]$
Ba		199,000	400,000	868	32.4	6.50
Ab		635,000	1,270,000	1835	39.6	24.5
M1 (74.2% Ba + 25.8% Ab)	Exp.	211,000	640,000	906	34.0	10.6
	Calcd.	243,000	623,000	..	..	11.2

Discussion of the Results

The first matter of interest is the comparison between the number average molecular weights obtained by osmotic pressure and by light scattering on the unfractionated sample. The first method gives 74,000, the second 94,000, the difference being of the order of 20%.

This difference is not surprising if one considers the lack of precision in the determination of the light scattering extrapolation, when curvature is so large. Further, the small range of angles investigated may not provide data far enough out to be truly asymptotic. These effects introduce an error which is always in the same direction, giving a larger M_n from light scattering than from osmotic pressure. In addition, even at their best, both light scattering and osmotic pressure cannot usually provide a molecular weight with better precision than $\pm 10\%$. Hence the agreement is as good as one can expect, and in addition the light scattering method allows a very rapid determination of M_n and M_w, giving a measure of the polydispersity.

The second point we wish to mention concerns the value of the effective bond length. Using as usual $\overline{r_z^2}$ and N_w for its determination, one finds b = 75 Å. instead of a value of 35 Å. But if one interprets the data as described above, the result is quite different and turns out to be 38 Å. This value is in fair agreeement with our results on the study of fractions and shows, as we have said, that it is useless to fractionate in certain cases, if one is interested only in the statistics of the chain.

In connection with the mixing experiment, it can be seen from Table I that agreement is satisfactory between the experimental molecular weights of the mixture, and the values calculated from the experiments on the fractions. It should be pointed out, however, that the weight average molecular weights for the fractions have been obtained only by assuming that the envelope remains linear through the entire angular range. The value of the effective bond length, b, determined from the asymptote is 34 Å., in excellent agreement with the results on cellulose trinitrate fractions.[7] Further, the shape of the function $P^{-1}(\theta)$ calculated from the $P^{-1}(\theta)$'s of the individual fractions, assuming the latter are linear, is in good agreement with the experimental curve for the mixture, showing the same amount of downward curvature (Fig. 6).

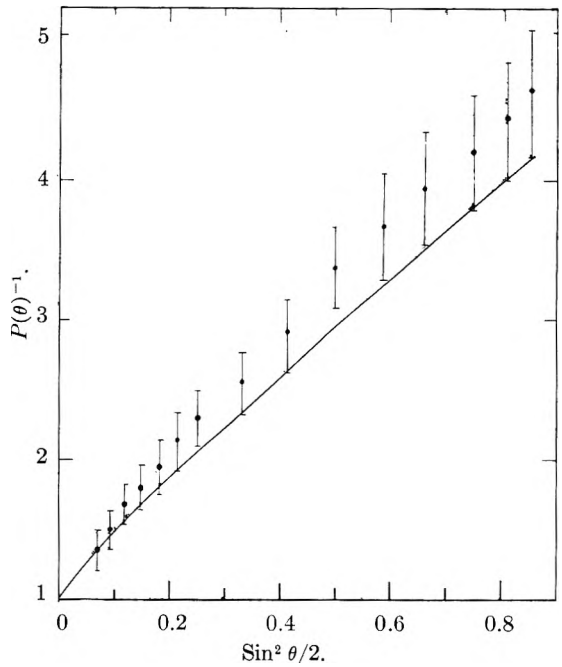

Fig. 6.—Comparison of calculated (solid curve) and experimentally determined (points) angular envelopes for mixture M1. The calculated curve was obtained from the envelopes of the component fractions, assuming the observed linearity persisted to zero angle. The points were obtained directly from the values of $(Kc/R\theta)_c$ = 0 from the experiment on the mixture, and the intercept $(1/M_w)$ of the latter with the θ = 0 axis.

As expected, the intrinsic viscosity of the mixture is, within experimental error, equal to the weight average of the intrinsic viscosities of the two com-

TABLE II

	z = ∞ (monodisperse)					z = 4 (M_z:M_w:M_n::6:5:4					z = 19 (M_z:M_w:M_n::21:20:19				
$N_w u = \langle u \rangle$	$P^{-1}(\theta)$	Asymptote	$\left(\frac{\text{Asymptote}}{P^{-1}(\theta)}\right)$	Limiting tangent	$\left(\frac{\text{Limiting tangent}}{P^{-1}(\theta)}\right)$	$P_4^{-1}(\theta)$	Asymptote	$\left(\frac{\text{Asymptote}}{P_4^{-1}(\theta)}\right)$	Limiting tangent	$\left(\frac{\text{Limiting tangent}}{P_4^{-1}(\theta)}\right)$	$P_{19}^{-1}(\theta)$	Asymptote	$\left(\frac{\text{Asymptote}}{P_{19}^{-1}(\theta)}\right)$	Limiting tangent	$\left(\frac{\text{Limiting tangent}}{P_{19}^{-1}(\theta)}\right)$
0	1.00	0.500	0.500	1.00	1.00	1.00	0.625	0.625	1.00	1.00	1.00	0.526	0.526	1.00	1.00
1	1.36	1.00	.74	1.33	0.98	1.42	1.13	.79	1.40	0.99	1.37	1.03	.75	1.35	0.98
2	1.76	1.50	.85	1.67	.95	1.86	1.63	.87	1.80	.97	1.70	1.53	.90	1.70	.95
3	2.19	2.00	.91	2.00	.91	2.32	2.13	.92	2.20	.95	2.22	2.03	.91	2.05	.92
4	2.65	2.50	.94	2.33	.88	2.78	2.63	.94	2.60	.93	2.68	2.53	.94	2.40	.89
5	3.12	3.00	.96	2.67	.85	3.27	3.13	.96	3.00	.92	3.15	3.03	.96	2.75	.87
6	3.60	3.50	.97	3.00	.83	3.75	3.63	.97	3.40	.91	3.63	3.53	.97	3.10	.85
7	4.08	4.00	.98	3.33	.82	4.23	4.13	.98	3.80	.90	..	..	..	..	..
8	4.57	4.50	.98	3.67	.80	4.72	4.63	.98	4.20	.89	4.61	4.53	.98	3.80	.82
9	5.07	5.00	.99	4.00	.79	5.20	5.13	.99	4.60	.88	..	..	..	..	..
10	5.56	5.50	.99	3.33	.78	5.71	5.63	.99	5.00	.88	5.59	5.53	.99	4.50	.81
∞	..	..	1.00	..	.667	..	..	1.00	..	.80	..	..	1.00	..	.70

ponents. The Staudinger constant for the mixture checks closely the value obtained from the individual fractions.

These observations offer further evidence for the validity of this method of treating light scattering data and demonstrate that data on the asymptote of the light scattering envelope provide the number average molecular weight and the effective bond length. The applicability of the method requires, of course, that the molecular size be sufficiently large. In the region where this condition is only approximately met, some precautions in interpretation are necessary. On the other hand, these experiments emphasize the need of making measurements at much lower angles when the weight average molecular weight of large polymer molecules is required.

Appendix

Correction Factors for Locating the Asymptote.—In the special case where the distribution corresponds to $M_z:M_w:M_n::3:2:1$, the plot of $P^{-1}(\theta)$ against $N_w u$ is linear and there are no difficulties in interpretation. For samples whose distribution is more narrow than this, the distribution suggested by Zimm[3] seems a reasonable approximation. If the parameter z which measures the width of this distribution, is assigned a value, data falling on the corresponding curve can be reduced to the asymptote by the use of correction factors which are listed in Table II for three values of z. Following Zimm we have used as the independent variables $N_w u$, which is equal to his $<u>$, and we have included, for the sake of completeness, his correction factors for obtaining the limiting tangent.

For samples whose distribution is broader than that for which $P^{-1}(\theta)$ is linear, more than one peak may be present. In this case Zimm's distribution, which is always single peaked, may be unrealistic. However, correction factors are given in Table III for one case. We note that in this case the curve reaches its asymptote only at much higher values of $N_w u$ than for the sharper distributions. If for a given value of M_w/M_n the value of M_z/M_w is greater than that given by the Zimm distribution (as in multipeaked distributions), the approach to the asymptote occurs at much lower values of the abscissa.

TABLE III

$z = 0.5(M_z:M_w:M_n::5:3:1)$

$N_w u = <u>$	$P_{0.5}^{-1}(\theta)$	Asymptote	$\left(\frac{\text{Asymptote}}{P_{0.5}^{-1}(\theta)}\right)$	Limiting tangent	$\left(\frac{\text{Limiting tangent}}{P_1^{-1}(\theta)}\right)$
0	1.00	1.500	1.50	1.00	1.00
1	1.54	2.0	1.30	1.56	1.01
3	2.59	3.0	1.16	2.67	1.03
5	3.64	4.0	1.10	3.78	1.04
10	6.18	6.5	1.05	6.56	1.06
15	8.75	9.0	1.03	9.33	1.07
20	11.2	11.5	1.02	12.1	1.08
25	13.8	14.0	1.01	14.9	1.08
30	16.3	16.5	1.01	17.7	1.09
∞	...	...	1.00	...	1.11

THE DISTRIBUTION OF PARTICLE SIZES IN POLYSTYRENE LATEX

BY R. H. EWART AND C. I. CARR

Contribution No. 137 from the General Laboratories of the United States Rubber Company, Passaic, N. J.

Received April 19, 1954

A study has been made of the distribution of particle sizes in polystyrene latices made by emulsion polymerization. The effect of some of the polymerization variables on the breadth of the distribution curve has been determined. A theory has been developed relating size distribution to fluctuations in the time that a particle contains a free radical.

I. Introduction

The size of colloid particles has long been a subject of interest to chemists and physicists. The light scattering method developed by Professor Peter Debye[1] has been a powerful tool for studies of this kind.

The measurement of particle diameters by sedimentation, light scattering and other techniques can be facilitated by comparison of the unknown material with particles of known diameter. The standard material should be stable and composed of particles which are individual spheres and of sufficient hardness to maintain their shape in the electron microscope. It is desirable that the particles be monodisperse so as to be easily isolated in electron microscope pictures and so that the diameters can be determined by a relatively small number count. Further, the monodispersity is of importance when using other techniques to measure the particle size, in order to eliminate the uncertainty arising from the different average diameters characteristic of the method. Victor K. La Mer[2] has done extensive work on monodisperse sulfur sols and has studied the conditions for their preparation.

Several years ago a sample of polystyrene latex was produced by the Dow Chemical Laboratories[3] which satisfied the above requirements. This has been widely used for calibration and study of methods for the determination of colloidal particle sizes. It would be desirable to have a method by which such uniform particle size latices could be produced and in a wide range of sizes.

It is the object of this paper to consider some of the principles which lead to uniform particles by emulsion polymerization and to report experimental studies on such preparations.

W. D. Harkins[4] has discussed the relative impor-

(1) P. Debye, *J. Appl. Phys.*, **15**, 338 (1944).

(2) V. K. La Mer, THIS JOURNAL, **52**, 65 (1948).

(3) R. C. Backus and R. C. Williams, *J. Appl. Phys.*, **20**, 224 (1949).

(4) W. D. Harkins, *J. Am. Chem. Soc.*, **69**, 1428 (1947).

tance of the aqueous phase, the soap micelles and the polymer particles as the locus of the emulsion polymerization process. In a general theory of the kinetics of emulsion polymerization, Smith and Ewart[5] have discussed some of the factors which determine the number of particles. In a study of the kinetics of styrene emulsion polymerization, Smith[6] has presented experimental data on the effect of several variables and has shown agreement with this theory of emulsion polymerization. M. Morton[7] and co-workers have continued the study of emulsion polymerization of styrene and of diene monomers along similar lines.

II. Factors which Determine Size Uniformity

According to the general theories of emulsion polymerization, as long as micelles are present new particles are formed. However, as the particles grow, soap is adsorbed and eventually no more micelles exist. The rate of new particle formation will then decrease rapidly until the concentration of soap in the aqueous phase is so low that very few new particles will be formed. After this, the particles continue to grow in size and the number of particles remains essentially constant. The mechanical stability of the latex may become reduced due to the decrease in surface concentration of the soap with particle growth.

The two primary factors which affect distribution of particle sizes are (1) the original distribution at the time when the number of particles becomes essentially constant, and (2) the growth of the particles.

1. The Original Distribution.—If all of the particles were formed in a very short time interval at the beginning of the polymerization, and if all of these were to grow at exactly the same rate, we would obtain a latex of only one particle size. However, if the particles are formed over a considerable time interval, those which are formed first would be expected to be larger than those which are formed later and a size distribution would result.

Evidence has been presented[6] that the number of particles is a function of the concentration of surface active material, catalyst and temperature of polymerization. It has been postulated[5] that the time interval during which particles are formed should also be a function of these variables. This leads to the conclusion that increased soap should give a broader distribution of particle sizes when the particles have reached the same size. Data will be presented on this point in the experimental part of this paper.

2. Particle Growth.—If the volume of all the particles were to increase at the same rate, the average deviation in the cube of the diameter, Δd^3, should remain about constant as the particles grow. This will be shown not to be the case in the experiments reported in the next section.

Even though the particles were originally all of the same size, some particles might grow faster than others. Let us consider the case where a particle contains an average of one free radical half of the time. For an individual particle, let t_0 be the total polymerization time; let t be the time that this particle contains a free radical and let $2a$ be the number of free radicals which have entered the particle in the time, t_0. Also let f be the fraction of the total time that this particle contains a free radical, thus

$$f = t/t_0 \qquad (1)$$

Although the average value of f is one-half, there will be fluctuations in its value. We assume that a particle contains a growing free radical only when an odd number of radicals have entered due to rapid recombination. It will be shown in the last section that the probability, dP, that a particle contains a free radical for a fraction of its time between f and $f + df$ is given by

$$dP = \frac{(2a-1)!}{(a-1)!^2} f^{a-1}(1-f)^{a-1}\,df \qquad (2)$$

It follows from (2) that

$$\left(\frac{\Delta f}{\bar{f}}\right)^2 = \frac{\overline{(f-\bar{f})^2}}{\bar{f}^2} = \frac{1}{2a} \qquad (3)$$

Consideration will be given in the discussion as to whether or not fluctuations of this sort are important in determining the size distribution.

Another factor which might cause larger particles to increase in volume faster than small particles is the higher solubility of styrene in the larger particles. W. V. Smith[6] has shown experimentally that there is a trend in this direction. It would be expected on the basis of lower vapor pressure of larger particles.

III. Experimental Details

The emulsion polymerization of styrene to 100% conversion readily lends itself to the preparation of hard individual spherical particles with a minimum of experimental difficulties. The number of particles initiated and their size distribution, although influenced by temperature, catalyst concentration, *p*H and salt concentration, is primarily determined by the concentration of emulsifier in the aqueous phase.

Latices with particle diameters in excess of 0.25 μ have been prepared which have at least 90% of the particles by number within a 5–6% diameter range. The remaining particles are normally smaller and can be readily distinguished in electron microscope pictures. They probably result from occasional particle formation in the aqueous phase after most of the emulsifier has been adsorbed by the growing particles.

Stable latices of fairly monodisperse particles with diameters less than 0.25 μ can be prepared by initiating a relatively small number of particles on a formula with a small styrene to water ratio to give a low solids latex.

The general formula used in these investigations was

0.01 *N* KOH	100
Potassium persulfate	0.2
Potassium laurate	Variable
Styrene	Variable

This emulsion was polymerized in glass bottles on a slow tumbler in a 50° water thermostat for about 16 hours. This was sufficient time in all cases to give complete polymerization of the styrene. 0.01 *N* KOH was used to keep the system alkaline since potassium persulfate develops acidity when it decomposes.

The potassium laurate was prepared as a 0.1 *N* solution by dissolving Matheson technical grade lauric acid in an aqueous solution of J. T. Baker Analyzed potassium hydroxide. Ten per cent. excess KOH over that required to

(5) W. V. Smith and R. H. Ewart, *J. Chem. Phys.*, **16**, 592 (1948).

(6) W. V. Smith, *J. Am. Chem. Soc.*, **70**, 3695 (1948); *ibid.*, **71**, 4077 (1949).

(7) M. Morton, P. P. Salatiello and H. Landfield, *J. Polymer Sci.*, **8**, 111, 215, 279 (1952).

neutralize the lauric acid was used. The amount of potassium laurate given in the tables and graphs is based on the lauric acid content of this solution. The potassium persulfate was also J. T. Baker Analyzed reagent. This was used in the form of a freshly prepared 2% solution.

A preliminary study was made to determine the number of particles formed as a function of the amount of potassium laurate per 100 cc. of water. The amount of styrene used was that required to give particles in about the right size range for easy measurement of particle size from electron microscope pictures.

Polymerizations were then carried out where three different numbers of particles were initiated. The amount of styrene used was selected so as to give an overlap in average diameters of the polystyrene particles. In this way the effect of number of particles initiated and fluctuations in polymerization time on the distribution of sizes could more easily be studied at about the same average particle size. The results of these experiments are given in Table I.

TABLE I

NUMBER OF PARTICLES *versus* POTASSIUM LAURATE AND STYRENE

Sample no.	Potassium laurate, g./100 cc. water	Styrene, g./100 cc. water	$\bar{d}$, cm. $\times 10^4$	$\bar{d^3}$, cm.$^3 \times 10^{14}$	No. of particles/cm.^{3} water $\times 10^{-13}$
2	0.10	2.64	0.2219	1.109	0.433
3	.10	8.90	.3177	3.305	0.490
4	.15	1.1	.1117	0.1430	1.40
5	.15	8.8	.1743	0.5515	2.90
6	.15	29.6	.2756	2.135	2.52
7	.21	3.3	.0998	0.1073	5.59
8	.21	26.4	.1754	0.5747	8.03
9	.21	53	.2394	1.429	8.01

The detailed counts for these experiments are listed in Tables IIa, b and c where the diameters, d, are given in millimeters as measured directly on the electron microscope pictures at 48,000× magnification. The average values were obtained by measuring 200–300 individual particles and were calculated from

$$\bar{d}(\text{cm.}) = \frac{\Sigma n_i d_i}{\Sigma n_i} \times \frac{10^{-4}}{48}$$

and

$$\bar{d^3}(\text{cm.}^3) = \frac{\Sigma n_i d_i^3}{\Sigma n_i} \times \left(\frac{10^{-4}}{48}\right)^3 \qquad (4)$$

The number of particles per cc. of water, N, in terms of the weight of styrene used, S, the density of polystyrene (1.05) and the average value, $\bar{d^3}$, is

$$N = \frac{S}{100 \times 1.05} \Big/ \frac{\pi}{6} \bar{d^3}$$

$$= 0.0182 S/\bar{d^3} \qquad (5)$$

The calculated number of particles for each run is given in Table I. Sample 1 containing a very small amount of styrene failed to polymerize normally due to unknown causes and has not been included. It will be noted that samples 4 and 7 have a smaller number of particles than the others in their groups. It is believed that this is due to the fact that the free styrene was used up by swelling the particles formed early in the polymerization before the normal number of particles were formed.

TABLE IIa

PARTICLE COUNTS ON 0.10 K LAURATE LATICES

Values of d are in mm. on electron microscope photographs at 48,000×; $d(\mu) = d/48$.

Sample 2 d	Sample 2 n	Sample 3 d	Sample 3 n
12.8	1	16.4	2
12.6	1	16.2	7
11.8	2	16.0	29
11.6	3	15.8	39
11.4	3	15.6	67
11.2	15	15.4	32
11.0	57	15.2	19
10.8	77	15.0	3
10.6	25	14.2	1
10.4	12	13.8	1
10.2	10	12.8	1
10.0	7	12.6	1
9.8	2	12.4	1
9.2	1	11.0	1
9.0	3	10.6	2
8.8	1	10.4	1
8.0	2	10.0	2
7.8	3	7.4	1
7.6	1	6.0	1
5.4	1	5.2	1
5.0	1	3.4	1
Sums			
n	228		213
nd	2,428.4		3,248.6
nd^2	26,021.44		50,158.12
nd^3	279,800		778,500
nd^6	354.700,400		2,955,647,000

TABLE IIb

PARTICLE COUNTS ON 0.15 K LAURATE SERIES

Sample 4 d	Sample 4 n	Sample 5 d	Sample 5 n	Sample 6 d	Sample 6 n
6.0	22	10.2	1	15.2	2
5.8	45	10.0	3	15.0	7
5.6	55	9.8	4	14.8	4
5.4	43	9.6	3	14.6	10
5.2	51	9.4	11	14.4	6
5.0	33	9.2	21	14.2	10
4.8	8	9.0	58	14.0	36
4.6	5	8.8	45	13.8	30
4.4	1	8.6	28	13.6	14
4.2	1	8.4	33	13.4	23
4.0	3	8.2	20	13.2	34
3.4	2	8.0	31	13.0	37
3.2	1	7.8	7	12.8	16
3.0	3	7.6	4	12.6	8
		7.4	11	12.4	7
		7.2	3	12.2	8
		7.0	6	12.0	9
		6.8	3	11.8	1
		6.6	2	11.4	4
		6.4	3	11.2	2
		6.2	4	11.0	6
		6.0	2	10.2	6
		5.2	2	8.2	2
		4.4	5	6.8	1
		3.0	2		
Sums					
n	273		312		283
nd	1,464.4		2,610.8		3.743.6
nd^2	7,924.00		22,177.2		49.866.56
nd^3	43,182		190,300		668,340
nd^6	7,200,024		125,459,400		1,652,620,300

IV. Discussion of Results

In order to study the distribution of sizes, the average differences in Δd and Δd^3 were calculated. These are defined by

$$\Delta d = \sqrt{\overline{(d - \bar{d})^2}} = \sqrt{\bar{d^2} - (\bar{d})^2} \qquad (6)$$

TABLE IIc

PARTICLE COUNTS ON 0.21 K LAURATE LATICES

Sample 7		Sample 8		Sample 9	
d	n	d	n	d	n
6.0	1	10.4	4	14.2	1
5.8	11	10.2	3	13.8	2
5.6	24	10.0	12	13.6	2
5.4	24	9.8	8	13.4	5
5.2	34	9.6	17	13.2	5
5.0	64	9.4	18	13.0	14
4.8	22	9.2	28	12.8	13
4.6	17	9.0	41	12.6	16
4.4	10	8.8	20	12.4	12
4.2	6	8.6	15	12.2	15
4.0	16	8.4	20	12.0	27
3.8	4	8.2	14	11.8	22
3.6	3	8.0	18	11.6	9
3.4	1	7.8	12	11.4	9
3.2	5	7.6	5	11.2	14
3.0	2	7.4	9	11.0	16
2.8	2	7.2	6	10.8	9
2.4	1	7.0	7	10.6	10
2.2	2	6.8	5	10.3	6
2.0	1	6.6	2	10.0	7
1.6	2	6.2	6	9.5	10
1.4	2	5.5	8	8.8	10
1.0	1	4.7	4	8.2	4
		4.0	3	7.0	5
		3.0	2		
Sums					
n	255		287		243
nd	1,220.4		2,417.0		2,793.0
nd^2	6,022.48		20,835.04		32,560.12
nd^3	30,259		182,430		384,140
nd^6	4,102,406		131,217,500		665,550,300

and

$$\Delta d^3 = \sqrt{\overline{(d^3 - \bar{d}^3)^2}} = \sqrt{\bar{d}^6 - (\bar{d}^3)^2} \qquad (7)$$

The values of these quantities are given in Table III. If there is an average of one free radical half of the time, and if fluctuations from this value are negligible, then the volume of each particle should increase the same amount in the same time. This would lead to a constant value of Δd^3 in any one series using constant soap. It will be seen that Δd^3 is not constant. If the radius increases at a constant rate, Δd would be constant in each series. This quantity has much better constancy and may indicate a different mechanism of growth for these large particles involving several free radicals per particle.

TABLE III

QUANTITIES MEASURING SIZE DISTRIBUTION

Sample no.	Δd, cm. $\times 10^4$	Δd^3, cm.^{3} $\times 10^{14}$	$\Delta d/\bar{d}$	$\Delta d^3/\bar{d}^3$
2	0.0175	0.201	0.079	0.182
3	.0356	.650	.112	.197
4	.0104	.0331	.094	.232
5	.0215	.156	.123	.284
6	.0231	.463	.084	.217
7	.0175	.0404	.176	.377
8	.0269	.208	.154	.363
9	.0285	.443	.120	.310

If the fluctuations from an average value of one-half a free radical per particle is the important cause of distribution from the beginning of particle growth, and since the theory requires

$$d^3 = kt = kt_0 f \qquad (8)$$

then from equation 3

$$\frac{\Delta d^3}{\bar{d}^3} = \frac{\Delta f}{\bar{f}} = \left(\frac{1}{2a}\right)^{1/2} \qquad (9)$$

Since the total number of free radicals which enter the particle, $2a$, increases with time, the quantity $\Delta d^3/\bar{d}^3$ should decrease as $\bar{d}$ increases in any one series. While this is the case, the decreasc is not as great as expected from this hypothesis.

V. Derivation of Probability Equation 1

Let us consider the case where a latex particle is small enough so that if an even number of free radicals have entered it all radicals are recombined and no polymerization is taking place. On the other hand, if an odd number have entered, there remains one free radical which is causing polymerization.

If the total time considered is t_0, there will be a total time, t, during which polymerization is taking place. Assume that in the time t_0 that $2a$ free radicals have entered the particle. Let us divide t_0 into a very large number, n, of very small time intervals of length Δt. Let us ask how many ways can a radicals be distributed in x of these time intervals (during which the particle is polymerizing) and a radicals in $n - x$ intervals (during which the particle is not polymerizing). The number of ways is

$$W_x = \binom{x-1}{a-1}\binom{n-x-1}{a-1}$$

where $t = x \cdot \Delta t$ and $t_0 = n \cdot \Delta t$

$$\binom{x-1}{a-1} = \frac{(x-1)!}{(x-a)!(a-1)!}, \text{ etc.}$$

The total number of ways that $2a$ radicals can be distributed in n time intervals is

$$W_t = \binom{n-1}{2a-1}$$

Hence the probability, P_x, that a radicals will be in x intervals and a in $(n - x)$ intervals is

$$P_x = \binom{x-1}{a-1}\binom{n-x-1}{a-1}\binom{2a-1}{n-1}$$

If Δt becomes very small so that n and x are large compared to a and unity

$$P_x = \frac{(2a-1)!}{(a-1)!^2}\frac{x^{a-1}(n-x)^{a-1}}{n^{2a-1}}$$

Let f equal the fraction of the total time during which polymerization is taking place

$$f = \frac{x}{n} = \frac{t}{t_0}$$

Also

$$\frac{dP}{df} = nP_x = \frac{(2a-1)!}{(a-1)!^2} f^{a-1}(1-f)^{a-1}$$

Since

$$\int_0^1 f^c(1-f)^b\,df = \frac{b}{c+1}\int_0^1 f^{c+1}(1-f)^{b-1}\,df, \text{ etc.}$$

$$= \frac{b!c!}{(c+b+1)!}$$

the average value of f and f^2 are

$$\bar{f} = \int_0^1 f\,dP = \frac{(2a-1)!}{(a-1)!^2}\int_0^1 f \times f^{a-1}(1-f)^{a-1}\,df$$

$$= \frac{(2a-1)!}{(a-1)!^2}\,\frac{(a-1)!a!}{2a!} = \frac{a}{2a} = \frac{1}{2}$$

$$\bar{f^2} = \int_0^1 f^2\,dP = \frac{(2a-1)!}{(a-1)!^2} \times$$

$$\frac{(a-1)!(a+1)!}{(2a+1)!} = \frac{(a+1)(a)}{(2a+1)(2a)}$$

The average deviation

$$\overline{(f-\bar{f})^2} = \int_0^1 (f-\bar{f})^2 dP = \int_0^1 f^2 dP - \bar{f}^2$$

$$= \frac{1}{4(2a+1)}$$

THEORY OF LIGHT SCATTERING AND REFRACTIVE INDEX OF SOLUTIONS OF LARGE COLLOIDAL PARTICLES

BY BRUNO H. ZIMM AND

General Electric Research Laboratories, The Knolls, Schenectady, N. Y.

WALTER B. DANDLIKER

The Department of Biochemistry, University of Washington, Seattle, Washington

Received April 19, 1954

A general equation for the intensity of light scattered by a suspension of independently scattering particles is derived $V_{0,v} = (Mcn^2/\lambda_0{}^4N_0)[4\pi^2(dn/dc)^2 + (\lambda_0{}^2/4)(\tau/c)^2]$. $V_{0,v}$ is the Rayleigh ratio of the vertically polarized component of the excess scattered light at $\theta = 0$ with the electric vector vertical in the incident light. The other quantities involved are the molecular weight M, concentration c, refractive index n of the solution, the wave length λ_0 *in vacuo*, Avogadro's number N_0, the refractive index increment (dn/dc) and the excess turbidity, τ, due to the solute. The second term of the equation, which is important in the case of very large particles, has usually been omitted in the past. For spheres, a general relationship between dn/dc, particle size α and refractive index of particle and medium can be deduced: $dn/dc = 3nR(i_1{}^*)/2\alpha^3D$ where $R(i_1{}^*)$ is obtained from tabulations of the Mie theory. The density of the particle is D and $\alpha = 2\pi r/\lambda$ where r is sphere radius and λ is the wave length in the medium. For small spheres the refractive index equation reduces to the well known result: $dn/dc = 3n/2D\,(m^2 - 1/m^2 + 2)$, where m is the relative refractive index.

Introduction

Interpretations of light scattering studies on macromolecular and colloidal systems have used either of two theories. The study of very large spherical colloidal particles[1-5] has been made possible by the Mie theory of scattering from spheres[6,7] and computations based on it.[8] On the other hand, Einstein's fluctuation theory,[9] and its limiting simple form for dilute solutions, the Rayleigh formula,[10] have been used for smaller colloidal particles and high polymer molecules.[11]

An adaptation of a treatment given by Schuster[12] allows one to connect these two theories and to obtain a general relation between the scattering and refractive index of a colloidal solution and the size of the particles. This relation is the extension of the Rayleigh relation to very large particles. The ordinary Rayleigh relation is found to be valid only if the amount of light scattered per particle is not too large, a phase shift of the scattered light having been ignored in its derivation. An approach related in some respects to the present one is given by van de Hulst.[13]

Theory

Let the incident light be plane-polarized with the electric vector defined by

$$E_0 = R_0 \cos(\omega t - kx)$$

where x is measured from a point in the scattering medium and k is 2π times the reciprocal of the wave length. The light scattering from a single particle can be represented by

$$E_s = R_0[A\cos(\omega t - kr) + B\sin(\omega t - kr)]f(\vartheta,\phi)/r \quad (1)$$

where r is the distance from the particle, ϑ and ϕ are angles relating the directions and states of polarization of the incident and scattered rays, and $f(\vartheta, \phi)$ is the function that describes the angular dependence of the scattering. We may set $f(0, 0)$ equal to unity. The quantity B allows for a change of phase.

Now let a parallel beam of light traverse a scattering medium containing N independent particles per unit volume and consider the scattering occurring within a thin layer of thickness Δx, the x-axis being the direction of propagation of the beam. The method described in the appendix enables us to calculate the total forward scattering in the direction of propagation of the incident beam at a distance x from the layer as

$$E_{ts} = R_0\lambda N\Delta x[A\sin(\omega t - kx) - B\cos(\omega t - kx)] \quad (2)$$

If the material is a solution, we take n as the refrac-

(1) V. K. La Mer and D. Sinclair, N.D.R.C. Report 57 (1941) and 1668 (1943).

(2) I. Johnson and V. K. La Mer, *J. Am. Chem. Soc.*, **69**, 1184 (1947).

(3) D. Sinclair and V. K. La Mer, *Chem. Revs.*, **44**, 245 (1949).

(4) M. Kerker and V. K. La Mer, *J. Am. Chem. Soc.*, **72**, 3516 (1950).

(5) W. B. Dandliker, *ibid.*, **72**, 5110 (1950).

(6) G. Mie, *Ann. Physik*, **25**, 377 (1908).

(7) H. C. van de Hulst, "Optics of Spherical Particles," Duwaer and Sons, Amsterdam, 1946.

(8) "Tables of Scattering Functions for Spherical Particles," National Bureau of Standards, Applied Mathematics Series 4 (1949).

(9) A. Einstein, *Ann. Physik*, **33**, 1275 (1910).

(10) Rayleigh, *Phil. Mag.*, **41**, 447 (1871).

(11) P. Debye, *J. Appl. Phys.*, **15**, 338 (1944); G. Oster, *Chem. Revs.*, **43**, 319 (1948).

(12) A. Schuster, "An Introduction to the Theory of Optics," Second Ed., Edward Arnold and Co., London, 1920, p. 325.

(13) H. C. van de Hulst, *Physica*, **15**, 740 (1949).

tive index of the solvent alone while n' is that of the solution as a whole. The wave length *in vacuo* is λ_0 while the wave length in solution is $\lambda = \lambda_0/n'$ and $k = 2\pi/\lambda$.

In the following discussion we shall neglect the scattering from the solvent itself so that the conclusions apply to the excess scattering due to the solute. In the forward direction the scattered wave adds to the incident wave to give the transmitted wave. The constant part, $(-kx)$, of the phase angle is the same in the incident and scattered waves and may be dropped. The electric vector in the transmitted wave is then found to be

$$E = E_0 + E_{ts} = R_0[(1 - BN\lambda\Delta x)\cos\omega t + (AN\lambda\Delta x)\sin\omega t] \quad (3)$$

This may be reduced to

$$E = R_0\sqrt{(AN\lambda\Delta x)^2 + (1 - BN\lambda\Delta x)^2}\cos\left(\omega t - \arctan\frac{AN\lambda\Delta x}{1 - BN\lambda\Delta x}\right) \quad (4)$$

or, since Δx may be made as small as desired

$$E = R_0(1 - BN\lambda\Delta x)\cos(\omega t - AN\lambda\Delta x) \quad (5)$$

From purely phenomenological theory we know that the transmitted wave is retarded in phase by an amount δ compared to the incident wave, where δ is related to Δx and the refractive indices by

$$\delta = 2\pi\left(\frac{n'}{\lambda_0} - \frac{n}{\lambda_0}\right)\Delta x \quad (6)$$

On the other hand from eq. 5 we see that

$$\delta = AN\lambda\Delta x \quad (7)$$

so that

$$A = \frac{2\pi n'(n' - n)}{\lambda_0^2 N} \quad (8)$$

The intensity of the transmitted beam I, the time average of E^2, is

$$I = \overline{E^2} = R_0^2(1 - BN\lambda\Delta x)^2/2 = R_0^2(1 - 2BN\lambda\Delta x)/2, \quad (9)$$

while that of the incident beam I is equal to $R_0^2/2$. The fractional decrease in intensity per unit length is defined as

$$\tau = (\Delta I/I)\Delta x \quad (10)$$

so

$$B = \tau/2N\lambda \quad (11)$$

Thus we have expressed the two scattering constants A and B in terms of the refractive index increment of the solution and the turbidity, τ.

We may also relate to our formulas the observed scattering at small angles. The scattered field from one particle with ϑ and ϕ equal to zero and observed a distance x from the particle is, from eq. 1

$$E_{s,0} = R_0[A\cos(\omega t - kx) + B\sin(\omega t - kx)]/x \quad (12)$$

The scattered intensity $I_{s,0}$ is proportional to the time average of $E_{s,0}^2$ which is

$$I_{s,0} = E_{s,0}^2 = R_0^2[A^2 + B^2]/2x^2 \quad (13)$$

The "Rayleigh ratio" is the quantity

$$V_{0,v} = NI_{s,0}x^2/I_0 = N(A^2 + B^2) \quad (14)$$

The symbol $V_{0,v}$ indicates that the vertically polarized component scattered at zero angle with vertically polarized incident light is being used.

These formulas have been derived for the case where only one kind of scattering particle is present. If there are several kinds of particles average values of A and B or A^2 and B^2 must be used in eq. 5 and 13. The same thing must be done if the scattering is depolarized and depends on the orientation of the scattering particles. When the phase-shift terms containing B are negligible these averages are simple and lead to the usual formulas with the weight-average particle weights and Cabannes depolarization factors.[11] However, if the terms containing B are important special assumptions must be made about the variation of B to obtain the averages. We do not care to investigate this subject further here, but restrict ourselves to the case of one type of particle and no depolarization of the forward-scattered light.

Substituting the values of A and B from eq. 8 and 11, we obtain

$$V_{0,v} = \frac{4\pi^2 n'^2(n' - n)^2}{\lambda_0^4 N} + \frac{\tau^2 n'^2}{4N\lambda_0^2} \quad (15)$$

The weight concentration, c, Avogadro's number, N_0, and the molecular weight, M, are now introduced, giving $N = N_0 c/M$. Also we assume $n' - n = c(dn/dc)$. These substitutions give

$$V_{0,v} = \frac{Mcn'^2}{\lambda_0^4 N_0}\left[4\pi^2\left(\frac{dn}{dc}\right)^2 + \frac{\lambda_0^2}{4}\left(\frac{\tau}{c}\right)^2\right] \quad (16)$$

The Refractive Index of a Suspension of Spheres

The results of Mie's[6] exact theory of the scattering from spheres may be related to $V_{0,v}$ in terms of the nomenclature of La Mer and Sinclair[1] by the equation

$$V_{0,v} = cN_0\lambda^2(|R(i_1^*) + iI(i_1^*)|)^2/4\pi^2 M \quad (17)$$

where the scattering functions $R(i_1^*)$ and $I(i_1^*)$ are to be evaluated for scattering in the direction of the incident beam. For small particles we know (τ/c) is small so that the first term in eq. 16 must be predominant for small particles. The same is true for $R(i_1^*)$, as we may see from the tabulations of the Mie theory. Thus from a comparison of eq. 17 with eq. 16 one finds that

$$R(i_1^*) = \frac{4\pi^2 n'^2 M(dn/dc)}{\lambda_0^3 N_0} \quad (18)$$

and

$$I(i_1^*) = \frac{\pi M n'^2}{\lambda_0^2 N_0}\left(\frac{\tau}{c}\right) \quad (19)$$

The relation between particle size and the quantities $R(i_1^*)$ and $I(i_1^*)$ may be conveniently represented by a type of plot used by van de Hulst.[7] Figure 1 gives the plot for different values of m, the refractive index of the sphere divided by n. Values of $\rho = 4\pi r(m - 1)/\lambda$, the phase shift, are shown along the curves, where r is the radius of the sphere. The points for $m = 1.55$ were taken from the tables[8] while the curve $m = 1$ was calculated from the equations given by van de Hulst.[7] The reader should note that the quantity $[R(i_1^*)]/\alpha^2$ corresponds to ImA of van de Hulst while our $[-I(i_1^*)]/\alpha^2$ corresponds to his ReA. (α is $r/2\pi\lambda$.)

From these curves we can show that (dn/dc) depends not only upon the refractive index of the particle and medium but also upon the particle size. The general relationship for isotropic spheres

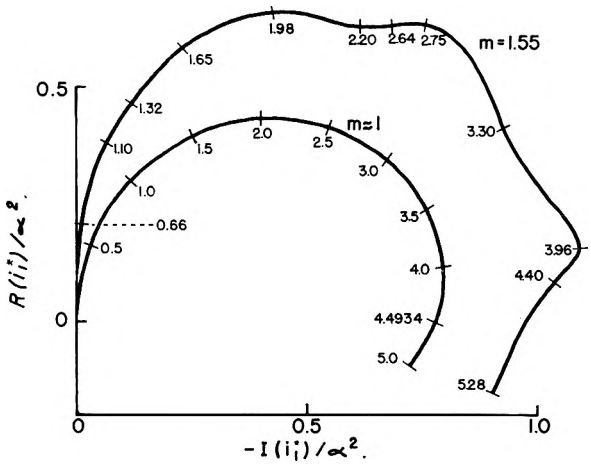

Fig. 1.—Amplitude function for forward scattering for two values of the relative refractive index (see eq. 18 and 19). Values of $\rho = 4\pi r(m-1)/\lambda$ are given along the curves.

is given by eq. 18. If D is the particle density, the molecular weight can be written

$$M = \frac{\alpha^3\lambda^3 N_0 D}{6\pi^2} \tag{20}$$

which with eq. 18 gives

$$\frac{dn}{dc} = \frac{3n' R(i_1^*)}{2\alpha^3 D} \tag{21}$$

In the limit for very small spheres

$$\frac{R(i_1^*)}{\alpha^3} = \frac{m^2-1}{m^2+2} \tag{22}$$

which reduces the general eq. 21 to

$$\frac{dn}{dc} = \frac{3n'}{2D}\left(\frac{m^2-1}{m^2+2}\right) \tag{23}$$

Equation 23 is equivalent to the refractive index equations given by Heller[14] and by Ewart, Roe, Debye and McCartney.[15]

Discussion

It is evident from eq. 16 that the calculation of molecular weights from measurements of the Rayleigh ratio involves a term in (τ/c) as well as the usual one in (dn/dc). The (τ/c) term, which arises from a phase shift in the scattering, is usually negligible, but must be taken into account when very large particles are encountered. It was important in the case of a polystyrene latex,[5] for example.

The use of eq. 21 and 23 for the refractive index can be illustrated by application to the sulfur hydrosols studied by La Mer and co-workers. Figure 2 shows the quantity

$$\frac{dn}{dc}\left(\frac{2D}{3n'}\right)\left(\frac{m^2+2}{m^2-1}\right) = \frac{R(i_1^*)}{\alpha^3}\left(\frac{m^2+2}{m^2-1}\right) = \frac{2R(i_1^*)}{\alpha^*\rho}\left(\frac{m^2+2}{m+1}\right)$$

plotted as a function of $\rho = 4\pi r(m-1)/\lambda$ for various values of m. We can determine from Fig. 2 that for sulfur sols in water (dn/dc) is zero at the green Hg line ($\lambda_0 = 5461$ Å.) when the particle radius is 2880 Å. It may be possible to test these

(14) W. Heller, *Phys. Rev.*, **68**, 5 (1945).

(15) R. H. Ewart, C. P. Roe, P. Debye and J. R. McCartney, *J. Chem. Phys.*, **14**, 687 (1946).

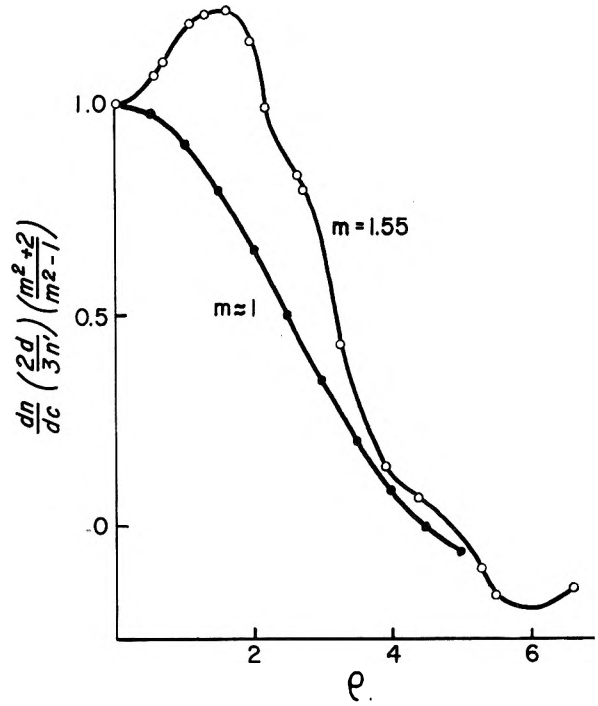

Fig. 2.—Dependence of the refractive index derivative (dn/dc) on size and relative refractive index, m.

predictions by direct refractive index measurements.

Heller[14] found that eq. 23 gave unreasonable values for the refractive index of large particles when applied to measured values of (dn/dc). He proposed an empirical correction equation which gives values approximating those from eq. 21 if the corrections are small. This may be regarded as support for eq. 21.

Some confusion may arise over two related points: the difference between the "observed" scattering at small angles and E_{ts} of eq. 2, and the requirement that the solution be composed of independent, *i.e.*, non-interacting, particles. The "observed" scattered intensity, $I_{s,0}$, from one particle was multiplied by N, the number of particles, to give the total scattering. This procedure cannot be used when the angle is so small that there is a correlation of phase between the waves scattered by the different particles. In the latter case the amplitudes must be added, as is done for E_{ts} in the Appendix. However, angles small from an observational standpoint are usually still large enough for the random positions of the particles to cause random phases in the scattered light so that the intensities, not the amplitudes, are to be added. The latter can only be done if the positions of the particles are strictly uncorrelated, hence the condition of non-interaction of the particles. In principle, this condition may always be satisfied by diluting the solution sufficiently.

Appendix

Derivation of the Amplitude and Phase of the Light Scattered Forward by a Thin Slab of Material.—Schuster[12] obtained Rayleigh's formula for the relation between the intensity of the scattered light and the refractive index of a medium containing independent scattering centers by summation

of the amplitudes of the waves scattered in the direction of the incident beam. The summation was assumed to be analogous to the familiar Fresnel zone procedure so that the results of the latter could be used without further analysis. It is not clear that the assumption is correct, since the Fresnel procedure assumes that the scattering decreases uniformly to zero as the angle increases so that the contribution of the outermost zone is negligible. The scattering does not generally go to zero at large angles, however. We attempt to improve the derivation in the following.

The problem is made as simple as possible by considering a parallel plane-polarized beam of light traversing a non-absorbing medium of constant refractive index n containing N scattering particles per unit volume. The apparent refractive index of the medium and scatterers as a whole is n'. The beam is moving in the direction of increasing x. We consider the effect on the beam of a thin slab of thickness Δx lying on the y–z plane and bounded at the edges by the curve C (Fig. 3). We take Δx small enough so that the retardation of the beam by the scattering particles in the slab, $(n' - n)\Delta x$, is much smaller than the wave length, λ.

From the macroscopic point of view such a slab affects the beam in three ways: it scatters a small amount of light to the side, reducing the intensity of the beam by the amount $\tau\Delta x$; it retards the phase of the beam by the amount $2\pi(n' - n)\Delta x/\lambda_0$, and finally, it produces a diffraction pattern dependent on the shape of its boundary C. If we had introduced surfaces across which the refractive index changed we would also have had to consider reflection. Oseen[16] has already treated the reflection problem, which is not of primary interest for this paper. Our problem here is to find the relation between the scattering and the intensity and phase changes of the main beam and to separate these from diffraction effects.

We take polar coördinates for points in the y–z plane, with σ the radius vector and ϕ the angle between the radius and the z-axis. It is convenient to represent the incident light apart from the oscillating time factor by the real part of

$$R_0 e^{-ikx} \qquad \text{(A-1)}$$

and the scattered light from a single particle at a distance r by the real part of

$$R_0 A f(\vartheta,\phi) e^{-i(kr + \epsilon)}/r \qquad \text{(A-2)}$$

with

$$\epsilon = \tan^{-1}(B/A) \qquad \text{(A-3)}$$

which corresponds with eq. 1 of the main part of the paper.

If there are N particles per unit volume, the average number whose centers lie in a unit area of slab is $N\Delta x$. We want the total amplitude of scattering at the point x on the x-axis. This is found by summing the individual amplitudes from all the particles in the slab, *i.e.*, by the integral

$$E_s = P_0 A N \Delta x e^{-i\epsilon} \int\int_0^C f(\vartheta,\phi)(e^{-ikr}/r)\sigma\,d\sigma\,d\phi \qquad \text{(A-4)}$$

Now let a be the distance from the origin to the nearest point of the boundary C and let b be the distance to the farthest point. The integration can be divided into two parts: one over the region with $\sigma < a$ and the other over the remainder. In this form the scattered amplitude is

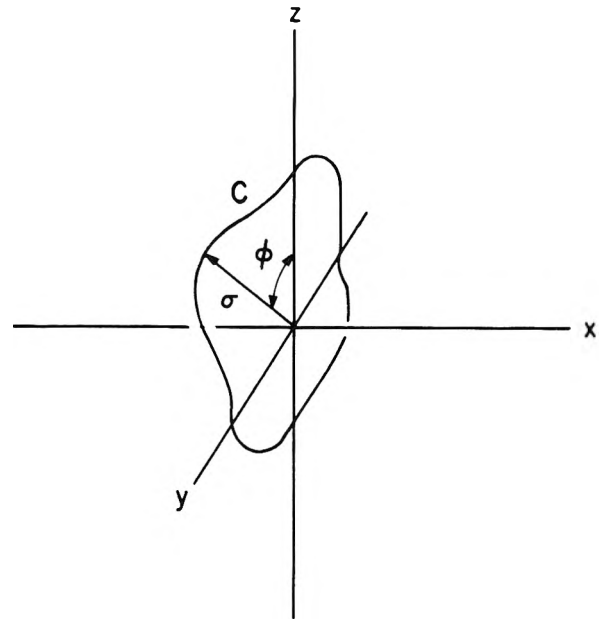

Fig. 3.—Diagram for the derivation of Schuster's formula for the scattering by a thin layer.

$$E_s = 2\pi R_0 A N \Delta x e^{-i\epsilon} \left\{ \int_0^a g(\sigma)(e^{-ikr}/r)\sigma\,d\sigma + \int_a^b h(\sigma)(e^{-ikr}/r)\sigma\,d\sigma \right\} \qquad \text{(A-5)}$$

where

$$g(\sigma) = \frac{1}{2\pi}\int_0^{2\pi} f(\vartheta,\phi)d\phi \qquad \text{(A-6a)}$$

$$h(\sigma) = \frac{1}{2\pi}\int_{\sigma<C} f(\vartheta,\phi)d\phi \qquad \text{(A-6b)}$$

The two integrals of eq. A-5 might be evaluated by the Fresnel method. However, this would require rather elaborate discussion to cover cases in which the scattering does not uniformly decrease with increasing angle. The following method seems to accomplish the same result in a simpler way. The two integrals of eq. A-5 may be simplified by the substitution

$$dr = \sigma d\sigma/r \qquad \text{(A-7)}$$

which follows from the relation between σ and r

$$r^2 = \sigma^2 + x^2 \qquad \text{(A-8)}$$

They may then be integrated by parts, to give the following

$$\int_0^a g(\sigma)(e^{-ikr}/r)\sigma d\sigma = \int_x^{\sqrt{a^2+x^2}} g(\sigma)e^{-ikr}dr = (-1/ik)[g(a)e^{-ik\sqrt{a^2+x^2}} - g(0)e^{-ikr} + (1/ik)\int_x^{\sqrt{a^2+a^2}} (dg/dr)e^{-ikr}\,dr \qquad \text{(A-9}$$

$$\int_a^b h(\sigma)(e^{-ikr}/r)\sigma\,d\sigma = (-1/ik)[h(b)e^{-ik\sqrt{b^2+x^2}} - h(a)e^{-ik\sqrt{a^2+x^2}} + (1/ik)\int_{\sqrt{a^2+x^2}}^{\sqrt{b^2+x^2}} (dh/dr)e^{-ikr}dr \qquad \text{(A-10)}$$

(16) C. W. Oseen, *Ann. Physik*, **48**, 1 (1915).

Now $f(\vartheta, \phi)$ is unity at $\vartheta = 0$, so $g(0) = 1$. Likewise $g(a) = h(a)$ and $h(b) = 0$. The last integral of eq. A-9 can be shown to be negligible by introducing a new scattering angle, $\psi = \cos^{-1}(x/r)$. Then we find

$$\frac{dg}{dr} = \frac{-\cos^2\psi}{x} \frac{dg}{d(\cos\psi)} \qquad \text{(A-11)}$$

For colloidal particles the variation of g with the cosine of the scattering angle ψ is such that $dg/d(\cos\psi)$ is not a large number. The size of the last term in eq. A-9 is then determined by the factor

$$1/ikx = \lambda/2\pi ix \qquad \text{(A-12)}$$

which is very small when x is of macroscopic size.

Caution must be used in applying a similar argument to the last term of eq. A-10 for the integral of $h(\sigma)$, because for certain shapes of boundary dh/dr may be infinite at points, as for example if C contains circular arcs centered on the origin. These are just the cases in which prominent diffraction effects are found. This term then gives a contribution dependent on the shape of the boundary which must be identified with the diffraction pattern of the boundary. However, if dh/dr is well behaved, as it will be in most cases, the factor $1/ikx$ makes the diffraction effects negligible.

The formula for E_s may now be written

$$E_s = iR_0NA\lambda\Delta x e^{-i(kx + \epsilon)} [1 + D(C)] \qquad \text{(A-13)}$$

where $D(C)$ arises from the last terms of eq. A-10 and represents the diffraction pattern of the boundary C. It is known that diffraction effects are negligible in comparison with the transmitted beam except in very special cases. If we omit $D(C)$ and write only the real part of eq. A-13, we get eq. 2 of the main part of the paper.

This result, with the omission of $D(C)$, is the same as the one Schuster obtained by the Fresnel method.

NON-NEWTONIAN BEHAVIOR OF SOLUTIONS OF MACROMOLECULES[1,2]

BY PAUL GOLDBERG[3] AND RAYMOND M. FUOSS

Sterling Chemistry Laboratory (Contribution No. 1213), Yale University, New Haven, Conn.

Received April 19, 1954

Using the assumption that the viscosity of a non-Newtonian liquid may be expanded as a power series in rate of shear, equations are derived which permit determination of the initial coefficients of the series from experimental data obtained using capillary viscometers. It is shown that measurements made at the same value of (Rp/L) in different viscometers agree; here, R = radius and L = length of capillary, and p is driving pressure. Furthermore, it is shown that non-Newtonian behavior of solutions can arise from molecular interaction or from a change of intrinsic viscosity with rate of shear; if the latter change is zero, plots of (η_{sp}/C) against C for different fixed values of $Q = Rp,g/2L\eta$ have the same intercept and if the interaction term vanishes, these curves have the same slope. In general, the (η_{sp}/C)-C curves at fixed Q have both different slopes and intercepts. Results on a number of systems indicate that the limiting dependence of apparent viscosity at low values of Q is linear in Q rather than quadratic.

Introduction

Viscosimetry has, since its introduction by Staudinger, been one of the standard tools of the polymer chemist. It represents an unusually apt illustration, however, of the cliché "all things are relative." It is fairly easy to obtain viscosity data with a precision of several per cent. for materials of moderate molecular weight using a capillary viscometer; this or better precision at molecular weights of the order of a million or more presents a number of experimental and theoretical complications. Many of these arise from the fact that solutions of polymers, especially polyelectrolytes, are non-Newtonian liquids. One of the goals of polymer chemistry is to obtain a one-to-one correlation between observable properties (such as viscosity) and a microscopic model of the polymer molecule: the theoretical treatments usually deal with the ideal limiting case of an isolated, undistorted, unoriented polymer molecule, while practical experimental conditions require us to work at non-zero concentration and rate of shear. An obvious prerequisite for comparison of theory and experiment therefore is the elimination of the effects of interaction and distortion or orientation by a double extrapolation to zero concentration and gradient. It is precisely here where the difficulties arise: for example, as concentration changes, viscosity naturally changes, and with it, the rate of shear for an otherwise fixed set of experimental conditions in a capillary viscometer. Also, the same driving pressure gives different rates of shear in viscometers with different radii and lengths; if hydrodynamic properties are a function of rate of shear, the apparent viscosity of a given solution may thus seem to change from one viscometer to the next. Furthermore, certain inherent characteristics of a capillary viscometer (such as the kinetic energy correction) masquerade as non-Newtonian behavior of the test liquid; these must be eliminated by design or calculation[4] before failure of Poiseuille's law may be ascribed to non-Newtonian behavior of the liquid.

It is the purpose of this paper to present the results of an experimental study of non-Newtonian liquids in the capillary viscometer in order to show how true volume properties may be obtained. As test liquids, we chose aqueous solutions of a polyelectrolyte of high molecular weight because these

(1) Presented at a Symposium held at Cornell University, March 15–16, 1954, in honor of the Seventieth Birthday of Professor P. J. W. Debye.

(2) Project NR 051-002 of the Office of Naval Research, Paper No. 43.

(3) Results presented in this paper are abstracted from a dissertation presented by Paul Goldberg to the Graduate School of Yale University in partial fulfillment of the requirements for the Degree of Doctor of Philosophy, June, 1953.

(4) H. T. Hall and R. M. Fuoss, *J. Am. Chem. Soc.*, **73**, 265 (1951).

are known to be extremely non-ideal in hydrodynamic behavior. The methods described first require the elimination of the essentially trivial but unfortunately not negligible effects of kinetic energy and similar apparatus characteristics. Then it will be shown that results which are independent of viscometer design are obtained if measurements in different instruments are compared at equal values of (Rp/L), where R is the radius of the capillary, L its length and p is the driving pressure. This is essentially the variable introduced by Reiner.[5] It is also implicit in the generalized Poiseuille equation which was derived by Tobolsky, Powell and Eyring[6] and used by Spencer and Dillon[7] in their treatment of the viscosity of molten polystyrene. The analysis of DeWind and Hermans[8] likewise uses (Rp/L) as the significant independent variable. Kroepelin[9] introduced the area-average gradient q_k; the latter has also been used[4,10] in the analysis of data on non-Newtonian liquids. We shall show that the Kroepelin average is different for Newtonian and non-Newtonian liquids, as is the maximum gradient G, which has also been used.[11] The variable $Q = Rpg/2L\eta$, where η is the limiting value of viscosity at zero rate of shear for non-Newtonian liquids (and obviously the viscosity itself for Newtonian), appears to be the most convenient variable for a self-consistent treatment of data obtained by means of capillary viscometers.

In general, a polymer solution may exhibit non-Newtonian behavior because the solute molecules are deformed or oriented by the flow, or because the energy of interaction between molecules is changed. An empirical extension of the Huggins formula, in which both $[\eta]$ and k' are considered to be possible functions of Q, can be derived for the case where the solution viscosity is linear in Q. Several examples will be discussed in the last section of this paper.

Modified Poiseuille Equation

Our discussion is based on the fundamental equation

$$F = \eta \text{ grad } v \qquad (1)$$

which relates a velocity gradient in a liquid to the shearing force necessary to maintain it; for Newtonian liquids, η is a constant and by definition, liquids for which $(F/\text{grad } v)$ is not a constant are called non-Newtonian. In cylindrical coördinates, eq. 1 takes the form

$$-dv/dr = rpg/2L\eta \qquad (2)$$

where r is the distance from the axis of the cylinder. For a Newtonian liquid, eq. 2 integrates immediately to Poiseuille's equation

$$\eta = \pi gR^4pt/8LV = Apt \qquad (3)$$

where t is the time required for a volume V to flow through a capillary of length L and radius R under a pressure p. If we are dealing with a non-Newtonian liquid, η depends on F and therefore implicitly on r through (dv/dr). We indicate this by writing

$$\phi(r) = 1/\eta(r) = (1/\eta)(1 - \alpha q + \beta q^2 \qquad (4)$$

where, for lack of theoretical guidance, we expand the fluidity in a power series and disregard terms beyond the quadratic. (Considerable algebraic simplification, especially in power series expansions, is achieved by considering fluidity ϕ rather than its reciprocal η.) Then α and β are empirical constants to be evaluated by experiment. The local gradient (dv/dr) is represented by q and from this point on, the *symbol η will mean the limit of the viscosity coefficient at zero gradient.* The total volume V flowing in t seconds is

$$V = t\int_0^R 2\pi rv\,dr$$

This equation can be put into a more convenient form for computation by a partial integration[8,12] and substitution of (2)

$$V/t = (\pi gp/2L)\int_0^R [r^3/\eta(r)]dr \qquad (5)$$

If now the approximation assumed in eq. 4 is substituted in eq. 5 and reiterated, we find to second order in gradient

$$\phi^* = (1/\eta)[1 + 4\alpha Q/5 + 2(\alpha^2 + \beta)Q^2/3] = 1/\eta^* \qquad (6)$$

where

$$Q = Rpg/2L\eta = |q(R)| \qquad (7)$$

and

$$\eta^* = \pi gR^4pt/8LV \qquad (8)$$

The quantity Q is the maximum gradient which would exist at the capillary walls if the fluid were Newtonian. By comparison with eq. 3, we recognize η^* as the *apparent viscosity, i.e.*, the viscosity which is obtained if the experimental pt product for a non-Newtonian liquid is multiplied by the calibration constant A (it being tacitly understood that A is determined by using Newtonian calibrating liquids and that pt is corrected for kinetic energy and so on). Granting our assumptions, eq. 6 states that the apparent viscosity η^* of a given non-Newtonian liquid will be the same if measured in different viscometers, provided conditions are such that Q, and hence (Rp/L) for the same liquid, is kept unchanged.

We next consider briefly Kroepelin's average[9] gradient which is defined as

$$q_K = (1/\pi R^2)\int_0^R (dv/dr)2\pi r\,dr \qquad (9)$$

For the Newtonian case, $q_K = 8V/3\pi R^3t = (Rpg/3L\eta) = 2Q/3$. But if eq. 4 is substituted in eq. 9, we find

$$q_K^* = (2Q/3)(1 + 4\alpha Q/5 + \ldots) \qquad (10)$$

Therefore the ratio of the area-average gradient to the limiting maximum gradient is itself a function of gradient and for example a quantity which is linear in Q would be quadratic in q_K^*. In other

(5) M. Reiner and R. Schoenfeld-Reiner, *Kolloid-Z.*, **65**, 44 (1933); M. Reiner, *J. Appl. Phys.*, **5**, 321 (1934).

(6) A. Tobolsky, R. E. Powell and H. Eyring in "Frontiers in Chemistry," Vol. I, Interscience Publishers, Inc., New York, N. Y., 1943, p. 179.

(7) R. S. Spencer and R. E. Dillon, *J. Colloid Sci.*, **3**, 163 (1948).

(8) G. DeWind and J. J. Hermans, *Rec. trav. chim.*, **70**, 521, 615 (1951).

(9) H. Kroepelin, *Kolloid-Z.*, **47**, 294 (1929).

(10) U. P. Strauss and R. M. Fuoss, *J. Polymer Sci.*, **8**, 593 (1952).

(11) T. G. Fox, Jr., J. C. Fox and P. J. Flory, *J. Am. Chem. Soc.*, **73**, 1901 (1951).

(12) W. Philippoff, *Kolloid-Z.*, **75**, 142 (1936).

words, a simple function could appear to be more complicated merely as a consequence of the choice of variable.

An estimate of the order of magnitude of the velocity gradient at which the series in eq. 6 differs appreciably from unity can be made as follows, according to a suggestion made by Professor L. Onsager. The quantity η grad v (units = dynes/cm.^{2}) is also numerically equal to the potential energy per unit volume (ergs/cm.^{3}) due to the velocity field. Then $(\eta - \eta_0)$ grad v is the excess momentum transport in the solution over that due to the solvent; if there are N molecules of molecular weight M in a total volume V, the corresponding average energy per molecule is (V/N) $(\eta - \eta_0)$ grad v. When this quantity equals kT, the energy imparted to a molecule by the flow process is of the order of the translational kinetic energy of the molecule; hence a critical range of gradient is defined by

$$(\text{grad } v)_{\text{crit}} = (NkT)/[V(\eta - \eta_0)] \qquad (11)$$

If we express concentrations in the usual units (g. solute/100 ml. solution), and let $z = (\eta - \eta_0)/c\eta_0$ be the reduced viscosity, eq. 11 becomes

$$(\text{grad } v)_{\text{crit}} = RT/100Mz\eta_0 \qquad (12)$$

At 25° and approximating 100 η_0 by unity (most solvents have a viscosity of about one centipoise), this becomes

$$(\text{grad } v)_{\text{crit}} \approx 2.5 \times 10^{10}/Mz \qquad (13)$$

Hence for a polymer of molecular weight one million and intrinsic viscosity 5, we would expect non-Newtonian behavior to be easily visible at a gradient of 5000 sec.$^{-1}$. This result is in accord with experience. The corresponding critical value for (Rp/L) is given by

$$(Rp/L)_{\text{crit}} = (2\eta/g)(\text{grad } v)_{\text{crit}} = 2\eta_r RT/100gMz \qquad (14)$$

Approximating the relative viscosity by two, eq. 14 gives at 25°

$$(Rp/L)_{\text{crit}} \approx 10^6/Mz \qquad (15)$$

Concentration Dependence

The non-Newtonian behavior of solutions of polymers can arise from one or both of two sources: shear dependence of the interaction between polymer molecules, and shear dependence of the intrinsic viscosity. In the former case, (α/c) will vanish at zero concentration and in the latter it will not. We present below a treatment of the Huggins equation[13] in which we shall initially assume that

$$z = [\eta] + k'[\eta]^2 c \qquad (16)$$

both $[\eta]$ and k' may depend on Q. In order to keep the algebra from becoming unwieldy, we shall limit the discussion to the range of low gradients, where the quadratic term in eq. 6 may be neglected. To this approximation

$$\phi^* = \phi(1 + 4\alpha Q/5) \qquad (17)$$

which can be rearranged to give

$$\eta^*_{sp} = \eta_{sp} - 4\alpha\eta^*_r Q/5 \qquad (18)$$

where η^*_{sp} and η^*_r denote, respectively, specific and relative viscosities as functions of Q. (Consistent with our convention for η, symbols without the asterisk mean the limits at $Q = 0$ of the corresponding quantities.) To simplify later equations, we introduce here the assumption

$$\alpha = ac + bc^2 + \ldots \qquad (19)$$

which includes the obvious fact that the solvent is Newtonian but permits the shear coefficient to depend on orientation, distortion or interaction of solute molecules. By dividing (18) by c and going to the limit $c = 0$, we find

$$[\eta^*] = [\eta] - 4aQ/5 \qquad (20)$$

because $\eta^*_r = 1$ at $c = 0$. We then define the shear dependent coefficient k^* by the equation

$$(\eta^* - \eta_0)/\eta_0 c = z^* = [\eta^*] + k^*[\eta^*]^2 c \qquad (21)$$

by analogy to (16). If we now substitute (16), (17) and (20) in (21), rearrange, divided by $[\eta]^2 c$ and let c go to zero, we obtain

$$k' - 4bQ/5[\eta]^2 - 4aQ/5[\eta] + (4aQ/5[\eta])^2 = k^*\{1 - 4aQ/5[\eta]^2\} \qquad (22)$$

This rather awkward expression can be put into more compact form

$$k^* = [k' - (B + 1 - x)x]/(1 - x^2) \qquad (23)$$

by using the abbreviations $x = 4aQ/5[\eta]$ and $B = b/a[\eta]$. When a is zero, we obtain directly from (22)

$$k^* = k' - 4bQ/5[\eta]^2 \qquad (24)$$

Equation 24 corresponds to $[\eta^*] = [\eta]$, *i.e.*, to the case where shear dependence is due to interaction only, while eq. 23 is for the more general case. Comparison with experiment for specific systems will show whether a vanishes.

Experimental

Apparatus.—Viscosities were measured in five different Bingham[14,15] viscometers, whose constants are given in Table I. The units in Table I are $[p]$ = g./cm.^{2}, $[t]$ = sec., viscosity = poise. Water[16] and aqueous sucrose solutions[17] were used as calibrating liquids; each viscometer was calibrated by using at least five standard liquids. The method of Hall and Fuoss[4] was used to determine the correction constants for kinetic energy, incomplete drainage and capillary end effects. One additional correction[18] is needed for work at low pressures in the Bingham viscometer, that due to the change in pressure due to the change in levels of the liquid in the draining and receiving bulbs of the viscometer. If disregarded, the pt–p plots become concave down at low pressures instead of remaining linear. The corresponding coefficient is most readily determined by plotting $F(x, p)$ against the reciprocal of the square of the

TABLE I

CONSTANTS OF VISCOMETERS

No.	R	L	$10^6 A$	$10^{13} A'$	$10^{18} aA^2/V_0$	V_0
1	0.01720	9.9	0.8523	0.103	0.26	4.00
2	.01884	11.0	1.091	.183	.31	4.02
3	.02020	11.0	1.495	.32	.34	4.02
4	.02536	11.0	3.620	2.0	1.9	4.02
5	.03038	10.8	7.566	9.8	3.6	4.02

(13) M. L. Huggins, *J. Am. Chem. Soc.*, **64**, 2716 (1942); D. J. Mead and R. M. Fuoss, *ibid*, **64**, 277 (1942).

(14) E. C. Bingham, "Fluidity and Plasticity," McGraw-Hill Book Co., Inc., New York, N. Y., 1922, p. 76.

(15) R. M. Fuoss and G. I. Cathers, *J. Polymer Sci.*, **4**, 97 (1949).

(16) J. F. Swindells, *J. Colloid Sci.*, **2**, 183 (1947).

(17) "Polarimetry, Saccharimetry and the Sugars," Circular C 440, National Bureau of Standards, 1942.

(18) E. C. Bingham, H. I. Schlesinger and A. B. Coleman, *J. Am. Chem. Soc.*, **38**, 27 (1916).

applied pressure; for our instruments, the correction height was found to lie between 2.3 and 2.7 cm. In our apparatus the range of pressure was from 20 to 200 cm. water. Flow times right-to-left and left-to-right were taken at the same applied pressure p_0 and averaged; this procedure eliminates certain asymmetry corrections.[14]

Having determined the calibration constants with Newtonian liquids, it is possible to calculate from observed (p, t) values for any liquid in the viscometer the quantity[10]

$$F(x,p) = x + (\alpha x^3 - \beta x)p$$

where

$$x = 1/pt,\ \alpha = A'\rho/A^3 \text{ and } \beta = aA^2/\rho V_0$$

For our range of working conditions, F and x differ by at most 1–2%. The function F represents the reciprocal pt product for non-Newtonian liquids, corrected for kinetic energy and so on, assuming that the corresponding coefficients (A', m, a) are the same for ideal and real liquids. This assumption is not strictly accurate because in principle each correction should be a function of Q, but it can be shown that the difference is of the order of a correction to a correction. The apparent viscosity η^* is then obtained by dividing A by F; apparent fluidity is F/A.

Materials.—Polyvinylpyridine was prepared by emulsion polymerization under nitrogen, using the recipe: 100 ml. of freshly distilled 4-vinylpyridine, 0.286 g. of azo-bis-isobutyronitrile, 200 ml. of water and 20 g. of Nekal AEMA. After 4 hr. stirring at 65°, the emulsion was broken by dilution and the polymer was washed thoroughly by decantation. Its reduced viscosity η_{sp}/c at 0.200 g./100 ml. in 95% ethanol was 5.44. A middle fraction was obtained by dissolving 50 g. in 1000 ml. of *t*-butyl alcohol, adding 700 ml. of benzene, centrifuging to remove a small amount of insoluble material, and then adding benzene to the cloud point at 25° (1610 ml. of benzene total). Then 15 ml. more of benzene were added and, after one hour, the gelatinous precipitate was centrifuged out and redissolved in 1000 ml. of *t*-butyl alcohol. Benzene (1335 ml. to cloud point plus 10 ml.) was added and after one hour, the precipitate was centrifuged out and redissolved in 500 ml. of *t*-butyl alcohol. This solution was frozen, and then solvent was sublimed off under vacuum; yield of middle-cut polymer, 30.0 g.; reduced viscosity at 0.200 g./100 = 6.18; estimated molecular weight, 2×10^6.

The polymer was partially quaternized as follows: 5.0 g. was dissolved in 220 g. of tetramethylene sulfone and heated for 3 hr. at 62° after addition of 33 g. of *n*-butyl bromide. The salt was recovered by pouring the reaction mixture into 2 l. of anhydrous dioxane, dissolving the precipitate in 10 ml. of methanol and reprecipitating in dioxane. This process was repeated twice; the third precipitate was dissolved in water and after freezing, water was sublimed off under *high* vacuum. The product is extremely hygroscopic. Bromine was determined by potentiometric titration: found average 25.9% Br; theoretical, 33.1%; the material is therefore 60.7% quaternized.

Method.—Materials were weighed out and polyelectrolyte plus solvent were placed on a shaker overnight. The next day, viscosities were determined in two or more viscometers. It was observed in the preliminary work that the viscosity slowly decreased on standing for several days; part of this change was due to the growth of several microorganisms in the solutions. Dr. S. Simmonds of the Biochemistry Department isolated two species: a small, pink Gram-negative rod and a large, cream-colored Gram-positive rod. The growth of these was rather surprising, because quaternary pyridinium salts are frequently used as fungicides and bactericides. They did not survive in 0.1% aqueous phenol, however, and all our final measurements were therefore made in 0.1% phenol as solvent. This solvent has a viscosity η_0 of 0.00903 at 25.00°. Even in 0.1% phenol, the viscosity decreased by several per cent. per 24 hr. on standing at room temperature; the rate of decrease was accelerated by heating to 65°. We also found that several hours at 5° would increase the 25° viscosity of the solutions; on standing or heating, the viscosity slowly decreased to the initial value and then below it. These observations suggest that both association and degradation may be occurring, but further work is needed to clarify these puzzles. In order to eliminate the aging effects, each solution was measured in the several viscometers within a period of 2–5 hr. and the viscosity in the first viscometer was always redetermined at the end of a sequence. Checks well within 1% were usually obtained.

Results and Discussion

The experimental results can best be presented graphically. In Fig. 1, we have plotted $(1/\eta^*) = F/A$ against driving pressure for a series of solutions of our polysalt in 0.1% aqueous phenol, which cover the range (top to bottom of Fig. 1) 0.00725 g./100 ml. to 0.2048. For orientation, we mention that the fluidity of the solvent would be represented by a horizontal line at $(1/\eta_0) = 110.8$ in Fig. 1. It is immediately obvious that the solutions are non-Newtonian, because the curves are not horizontal straight lines. Furthermore the apparent viscosity of a given solution measured at the same pressure in different viscometers is different; the differences are far from negligible. But if the apparent fluidities are plotted against (Rp/L) as in Fig. 2, all the data for a given solution lie on a single curve. This result confirms the statement made in the introduction that (Rp/L) is the rational independent variable to use for treating data obtained by the use of capillary viscometers.

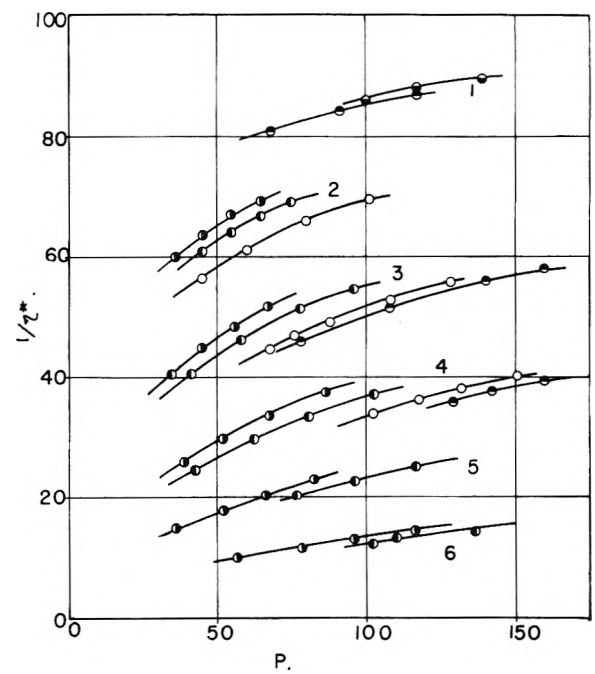

Fig. 1.—Apparent fluidity as function of pressure, solutions of poly-*n*-N-butyl-4-vinylpyridine in different viscometers: lower black circles, viscometer No. 1 (Table I); upper black, No. 2; open, No. 3; left black, No. 4; right black, No. 5. Concentrations: 1, 7.25 mg. polysalt/100 ml. solution; 2, 13.64; 3, 25.26; 4, 52.8; 5, 103.2; 6, 204.8.

The curves of Fig. 2 are of the general form required by eq. 6; since they are concave down, we conclude that β is negative and numerically larger than α^2. The shear dependence of the solution evidently goes through a maximum as we go from concentrated to more dilute solutions; other work[10] has shown that the partial contribution to the shear dependence which is due to the solute increases with increasing dilution for polyelectrolytes. The data shown in Fig. 2 are all in the range where (Rp/L) is much larger than the critical value given

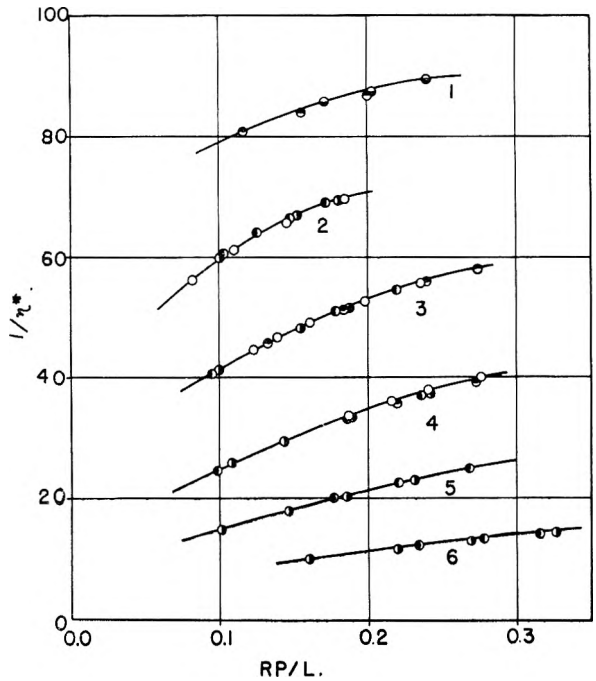

Fig. 2.—Apparent fluidity as function of (Rp/L). Same code as Fig. 1.

by eq. 11; in fact for solutions 2 and 3 at least, they are beyond the range where the quadratic term included in eq. 4 and 6 suffices to account for the curvature. Consequently extrapolation of these data to zero gradient has not been attempted.

We next turn to a consideration of eq. 21 using as an example nitrocellulose in butyl acetate.[19] The original data are reported as η^*/c for various values of q_K, the Kroepelin average. In order to obtain values as a function of Q, $(1/\eta^*_r)$ was plotted against $(q_K\eta^*_r)$ at each concentration, and extrapolated to zero gradient in order to obtain $(1/\eta_r)$ values. These in turn were used to calculate Q for each point by means of the relation

$$Q = 3\eta^* q_K/2\eta = 3\eta^*_r q_K/2\eta_r$$

Then plots of $(1/\eta^*_r)$ against Q were constructed for each concentration; they were linear up to Q = 20,000 sec.$^{-1}$. From these graphs, values of $(1/\eta^*_r)$ were read off at round values of Q; these data were then used to compute the points for the (η^*_{sp}/c)–c plot shown in Fig. 3. It will be noted that the different curves extrapolate to the same value; hence the intrinsic viscosity is independent of rate of shear for this system. It should be mentioned at this point that (η_{sp}/c)–c curves constructed at constant q_K give *different* intercepts, and would therefore mislead one into concluding that $[\eta]$ depended on shear. From the slopes of the curves of Fig. 3, we obtain k^* as a function of Q; according to eq. 24, k^* is linear in Q when $[\eta]$ is independent of Q. The top plot on Fig. 3 verifies this conclusion. Finally, from the slope of the k^*–Q plot, we obtain a value for b equal to 0.0112. The bottom curve of Fig. 3 shows (α/c) from the slopes of the $(1/\eta^*)$–Q plots as a function of concentration. It will be seen that higher terms in concentration than quad-

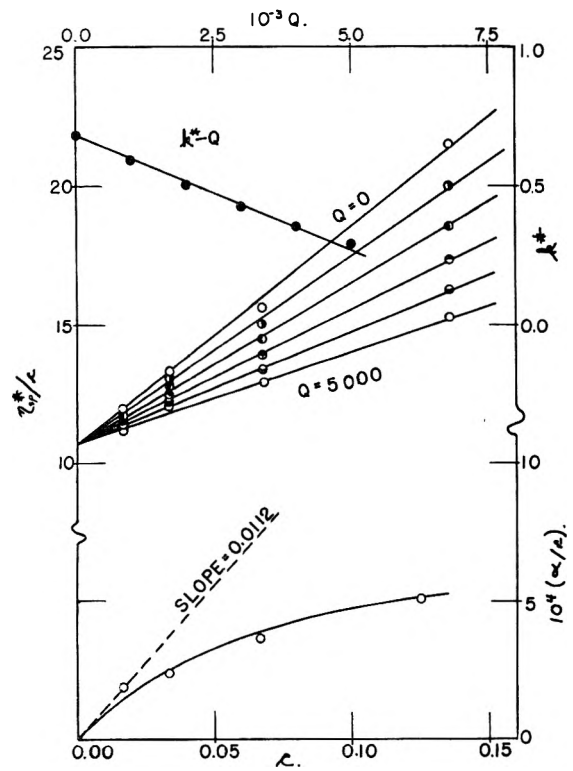

Fig. 3.—Nitrocellulose in butyl acetate: central lines, (η_{sp}/c) *vs.* c; coördinates left and bottom; 10^{-3} Q = 0, 1, 2, 3, 4 and 5. Bottom curve, (α/c) *vs.* c; coördinates right and bottom. Top line, k^* *vs.* Q, coördinates right and top.

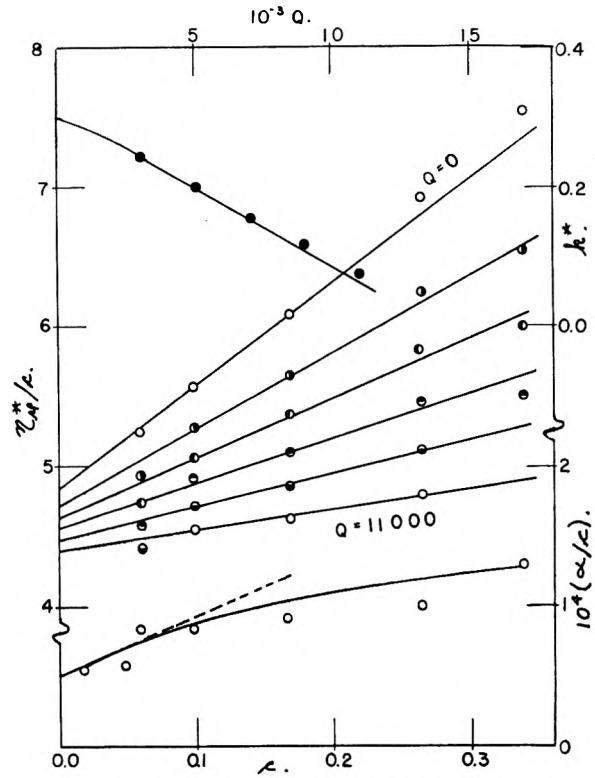

Fig. 4.—Polyvinylpyridine in methanol: central lines, (η^*_{sp}/c) *vs.* c; coördinates left and bottom; 10^{-3} Q = 0, 3, 5, 7, 9 and 11. Bottom curve, (α/c) *vs.* c, coördinates right and bottom. Top curve, k^* *vs.* Q, coördinates right and top.

(19) H. Staudinger and M. Sorkin, *Ber.*, **70**, 1993 (1937).

ratic are needed in eq. 19. But the equation is satisfactory to give the limiting behavior; the tangent to the (α/c)–c curve of Fig. 3 is drawn with a slope of 0.0112, the value obtained from the k^*–Q plot.

As an example of a system in which both $[\eta]$ and k' depend on shear, we consider next poly-4-vinylpyridine in methanol.[20] These data were obtained using viscometer 2 of Table I; the $(1/\eta^*)$–Q plots were linear over the range 2000–15,000 sec.$^{-1}$. Figure 4 shows plots of η^*_{sp}/c against c for round values of Q. In contrast to nitrocellulose, the lines now have different intercepts at $c = 0$, and we conclude that $[\eta]$ depends on rate of shear. This result seems compatible with the difference in stiffness between nitrocellulose and polyvinylpyridine. The lower curve of Fig. 4 is a plot of (α/c) against c; the limiting value at $c = 0$ is 0.50×10^{-4}, which evaluates a of eq. 19. In order to obtain b, we plotted $k^*(1 - x)^2$ against x; the curve is nearly linear and, from its limiting tangent, we obtain B and then b. The value so obtained, 4.4×10^{-4}, was used to draw the tangent to the (α/c)–c curve of Fig. 4; it is consistent with the observed curve. Finally, eq. 23 was used to compute values of k^* for different values of Q using the values of a and B obtained above. The result is shown as the solid curve at the top of Fig. 4. Evidently, eq. 23 represents the shear dependence of the concentration coefficient within our experimental error.

(20) R. A. Mock, Thesis, Yale University, 1951.

Our results, as well as those of other observers, show that the empirical limiting relation between the viscosity of polymer solutions and the rate of shear is a linear one. This implies the theoretical absurdity that mere reversal of the direction of shear would reverse the sign of the viscosity change; the dilemma cannot be evaded by postulating linearity in the absolute value of the velocity gradient, because absolute value is a function whose derivative is discontinuous at the origin. The available theoretical analyses all call for a quadratic dependence of viscosity on gradient, but no experimental evidence supporting this result has been reported. Possibly the function involved is something like the square root of the square of the gradient plus a small constant, $(1 + 2b \text{ grad}^2 v)^{1/2}$ which expands to $(1 + b \text{ grad}^2 v)$ when the second term is very small and which behaves like $(2b)^{1/2} \text{ grad } v$ when it is large. The situation is reminiscent of Kohlrausch's insistence that the conductance of strong electrolytes in water was linear in root concentration, in the face of the prestige of the Arrhenius dissociation theory and the Ostwald dilution law which called for a limiting linear dependence on the first power of concentration. Half a century later, Debye produced the theoretical interpretation which justified Kohlrausch's confidence in his experimental results.

INTRINSIC VISCOSITIES OF POLYELECTROLYTES. POLY-(ACRYLIC ACID)[1]

BY PAUL J. FLORY AND JEAN E. OSTERHELD

Department of Chemistry, Cornell University, Ithaca, New York

Received April 19, 1954

Intrinsic viscosities $[\eta]$ of poly-(acrylic acid) neutralized to varying degrees have been determined in the presence of NaCl, Na_2SO_4, $CaSO_4$ and $CaCl_2$. Measurements at several rates of shear over the range from 2000 to 200 sec.$^{-1}$ permitted extrapolation to zero shear rate. The intrinsic viscosity at the Θ-point (*ca.* 32°) for one-third neutralized polymer in 1.245 molar aqueous NaCl agrees within experimental error with the value found for the non-ionized polyacid at the Θ-point (30°) in pure dioxane. Equivalent configurations for the unperturbed poly-salt and for the polyacid chain are thus indicated. Expansion factors α^3 have been calculated from intrinsic viscosities determined in other aqueous media using the relation $\alpha^3 = [\eta]/[\eta]\Theta$. Values of $\alpha^5 - \alpha^3$ for polymer fractions of $M \cong 8 \times 10^6$ at fixed degrees of neutralization i (= 1.00, 0.333 and 0.100) increase linearly with the reciprocal ionic strength S^* of the aqueous NaCl solution. The slopes are considerably lower than theoretically predicted, and the disparity increases with i. It is suggested that suppression of the mean ion activity, owing to the comparatively high charge on the polymer chain, is responsible for the result. At the same ionic strength Na_2SO_4 is equivalent to NaCl in its effect on the molecular configuration; the lower intrinsic viscosities observed in the presence of Ca salts are attributed to stronger electrostatic interaction of divalent cations with the charged chain molecule. The validity of the Donnan approximation used in treating the polyelectrolyte molecule is discussed, and it is shown that the ease of molecular expansion tends to preclude the occurrence of large differences in chemical potentials for mobile ions inside and outside the molecular domain. The net charge acquired by the molecule is small in comparison with the number of charge sites on the chain down to very low salt concentrations. Even in the total absence of added electrolyte, the ions present in pure water should be sufficient to prevent close approach to full extension of the polyelectrolyte molecule and the removal of a preponderance of its complement of counter ions contrary to presumptions in the polyelectrolyte literature.

Introduction

During the past few years procedures for treating the influence of long range intramolecular interactions in uncharged polymer molecules have been fairly well established.[2,3] The average linear expansion α resulting from these interactions has been predicted theoretically to increase non-asymptotically with the chain length, and this prediction

(1) (a) Presented before the Debye 70th Anniversary Symposium, Cornell University, March 15 and 16, 1954. (b) The work discussed herein was performed as a part of the research project sponsored by the Reconstruction Finance Corporation Office of Synthetic Rubber, in connection with the Government Synthetic Rubber Program.

(2) See for example T. G. Fox, Jr., and P. J. Flory, *J. Am. Chem. Soc.*, **73**, 1905, 1909, 1915 (1951); L. H. Cragg, E. T. Dumitru and J. E. Simkins, *ibid.*, **74**, 1977 (1952).

(3) P. J. Flory, "Principles of Polymer Chemistry," Cornell Univ. Press, Ithaca, N. Y., 1953, Chap. XIV.

has received gratifying confirmation from experiment. Out of these investigations it has been shown that the intrinsic viscosity $[\eta]$ is directly proportional to the volume molecular expansion α^3. Thus, this factor which characterizes the configuration under given conditions is readily accessible experimentally through the relationship

$$\alpha^3 = [\eta]/[\eta]_\Theta \qquad (1)$$

where $[\eta]_\Theta$ is the intrinsic viscosity of the same polymer sample at the same temperature in the absence of perturbations due to long range interactions between chain elements (*i.e.*, between elements situated some distance apart along the polymer chain). The "Θ-point," at which this condition of ideality holds, is realized in a solvent medium where the covolume of the chain elements is zero (and, consequently, the covolume of the molecule as a whole is zero also).

More recently, the treatment of intramolecular interactions in polymer molecules has been extended to polyelectrolyte chains immersed in a solution of an ordinary electrolyte.[4,5] If the molecular weight of the polymer molecule is reasonably high and the ionic strength S^* of the surrounding solution is not extremely low (*e.g.*, if $S^* > 10^{-4}$ molar), then, as Kimball, Cutler and Samelson[6] have shown, the net charge acquired within the domain of the polymer molecule should be small compared with the total charge of the ionic centers bound to the polymer chain.[7] It is essential merely that the size of the polymer domain shall be large compared with $1/\kappa$, the radius of the Debye–Hückel atmosphere about an ion. If the root-mean-square end-to-end distance is adopted as a measure of the former quantity, then it is required that $\kappa\sqrt{\overline{r^2}} << 1$.[6,7]

When this condition is met, mobile ion concentrations within the domain of the polymer molecule may be calculated in the Donnan electroneutrality approximation, the more laborious derivation of the potential and the electrical free energy being unnecessary.[5] Deformation of the polymer molecule is appropriately attributed to the osmotic activities of the mobile ions, which occur at somewhat greater concentration within the polymer domain than in the outer solution, in the manner dictated by the usual Donnan equations. The average mobile ion concentration in each volume element may be related to the average concentration of charged polymer units in that volume element, and the total osmotic effect of the mobile ions may be obtained by integration. Thus, the effects of the icns on the configuration of the polymer chain may be treated in a manner paralleling the previous treatment[2,3] of long range intramolecular interactions in non-ionic polymer molecules. The following relationship has been established[5] by this procedure.

$$\alpha^5 - \alpha^3 = 2C_M\psi_1(1 - \Theta/T)M^{1/2} + 2C_I i^2 M^{1/2}/S^* + 2C'_I i^3 (z_- - z_+)/(S^*)^2\alpha^3 + 2C''_I i^4[z^2_- - (5/2)z_+ z_- + z_+^2]/M^{1/2}(S^*)^3\alpha^6 + \ldots \qquad (2)$$

where C_M and ψ_1 are parameters previously defined[2,3] for non-electrolyte chains, M is the molecular weight, S^* the ionic strength of the external solution expressed in moles per liter, i is the degree of ionization or number of (negative) electronic charges[8] per unit of the polymer chain, z_+ and z_- are the magnitudes of the electronic charge numbers for the ions of the added electrolyte, and

$$C_I = 10^3(2^{-6/2}2^{-2})(3\pi^{-1/2})^3[(M/\overline{r_0^2})^{3/2}/\mathbf{N}M_u]/M_u$$
$$C_I' = 10^6(3^{-6/2}2^{-3})(3\pi^{-1/2})^6[(M/\overline{r_0^2})^{3/2}/\mathbf{N}M_u]^2/M_u \qquad (3)[9]$$
$$C_I'' = 10^9(4^{-5/2}2^{-4})(3\pi^{-1/2})^9[(M/\overline{r_0^2})^{3/2}/\mathbf{N}M_u]^3/M_u$$

Here $\overline{r_0^2}$ is the mean-square unperturbed end-to-end length of the polymer chain, M_u is the molecular weight of the polymer unit, and **N** is Avogadro's number.

The first term occurring on the right-hand side of equation 2 is due to the interactions between polymer chain elements, apart from coulombic effects; it is formally identical with the expression for non-ionic polymers. The second term represents the principal ionic term; under the conditions of our experiments the remaining terms appear to be comparatively small. Thus, the quantity $\alpha^5 - \alpha^3$ should vary linearly with i^2/S^*.

The present investigation was undertaken with the object of exploring the validity of the foregoing equations. Polyacrylic acid fractions of high molecular weight were chosen, and these were neutralized to varying degrees in aqueous solutions containing sodium chloride or other electrolytes at various ionic strengths S^*.[10] The values of α were calculated from intrinsic viscosities $[\eta]$ through the use of equation 1. It is assumed, therefore, that the intrinsic viscosity of the polyelectrolyte molecule is the same function of molecular dimensions as for uncharged polymers. This assumption receives support in the previous work of Oth and Doty[11] in which molecular dimensions of polymethacrylic acid salts, determined by light scattering disymmetry measurements, were compared with intrinsic viscosities at various degrees of neutralization.

Experimental

Poly-(acrylic Acid).—The fractions used in this investigation were prepared by Newman, *et al.*,[12] as described elsewhere. Series A fractions, the final step in the preparation of which involved reprecipitation from dioxane solution using benzene, contained in the neighborhood of 5% of moisture and solvent. Series B fractions, freeze dried without reprecipitation retained up to 15% of solvent and around 2% of moisture. (Series B fractions were used only for precipitation temperature determinations.) It was

(4) T. L. Hill, *J. Chem. Phys.*, **20**, 1173 (1952).

(5) P. J. Flory, *ibid.*, **21**, 162 (1953).

(6) G. E. Kimball, M. Cutler and H. Samelson, THIS JOURNAL, **56**, 57 (1952).

(7) The same conclusion is contained in the earlier work of J. J. Hermans and J. Th. G. Overbeek, *Rec. trav. chim.*, **67**, 761 (1948), and also in the more recent treatment given by F. Osawa, N. Imai and I. Kagawa, *J. Polymer Sci.*, **13**, 93 (1954), concerning a polyelectrolyte molecule distributed uniformly within a sphere.

(8) In consideration of the polyacrylate chain employed in this investigation, the charges on the polymer chain are taken to be negative rather than positive as assumed in the previous paper.[5] This accounts for the appearance of $(z_- - z_+)$ instead of $(z_+ - z_-)$ in the third term on the right.

(9) These relations were previously given[5] in error by factors $1/v_1$, where v_1 is the molar volume of the solvent.

(10) Preliminary results were presented previously by P. J. Flory, W. R. Krigbaum and W. B. Shultz, *J. Chem. Phys.*, **21**, 164 (1953).

(11) A. Oth and P. M. Doty, THIS JOURNAL, **56**, 43 (1952).

(12) S. Newman, W. R. Krigbaum, C. Laugier and P. J. Flory, *J. Polymer Sci.*, in press.

necessary, therefore, to accurately measure the poly-(acrylic acid) content of each sample in order to prepare solutions of known concentration and at specified degrees of neutralization. Preceding the preparation of solutions for viscosity or precipitation measurements, each sample was titrated with carbonate-free 0.05 *M* NaOH. Sufficient NaCl was added to render the solution approximately 0.1 *M* in salt in order to sharpen the otherwise ill-defined end-point which is characteristic of a polymeric weak acid. Preliminary potentiometric titrations, using the glass electrode and KOH instead of NaOH displayed sharp inflection points in the presence of 0.1 *M* KCl, and the positions of these end-points were unchanged in 0.24 *M* KCl. Thereafter the titrations were carried out as described above using phenolphthalein as the indicator.

Molecular weights of the fractions were taken from the light scattering results of Newman, *et al.*,[12] or, where they were not measured directly, values were estimated by interpolation. Precise values are unimportant for the purposes of this investigation.

Preparation of Aqueous Solutions.—A solution of the highest polymer concentration required for a series of measurements at a given degree of neutralization i and ionic strength S^* of added salt (usually sodium chloride) was prepared as follows. A weighed quantity of the polymer sample, previously titrated for poly-(acrylic acid) content, was introduced into a volumetric flask (10 ml. for solutions to be used for precipitation measurements, 25 or 50 ml. for viscosity determinations). The amount of the added electrolyte required for the ionic strength S^* was weighed into the flask, and carbonate-free aqueous sodium hydroxide was added in the precise proportion required for the desired degree of neutralization. Solution was effected by mild shaking under a heat lamp. The solution was then diluted to volume at 30° with decarbonated distilled water.[13] Partial precipitation sometimes occurred during the operation; in such instances complete homogeneity was restored by further warming and agitation.

Solutions used in the precipitation determinations (degree of neutralization $i = 0.333$, sodium chloride at $S^* = 1.245$ molar) were reduced to successively lower polymer concentrations by adding suitable measured volumes of aqueous sodium chloride at the same ionic strength. The polymer concentration here is not critical, hence small errors in the dilution procedure were of no importance. Precise control of the degree of neutralization and, to a somewhat lesser extent, of the ionic strength of the salt, was essential, however. For convenience, the polymer concentrations used in these experiments are expressed in per cent. of poly-(acrylic acid) by weight.

In carrying out a series of viscosity measurements at a given degree of neutralization i and an ionic strength S^* it was expedient likewise to prepare solutions of lower concentration from those of higher concentration by successive dilution. Avoidance of accumulated error from the successive dilutions was highly important here and for this reason it was considered desirable to determine the dilution (with salt solution of the given S^*) by weighing. Some of the less viscous solutions (with relative viscosity < 1.5) were, however, diluted volumetrically using a pipet, the drainage error being small in such cases. Polymer concentrations are expressed in g. of poly-(acrylic acid) per 100 ml. of solution at 30° for all solutions used in the viscosity measurements.

Precipitation Measurements.—The procedure here resembled that described by Shultz and Flory.[14] A ruled scale was observed visually through the stirred solution with illumination transverse to the direction of observation. The aqueous solution of the one-third neutralized polyacid in 1.245 *M* NaCl was cooled slowly until the lines of the scale appeared blurred. The temperature T_p at which this first became apparent was taken as the precipitation temperature, which could be defined within ±0.5° (usually ±0.2°). In order to compensate the decreased quantity of polymer in the path of observation at the higher dilutions, a larger flask was employed. The precipitation was reversible with increasing temperature.[15] Minute variation in the degree of neutralization probably was the major source of error in these measurements.

Precipitation measurements in dioxane were conducted in a similar fashion. Owing to inversion of the usual solubility–temperature relationship in this case, the precipitation was observed with gradual warming of the solution.

Solution Viscosities.—Dilute solution viscosities were measured in Ubbelohde (No. 1) viscometers (flow time for water at 30°, *ca.* 100 sec.) immersed in a water-bath at 30.00 ± 0.05°. Kinetic energy corrections were employed throughout. Freshly prepared solutions were used. They were filtered into the viscometer through sintered glass frits. After each determination the viscometer was flushed at least five times with distilled water before rinsing with acetone preparatory to drying. This procedure was important inasmuch as acetone is a powerful precipitant for the polymer. For the same reason, acetone vapor was thoroughly removed before the introduction of the next solution. The solvent viscosity used in computing the relative viscosity of aqueous polymer solutions was taken as that observed for the aqueous solution of the salt at the same ionic strength S^* as that employed in the presence of polymer.

The influence of rate of shear on the viscosities of various polyacrylate solutions was investigated with the aid of the low shear capillary viscometer previously described.[16] The two upper bulbs only were used; these gave rates of shear γ at the capillary wall (*i.e.*, maximum shear rates) in the neighborhood of 250 and 500 sec.$^{-1}$. Results so obtained in conjunction with that for the Ubbelohde viscometer, which operated at $\gamma \sim 2000$ sec.$^{-1}$ permitted evaluation of the shear coefficient for a given solution, and from this coefficient the intrinsic viscosity at $\gamma = 0$ could be estimated.

Results

Determination of Theta Points.—The system water–sodium chloride–poly-(acrylic acid) at fixed degree of neutralization may be treated as one of three components after the manner described in previous publications.[17,18] The plait point for such a system in the limit of infinite molecular weight occupies a role corresponding to the Θ-point in a system of two components. The plait point merges with the solvent–non-solvent axis of the triangular phase diagram as $M \rightarrow \infty$, hence the plait point in this limit specifies a unique solvent composition. Shultz[18] designates this the critical consolute mixture (CCM). The equivalence of the CCM to the Θ-point for a single solvent follows from the fact that the second coefficient in the expansion of the osmotic pressure in powers of the polymer concentration must equal zero when the solvent–non-solvent ratio corresponds to the CCM.[18,19] In this paper we employ the term "Θ-point" in the sense of including the CCM for mixed solvents as well.

Instead of locating the CCM for partially neutralized polymer in mixtures of water and salt at a given temperature, we have chosen to follow the procedure of Mandelkern[17] involving location of the temperature at which a given solvent mixture becomes the CCM for the polymer. We then designate this temperature as the Θ-point. The degree

(13) A temperature of 31.6° was adopted for solutions near the Θ-point, *i.e.*, for $i = 0.333$ and $S^* = 1.245$ molar, in order to avoid incipient precipitation.

(14) A. R. Shultz and P. J. Flory, *J. Am. Chem. Soc.*, **74**, 4760 (1952).

(15) Some of the samples of fractions A-6 and A-7 yielded solutions containing minute amounts of suspended, relatively unswollen matter, presumed to be undissolved polymer. On the other hand, solutions of composition well removed from the Θ-point, such as were used for most of the viscosity measurements, gave no evidence of an insoluble residue.

(16) W. R. Krigbaum and P. J. Flory, *J. Polymer Sci.*, **11**, 37 (1953).

(17) L. Mandelkern and P. J. Flory, *J. Am. Chem. Soc.*, **74**, 2417 (1952).

(18) A. R. Shultz and P. J. Flory, *ibid.*, **75**, 5681 (1953).

(19) R. L. Scott, *J. Chem. Phys.*, **17**, 268 (1949).

of neutralization $i = 0.333$ and the sodium chloride concentration $S^* = 1.245$ molar were selected with the object of securing a Θ-point at a temperature in the neighborhood of the Θ-point for dioxane, namely, about 30° (*cf. seq.*).

The results of precipitation measurements on various poly-(acrylic acid) fractions, one-third neutralized with NaOH and dissolved in 1.245 *M* aqueous NaCl in each case, are shown in Fig. 1 where they are plotted against the polymer concentration expressed in per cent. by weight of the polyacid. While these curves rapidly approach the ordinate axis, they must eventually become asymptotic to it (so long as *M* is finite). It will be seen that the curves do not occur in the order of their molecular weights. This irregularity probably is related to the difficulty of achieving identical degrees of neutralization with different samples (see Experimental section).

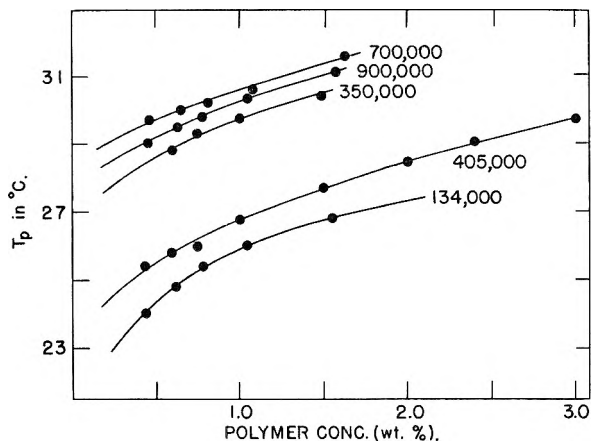

Fig. 1.—Precipitation temperatures T_p for one-third neutralized poly-(acrylic acid) fractions dissolved in 1.245 *M* aqueous NaCl plotted against the polymer concentration expressed as per cent. by weight of the polyacid. Molecular weights are indicated with each curve.

Precipitation temperatures for a polymer concentration of 0.50 weight per cent., determined by interpolation along the curves of Fig. 1, are represented by the lower set of data shown in Fig. 2 where they are plotted against the value of $M^{-1/2}$

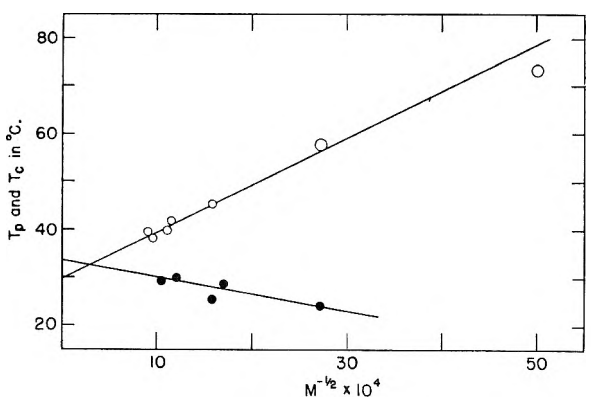

Fig. 2.—The solid points represent precipitation temperatures T_p interpolated from the curves of Fig. 1 for solutions of the one-third neutralized polymer at a concentration of 0.5 g. of polyacid per 100 g. of solution. The open circles are critical miscibility temperatures T_c for the polyacid in dioxane.

for the fraction. Similar plots of the values of T_p for higher concentrations would describe lines above the one shown. The Θ-point corresponds to the point of convergence of the intercepts of the family of these plots as the concentration becomes zero.[17] The intercept of the line drawn in Fig. 2 is 33° which by extrapolation to $c = 0$ leads to a value of 32 ± 3° for the Θ-point of this system.

Also shown in Fig. 2 are the critical miscibility temperatures for poly-(acrylic acid) fractions in pure, anhydrous dioxane. The solubility decreases with temperature in this system, hence T_p increases with decrease in the molecular weight *M*. A value of 30 ± 1° for the Θ-point of this system is indicated by the usual linear extrapolation.

Intrinsic Viscosities at the Θ-Points.—Results of dilute solution viscosity measurements on fraction A-7, having a molecular weight of 768,000, are shown in Fig. 3. The open circles represent

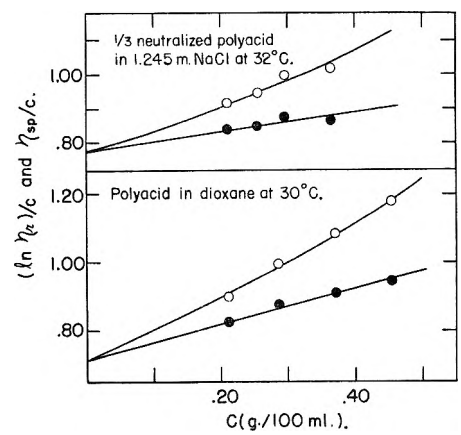

Fig. 3.—Viscosity–concentration plots of fraction A-7 in the Θ-solvents indicated.

η_{sp}/c, the filled circles $(\ln \eta_r)/c$. In conformity with previous work,[2,20] the slopes of these plots are unusually large in the vicinity of the Θ-point, *i.e.*, the Huggins k' exceeds 0.50. The intercept for the polyacid in dioxane at 30° gives $[\eta]_\Theta = 0.71 \pm 0.02$. For the one-third neutralized polyacid in 1.245 molar aqueous NaCl, $[\eta]_{32°} = 0.77 \pm 0.03$. Similar measurements made in the same solvent mixture at 29° yielded $[\eta]_{29°} = 0.67 \pm 0.02$. Recalling the uncertainty in the Θ-point for this mixture, we conclude that for the polyelectrolyte in salt solution $[\eta]_\Theta = 0.77 \pm 0.10$. Thus, within the unfortunately large experimental error, *the intrinsic viscosities of the polyacid in an organic solvent and of the polyacid salt in an aqueous medium are substantially the same.* It is worth noting that the uncertainty with which this conclusion must be qualified is dwarfed by the viscosities attained by the polyelectrolyte in more favorable media, *i.e.*, at lower concentrations of salt.

In view of the comparatively large uncertainty in $[\eta]_\Theta$ for the polyelectrolyte in aqueous solutions, we shall adopt the value found for the polyacid in dioxane, namely, 0.71 for fraction A-7, for use in treating the results which follow. None of the conclusions reached would be altered seriously, how-

(20) P. J. Flory, L. Mandelkern, J. Kinsinger and W. B. Shultz, *J. Am. Chem. Soc.*, **74**, 3364 (1952).

ever, if the value 0.77 indicated by measurements in aqueous salt were employed instead.

Intrinsic Viscosities in Aqueous NaCl Solutions.—Solutions of polymer fraction A-7 were investigated at degrees of neutralization from 1.00 to 0.10 and over ranges in ionic strength of NaCl from the lowest at which reasonably reliable shear corrections could be made up to ionic strengths at which molecular expansion owing to the osmotic action of the gegenions was largely suppressed. Primary measurements were carried out in the No. 1 Ubbelohde viscometer which operates at a rate of shear of about 2000 sec.$^{-1}$. Corrections for the effect of shear rate were introduced in the manner to be described in the following section.

Typical viscosity–concentration plots are shown in Fig. 4. At degrees of neutralization greater than 0.10 extrapolation to $c = 0$ for the purpose of evaluating $[\eta]$ presented no difficulties. The slopes of the plots were observed to vary with the degree of neutralization and with the ionic strength in a somewhat irregular manner. The intercepts, given in column two of Table I, are believed to be accurate within one per cent. for $i = 1.00$ and 0.333, except at the highest values of $[\eta]$ where the percentage error may be twice as great.

At the lowest degree of neutralization, $i = 0.100$, upward curvature invariably was observed at low concentrations, as is illustrated by the two examples included in Fig. 4. This behavior appears to

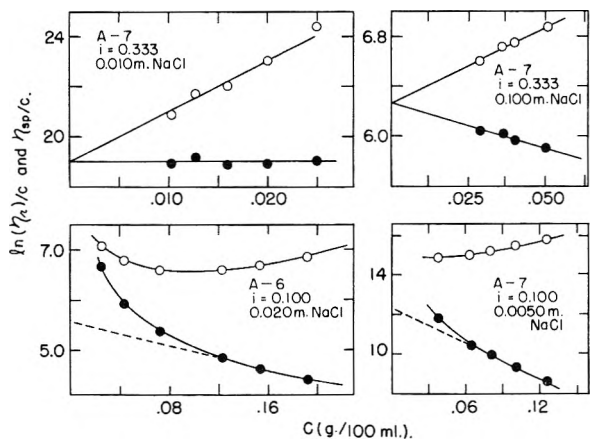

Fig. 4.—Typical viscosity–concentration plots for various degrees of neutralization and salt concentrations as indicated: open circles, η_{sp}/c; filled circles, $(\ln \eta_r)/c$; (Ubbelohde viscometer, shear rate approximately 2000 sec.$^{-1}$).

be due to enhanced ionization according to the process

$$COOH + (Na^+)^* \rightleftharpoons COO^- + Na^+ + (H^+)^* \quad (4)$$

where the asterisk designates species located outside the domain of the polymer coil. If we neglect the restraining influence of the small (*cf. seq.*) potential difference between the domain of the polymer molecule and the surrounding solution, then

$$[H^+]^* = K[COOH]/[COO^-] \cong K/i \quad (5)$$

Assuming that $K \cong 10^{-5}$ mole/liter, it is apparent that if $i \cong 0.10$ then process (4) should make an appreciable contribution to the degree of ionization when the concentration of carboxylate ion in the system as a whole falls below about 10^{-3} molar. This occurs in the vicinity of $c = 0.1$ g./100 cc., in good agreement with the location observed for the onset of the deviation.

The intrinsic viscosities given for $i = 0.100$ in Table I have been obtained by linear extrapolation of the points at higher concentration after the manner indicated by the broken lines shown in the two lower diagrams of Fig. 4. The estimated error in this procedure amounts to about 4% of the intrinsic viscosity.

TABLE I

INTRINSIC VISCOSITIES OF POLYMER FRACTION A-7 IN AQUEOUS SODIUM CHLORIDE SOLUTIONS AT 30°

S^*, mole/l.	$[\eta]$ Obsd.	$[\eta]$ Corrected	α^3	$\alpha^5 - \alpha^3$	$i/\alpha^3 S^*$
		$i = 1.00$			
0.250	5.51	5.54	7.80	22.9	0.51
.100	8.65	8.8	12.4	54.1	.81
.060	11.3	11.7	16.5	90	1.01
.0400	14.8	15.4	21.7	147	1.15
.0200	19.8	21.5	30.3	269	1.65
		$i = 0.333$			
0.200	4.24	4.26	6.00	13.8	0.28
.100	6.26	6.32	8.90	29.3	.37
.0200	13.9	14.8	20.8	136	.80
.0100	19.0	21.3	30.0	260	1.11
		$i = 0.100$			
0.0200	5.6	5.6	7 9	22.7	0.63
.0160	6.35	6.4	9.0	30	.69
.0120	7.8	8.0	11.2	45	.74
.0100	9.0	9.2	13.0	59	.77
.0050	12.2	12.7	17.9	105	1.12
.00250	17.6	19.3	27.2	219	1.45

The Shear Correction.—Viscosities of various solutions of completely neutralized and of one-third neutralized polymers were measured at the low rates of shear γ attainable in the shear viscometer. Typical results are shown in Fig. 5. The point at the highest value of γ was obtained using the Ubbelohde viscometer, and the other two points using the upper bulbs of the shear viscometer. The effect of rate of shear appeared to be linear, and at low concentrations the slope showed no definite trend with concentration.

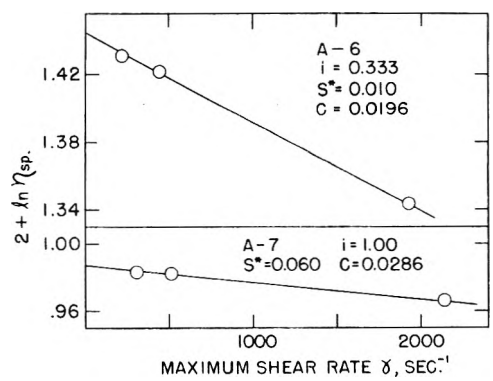

Fig. 5.—Dependence of specific viscosity on maximum rate of shear (*i.e.*, shear at capillary wall) for two solutions.

The slopes of such plots, expressed as[16,21] $\varphi =$

(21) T. G. Fox, Jr., J. C. Fox and P. J. Flory, *J. Am. Chem. Soc.*, **73**, 1901 (1951).

100 d ln $\eta_{sp}/d\gamma$, are plotted in Fig. 6 against the square of the intrinsic viscosity. While the scatter of the points precludes definition of any sort of quantitative relationship between the shear coefficient and the intrinsic viscosity, the data are nevertheless sufficiently coherent to provide a basis for empirical correction. The points for the one-third neutralized polymer indicate a somewhat greater effect than do those for complete neutralization. Accordingly, separate lines have been drawn. For $i = 1.00$

$$\varphi = 0.78 \times 10^{-5} [\eta]^2_{obs}$$

and for $i = 0.333$

$$\varphi = 1.14 \times 10^{-5} [\eta]^2_{obs}$$

The percentage corrections applicable to intrinsic viscosities determined with the Ubbelohde viscometer, and recorded in the second column of Table I, were obtained by taking the product of φ and γ. Inasmuch as the observed intrinsic viscosities have been deduced by extrapolating empirically to $c = 0$, the rate of shear γ refers to that for the solvent mixture—about 2800 sec.$^{-1}$. Intrinsic viscosities corrected in this manner are given in the third column of Table I. The influence of rate of shear at $i = 0.100$ was not investigated. Instead, the relationship for $i = 0.333$ has been assumed to hold sufficiently at the lowest degree of ionization.

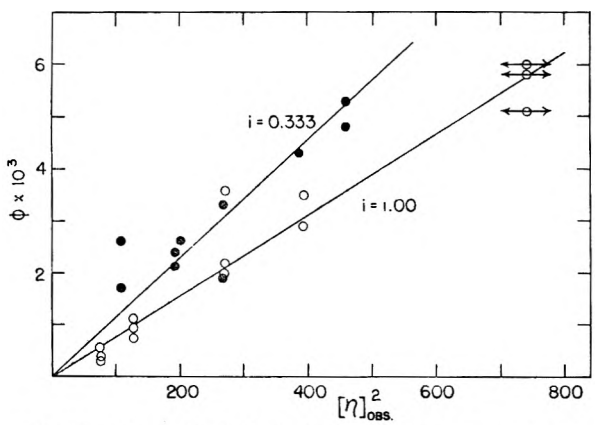

Fig. 6.—Slopes ($\phi/100$) of plots like those shown in Fig. 5 plotted against $[\eta]^2_{obs}$: ●, $i = 0.333$, fraction A-6 except for two points (at $[\eta]^2_{obs} = 194$) on A-7; ○, $i = 1.00$, fraction A-7.

Values of α^3 were calculated from equation 1 with $[\eta]_\Theta = 0.71$ for fraction A-7 (see above). The quantity $\alpha^5 - \alpha^3$ given in the next to the last column of Table I is plotted against $1/S^*$ in Fig. 7. The relationship appears to be linear within experimental error at each degree of ionization. This is in conformity with equation 2 if $C_M\psi_1(1 - \Theta/T)$ may be assumed independent of S^* and if terms in higher powers of $1/S^*$ make a negligible contribution. In the case of NaCl, $z_+ = z_-$, making the term in $(1/S^*)^2$ zero; it may readily be shown that the term in $(1/S^*)^3$ should be altogether negligible in comparison with the major ionic term (*cf. seq.*).

The term containing $C_M\psi_1(1 - \Theta/T)$, and representing the interaction between chain elements in the solvent medium, must vary to some extent as the solvent medium is changed by increasing the salt concentration. We should, in fact, expect it to decrease with increase in ionic strength owing to salting out effects. On the scale of Fig. 7, however, the contribution of this term may be presumed to be almost negligible, *i.e.*, except at the highest ionic strengths, the osmotic effect of the mobile ions far outweighs the polymer–polymer interaction. It may be significant, however, that the intercepts in Fig. 7 appear to decrease slightly with decrease in i, indicating decreased solubility of the polymer. Thus, at $i = 0.333$ experiments on the determination of the Θ-point showed that the sum of the terms on the right-hand side of equation 2 reduces to zero at $S^* = 1.245$ molar (at about 32°), giving $\alpha^5 - \alpha^3 = 0$, or $\alpha = 1$. We may conclude that $\psi_1(1 - \Theta/T)$ is then somewhat negative. The extent of the salting out contribution to the value of this quantity cannot be ascertained from the data, however.

Consideration of the slopes of the plots in Fig. 7 is deferred for later discussion.

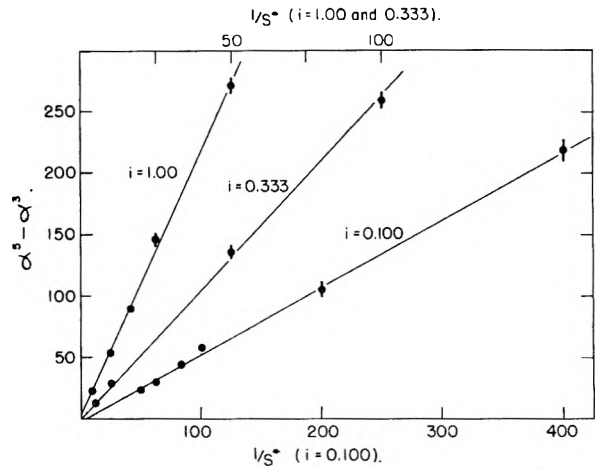

Fig. 7.—$\alpha^5 - \alpha^3$ for fraction A-7 in the presence of NaCl plotted against $1/S^*$ in accordance with equation 2. Upper scale is for $i = 1.00$ and 0.333, lower scale for $i = 0.100$.

Experiments with Various Electrolytes.—Owing to depletion of fraction A-7, it became necessary to conduct these experiments, concerned with salts of other valence types, using the fraction A-6 of slightly higher molecular weight (*ca.* 800,000). All measurements were made at the degree of neutralization 0.100 reached by adding NaOH as above. In the presence of a salt having a different cation (*e.g.*, Ca^{++}), exchange of course will occur. Since determination of the intrinsic viscosity involves extrapolation of the polymer concentration to zero while the added salt concentration remains fixed, the concentration of the ions (Na^+) introduced in neutralization vanishes in this limit, the environment of the polymer chain being dominated completely by the ions of the added salt.

Results derived in the manner previously discussed are summarized in Table II. Values of α^3 were computed from $[\eta]_\theta = 0.75$ for fraction A-6. The measurements in NaCl yielded values for α^3, and also for $\alpha^5 - \alpha^3$, slightly higher than those for A-7 at the same ionic strength (compare Table I). The differences are consistent with equation 2 in view of the slightly greater molecular weight of fraction A-6.

TABLE II

VISCOSITIES IN THE PRESENCE OF VARIOUS ELECTROLYTES AT 30° (POLYMER A-6 WITH i = 0.100)

Electrolyte	S^*	$[\eta]$ Obsd.	$[\eta]$ Corrected	α^3	$\alpha^5 - \alpha^3$
NaCl	0.0050	13.2	13.9	18.5	111
	.0025	18.6	20.7	27.6	224
Na_2SO_4	.0050	13.4	14.1	18.8	114
	.0025	18.2	20.1	26.8	213
$CaSO_4$	.0050	5.25	5.3	7.1	19.1
	.0025	8.0	8.15	10.9	43
$CaCl_2$	.0050	4.45	4.48	6.0	13.8
	.0025	6.8	6.9	9.2	31
$CuSO_4$	.0025	0.5 (±0.3)	0.5		

The results are shown graphically in Fig. 8. Those for Na_2SO_4 coincide with those for NaCl within experimental error.[22] Thus, at the same ionic strength these salts of 1:2 and 1:1 valence types are equivalent in their influence on the viscosity, and therefore on the configuration of the polymer molecule.

Calcium salts suppress the molecular expansion considerably more than do the 1:1 and 1:2 electrolytes (Table II and Fig. 8). Moreover, negative intercepts with the ordinate axis are definitely indicated, which suggests that the non-ionic interaction term assumes a more negative value in the presence of calcium ions. Possibly this may be attributed to a stronger salting out effect of the divalent cation.

Copper sulfate (Table II) was most effective in suppressing the viscosity exhibited by the polyacrylate chain. The plot of η_{sp}/c against c displayed in this case an unprecedented high slope—so great that only a rough estimate of $[\eta]$ was possible. The value of $[\eta]$ is near $[\eta]_\Theta$, or possibly somewhat less. This suggests that the system bordered on precipitation. Wall[23] has called attention to the importance of the formation of complexes between cupric ions and carboxyl groups of the poly-acrylate chains, as evidenced, for example, by the intense blue color. If the complexes involve carboxyl groups well separated in sequence along the chain, or belonging to different molecules if the concentration is sufficiently great, an explanation is at hand for both the strong dependence of η_{sp}/c on c and for the low value of the intercept ($[\eta]$).

Discussion

The observation that $[\eta]_\Theta$ for the partially neutralized polyacid in aqueous salt solution closely approximates the value of $[\eta]_\Theta$ for the non-ionized polyacid in dioxane is perhaps the most significant feature of this investigation. While it may be hazardous to generalize in advance of additional similar determinations on other polymers and with various salts, the result suggests that the chain flexibility is nearly independent of the medium and of the presence or absence of charged substituents on the poly-(acrylic acid) chain. We have assumed in arriving at this somewhat tentative conclusion that the contribution of the polyelectrolyte molecule to the viscosity depends on its size by the same relationship as holds for non-ionic polymers. While it is possible that a difference in molecular size at the two Θ-points might be obscured by a compensating difference in hydrodynamic behavior of the two molecular forms, such a possibility seems quite unlikely.[24]

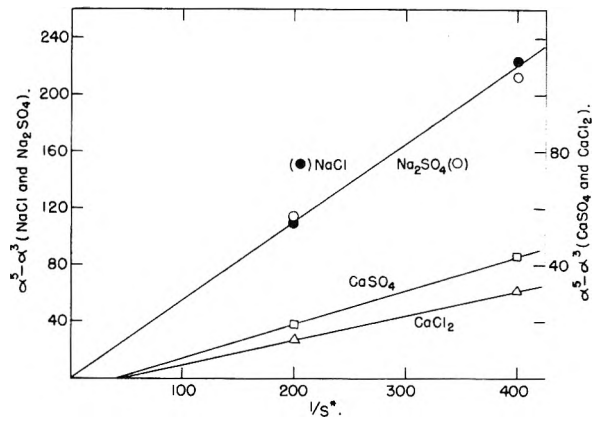

Fig. 8.—$\alpha^5 - \alpha^3$ for polymer fraction A-6 in solutions of various salts plotted against $1/S^*$. Left-hand ordinate scale is for NaCl and Na_2SO_4 solutions; right-hand scale for $CaSO_4$ and $CaCl_2$.

The slopes of the lines drawn in Figs. 7 and 8 are presented in Table III where they are compared with those calculated from the theoretical equations 2 and 3, taking $(\overline{r_0^2}/M)^{1/2} = 7.7 \times 10^{-9}$ cm. (see ref. 10), $M_u = 72$, and $M = 7.68$ and 8.0×10^5 for fractions A-7 and A-6, respectively. The observed slopes are much smaller than those calculated, but the discrepancy decreases with decrease in i. At $i = 0.100$ and in the presence of the sodium cation the discrepancy is about fivefold. Closer approach to theory might be expected at still lower degrees of ionization, which were not investigated owing to complications from ionization of the carboxyl groups with dilution. It is to be noted that the direction of the discrepancy is the same as occurs for non-ionic polymers. In the latter case, the thermodynamic parameter ψ_1 calculated from the intrinsic viscosity (*i.e.*, from α^3) is smaller than can be reconciled with the other measurements by a factor of at

TABLE III

COMPARISON OF OBSERVED AND CALCULATED SLOPES OF $\alpha^5 - \alpha^3$ AGAINST $1/S^*$

Polymer frac.	i	Salt	Slope Obs.	Slope Calcd.	Obsd./calcd.
A-7	1.00	NaCl	5.5	265	0.021
A-7	0.333	NaCl	2.6	29.4	.089
A-6	.333	NaCl	3.0[a]	30.0	.100
A-7	.100	NaCl	0.54	2.65	.20
A-6	100	NaCl	.55	3.0	.18
A-6	.100	Na_2SO_4	.55	3.0	18
A-6	.100	$CaSO_4$	.120	3.0	.040
A-6	.100	$CaCl_2$	.088	3.0	.029

[a] Based on the following intrinsic viscosities $[\eta]_{cor}$ determined at S^* = 0.040, 0.020 and 0.010 molar, respectively, 11.4, 17.7 and 24.5.

(22) In experiments not reported here, sodium acetate was found to be equivalent in its effect to NaCl at the same ionic strength.

(23) F. T. Wall, private communication.

(24) The contribution of the classical electro-viscous effect should obviously be unimportant inasmuch as the double layer thickness is small compared with the size of the macromolecule in solution.

least two[25] and perhaps by as much as seven[26]; *i.e.*, if values are used for ψ_1 which are acceptable on other grounds, calculated values for $\alpha^5 - \alpha^3$ exceed those observed to a degree which resembles the residual discrepancy in the ion effect at a low degree of ionization.

In treating[4-7] the osmotic effects of the ions, it has been assumed that the charge on the polymer chain is distributed continuously over the volume occupied by the molecule. If the units of the chain were dissected from one another, but distributed with radial density in the manner assumed (*i.e.*, Gaussian), our model would involve no more serious approximation than the replacement of the Debye–Hückel activity coefficient by unity. Since the mean ion concentrations involved generally are less than 0.1 molar, this would appear to be a reasonable first approximation. At higher degrees of neutralization, however, consecutive charged sites along the chain are considerably closer to one another than would be the case if the units were dissected and distributed in the manner mentioned. At $i = 0.333$, for example, the average distance between consecutive carboxylate ions is only about 8 Å. whereas the radius of the Debye–Hückel atmosphere is already about 10 Å., even at an ionic strength of 0.10 molar. At $i = 0.10$, the former average distance may be about 15 to 20 Å. The electrostatic attraction exerted by the chain on a gegenion consequently should be much greater, at high degrees of ionization at least, than the force between a pair of oppositely charged monovalent ions. We suggest, therefore, that the increasing discrepancy between experiment and theory as the degree of ionization increases is due to electrostatic "binding" of gegenions by the relatively large potential in the vicinity of the polymer chain. This will be manifested by depression of activity coefficients within the polymer domain and, consequently, by a diminished osmotic effect. Such effects should be greater for the divalent cation Ca^{++} than for Na^+. The suppression of the swelling of the polyelectrolyte molecule in the presence of Ca^{++} gegenion compared with its behavior in the presence of Na^+ probably can be accounted for on this basis alone. It seems unnecessary to postulate formation of complex or cross-linkages by Ca^{++} ion as proposed by Wall and Drenan[27] to account for the precipitation of polyacrylate chains in the presence of salts of alkaline earths.

There is unfortunately no suitable theory of the activity of ions in the neighborhood of an electrically charged polymer chain.[28] It is possible to show, however, that for a symmetrical added electrolyte the factor γ^2/γ^* should be included in the first ionic term in equation 2; γ and γ^* are the mean ion activity coefficients inside and outside the polymer, respectively. The constancy of slope implies that this activity coefficient factor γ^2/γ^* is insensitive to the value of S^*, although it decreases considerably with increase in i. The expected decrease in γ^2 with the increase in internal ion concentration as S^* increases may be moderated by the increased shielding of the high charge on the polymer chain. The problem obviously is in need of further theoretical study.

Throughout our experiments the mean concentration of fixed charge sites within the domain of the polymer molecule was small compared with the concentration of added electrolyte. The mean concentration $\bar{c}_2$ of polymer units within the domain of the polymer can be specified for the purposes of the present discussion in terms of an equivalent sphere, whose radius $\mathcal{R}_e$ may be taken[29] equal to $(1/2)(\overline{r^2})^{1/2} = (\alpha/2)(\overline{r_0^2})^{1/2}$. With $(\overline{r_0^2})^{1/2} = 6.8 \times 10^{-6}$ cm. for the fraction A-7 (ref. 10), we obtain $\bar{c}_2 = 0.11/\alpha^3$ moles per liter. Hence, the ratio of the mean concentration of charge sites to the external ionic strength is estimated in this manner to be

$$i\bar{c}_2/S^* = 0.11(i/\alpha^3 S)^* \qquad (6)$$

Values of the quantity in parentheses, given in the last column of Table I, yield ratios in the range from 0.03 to 0.18 under the conditions of the various experiments in which NaCl was used. Allowance for the depressed ion activities within the molecule, as explained above, would lead to lower values for the ratio of charge sites to external ionic strength (*i.e.*, the effective value of i is lower than the actual, especially for larger i).

Consideration of the Donnan equilibrium relation shows at once that the ratio of the mean Na^+ ion concentration within the polymer domain to that outside ranged from 1.015 to 1.09 in our experiments. The corresponding maximum Donnan potential ψ is only about 2 mv. If we accept as a model the equivalent sphere of uniform density used above for calculating $\bar{c}_2$, and consider further that it is a conducting one whose net charge will therefore be concentrated at its surface, the net charge $q = D\psi\mathcal{R}_e$ corresponding to this potential would amount to about ten electronic charges; *i.e.*, the net charge would correspond at most to less than 1% of the charge sites. Smaller estimates of the Donnan potential and of the net charge would result if account were taken of the activity coefficient.

While equation 2 has been derived[3,5] for a continuously varying distribution of polymer density, without resorting to the uniform sphere model temporarily adopted above, its convergence depends also on the ratio $i/\alpha^3 S^*$. The factor $(z_- - z_+)$ in the second ionic term of equation 2 is zero for NaCl and unity for Na_2SO_4; the corresponding valence factor in the third ionic term is zero for Na_2SO_4 and $-1/2$ for NaCl. (The mere fact that results for Na_2SO_4 are superimpossible on those for NaCl indicates, therefore, that contributions of higher ionic terms are negligible). Considering the case of Na_2SO_4, the ratio of the second to the first ionic term according to equations 2 and 3 should be

$$\rho_{21} = (2/\pi)^{3/2} \times 3^{1/2} \times 10^3(\overline{r_0^2}/M)^{-3/2} (\mathbf{N}M_u)^{-1}(i/M^{1/2}S^*\alpha^3) \qquad (7)$$

(25) W. R. Krigbaum and P. J. Flory, *J. Am. Chem. Soc.*, **75**, 5254 (1953); W. R. Krigbaum, *ibid.*, in press.

(26) A. R. Shultz and P. J. Flory, *ibid.*, **75**, 3888 (1953).

(27) F. T. Wall and J. W. Drenan, *J. Polymer Sci.*, **7**, 83 (1951).

(28) R. M. Fuoss, A. Katchalsky and S. Lifson, *Proc. Natl. Acad. Sci. U. S.*, **37**, 579 (1951), and T. Alfrey, P. W. Berg and H. Morawetz, *J. Polymer Sci.*, **7**, 543 (1951), have treated the case of a solution of parallel charged rods, infinite in length, and surrounded by gegenions only. Their treatment is inapplicable to solutions containing an additional electrolyte.

(29) P. J. Flory, *J. Chem. Phys.*, **17**, 303 (1949).

substituting $(\overline{r_0^2}/M)^{1/2} = 7.7 \times 10^{-9}$ cm. (see ref. 10), $M_u = 72$, and $M = 8.0 \times 10^5$, we obtain for fraction A-6

$$\rho_{2i} = 0.050(i/S^*\alpha^3) \qquad (7')$$

Introduction of the actual values for $i/S^*\alpha^3$ leads to the conclusion that the second ionic term should be quite negligible throughout our experiments. Allowing for the depressed internal activities, it should be even smaller than this calculation indicates. The third ionic term (for NaCl) is of course altogether insignificant.

With further decrease in ionic strength the quantity $i/\alpha^3 S^*$, and therefore the concentration ratio $i\bar{c}_2/S^*$ also, may be increased appreciably beyond the values prevailing in our experiments. By extrapolation of observed relationships we may arrive at an estimate of the range over which the present treatment may be expected to hold. When α^5 is large, the first term (non-ionic) in equation 2 is negligible and $\alpha^5 > > \alpha^3$, hence

$$\alpha^5 \cong B/S^* + \ldots. \qquad (8)$$

where B is chosen to represent the observed slope in Fig. 7 as recorded in Table III. Neglecting higher terms in the series and employing this relation to eliminate α^3, we have

$$i/\alpha^3 S^* \cong iB^{-3/5}(S^*)^{-2/5} \qquad (9)$$

from which the ratio of interest is seen to vary with an inverse small power of the ionic strength. From a physical point of view, the molecule responds to a decrease in external ionic strength by expanding, thereby reducing its internal average concentration $i\bar{c}_2$ of charge sites. The change in the ratio of single ion concentrations inside and outside the domain is thus greatly reduced, as is also the associated Donnan potential and net charge. In other words, over a wide range in S^*, the randomly coiled polymer molecule alters its configuration in such a manner as to avoid a large mobile ion concentration ratio between the domain and the surroundings.

To pursue the matter further, consider the case of one-third neutralization. Upon inserting the experimental value for B—about 2.8, see Table III—in equation 8, consistency demands use of the effective value for i. The results indicate a correction factor of the order of $^1/_3$, hence we may take $i = 0.10$, giving

$$(i/\alpha^3 S^*)_{\text{effective}} = 0.055(S^*)^{-2/5}$$

At an ionic strength of 10^{-5} molar this ratio becomes 5.5, and higher ionic terms (see equation 7') should begin to assume importance; the series still converges fairly rapidly, however. The mean internal concentration of charged sites on the polymer is then about one-half the external ionic strength, and the ratio of the single ion activities is in the neighborhood of 1.3. The net charge remains a small fraction of the total charged sites on the chain, therefore.

Under these same conditions we calculate from equation 8 that $\alpha \cong 12$. The unperturbed end-to-end distance, $(\overline{r_0^2})^{1/2} \cong 675$ Å., for polymer fraction A-7 is about 2.5% of its fully extended length, $r_{\max} = 2.7 \times 10^4$ Å. Hence, the estimated ratio $(\overline{r^2})^{1/2}/r_{\max}$ for $i = 0.33$ and $S^* = 10^{-5}$ is *ca.* 0.30. With further expansion we may expect incipient failure of the spherically symmetric model, both in regard to the treatment of intramolecular interactions (equation 2) and the hydrodynamic behavior[30] (equation 1). Thus, it appears that deviation from average spherical symmetry assumed in deriving equation 2, rather than convergence of the series or failure of the Donnan approximation (which is tantamount to occurrence of an appreciable net charge), sets a theoretical limit on the application of this relation to polyelectrolyte molecules.

At $i = 0.33$ and $S^* = 10^{-5}$ molar the estimated α^3 is *ca.* 1.8×10^3, corresponding to an intrinsic viscosity of 1.3×10^3 deciliters/g.! An intrinsic viscosity of this magnitude probably never has been measured for any polymer. The rate of shear correction doubtless would pose a serious obstacle to quantitative determination by any presently known method—an obstacle more formidable than limitations of the theory as discussed above.

The polyelectrolyte molecule at infinite dilution in the absence of added electrolytes has been the subject of much discussion.[31] Under this circumstance the molecule is considered to be fully extended and bereft of gegenions. Presuming the solvent to be water, these considerations are open to serious objections inasmuch as the minimum ionic strength is then 10^{-7} molar. Extending the foregoing estimates to this limit, we may expect significant deviation from Gaussian chain statistics, but *by no means full extension of the chain.* Moreover, retention of ions of opposite charge may still be expected to dominate the scene, although these ions will (at infinite dilution) consist of one or the other of the ions formed by dissociation of the solvent; *i.e.*, hydrolysis will occur with the formation of the poly acid or base, which, if it is a strong acid or base, may yet be highly ionized. The highly charged polyelectrolyte molecule without the preponderance of its complement of gegenions nearby, *i.e.*, within a distance small compared with the molecular dimension if the chain length is reasonably great, is experimentally unrealizable—in water at any rate.

It follows also that at very low ionic strengths, or in the total absence of added electrolyte, the polyelectrolyte configuration may be profoundly affected by mere traces of ions, and in particular by polyvalent ions of opposite charge. Recent results[32,33] indicating a decrease in the reduced viscosities η_{sp}/c of polylelectrolytes with dilution in the absence of salt should be examined critically from the point of view of this possibility.

(30) S. Newman and P. J. Flory, *J. Polymer Sci.*, **10**, 121 (1953).

(31) See, for example, S. Lifson and A. Katchalsky, *ibid.*, **13**, 43 (1954).

(32) J. A. V. Butler and B. E. Conway, *Nature*, **172**, 153 (1953); *J. Polymer Sci.*, **11**, 277 (1953).

(33) H. Eisenberg and J. Poyuet, *ibid.*, **13**, 85 (1954).

THE DEPENDENCE OF BOND ENERGY ON BOND LENGTH

BY LINUS PAULING

Contribution No. 1900 from the Gates and Crellin Laboratories of Chemistry, California Institute of Technology, Pasadena, Calif.

Received April 19, 1954

It is suggested that in a series of similar bonds the bond energy is proportional to the reciprocal of the equilibrium interatomic distance (the bond length). This relation is supported by experimental values for some sequences, such as O_2, S_2, Se_2, Te_2. Application of the relation to other sequences is shown to support the values 170 kcal./mole for the heat of dissociation of N_2 and 139 kcal./mole for the heat of sublimation of carbon. The dependence of bond energy on other factors, including character of bond orbitals, energy of resonance of bonds among alternative positions, and repulsion of unshared electron pairs on the bonded atoms, is discussed.

No generally applicable empirical system of bond energies has been formulated. The difference of the energy of a single bond between unlike atoms, A–B, and the average of the single bonds between the corresponding like atoms, $^1/_2$(A–A + B–B), can be calculated approximately from the difference in electronegativities of the atoms.[1] The magnitude of the energy of a single bond depends upon the hybrid character of the bond orbitals, and it has been suggested that it is approximately proportional to the product of the bond strengths S of the orbitals, where S represents the concentration of the orbital in the bond direction, as determined by the angular wave functions.[2]

Let us tabulate the factors that might be expected to be important in determining bond energies.

1. The type of bond as determined by the number of electrons involved—whether it is a single bond, a double bond, a triple bond, a one-electron bond, a three-electron bond, etc.
2. The atomic reference state—bond-energy values should in general be referred to the valence states of atoms, rather than to their normal states.
3. The angular part of the bond orbitals; the bond energy may be approximately proportional to the product of the bond strengths S, as mentioned above.

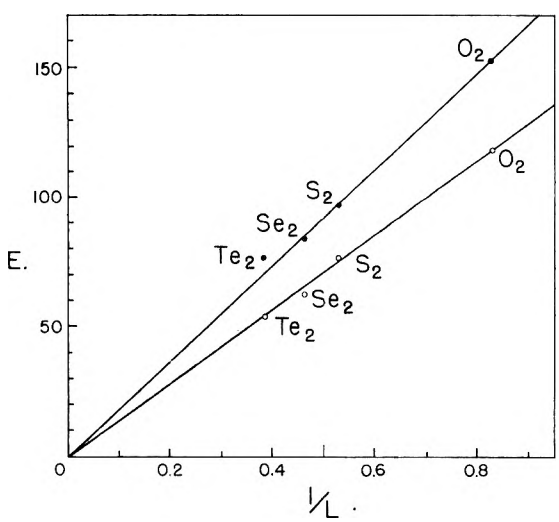

Fig. 1.—Bond energies for O_2, S_2, Se_2 and Te_2, plotted against the reciprocal of bond length. The open circles are bond energies referred to the normal states of the atoms, and the solid circles are bond energies referred to the valence states.

4. The radial part of the bond orbitals; the bond energy might be expected to vary both with the total quantum number and with the equilibrium internuclear distance.
5. The repulsion of unshared electron pairs on the bonded atoms.
6. The energy of resonance of bonds among alternative positions in the molecule or crystal.

Bond Energy and Bond Length

We shall discuss first the dependence of bond energy on equilibrium internuclear distance and total quantum number.

The potential-energy terms in the Hamiltonian function are coulombic, and hence inversely proportional to distance, and it might hence be expected that the bond energy for a sequence of molecules with constant bond type would be inversely proportional to the equilibrium internuclear distance.

The molecules O_2, S_2, Se_2, and Te_2 constitute a sequence in which the bond type may be expected to be constant. The normal molecular state is $^3\Sigma$, involving eight bonding electrons, which may be described as forming a single σ bond plus two three-electron π bonds. Values of the bond energy D_0 are given by the points close to the lower line in Fig. 1, plotted against the reciprocal of the equilibrium internuclear distance L. All values of bond energies are enthalpies of dissociation as given in the Bureau of Standards Circular[3] unless otherwise stated. For O_2, S_2, Se_2, and Te_2 the values of D_0 and L are those shown in Table I. It is seen that the points lie close to a straight line passing through the origin.

TABLE I

ENERGY AND BOND-LENGTH VALUES FOR O_2 AND RELATED MOLECULES

D_0 = dissociation energy to normal states of atoms, in kcal./mole. E = dissociation energy to valence states, in kcal./mole.

	D_0	E	L, Å.	Valence-state energy, kcal./mole	
O_2	118.3	152.9	1.208	O	17.3
S_2	76.6	96.8	1.89	S	10.1
Se_2	62.9	83.7	2.16	Se	10.4
Te_2	54.2	77.2	2.59	Te	11.5

It is preferable to refer the bond energies to the valence states of the atoms. The valence state of oxygen has been evaluated as 17.3 ± 1.2 kcal./mole.[4] This value is 38.3% of the separation of

(1) L. Pauling, *J. Am. Chem. Soc.*, **54**, 3570 (1932).
(2) L. Pauling, *ibid.*, **53**, 1367 (1931).
(3) "Selected Values of Chemical Thermodynamic Properties," Circular of the Bureau of Standards 500, U. S. Government Printing Office, 1952.
(4) L. Pauling, *Proc. Natl. Acad. Sci.*, **35**, 229 (1949).

the normal state, $1s^2 2s^2 2p^4\ ^3P$, of the oxygen atom, and the first excited state, $1s^2 2s^2 2p^4\ ^1D$. Values of the valence-state energy of sulfur, selenium, and tellurium may be estimated by the assumption that the same relation exists with $^1D - {}^3P$. These values are given in Table I, as well as the values of the bond energy E referred to the valence state. The latter values are plotted in Fig. 1 as the points close to the upper line. It is seen that for these values also, except for Te_2, there is good proportionality to the reciprocal of the bond length. We assume from this result and the results of similar considerations with other sequences that in general the dependence of bond energy on bond length is an inverse proportionality in case that other factors remain constant.

Bond Energies for Nitrogen and Phosphorus

Values of bond energies and bond lengths for N_2, P_2, As_2, Sb_2, and Bi_2 are given in Table II. For both N_2 and P_2 there has been uncertainty about the bond energy, and two values are given in the table for each of these molecules. The valence-state energy of nitrogen has been evaluated as 42.4 kcal./mole.[5] This value is 77.5% of the separation of the normal spectroscopic state $1s^2 2s^2 2p^3\ ^4S$ and the first excited state $1s^2 2s^2 2p^3\ ^2D$, and values for the valence-state energies of phosphorus, arsenic, antimony, and bismuth as calculated by the assumption of the same relation are given in Table II.

TABLE II

ENERGY AND BOND-LENGTH VALUES FOR N_2 AND RELATED MOLECULES

	D_0	E	L, Å.	Valence-state energy, kcal./mole	
N_2	170	255	1.094	N	42.4
	225	310			
P_2	95.0	150	1.89	P	27.5
	116.5	171			
As_2	91.7	146.1	2.08	As	27.2
Sb_2	69.6	123.8	2.48	Sb	27.1
Bi_2	40.0	124	2.68	Bi	42

It is seen in Fig. 2 that the low bond-energy values for P_2 and N_2 lie near a straight line through the origin and the values of As_2 and Sb_2, when plotted against the reciprocals of the bond lengths. The circles near the lower line show the bond energies referred to the normal state, and those near the upper line the bond energies referred to the valence state. The squares in Fig. 2 represent the high proposed values for P_2 and N_2, referred to the normal state of the atoms; they lie about 25% above the values predicted on the assumption of proportionality to the reciprocal of the bond length.

It is interesting that the slope of the line representing bond energy relative to the valence state is 279 kcal. A/mole in Fig. 2, and 185 kcal. A/mole in Fig. 1, the ratio being 3/1.99. Inasmuch as the bond in N_2 and related molecules is a triple bond, and that in O_2 and related molecules, which may be described as a single bond plus two three-electron bonds, is a kind of double bond, the approximation of this ratio to 3/2 is satisfying.

(5) L. Pauling and W. F. Sheehan, Jr., *Proc. Natl. Acad. Sci.*, **35**, 359 (1949).

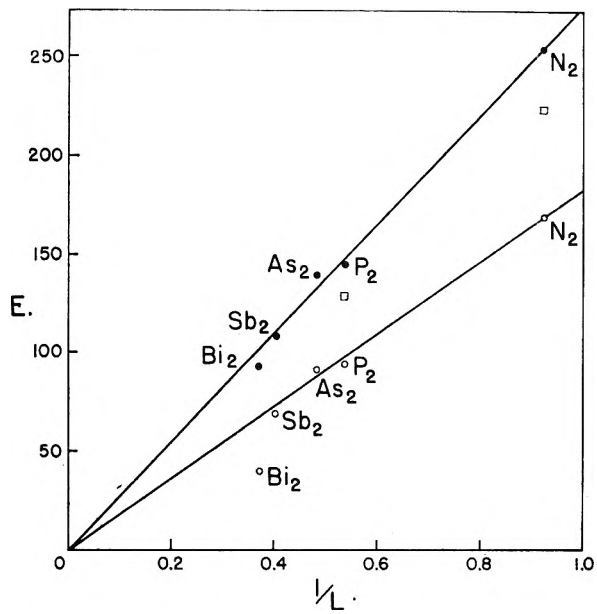

Fig. 2.—Bond energies for N_2, P_2, As_2, Sb_2 and Bi_2, plotted against the reciprocal of bond length. The open circles are bond energies referred to the normal states of the atoms, and the solid circles are bond energies referred to the valence states. The squares represent the higher of alternative values proposed for N_2 and P_2, referred to the normal states of the atoms.

Tetrahedral Bonds in Diamond and Related Crystals

In the discussion of carbon and its congeners with the diamond structure, silicon, germanium, and gray tin, it is necessary to refer the bond energies to the valence states of the atoms, which lie far above the normal states in energy. The valence state of carbon has been discussed in detail by Van Vleck[6] and Voge.[7] Van Vleck showed that the wave function for a quadrivalent carbon atom with tetrahedral symmetry can be formulated by hybridization of seven states of the carbon atom, the states ^3P and ^1D based upon the configuration $1s^2 2s^2 2p^2$, the states ^5S, ^3D, and ^1D based upon $1s^2 2s 2p^3$, and the states ^3P and ^1D based upon $1s^2 2p^4$. The ideal quadrivalent structure lies 161 kcal./mole above the normal state of the atom. Voge found that in methane the carbon atom is represented as a hybrid of this ideal quadrivalent structure and the bivalent structure, with the zero-valent structure also making a small contribution. The effective valence-state energy is calculated to be about 100 kcal/mole; that is, it is close to the promotion energy to the spectroscopic state $1s^2 2s^2 2p^3\ ^5S$, which lies 96.0 kcal./mole above the normal state. The quadrivalent carbon atom is not purely quadrivalent in the quantum-mechanical sense; instead, if we accept Voge's calculations, it involves resonance between the structure with four bonding electrons, which contributes about 63%, and the six structures with two bonding electrons and an unshared electron pair in the L shell, which together contribute most of the remaining 37%. In the following discussion we shall refer to an atom with a

(6) J. H. Van Vleck, *J. Chem. Phys.*, **1**, 177 (1933); **1**, 219 (1933); **2**, 20 (1934).

(7) H. H. Voge, *ibid.*, **4**, 581 (1936); **16**, 984 (1948).

hybrid valence state such as that described by Voge for carbon in methane as a quadrivalent atom, and shall assume that the valence-state energy of quadrivalent carbon is 96.0 kcal./mole, the promotion energy to the ^5S state.

Values of the enthalpy of sublimation, the equilibrium internuclear distance, the valence-state energy, and the bond energy referred to the valence state are given for carbon and its congeners in Table III. The spectroscopic states ^5S have not been observed for silicon, germanium, and tin; the values of the valence-state energy given in the table have been calculated from the value 96.0 kcal./mole for carbon by the assumption of proportionality to the first ionization potentials of the atoms.

TABLE III

ENERGY AND BOND-LENGTH VALUES FOR C, Si, Ge AND Sn

S = heat of sublimation to normal states of atoms, in kcal./mole. E = single-bond energy referred to valence states, in kcal./mole.

	S	E	L, Å.	Valence-state energy, kcal./mole
C	139	117.5	1.544	96.0
	170	133		
Si	88.0	78.7	2.346	69.4
Ge	78.4	72.8	2.445	67.2
Sn	71	67	2.80	62.5

In Fig. 3 values of the bond energy referred to the valence state are plotted against the reciprocal of the bond lengths. It is seen that a straight line through the origin with slope 182 kcal. A/mole passes very close to the points for tin, germanium, and silicon, and the lower of the two points for carbon. This point corresponds to the value 139 kcal./mole for the heat of sublimation of carbon, and the upper point, represented in Fig. 3 by a square, to the value 170 kcal./mole. The question of the choice between these two values has not yet been finally settled, and the foregoing argument provides additional support for the low value.

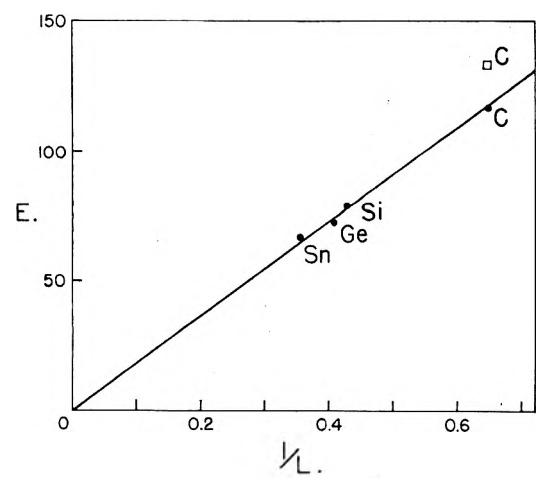

Fig. 3.—Bond energies for crystalline C, Si, Ge, and Sn, referred to the valence states of the atoms. The square corresponds to the higher of the two proposed values for the heat of sublimation of carbon.

The Alkali and Alkaline Earth Metals

The alkali metals form gaseous molecules Li_2, Na_2, K_2, Rb_2, and Cs_2, with dissociation energies D_0 as given in Table IV. The bonds involved hybrid orbitals with a large amount of s character and a small amount of p character. Evaluation of the amounts of p character and of the bond energies for pure s bonds has been reported in an earlier paper.[8] If it is assumed that the bond-forming power of an orbital is proportional to its concentration in the bond direction, as measured by the angular dependence of the wave function, and that the bond energy between like atoms is proportional to the square of this bond strength S, the bond energy for pure s bonds and the amount of p character of the bond orbitals can be evaluated by solution of a secular equation, with use of the s-p promotion energy. The dissociation energies of the molecules vary from 26.8 kcal./mole for Li_2 to 10.4 kcal./mole for Cs_2, and the calculated bond energies for pure s bonds, E, from 15.6 kcal./mole to 7.4 kcal./mole, as given in Table IV. The amount of p character is significantly larger for Li_2, 14.0%, than for the other four, 5.0 to 6.8%.

TABLE IV

ENERGY AND BOND-LENGTH VALUES FOR MOLECULES OF ALKALI METALS

D_0 = dissociation energy to normal states of atoms, in kcal./mole. E = calculated bond energy for pure s bonds, in kcal./mole.

	D_0	E	L, Å.	p-character, %
Li_2	26.8	15.6	2.67	14
Na_2	17.9	12.2	3.08	6.8
K_2	11.8	8.4	3.92	5.5
Rb_2	11.2	8.0	4.19	5.0
Cs_2	10.4	7.4	4.57	5.5

Values of the s-bond energy for the five molecules are shown in the lower part of Fig. 4 as a function of the reciprocal of the bond lengths. There is an approximate linear relationship. The slope of the straight line shown, passing through the point for Na_2, is 38 kcal. A/mole. If the proportionality of

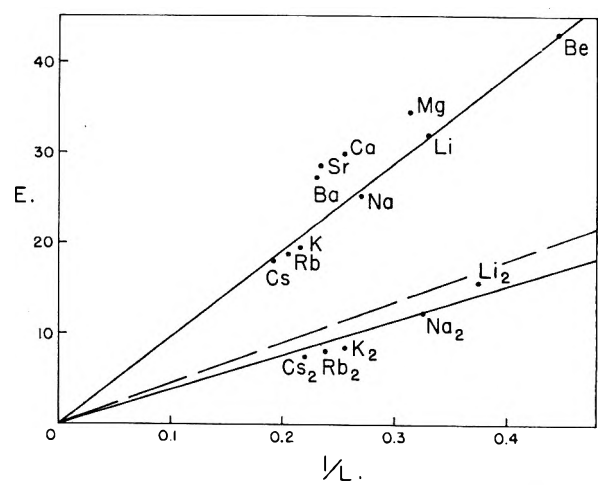

Fig. 4.—The points in the lower part of the figure represent the values of pure s-bond energy of Li_2, Na_2, K_2, Rb_2, and Cs_2, calculated from the dissociation energies of the molecules by correcting for p character of the bond orbitals. The circles near the upper line represent the energy of resonating s bonds in the alkali metals and alkaline earth metals, obtained by correcting for the p character of the bond orbitals.

(8) L. Pauling, *Proc. Roy. Soc.* (*London*), **A196**, 343 (1949).

bond energy to the square of the bond strength, S^2, were valid, a slope 45.5 would be predicted for bonds between s orbitals from the value 182 for the sp^3 bonds in diamond. The line corresponding to this predicted slope is the dashed line in the figure. We conclude that there is rough substantiation of the proportionality between bond energy and S^2.

The results of similar calculations for the crystalline alkali metals and alkaline earth metals are given in Table V, taken from the earlier paper.[8] Values of the bond energy E for resonating s bonds are plotted in Fig. 4 against the reciprocal of the internuclear distance in the metals. It is seen that a straight line through the origin and the point for beryllium passes close to the points for all five of the alkali metals. The values for magnesium, calcium, strontium, and barium lie about 5 kcal./mole above this line. It seems not unlikely that the bonds in these metals have also a significant amount of d character, and that if the correction for d character were to be made the calculated values of the s-bond energy would lie near the line for the other metals.

TABLE V

CALCULATED S-BOND ENERGY AND BOND-LENGTH VALUES FOR ALKALI AND ALKALINE EARTH METALS

	E, kcal./mole	L, Å.		E, kcal./mole	L, Å.
Li	32.0	3.04	Be	43	2.25
Na	25.3	3.72	Mg	34.5	3.20
K	19.5	4.62	Ca	30.0	3.94
Rb	18.7	4.87	Sr	28.6	4.30
Cs	18.1	5.24	Ba	27.3	4.34

The slope of the line for resonating s bonds is 97 kcal. A/mole. We conclude, in agreement with the earlier discussion,[8] that the energy of a resonating bond in the alkali and alkaline earth metals is somewhat more than twice the energy of a non-resonating bond.

The Transition Metals

Some information about the valence of the transition metals may be obtained by consideration of the bond energies. There has been argument, for example, about whether the copper atom in copper metal should be assigned the valence 1, or a higher value. The normal state of the copper atom is $3d^{10}4s\ ^2S$, and if the element were univalent in the metal the bonds formed would be essentially s bonds. The heat of sublimation of copper is 81.5 kcal./mole, which corresponds to a bond energy, if the atoms are univalent, of 163 kcal./mole. Multiplying by the bond length, 2.551 Å., we obtain the value 416 kcal. A/mole for the EL product. This value is over four times the expected value, 97 kcal. A/mole, given above for a resonating s bond. We accordingly conclude that the assumption of univalence of copper in the metal is incorrect.

In the resonating valence-bond theory of metals[8] copper is assigned the valence 5.5, which corresponds to the configuration $3d^{7.75}4s4p^{2.25}$. The promotion energy of the copper atom to the state $3d^94s4p\ ^4P$ is 113.0 kcal./mole. If the assumption is made that the same promotion energy is needed to raise additional electrons from the 3d level to the 4p level, the valence-state energy for the 5.5-valent state is 246 kcal./mole, and the energy per bond is 119 kcal./mole. This leads to the value 304 kcal. A/mole for the EL product, which, for resonating dsp bonds, is not unreasonable in comparison with the value 182 kcal. A/mole for non-resonating sp^3 bonds. We conclude that the proposed metallic valence 5.5 for copper is compatible with the energy of the crystal.

Similar bond-energy values are found also for other transition metals for which spectroscopic values of promotion energies are at hand. Scandium, for example, has heat of sublimation 93 kcal./mole and promotion energy, from the normal state $3d\text{-}4s^2\ ^2D$ to the trivalent state $3d4s4p\ ^4S$, 45.0 kcal./mole. These values correspond to the bond energy 92 kcal./mole, and, with bond length 3.21 Å., to the value 295 kcal./mole for the EL product.

The Bond Strengths of Hybrid Orbitals

The suggestion was made in 1931 that the quantity S, proportional to the value of the angular part of the wave function of a bond orbital along the axis of the bond, may be taken as a measure of the bond-forming power of the orbital, and that the energy of a bond is roughly proportional to the products of the strengths S of the two orbitals involved in the bond. This argument leads to the conclusion that tetrahedral sp^3 bond orbitals should form bonds four times as strong as those formed by s orbitals, and that the best dsp hybrid bond orbitals should form bonds nine times as strong as those formed by s orbitals. It has been shown in the preceding paragraphs that the ratio of bond energies of sp^3 bonds and s bonds is approximately four, in agreement with the simple argument based upon the bond strength S.

However, as has been pointed out by Craig, *et al.*, from consideration of overlap integrals,[9] hybrid bond orbitals with some d character seem not to form such strong bonds as is predicted for them by the simple function S. For example, the spd resonating bonds in scandium have been calculated above to have the function EL = 295 kcal. Å/mole. This is approximately equal to the value 301 kcal. A/mole found for aluminum, with heat of sublimation 75.0 kcal./mole, promotion energy to $3s3p^2\ ^4P$ = 82.8 kcal./mole, and bond length 2.858 Å. The increase of the value over the value 182 for non-resonating sp^3 bonds may be attributed largely to the resonance energy of the bonds among the twelve alternative positions in the closest packed crystals, and the conclusion may be drawn that the dsp hybrid bond orbitals in scandium have not much greater bond-forming power than the sp^2 bond orbitals in aluminum, after correction is made for the bond length.

The energy of a bond is determined by the product of the two orbitals throughout the region between the two atomic nuclei, and not just along the internuclear axis. The bond strengths S = 1, 1.73, and 2.24 calculated for s, p, and d orbitals along the axis maximize the differences in the values of the orbitals. It might be estimated that the region of significance for the overlapping of the bond orbitals extends as far as 45° from the bond di-

(9) D. P. Craig, A. Maccoll, R. S. Nyholm, L. E. Orgel and L. E. Sutton, *J. Chem. Soc.*, 332 (1954).

rection, and that an average region is at 30°. The relative magnitudes of s, p, and d orbitals in the direction 30° from the bond axis are 1:1.50:1.40; that is, because of the rapid decrease in its value with increasing angle from the bond direction the d orbital becomes smaller than the p orbital at 30° from the bond axis, and it might well be that the bond-forming power of a d orbital is less than that of a p orbital. Use of the value of the bond orbital in a direction 30° from the bond axis to calculate the bond strength S of the orbital does not make much change in the calculations involving only s and p orbitals; for example, the bond strength of a tetrahedral sp^3 orbital is calculated to be 1.80 in this way, rather than 2.00; but it makes a large change in calculations involving d orbitals.

The Repulsion of Unshared Electron Pairs

It has been pointed out by Pitzer[10] that bonds between light atoms are seriously affected by the repulsion of unshared pairs of electrons on the adjacent atoms, and that this repulsion is much greater for atoms of the first row in the periodic table than for heavier atoms. The effect of this repulsion is clearly evident in the values of EL for the halogen molecules. These values, calculated with the enthalpies of dissociation 38, 57.8, 46.1, and 36.2 kcal. mole for F_2, Cl_2, Br_2, and I_2, respectively, and the bond lengths 1.48, 1.989, 2.284, and 2.667 Å., are 56, 115, 105, and 97 kcal. A/mole. The predicted value of EL for p bonds is 136, which is $^3/_4$ times the value 182 for sp^3 bonds.

The example of the halogens, in which the bond energy is greatly affected by repulsion of unshared electron pairs, shows that care must be taken in the application of the rule of the constancy of the product EL to a set of molecules which might be assumed to contain bonds of the same type.

(10) K. S. Pitzer, *J. Am. Chem. Soc.*, **70**, 2140 (1948).

THE VAPOR PRESSURES OF *d*- AND *dl*-DIMETHYL TARTRATE[1]

BY THOMAS I. CROWELL AND GEORGE L. JONES, JR.

Cobb Chemical Laboratory, University of Virginia, Charlottesville, Virginia

Received March 10, 1954

The vapor pressure curves of *d*- and *dl*-dimethyl tartrate, obtained by the effusion method in the temperature range 30–92°, were found to coincide at the melting point of *dl*-dimethyl tartrate, indicating that no racemic compound exists in the liquid state. Molar heats of vaporization, sublimation and fusion were calculated from the vapor pressures.

The possibility of the existence of racemic compounds in the liquid state or in solution has led to a variety of physical measurements. Vapor pressure data are lacking; however, if compound formation occurs in a liquid mixture of enantiomers, it should be detectable by vapor pressure measurements near the melting point. In this paper, the vapor pressure of *d*-dimethyl tartrate, m.p. 48°, is compared with that of the racemic compound *dl*-dimethyl tartrate, m.p. 89°.

Experimental

Materials.—*d*-Dimethyl tartrate was prepared by refluxing one part commercial tartaric acid with two parts methanol for seven hours as in the preparation of the diethyl ester.[2] The solvent was rapidly distilled off, an amount of fresh solvent equal to the original amount added, and the solution refluxed further for seven hours. After the solvent was again removed, the viscous liquid was vacuum-distilled at about 5 mm., the 130–150° fraction being retained. The very hygroscopic ester was recrystallized from absolute ethanol and dried in a vacuum oven at 60°; m.p. 48°; assay (neutral equivalent) 100.0 ± 0.1%. The allotropes melting at 50 and 61.5° were not encountered in this work.

dl-Tartaric acid was prepared by racemization of commercial *d*-tartaric acid.[3] The purified *dl*-tartaric acid (one part) was refluxed with methanol (10 parts) and a little hydrochloric acid, for eight hours.[4] The ester was purified as described above; m.p. 89°; assay 100.0 ± 0.1%; $[\alpha]^{25}D$ 0.00°.

Procedure.—Vapor pressure was measured by effusion from a brass cylinder 2 cm. in diameter and 3 cm. high. The screw cap contained a window of 0.05-mm. copper in which was bored a 0.79-mm. hole. About 2 g. of the compound was placed in this vessel and the cap was screwed down on a lead washer and sealed with a non-volatile wax. The vessel was placed on a lead block in a glass tube which was immersed in the oil thermostat (±0.1°) and evacuated to 10^{-4} mm. or better. After outgassing, the vessel was accurately weighed and the loss of sample by effusion was determined. The time necessary to build up maximum vacuum (30–45 seconds) was usually rendered negligible by the length of the run.

The method was checked by measuring the vapor pressure of naphthalene: the value of 0.1184 mm. obtained at 25.9° differs from that of 0.1169 mm. calculated from the equation of Sears and Hopke[5] by 1.3%. The average deviation from the mean of seven runs was 0.6%.

Results

The vapor pressures, calculated by the equation of Knudsen,[6] are shown in Table I. Each value is the mean of six determinations. The average deviation is less than 1% in all cases except two, where it is 1.3%.

A plot of $\log p$ *vs.* $1/T$ is shown in Fig. 1. The vapor pressure of solid *dl*-ester is lower than that of solid *d*-ester: the racemic crystal is the more stable with respect to both vaporization and fusion. Equations were derived from the data of Table I by least squares

$$d\text{ (solid)}: \log p = -5903.2/T + 16.6104 \quad (1)$$

$$d\text{ (liquid)}: \log p = -3993.1/T + 10.7296 \quad (2)$$

$$dl\text{ (solid)}: \log p = -5941.3/T + 16.1268 \quad (3)$$

Simultaneous solution of (1) and (2) gives a calculated melting point of 51.6° for the *d*-ester; the

(1) From the dissertation of George L. Jones, Jr., University of Virginia, 1952.

(2) T. M. Lowry and J. O. Cutter, *J. Chem. Soc.*, **121**, 533 (1922).

(3) "Organic Syntheses," Coll. Vol. I, John Wiley and Sons, Inc., New York, N. Y., 1941, p. 497.

(4) T. S. Patterson and C. Dickinson, *J. Chem. Soc.*, **79**, 280 (1901).

(5) G. W. Sears and E. R. Hopke, *J. Am. Chem. Soc.*, **71**, 1632 (1949).

(6) M. Knudsen, *Ann. Physik*, **28**, 999 (1909); **29**, 179 (1909).

TABLE I

VAPOR PRESSURES OF DIMETHYL TARTRATES

t, °C.	$10^3 p$, mm.	t, °C.	$10^3 p$, mm.
d-Dimethyl tartrate (s)		*dl*-Dimethyl tartrate (s)	
35.4	3.02	42.5	1.98
40.4	6.16	49.5	5.33
44.2	10.23	55.8	11.65
		65.6	39.6
d-Dimethyl tartrate (l)		72.9	90.0
49.5	22.6	85.2	275
55.8	39.1		
63.3	73.5	*dl*-Dimethyl tartrate (l)	
85.2	381	91.8	621
91.8	625		

observed value (experimental section) was 48°. The vapor pressures of the *d*- and *dl*-ester are equal, within experimental error, at 91.8°, where both are liquid. The intersection of the curves given by (2) and (3) is at 87.8°; the observed value of the melting point of the *dl*-ester is 89°. Since both esters boil at about 280° at atmospheric pressure, the curves may be assumed to coincide at temperatures above 89°.

These relationships between the three vapor pressure curves are just the ones expected of a system of two enantiomers in which the solid racemic crystal is more stable than the crystal of one isomer, but in which the physical properties of the liquid do not depend markedly upon the configuration of the constituents.

The molar heats of sublimation of *d*- and *dl*-dimethyl tartrate, calculated from the slopes of curves (1) and (3), are 27.01 and 27.19 kcal., respectively. The heat of racemization in the solid state is therefore very small. The heats of combustion of the two esters are reported to differ by 1.0 kcal./mole.[7] Rosenberg,[8] however, has found by measurement of the heat of solution of tartaric acid that the molar heat of racemization is only about 0.15 kcal.

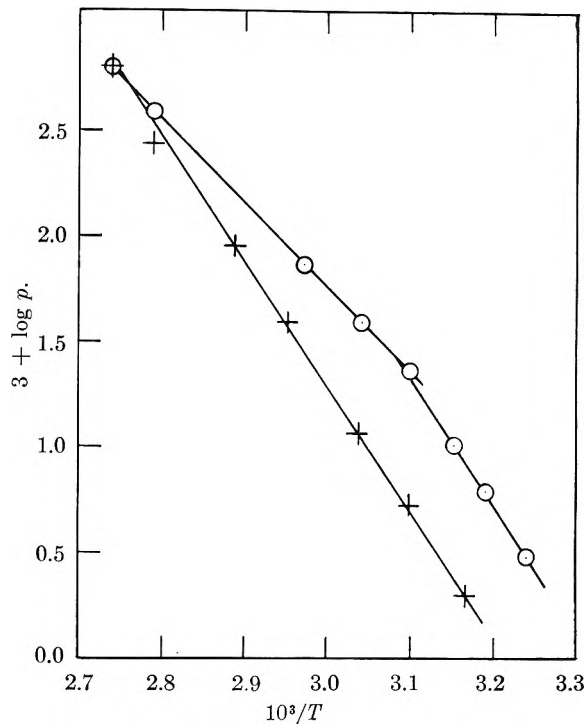

Fig. 1.—Vapor pressure of *d*-dimethyl tartrate, ○; and *dl*-dimethyl tartrate, +.

The calculated molar heat of vaporization of liquid *d*-dimethyl tartrate is 18.26 kcal. Assuming the same value for the racemic ester, the molar heats of fusion are 8.75 and 8.93 kcal. Wasserman[7] found 3.63 kcal. for the molar heat of fusion of *d*-diethyl tartrate and 5.21 kcal. for *meso*-diethyl tartrate.

(7) A. Wasserman, *Z. physik. Chem.*, **A146**, 446 (1930).
(8) T. Rosenberg, *Acta Chem. Scand.*, **2**, 740 (1948).

THE THERMAL DECOMPOSITION OF NICKEL OXALATE

BY J. A. ALLEN AND D. E. SCAIFE

Department of Chemistry, University of Tasmania, Hobart, Tasmania

Received March 17, 1954

The kinetics of the thermal decomposition of anhydrous nickel oxalate have been studied in the range 280–320° by measuring the rate of evolution of carbon dioxide into an atmosphere of pure nitrogen. The reaction falls into two parts, (i) an initial reaction following an equation, $V = k_1(t - t_0)^{1/2}$, where V is the volume of carbon dioxide, t the time and t_0 a correction factor, which is succeeded by (ii) a reaction with a constant initial rate, $V = k_2 t$, but which soon falls off. The activation energies for the two parts are, respectively, 47.6 and 36.4 kcal. A mechanism for the reaction is proposed in which the rate-determining step in (i) is the diffusion of anions to the free surface and in (ii) the transfer of electrons from the oxalate ion. X-Ray measurements show the absence of metallic nickel throughout (i) and its presence in (ii).

Many irreversible thermal decomposition reactions of the general type

$$\text{A(solid)} \longrightarrow \text{B(solid)} + \text{C(gas)}$$

have been studied, but only in cases in which B is a metal and C a single gas are the results likely to be interpretable in terms of our present knowledge of electronic and ionic processes in the solid state. Silver oxalate is the only metal oxalate conforming to these restrictions which has been investigated, but the photosensitivity of this substance[1] and its molecular layer lattice[2] suggest that it should not be considered as a general case.

Anhydrous nickel oxalate appeared to fulfill most of the requirements for such an investigation. It is one of the few metallic oxalates which decompose to give the metal and carbon dioxide, although traces of oxide and carbonate have been reported.[3] The salt is prepared as the dihydrate, $NiC_2O_4 \cdot 2H_2O$, by precipitation from solutions of nickel sulfate

(1) F. C. Tompkins, *Trans. Faraday Soc.*, **44**, 203 (1948).
(2) R. L. Griffith, *J. Chem. Phys.*, **14**, 408 (1946).
(3) M. Herschkowitsch, *Z. anorg. allgem. Chem.*, **115**, 159 (1921).

and oxalic acid and investigations on its preparation and dehydration have already been published.[4,5]

The dihydrate may be dehydrated under controlled conditions at a temperature of about 90° below that of decomposition which takes place at measurable rates in the range 280–320°. Nickel oxalate dihydrate is stable in air and is unaffected by prolonged exposure to ultraviolet light. There is no evidence of photosensitivity of the anhydrous salt and it is unlikely to possess a layer lattice.

The aim of the present work was to study the kinetics of the thermal decomposition of anhydrous nickel oxalate and, if possible, to formulate a mechanism for the reaction.

Experimental

(a) **Nickel Oxalate.**—Nickel oxalate dihydrate from three different sources with the characteristics listed in Table I was used as starting material.

TABLE I

Source	Description	Surface area of dihydrate, cm.² per g.	Particle character
A	Standard May and Baker	6700	Very uneven
B	Rapid precipitation from soln. 0.4 *N* $H_2C_2O_4$ and 0.2 *N* $NiSO_4$	4700	Even
C	Slow precipitation from soln. 0.02 *N* $H_2C_2O_4$ and 0.4 *N* $NiSO_4$	10000	Flaky

A was adopted as the standard material since its properties were intermediate between B and C prepared under the widely differing conditions. Unless otherwise specified all results refer to A. Dehydration to the anhydrous salt was carried out *in vacuo* at 190° for a minimum of 4 hours. For 0.2 g. of dihydrate normally used this was complete in 2 hours, the evolution of further water vapor thereafter being undetectable over 10-minute intervals. The completeness of dehydration was checked gravimetrically in test experiments.

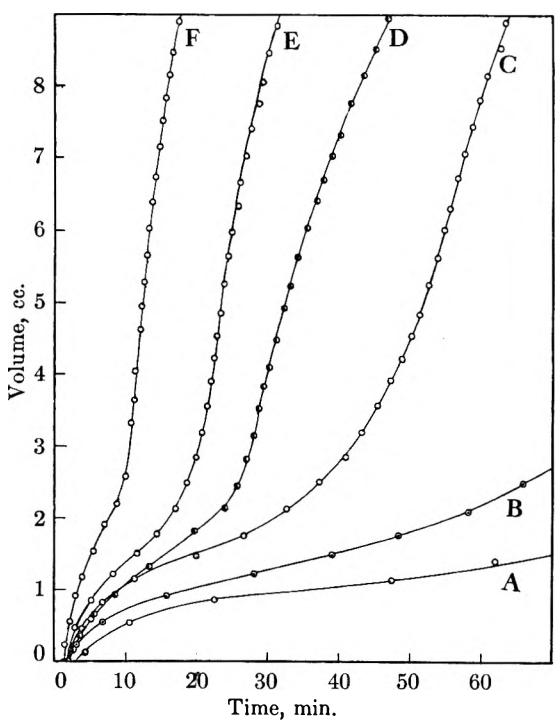

Fig. 1.—A, 279.2°; B, 291°; C, 298.5°; D, 303°; E, 309°; F, 320°.

The oxalate was enclosed in a thin-walled Pyrex ampoule about 6 mm. internal diameter; one end of this was drawn down to a strong capillary which was then bent into a hook. A loose plug of glass wool was packed into this constricted end and the sample of dihydrate weighed into the tube which was subsequently sealed off at the opposite end.

(b) **Apparatus.**—The decomposition was carried out into an atmosphere of pure nitrogen acting as a buffer gas so that the volume of carbon dioxide could be measured at constant pressure over a convenient range. The purification system for the nitrogen was similar to that used by Herington and Martin.[6]

The experimental apparatus consisted of a wide bore glass tube heated at the top by a mercury vapor jacket and cooled at the bottom by a lead coil carrying cold water. The ampoule was suspended by a thin platinum wire and could be moved in the reaction tube by means of a winch around which the wire was wound. The pressure of the pure nitrogen was measured by a wide bore mercury manometer and the volume of the carbon dioxide evolved in the reaction was measured in a water jacketed gas buret. The pressure was kept constant by using a leveling reservoir in conjunction with a differential oil manometer. The whole apparatus could be evacuated to a pressure of less than 10^{-5} mm. by a pumping system of conventional design.

The temperature gradient in the heated tube was measured and a region of sufficient length over which the variation was less than 1° was determined. This was located from a predetermined number of turns of the winch.

(c) **Procedure.**—The ampoule containing the dihydrate was attached to the platinum wire and wound into the cold section. The apparatus was continuously evacuated, the temperature of the hot section adjusted to 190° and the ampoule then wound up into this section. When dehydration was complete the ampoule was wound down to the cold section and the temperature of the hot section adjusted to that for the decomposition, 280–320°. The system was isolated from the pumps, the nitrogen admitted to the desired pressure and the differential manometer set. The ampoule was then raised into the heated section and the evolution of gas measured with time. There was an initial drop in pressure due to cooling of the gas in the heated section by the cold ampoule and it took 1.5–2.5 minutes for the sample to reach the decomposition temperature when the reaction started immediately.

Results

(a) **General Form of the Rate Curve.**—The volume of gas evolved per 0.1 g. of anhydrous nickel oxalate reduced to N.T.P. is plotted against time in Fig. 1 for a series of temperatures between 280 and 320°. The initial reaction follows the equation

$$V = k_1(t - t_0)^{1/2} \qquad \text{(i)}$$

as shown in Fig. 2, where V is the volume of carbon dioxide per 0.1 g. of anhydrous oxalate, t is the time and t_0 is a time correction for the period of heating. The initial reaction represents an average of 5.8% of the total reaction.

The second part of the rate curve does not fit any of the equations reported in the literature for reactions of a similar kind. Detailed examination of this part of the reaction, particularly at the higher temperatures, showed that it may be treated as an initially linear relation

$$V = k_2 t \qquad \text{(ii)}$$

the maximum slope k_2 being characteristic of this part of the reaction. The early falling off from linearity, referred to as the decay, is not unimolecular.

(4) J. A. Allen, THIS JOURNAL, **57**, 715 (1953).
(5) J. A. Allen and D. E. Scaife, *ibid.*, **57**, 863 (1953).
(6) E. F. G. Herington and J. F. Martin, *Trans. Faraday Soc.*, **49**, 154 (1953).

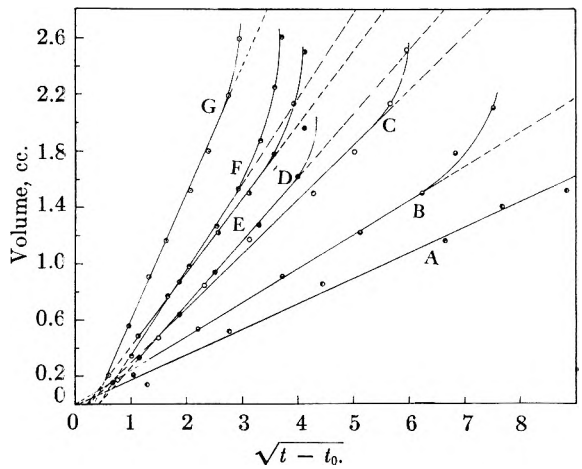

Fig. 2.—A, 279.2°; B, 291°; C, 298.5°; D, 303°; E, 309°; F, 313°; G, 320°.

(b) **Reproducibility.**—For similar samples under identical conditions the initial reaction rate is very reproducible. The duration of the initial reaction varies irreproducibly within the limits of ±20% about a mean. The initial rate of the second part of the reaction, defined by k_2 is reproducible to within ±5%. The onset of the decay tends to be variable. Typical results of identical experiments are shown in Table II.

TABLE II

Run	k_1	k_2	Duration of initial reaction, min.
17	0.45	0.45	20
18	.45	.41	25
19	.45	.44	27

(c) **Mass of Sample and Pressure of Buffer Nitrogen.**—A standard amount of 0.2 g. of dihydrate was used in most experiments. Test experiments using 0.1 g. did not yield significantly different results. For quantities ≤0.05 g. the initial reaction was too small to be followed accurately at the standard buffer pressure.

A pressure of 30 cm. of nitrogen was used in most experiments. Increasing this to 50 cm. did not yield significantly different results.

(d) **Samples of Different Origin.**—Typical results of identical experiments using samples from the three sources listed previously are shown in Table III.

TABLE III

Source	k_1	k_2	Duration of initial reaction, min.
A	0.45	0.44	27
B	.75	.43	23
C	.41	.41	31

The initial rate of the second part of the reaction is the same within the limits of reproducibility for all samples. The rate of the initial reaction is different for samples of different origin.

(e) **Purity of Nitrogen.**—The presence of oxygen in the buffer gas has a marked effect on the rate of decomposition. Figure 3 shows curves obtained from experiments in which pure nitrogen, impure nitrogen containing less than 1% oxygen and air, respectively, were used, all other conditions being identical. The features are the small effect of oxygen on the initial reaction and the systematic decrease in the initial rate of the second part of the reaction for experiments carried out in impure nitrogen and in air. The decay also appears to set in earlier with these experiments.

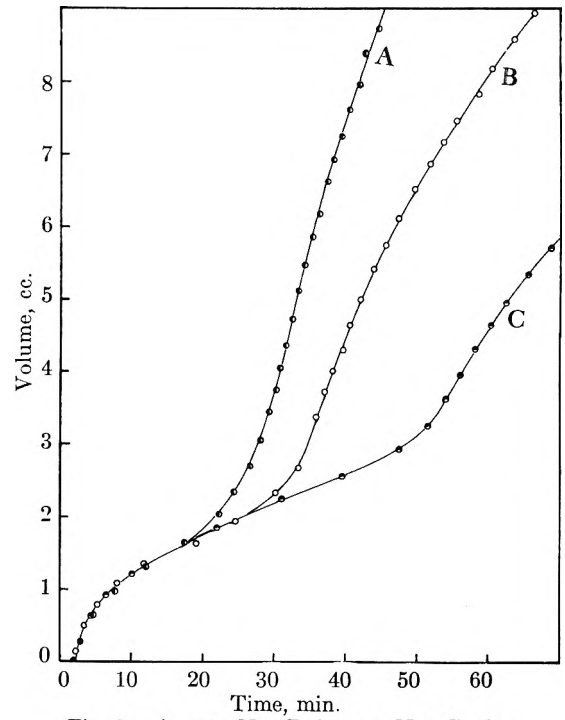

Fig. 3.—A, pure N_2; B, impure N_2; C, air.

(f) **Temperature of Dehydration.**—Dehydration at 220° instead of 190° generally employed halved the time of dehydration, but did not significantly influence the subsequent thermal decomposition. A more detailed study of this variable, particularly in relation to the surface area of the dehydrated oxalate, is to be undertaken.

(g) **Completeness of Decomposition.**—In a number of experiments the gases were evacuated from the apparatus when about 30% of the total decomposition had taken place and the remainder of the reaction carried out *in vacuo*. The yield of metallic nickel determined gravimetrically immediately after the experiment corresponded to the theoretical value to within 1.8%. The ampoule was sealed immediately on removal from the apparatus in order to minimize oxidation of the nickel. In addition, experiments using 0.05 g. of dihydrate were carried on for a long period in the presence of the nitrogen and carbon dioxide. It was found that when the reaction had proceeded to the extent of 75% the rate of evolution of gas had become very slow.

If the decomposition was interrupted by lowering the ampoule out of the heated section, the smooth curve was resumed without a break on resumption of heating. Metallic nickel residue from a previous experiment mixed in a fresh charge of oxalate to the extent of about 30% by weight prolonged the initial reaction for as much as 150 minutes. It should be noted, however, that the metallic residue used would have been contaminated with oxide as a result of exposure to the air during mixing.

(h) **Effect of Temperature.**—The over-all effect of temperature on the rate curve is seen from Fig. 1. The plot of log k_1 against $1/T$, Fig. 4, yields, by the method of least squares, the equation

$$\log_{10} k_1 = \frac{-5202}{T} + 8.669 \qquad \text{(iii)}$$

The specific reaction rate corresponding to the differential form of equation (i) is k_1^2 whence the activation energy for the initial reaction is 47.6 kcal. per mole.

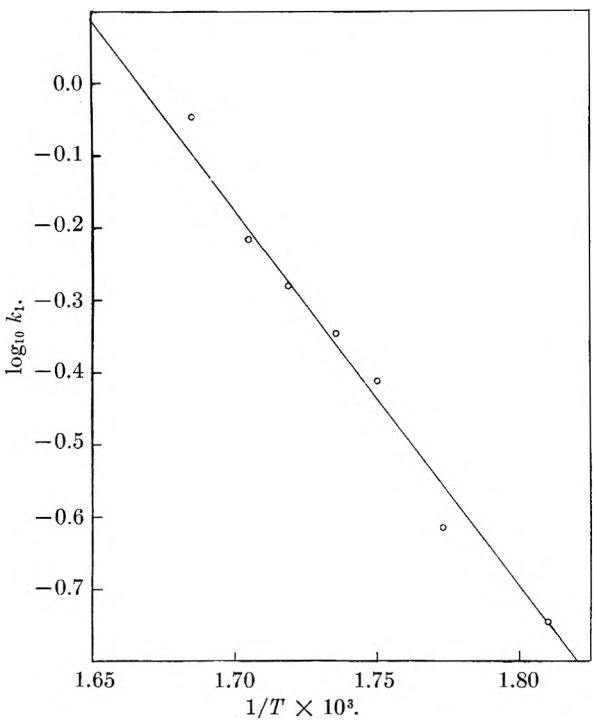

Fig. 4.

For the second part of the reaction log k_2 plotted against $1/T$, Fig. 5, gives

$$\log_{10} k_2 = \frac{-7946}{T} + 13.46 \qquad \text{(iv)}$$

whence the activation energy is 36.4 kcal. per mole.

(i) **X-Ray Analyses.**—Four samples of partly decomposed oxalate, two taken during the initial reaction and two during the second part, were examined with unfiltered copper radiation in sealed quartz tubes by Dr. G. F. Walker of the Commonwealth Scientific and Industrial Research Organization. He reported that the two samples taken during the initial reaction gave patterns identical with the undecomposed anhydrous nickel oxalate, whereas the two samples taken during the second part gave, in addition, patterns corresponding to metallic nickel. It was estimated from synthetic mixtures that 1% of metallic nickel would be observable. There was no evidence of the presence of nickel oxide or nickel carbonate in any of the samples although in the case of the latter as much as 10% might escape detection.

Discussion

The present results are substantially different from those reported for barium azide and silver oxalate for which some theoretical work has been

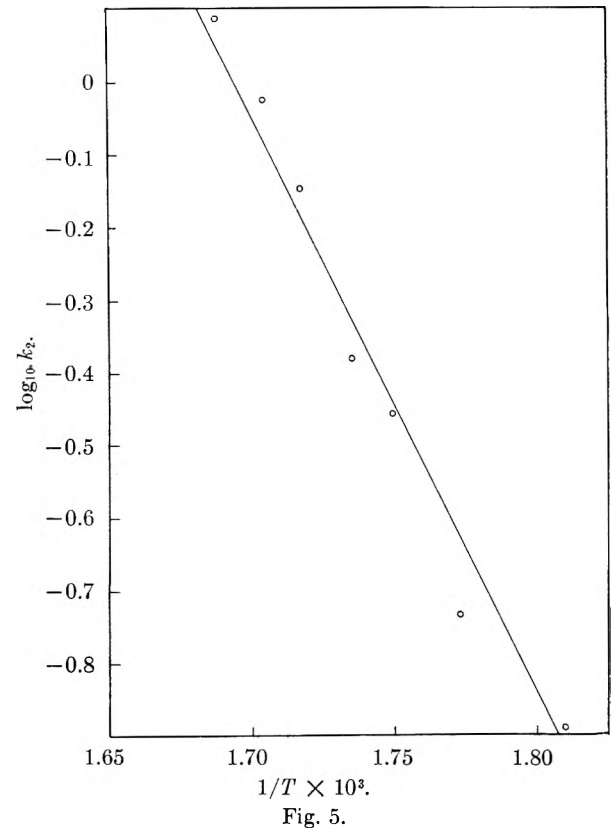

Fig. 5.

carried out.[7] For the initial reaction the following mechanism is proposed.

An anion situated at a favorable site at the surface loses its electrons which are trapped at impurity centers or existing vacant anion sites. The oxalate radical breaks down to give carbon dioxide which escapes leaving a vacant anion site which may function as a further electron trap.

The vacant anion sites diffuse into the body of the crystal, but, because of the large size of the anions and their expected low mobility, a quasi-equilibrium of vacant anion sites is set up in the surface layers of the crystal. The concentration gradient controlling diffusion of anions to the free surface will, under these conditions, be inversely proportional to the extent of the reaction; that is, provided the rate-determining step is the diffusion of anions to the free surface

$$\frac{dV}{dt} \propto \frac{1}{V} \qquad \text{(v)}$$

from which the experimentally found equation (i) follows.

At the end of the initial reaction the lattice in the upper surface layers has become so defective that it collapses to form metallic nuclei. An anion at the free surface so produced may now lose its electrons, the oxalate radical breaking down to yield carbon dioxide. The trapped electrons migrate to a cation adjacent to a metallic nucleus to which the resulting metal atom joins. There will now be a continuous exposure of fresh oxalate ions at the free surface in positions favorable for decomposition. This

(7) *E.g.*, J. G. N. Thomas and F. C. Tompkins, *Proc. Roy. Soc.* (*London*), **A210**, 111 (1951).

mechanism would lead to a reaction of initially constant rate, *cf.* equation (ii).

The X-ray data give clear evidence of the absence of metallic nickel in the initial reaction and the presence of it in the second part of the reaction. The activation energy of 47.6 kcal. per mole for the initial reaction is interpreted as the activation energy for diffusion while the 36.4 kcal. per mole for the initial rate of the second part of the reaction is to be associated with the transfer of electrons from an oxalate ion at a position suitable for reaction.

The early decay of the initial rate of the second part of the reaction is attributable primarily to interference with the electron transfer processes by the gaseous product of the reaction. The decrease in the area of the free surface of the oxalate as the amount of metallic nickel increases may also be important when the reaction is well advanced.

The experimental observations are consistent with the view that both oxygen and carbon dioxide are effective poisoning agents of the surfaces of the metallic nuclei. The actual formation of a small amount of surface oxide on the metallic nuclei by reduction of the carbon dioxide is feasible thermodynamically and cannot be ignored. The effect of oxygen in extending the duration of the initial reaction is explicable since the diffusion of oxygen into the highly defective surface layers would retard the collapse to form the metal lattice.

The proposed mechanism is based on the hypothesis, that the oxalate ions can diffuse in the surface layers. To test this, ionic diffusion measurements are required and these will be undertaken in a future investigation.

Acknowledgments.—We wish to thank Dr. G. F. Walker for the X-ray analysis and Professor I. Lauder of the University of Queensland for a useful discussion of some aspects of the reaction. The work was supported by the University of Tasmania Research Fund and we are indebted to Commonwealth Industrial Gases Ltd., Tasmania, for a gift of liquid air.

NOTE

A SIMPLE CORRELATION OF GAS SOLUBILITIES

By J. H. Hildebrand

Department of Chemistry, University of California, Berkeley, Calif.

Received April 9, 1954

The fact that the solubilities of the more "permanent" gases decrease with increasing "internal pressures" of the solvent was pointed out[1] in 1916. In 1924 the relation was put upon an approximately quantitative basis by aid of the theory of regular solutions.[2] In 1940, Gonikberg[3] applied this relation rather successfully to solubilities of hydrogen. (The one discordant case, in carbon disulfide, can now be definitely ascribed to an inaccurate measurement.) In 1949 Gjaldbaek[4] and I published a detailed treatment of solubility data for nitrogen by means of the equations for regular solutions, both with and without the Flory–Huggins correction for unequal molar volumes.

The Flory–Huggins expression for the entropy of athermal mixing of two liquids of unequal molar volumes contains the implicit assumption that the free volumes of the pure liquids and the solution are simply related if the appropriate one of the several kinds of free volume is selected.[5] But a good part of the considerable success of that formulation, as indeed of regular solution theory, comes from the fact that, as Scott[6] has recently stated, "the solution properties which interest us . . . are usually differences or ratios referred to the pure

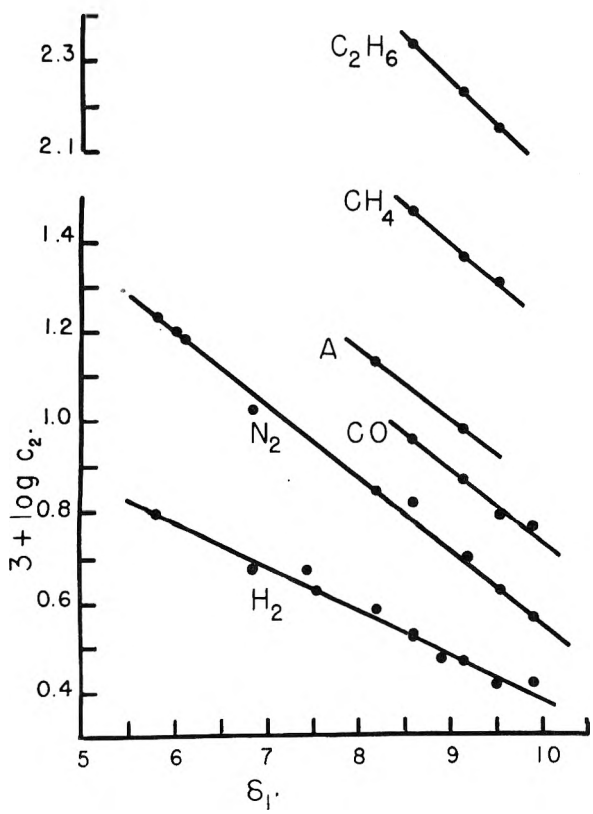

Fig. 1.—Relation between molar concentrations of gases and solubility parameters of solvents.

(1) J. E. Hildebrand, *J. Am. Chem. Soc.*, **38**, 1452 (1916). See also *Phys. Rev.*, **21**, 46 (1923); N. W. Taylor and J. H. Hildebrand, *J. Am. Chem. Soc.*, **45**, 682 (1923).

(2) J. H. Hildebrand, "Solubility of Nonelectrolytes," 2nd Edition, 1924, p. 135; 3rd Edition, with R. L. Scott, 1950, p. 244, Reinhold Publ. Corp., New York, N. Y.

(3) M. G. Gonikberg, *J. Phys. Chem., U.S.S.R.*, **14**, 582 (1940).

(4) J. C. Gjaldbaek and J. H. Hildebrand, *J. Am. Chem. Soc.*, **71**, 3147 (1949).

(5) A. Bondi, in preparation.

(6) R. L. Scott, *J. Chem. Educ.*, **30**, 542 (1953).

TABLE I

SOLUBILITY PARAMETERS OF SOLVENTS, δ_1, AND SOLUBILITY OF GASES EXPRESSED AS MOLES PER LITER, c_2, AT 1 ATMOSPHERE AND 25°

Solvent	δ_1	$10^3 c_2$ H_2	N_2	CO	A	CH_4	C_2H_6
n-C_7F_{16}	5.8	6.25[10]	17.15[4]	17.08[10]			
		6.22[8]					
$C_6F_{11}CF_3$	6.0		16.73[4]				
$C_6F_{10}(CF_3)_2$	6.1		14.63[14]				
i-C_8H_{18}	6.9		10.65[4]				
n-C_7H_{16}	7.5	4.67[8]		11.68[10]			
n-C_8H_{18}	7.6	4.18[8]					
c-C_6H_{12}	8.2		6.97[4]		11.34[9]		
CCl_4	8.6	3.33[7]	6.63[7]	8.94[7]		14.68[7]	23.31[7]
		3.30[8]					
$C_6H_5CH_3$	8.9	3.39[8]					
C_6H_6	9.15	2.92[7]	5.09[4]	7.44[7]	9.94[9]	13.65[7]	22.29[7]
		2.89[8]	4.95[7]	7.56[10]			
C_6H_5Cl	9.5	2.71[7]	4.20[7]	6.19[7]		13.09[7]	21.61[7]
CS_2	9.9	2.71[10]	3.67[4]	5.92[10]			
		2.64[3]					

liquid as standard state. If we assume that the unknown features of liquids persist unchanged into the solutions, these features cancel out and can therefore be ignored." If we break down the mixing process into two steps, first, the evaporation of the pure components, second, their condensation into solution, we have to confess that we know less about the separate steps than about the total process, in which we cancel some of our ignorance. But that is not a fully satisfactory way to deal with ignorance, and I think we should try to learn something about the second step above, the one concerning which we are most ignorant.

The entropy of solution of gases is susceptible to experimental measurement and offers the advantage that one can work with extremely dilute solutions, where solute–solute interaction is negligible. New experimental data are badly needed, because there are only a few accurate measurements of gas solubility even at one temperature, and data over a range of temperature are needed, sufficiently reliable to permit calculation of entropies of solution.

In the course of preliminary study of this problem, I had occasion to calculate the volumes of different solvents required to dissolve one mole of gas, and discovered, as a by-product, the remarkably simple correlation between concentrations of dissolved gas and solubility parameters of solvents shown in Fig. 1. The ordinates represent the logarithms of the solubilities of the gases, c_2, expressed as moles of gas per liter of solvent, with the gas at 1 atmosphere and 25°. The abscissas are the solubility parameters of the solvents, δ, as given in "Solubility of Nonelectrolytes." The figures for log c_2 have been calculated from the measured values of Horiuti,[7] Gjaldbaek and Hildebrand,[4] Hanson and Cook,[8] Lannung,[9] and Gjaldbaek.[10] The data plotted are given in Table I. The δ-values serve to identify the solvents. They have not been adjusted empirically in the manner I once suggested.[11]

Each line would, of course, be displaced vertically by an amount calculable by aid of Henry's law for gas at another pressure. The parallelism between all the lines except hydrogen is striking, and their displacements are obviously related to their relative vapor pressures in the liquid state. Fragmentary data for helium and neon suggest that the slopes decrease in the order Ne, H_2, He.

Solvents such as ether, alcohols, ester, acetone and water are not included, because their solvent powers are not uniquely determined by solubility parameters.

This simple correlation is considerably better than the one for nitrogen given in reference 2, and I publish it now for the sake of its evident practical value without awaiting the outcome of the study to which it gave rise.

This work has had the support of the Atomic Energy Commission.

(7) J. Horiuti, *Sci. Papers, Inst. Phys. Chem. Research, Tokyo Univ.*, **17**, No. 311. 125 (1931).

(8) D. N. Hanson and M. W. Cook, Radiation Lab., Univ. Calif., Berkeley, unpublished measurements.

(9) A. Lannung, *J. Am. Chem. Soc.*, **52**, 68 (1930).

(10) J. C. Gjaldbaek, *Acta Chem. Scand.*, **6**, 623 (1952).

(11) J. H. Hildebrand, *J. Chem. Phys.*, **18**, 1337 (1950).

AZEOTROPIC DATA

-- Advances in Chemistry Series Volume No. 6

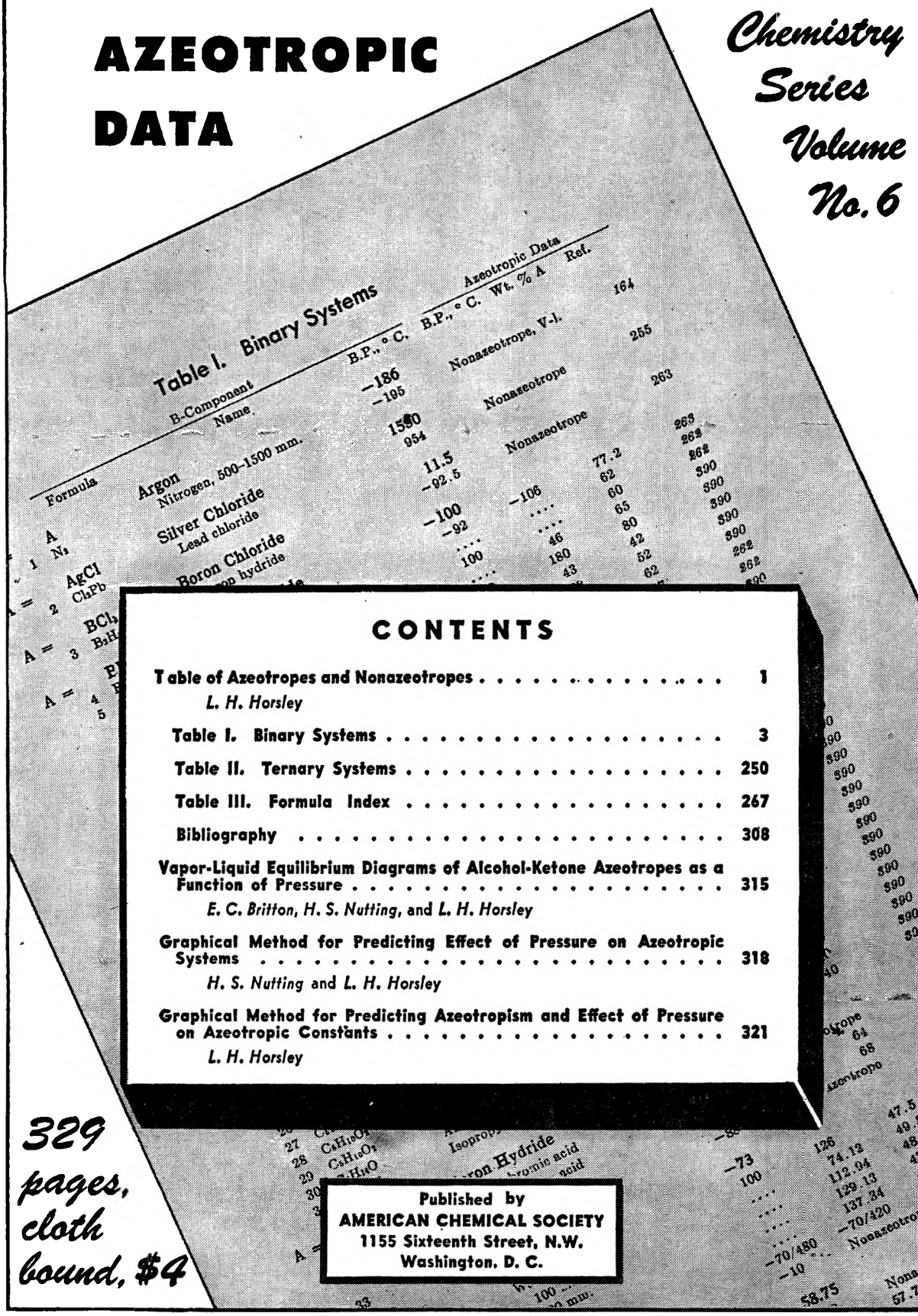

CONTENTS

329 pages, cloth bound, $4

Published by
AMERICAN CHEMICAL SOCIETY
1155 Sixteenth Street, N.W.
Washington, D. C.